USING HIGH-THROUGHPUT PALEOLIMNOLOGICAL METHODS TO EVALUATE THE DISTRIBUTION AND TRANSPORT OF LEAD IN NORTHEASTERN NORTH AMERICA

by

Dewey W. Dunnington

Submitted in partial fulfillment of the requirements
for the degree of Doctor of Philosophy

at

Dalhousie University
Halifax, Nova Scotia
August 2020

For Clementine Louise

Table of Contents

List of Tables . . . . . **viii**

List of Figures . . . . . **ix**

Abstract . . . . . **xii**

List of Abbreviations Used . . . . . **xiii**

Acknowledgements . . . . . **xv**

Chapter 1 Introduction **1**

Chapter 2 A Global Review of the Timing, Distribution, and Transport of Trace Metals in Freshwater Sediments **4**

2.1 Abstract 4

2.2 Introduction 4

2.3 Point Source Trace Metal Inputs 5

2.4 Deposition of Trace Metals in Remote Regions 7

2.5 Pre-Industrial Trace Metal Mobilization 8

2.6 Short- and Medium-Range Transport of Trace Metals 10

2.6.1 Europe 10

2.6.2 West, South, and Central North America 11

2.6.3 Northeast United States 14

2.6.4 Eastern Canada 16

2.7 Conclusion 18

Chapter 3 Evaluating the Utility of Elemental Measurements Obtained from Factory-Calibrated Field-Portable X-Ray Fluorescence Units for Aquatic Sediments 20

3.1 Abstract 20

3.2 Introduction 21

3.3 Materials and Methods 22

3.3.1 Sediment Sampling & Preparation 22

3.3.2 XRF Analysis 23

3.3.3 Data Quality 24

3.3.4 Precision of Replicate Measurements 26

3.3.5 Accuracy of Calibrated Total Concentrations 26

3.3.6 Comparability of Calibrated Extractable Concentrations 27

3.4 Results 27

3.4.1 Precision of Replicate Measurements 27

3.4.2 Accuracy of Calibrated Total Concentrations 29

3.4.3 Comparability of Calibrated Extractable Concentrations 29

3.5 Discussion 31

3.5.1 Data Quality Relationships 31

3.5.2 Analyzer Data Quality 32

3.5.3 Elemental Data Quality 33

3.5.4 Suitability for Environmental Pollution Studies 34

3.5.5 Improving Quantification 36

3.6 Conclusion 37

Chapter 4 Visualizing Paleoenvironmental Archives 38

4.1 Abstract 38

4.2 Introduction 39

4.3 Example Data 40

4.4 Design and Implementation . . . 41
4.4.1 Data . . . 41
4.4.2 Scales . . . 43
4.4.3 Geometries . . . 45
4.4.4 Facets . . . 47
4.4.5 Theme Elements . . . 50
4.4.6 Statistical Helpers . . . 51
4.5 Example . . . 54
4.6 Discussion . . . 56
4.7 Conclusion . . . 61
Chapter 5 Anthropogenic Activity in the Halifax Region, Nova Scotia, Canada, as Recorded by Bulk Geochemistry of Lake Sediments . . . 62
5.1 Abstract . . . 62
5.2 Introduction . . . 63
5.3 Study Site . . . 64
5.4 Materials and Methods . . . 65
5.4.1 Historical Methods . . . 65
5.4.2 Coring and Sampling . . . 67
5.4.3 Bulk Sediment Geochemistry . . . 68
5.4.4 Age-Depth Models . . . 69
5.4.5 Numerical Analyses . . . 69
5.5 Results . . . 70
5.5.1 Historical Observations . . . 70
5.5.2 Age-Depth Models . . . 72
5.5.3 Numerical Analyses . . . 72
5.5.4 Bulk Sediment Geochemistry . . . 74

5.6 Discussion . . . 77
5.6.1 Watershed Disturbances . . . 77
5.6.2 Interpretation of Geochemical Parameters . . . 81
5.6.3 Comparison to Bioindicator Studies . . . 82
5.7 Conclusion . . . 83
Chapter 6 Evaluating the Performance of Calculated Elemental Measures in Sediment Archives . . . 84
6.1 Abstract . . . 84
6.2 Introduction . . . 85
6.3 Materials and Methods . . . 87
6.3.1 Example Data . . . 87
6.3.2 Synthesized Data . . . 88
6.3.3 Software . . . 90
6.4 Results . . . 92
6.4.1 Example Data . . . 92
6.4.2 Synthesized Data . . . 92
6.5 Discussion . . . 96
6.5.1 Measure Performance Using Example Data . . . 96
6.5.2 Measure Performance Using Synthetic Data . . . 96
6.5.3 Geochemical Assumptions . . . 98
6.5.4 Reporting of Elemental Concentrations . . . 101
6.6 Conclusion . . . 102
Chapter 7 The Distribution and Transport of Lead Over Two Centuries as Recorded by Lake Sediments from Northeastern North America . . . 103
7.1 Abstract . . . 103
7.2 Introduction . . . 104

7.3 Methods . . . 105
7.3.1 Record Selection and Parameter Measurement . . . 105
7.3.2 Age-Depth Models . . . 106
7.3.3 Cumulative Anthropogenic Pb Deposition . . . 108
7.3.4 Timing of Pb Deposition . . . 109

7.4 Results and Discussion . . . 110
7.4.1 Pb Concentrations . . . 110
7.4.2 Cumulative Anthropogenic Pb Deposition . . . 111
7.4.3 Timing of Deposition . . . 117
7.4.4 Implications for Pb Transport . . . 118

7.5 Conclusion . . . 121

Chapter 8 Conclusion . . . 123

8.1 Conclusion and Implications . . . 123

8.2 Recomendations for Future Research . . . 125

References . . . 127

Appendix A Copyright Permissions . . . 155

Appendix B Supplemental Information: Evaluating the Utility of Elemental Measurements Obtained from Factory-Calibrated Field-Portable X-Ray Fluorescence Units for Aquatic Sediments . . . 160

Appendix C Supplemental Information: Anthropogenic Activity in the Halifax Region, Nova Scotia, Canada, as Recorded by Bulk Geochemistry of Lake Sediments . . . 169

Appendix D Supplemental Information: The Distribution and Transport of Lead Over Two Centuries as Recorded by Lake Sediments from Northeastern North America . . . 172

List of Tables

3.1 Details of pXRF instruments used in this chapter. 24

3.2 Data and criteria used in this study to establish data quality. 25

3.3 Number of analyzers with a definitive level of data quality. 35

6.1 Parameters controlling the mass input time series for each source. . . . 91

B.1 Relative standard deviations of replicate values from study pXRF analyzers. 161

B.2 Pearson correlation coefficient and RD values between total concentrations and pXRF measurements. 162

B.3 Pearson correlation coefficient and RD values between extractable concentrations and pXRF measurements. 164

C.1 Selected watershed parameters for lakes in Chapter 5. 170

D.1 List of cores included in this study and associated metrics. 173

D.2 Annual precipitation estimates, collection methods, and references for lakes included in Chapter 7. 175

D.3 List of independent age-depth markers used to assess reconstructed age-depth models. 179

List of Figures

3.1 Schematic of sample analysis using the pXRF. 25

3.2 Relative standard deviations of replicate values from study pXRF analyzers for elements with a definitive overall level of data quality. . . . 28

3.3 Relative difference between calibrated pXRF values and total concentrations. 30

3.4 Relative difference between calibrated pXRF values and extractable concentrations. 32

4.1 Geochemical measurements from Kellys Lake, Nova Scotia, Canada. . 41

4.2 Microfossil zooplankton (Cladocera) relative abundances from Kellys Lake, Nova Socita, Canada. 42

4.3 Age-depth transformation and scales applied to a stratigraphic plot of geochemical measurements. 44

4.4 Exaggerated line and area geometries for highlighting relative change of parameters with a large change in magnitude. 47

4.5 Column segment, line, area, and combinations commonly used to represent relative abundance values on stratigraphic diagrams. 48

4.6 Adding units to multi-parameter plots using the geochemistry labeller. 50

4.7 Relative abundances and cluster analysis of microfossil diatom relative abundance from two lakes in Kejimkujik National Park, Nova Scotia, Canada. 57

4.8 A stratigraphic diagram created using the *analogue* package. 59

4.9 A stratigraphic diagram created using the *rioja* package. 60

4.10 A stratigraphic diagram created using *TiliaGraph* software. 60

4.11 A stratigraphic diagram created using *C2* software. 61

5.1 Overview of chapter study lakes in the context of the Halifax Regional Municipality (HRM). 66

5.2 ^{210}Pb activity and age for ^{210}Pb-dated cores in this chapter. 73

5.3 Bulk geochemistry, PC1 scores, and periods of probable land disturbance for Lake Major, Pockwock Lake, Bennery Lake, and Second Lake. 75

5.4 Bulk geochemistry, PC1 scores, and periods of probable land disturbance for Lake Fletcher, Lake Lemont, First Lake, and First Chain Lake. 78

6.1 A conceptual model of sediment sources to the simplified lake sediment archive. 89

6.2 Elemental concentrations and ratios at First Chain Lake and Pockwock Lake. 91

6.3 Model results and tracer element measures for the modeled scenarios. . 94

6.4 Visualization of the Pb-Ti relationship in the model results. 95

6.5 Pb concentrations vs. Ti concentrations at First Chain Lake and Pockwock Lake. 100

7.1 Pb concentrations vs. median age of sediment intervals. 112

7.2 Relationship of cumulative focus-corrected anthropogenic Pb deposition to watershed variables. 115

7.3 Principal components analysis (PCA) biplot of PC1 and PC2 scores with loadings of input variables overlayed. 116

7.4 Relative anthropogenic Pb concentrations vs. median age (top) and age distributions of breakpoints (bottom). 119

7.5 Relative anthropogenic Pb for cores collected after 2006. 121

B.1 Total concentrations (4-acid digestion/ICP-OES) compared to pXRF values. 165

B.2 Total concentrations (4-acid digestion/ICP-OES) compared to calibrated pXRF values. 166

B.3 Extractable concentrations ($HClO_4$ digestion/ICP-OES) compared to pXRF values 167

B.4 Extractable concentrations ($HClO_4$ digestion/ICP-OES) compared to calibrated pXRF values 168

C.1 Total elemental Pb concentrations for First Lake and Second Lake. . . 171

C.2 PCA loadings for the first principal component for lakes in Chapter 5. 171

D.1 Location of cores included in Chapter 7. 182

D.2 Total ^{210}Pb activities and calculated background values. 183

D.3 Comparison of recalculated age-depth models with original published models. 184

D.4 Total Pb and Total Ti concentrations for study lakes. 185

D.5 Pb concentrations vs. median age of sediment intervals. 186

D.6 Calculated backgrounds and inventories for each location. 187

D.7 Explanatory variable values for each lake. 188

Abstract

Using high-throughput paleolimnological methods, this thesis evaluated anthropogenic Pb deposition along a west-east transect from the Adirondack Mountains, New York, USA (ADIR) region, the Vermont-New Hampshire-Maine, USA (VT-NH-ME) region, and Nova Scotia, Canada (NS) region using 47 ^{210}Pb-dated lake sediment records. This thesis reviewed the distribution and transport of trace metals at a global scale, developed a high-throughput analytical method to measure the elemental composition of low-mass aquatic sediment samples, developed a software package to visualize and analyze measurements from many lake sediment records, validated the sensitivity of elemental measurements in lake sediments to watershed-scale disturbance, and evaluated calculated elemental measures to deconvolute multiple sources of trace metals to lake sediment records. Finally, this thesis used focus-corrected Pb inventories to evaluate cumulative deposition and breakpoint analysis to inform west-east transport of Pb in northeastern North America. Peak Pb concentrations decreased from west to east (ADIR region: 52-378 mg kg^{-1}, VT-NH-ME region: 54-253 mg kg^{-1}, NS: 38-140 mg kg^{-1}). Cumulative deposition of anthropogenic Pb also decreased from west to east (ADIR region: 791-1,344 mg m^{-2}, VT-NH-ME region: 209-1,206 mg m^{-2}, NS: 52-421 mg m^{-2}). The initiation of anthropogenic Pb deposition occurred progressively later along the same transect (ADIR region: 1869-1900, VT-NH-ME region: 1874-1905, NS region: 1901-1930). Previous lead isotope studies suggest that eastern Canadian Pb deposition over the past ~150 years has originated from a mix of both Canadian and U.S. sources. The results of this thesis indicate that anthropogenic Pb from sources west of the ADIR region were deposited in lesser amounts from west to east and/or Pb sources reflect less population density from west to east. The timing of the initiation of anthropogenic Pb deposition in the NS region suggests that Pb from gasoline may be an important source in this region. The high-throughput methods developed in this thesis may further the application of paleolimnological studies to regional contaminant transport, contaminated aquatic sediment assessment, and water infrastructure design.

List of Abbreviations Used

ADIR - Adirondack Mountain Region, New York

AMS - Atomic Mass Spectrometry

ANOVA - Analysis of Variance

ARD - Acid Rock Drainage

CCME - Canadian Council of Ministers for the Environment

CRM - Certified Reference Material

CRS - Constant Rate of Supply

DEM - (Nova Scotia) Department of Energy and Mines

DI-SC - Diatom-Inferred Specific Conductance

DI-TP - Diatom-Inferred Total Phosphorus

HRM - Halifax Regional Municipality

ICP-MS - Inductively-Coupled Plamsa Mass Spectrometry

ICP-OES - Inductively-Coupled Plasma Optical Emission Spectrometry

IQR - Inter-Quartile Range

ISQG - Interim Sediment Quality Guideline

LOD - Limit of Detection

LOI - Loss On Ignition

MAR - Mass Accumulation Rate

ME - Maine

NB - New Brunswick

NH - New Hampshire

NS - Nova Scotia

NSERC - Natural Sciences and Engineering Research Council (of Canada)

PCA - Principal Components Analysis

PEC - Probable Effect Concentration

PEL - Probable Effect Level

PIRLA - Paleoecological Investigation of Recent Lake Acidification

PLR - Piecewise Linear Regression

pXRF - Portable X-Ray Fluorescence

QC - Quebec

RD - Relative Deviation

RDL - Reporting Detection Limit

RSD - Relative Standard Deviation

RSE - Relative Standard Error

SAR - Sediment Accumulation Rate

SINLAB - Stable Isotopes in Nature Laboratory (University of New Brunswick)

TEC - Threshold Effect Concentration

TEL - Tetra-Ethyl Lead

USA - United States of America

USEPA - United States Environmental Protection Agency

USGS - United States Geological Survey

VPDB - Vienna Pee Dee Belemnite

WD-XRF - Wavelength-Dispersive X-Ray Fluorescence

XRF - X-Ray Fluorescence

Acknowledgements

This thesis contains data obtained from over 50 sediment cores, none of which were collected by me alone. I am grateful to Kirklyn Davidson, Adam Godfrey, Baillie Holmes, Joshua Kurek, Amanda Loder, Heather McGuire, Ben Misiuk, Steve Norton, Dave Redden, Sarah Roberts, Ian Spooner, and Drake Tymstra for letting me write about cores they worked hard to collect and analyze. Barry Geddes, Beth Lowe, Adam McKnight, Rebecca Betts and Gabriel Sombini provided additional field support, laboratory support, and/or data; Dominique Huot (REFLEX Instruments), Stephen Williams (Panalytical), Beth McClenaghan (Geological Survey of Canada), and Jack Cornett (University of Ottawa) provided standards and analytical support; and Al Sosiak (Lake and Reservoir Management), Euan Reavie (Lake and Reservoir Management), Mark Brenner (Journal of Paleolimnology), and a number of anonymous reviewers provided valuable feedback on the manuscript submissions resulting from this thesis. Jack Cornett, Graham Gagnon, Braden Gregory, Jane Kirk, Wendy Krkošek, Joshua Kurek, Nell Libera, Mark Mallory, Ben Misiuk, Derek Muir, Steve Norton, Sarah Roberts, Ian Spooner, Drake Tymstra, and Chris White all co-authored one or more manuscripts in this thesis and provided invaluable comments during the preparation and submission process.

This thesis was assembled using the *knitr*, *rmarkdown*, and *bookdown* packages for R statistical software (R Core Team 2019; Xie 2020; Allaire et al. 2019; Xie 2019). Tables were created using the *kableExtra* package, graphics were created using the *ggplot2* package, and maps were created using QGIS (Zhu 2019; Wickham et al. 2020a; QGIS Development Team 2020). Finally, the unseen work of making raw data usable would not have been possible with out the *tidyverse* (Wickham 2019). I owe the authors of these software packages a debt of gratitude.

Funding for this work was provided by the Natural Sciences and Engineering Research Council (NSERC) Canada Graduate Scholarship, ENGAGE/ENGAGE Plus (I. Spooner, Halifax Water, and Cape Breton Water Utility), Discovery (I. Spooner, J. Kurek, and G. Gagnon), and Industrial Research Chair (G. Gagnon) grant programs. The Centre for Water Resources Studies, Dalhousie University, and Acadia University provided additional support.

I would like to thank my supervisory committee (Graham Gagnon, Rob Jamieson, Ian Spooner,

and Joshua Kurek) for taking the time to read and comment on many versions of this thesis and the manuscripts, proposals, and comprehensive exams that contributed to its completion. In particular, I would like to thank my supervisor Graham Gagnon for his support and his willingness to accept a geoscientist into a Ph.D. program in Civil Engineering.

Ian Spooner is responsible for my involvement with lake sediment geochemistry, and provided the inspiration for many of the ideas presented in this thesis. His guidance and friendship are responsible for many important things in my life, including this thesis.

Finally, it is my wife Catherine who ensured I had food, excercise, and a clean place to live during the many months that I was absorbed in this thesis. It would never have been finished (or I would have been) without her support.

Chapter 1

Introduction

In 1923, the first gasoline containing tetraethyl lead (TEL) was sold in Dayton, Ohio (Nriagu 1990). By 1975, motorists in the United States were consuming over 140,000 metric tons of elemental lead (Pb) annually as TEL in gasoline (Nriagu 1990; Oudijk 2010; Mielke et al. 2011). Human health and environmental concerns led to the replacement of Pb in gasoline with other additives during the 1970s and 1980s, and by 1990 there was little atmospheric deposition of Pb from leaded gasoline in North America (Nriagu 1990). Along with coal burning, waste incineration, municipal wastewater input, and smelting, freshwater bodies in northeastern North America have been exposed to more than a century of substantial anthropogenic Pb input (Gallon et al. 2005; Graney et al. 1995; Gobeil et al. 2013).

Lead can travel long distances in the atmosphere before deposition on to the landscape (Marx et al. 2016). Boyle (2001) and Rose et al. (2012) both noted that continued research was needed to characterize the redistribution of Pb in watershed soils. Furthermore, concentrations of Pb in soil dust have been linked to blood Pb levels in children (Dixon et al. 2009). The introduction of the Clean Air Act in 1970 in the United States mitigated atmospheric deposition of Pb from some sources (Mahler et al. 2006; Nriagu 1990). However, Pb deposited on the landscape is still a likely source of Pb in urban dust (Mielke et al. 2011) and production of TEL as an additive in fuel for small airplanes continues (United States Environmental Protection Agency 2020; Federal Aviation Administration 2019). Non-atmospheric and proximal point-sources of Pb may be locally important (Norton et al. 2004; Horowitz et al. 1995; Thienpont et al. 2016); however, the past and potential for future atmospheric transport and deposition of Pb at a regional scale remains relevant and should be investigated. Finally, the past and potential for future transport of other compounds in northeastern North America may have important implications for water treatment infrastructure (Evans et al. 2005a; Anderson et al. 2017).

Lake sediment records are often used to reconstruct input of pollutants when little or no monitoring data are available (Kay et al. 2020), and are particularly well-suited for elements such as

Pb, for which post-depositional mobility is minimal (Norton et al. 1992). Many lake sediment Pb records from northeastern North America show a pattern of increasing Pb accumulation rate or concentration starting in the mid-1800s; however, the regional timing of this increase is not well-constrained (Blais et al. 1995; Norton et al. 1992). Anthropogenic Pb deposition has been estimated for groups of lakes in close proximity; a synthesis of these results suggests that different amounts of Pb were deposited in different regions in northeastern North America (Kada and Heit 1992; Blais and Kalff 1993; Dillon and Evans 1982; Evans and Rigler 1985; Roberts et al. 2019). Despite previously-published Pb records from lake sediments from northeastern North America, there is a lack of consistent data treatment among those studies, and few published Pb records exist from Maritime Canada (Roberts et al. 2019), where west-to-east upper-atmosphere circulation has led to the region being called the "tailpipe of North America" (Nova Scotia Environment 2017). Whereas regional syntheses exist for other contaminants (Perry et al. 2005), other regions (Renberg et al. 1994; Renberg et al. 2000; Verta et al. 1989), or both (Landers et al. 1998), the spatial component of anthropogenic Pb deposition in northeastern North America is poorly characterized.

Few paleolimnological studies have been attempted at the scale required to adequately characterize the distribution and transport of Pb in northeastern North America. Traditional analytical methods can be time- and/or cost-prohibitive (Croudace et al. 2006), and traditional techniques for assembling, plotting, and applying statistical techniques to time-stratigraphic data are poorly equipped for use with many lake sediment archives (Dunnington and Spooner 2018). Furthermore, separating the effects of multiple contributions (e.g., land-use change and/or atmospheric deposition) of an element to the geochemical record is difficult, and, in some cases, poorly understood (Boyle 2001). The ability to assemble evidence from many high-resolution records offers investigators the opportunity to add robustness to paleolimnological investigations of regional contaminant transport in addition to planning of water and wastewater treatment infrastructure, recent literature for which highlights the need for a long-term perspective on source and/or receiving water quality (Anderson et al. 2017; Delpla et al. 2009).

Using newly developed, high-throughput paleolimnological methods, this thesis will evaluate the spatial distribution of anthropogenic Pb deposition and inform the nature of west-east Pb transport in northeastern North America. In particular, this thesis will answer two questions. First, was Pb transported to Nova Scotia from U.S. sources? Second, is Nova Scotia the

"tailpipe of North America"? To do so, Chapter 2 will review previous studies of trace metal deposition to build the case for lake sediment records of Pb as indicators of atmospheric transport, Chapter 3 will establish portable X-Ray fluorescence (pXRF) as a reliable quantitative method with which to analyze Pb concentrations and important land-use change indicators that may affect Pb concentrations in lake sediments, Chapter 4 will introduce a new software package that can be used to visualize and analyze data from many lake sediment archives, Chapter 5 will test the application of land-use change indicators that may affect Pb concentrations observed in lake sediment records, Chapter 6 will evaluate methods with which Pb from multiple sources might be separated using land-use change indicators, and Chapter 7 will apply these techniques to 47 dated lake sediment cores along a west-east transect from the Adirondack Mountains, New York to Nova Scotia, Canada to inform west-east transport of Pb in northeastern North America. Finally, Chapter 8 will discuss the implications of west-east Pb transport, possible applications of high-throughput paleolimnological techniques, and directions for future research.

Chapter 2

A Global Review of the Timing, Distribution, and Transport of Trace Metals in Freshwater Sediments

This chapter has not been submitted for publication.

2.1 Abstract

A large number of studies have reported trace metal concentrations from lake sediment samples around the world. This review focuses on the observed concentrations, accumulation patterns, and geographic distribution and temporal distribution of As, Cd, Cr, Cu, Hg, Ni, Pb, and Zn, as established by concentrations in lake sediments, peat cores, and ice cores. Unsurprisingly, lakes exposed to a proximal point source of trace metal input report high concentrations of the trace metal(s) associated with the pollution source; however, trace metal input generally occurs long after direct input from the point source. There is considerable evidence for transport of Pb, Hg, Cd, and Zn to remote locations (e.g., high arctic), although concentrations of these elements tend to be higher near populated areas. There is less evidence for transport of As, Cr, Cu, and Ni to remote locations; however, increases in concentration near populated areas are common. Despite the ubiquitous nature of elevated concentrations, the timing and magnitude of trace metal deposition can vary within small distances. Watershed-scale processes such as erosion and land-use change are often cited as reasons for this variability, although few studies characterize these processes precisely.

2.2 Introduction

Considerable study has been devoted to the occurrence of trace metals in freshwater and freshwater sediments (Norton et al. 1990; Norton et al. 1992; Blais and Kalff 1993; Blais et al. 1995; Dunnington et al. 2017). These studies have established that through atmospheric deposition and watershed disturbance, both natural and anthropogenic activity can affect the spatial

and temporal distribution of trace metals in both water and sediment (Dunnington et al. 2017; Thienpont et al. 2016). While several reviews have focused on specific facets of trace metals in lakes (Grégoire and Poulain 2018; Norton et al. 1990; Blais et al. 1995), a global aggregation of regional patterns in trace metal deposition to identify literature gaps has hitherto not been attempted.

In this review we use several conventions: Peak Hg concentrations, where reported as concentrations from lake sediment, are conveyed in parts per billion (ppb). Other trace metal concentrations from lake sediments are reported in parts per million (ppm). We also note where peak values are concentrations or accumulation rates. While accumulation rates are sometimes preferable to concentrations (Norton 2007), they are not often calculated, and it is beyond the scope of this study to obtain the required data to recalculate them. Therefore, we report values as concentrations where possible. Non-lake sediment archives of environmental change through time such as ice cores and peat cores provide useful information about the atmospheric transport and deposition of trace metals; references to these studies are provided where they add context to studies of freshwater sediments. In general, we highlight the maximum and minimum concentrations that occur by region, and common temporal patterns of increase and decrease in concentration.

2.3 Point Source Trace Metal Inputs

It comes as no surprise that high concentrations of trace metals in lake sediments can be found in close proximity to industrial point sources, particularly when these sources discharge directly to a water body. Horowitz et al. (1995) observed over 20,000 ppm of Pb, 10,000 ppm of Zn, 600 ppm of Cu, 80 ppm of Cd, 600 ppm of As, and 10,000 ppb of Hg at a large lake in Idaho, USA, where tailings for many mines were allowed to mobilize within the catchment for almost 100 years before tailings ponds were constructed; Gallagher et al. (2004) observed Hg concentrations of up to 150 ppb in a lake whose watershed contained Hg mining operations in northern British Columbia. High concentrations of Cr (>4,000 ppm) in aquatic sediments have been observed near the outflow of a leatherworking facility in eastern Massachusetts (Hubeny et al. 2018). High Cr (>50,000 ppm), As (>1,000 ppm), Cd (>200 ppm), and Hg (>29,000 ppb) concentrations were also observed at a superfund site in the same area as a result of point source pollution from military operations (Norton et al. 2004). Pulp mill effluent is also a direct input

to some freshwater systems: Hoffman et al. (2017) observed concentrations of Zn >1,200 ppm in an effluent pond in Nova Scotia, Canada.

Some trace metals also appear in increased concentrations in lake and bog sediments when industrial point sources are outside the watershed, suggesting atmospheric transport as an important mechanism for transporting many trace metals. In particular, smelting operations appear often in the literature. Crecelius and Piper (1973) were some of the first to document this effect in North American lake sediments, finding increased Pb concentrations (up to 400 ppm) in response to vehicle emissions and a Pb smelter in Seattle, Washington. Similar concentrations of Pb in a peat deposit were reported near a Pb smelter in the Czech Republic accompanied by elevated concentrations of Hg (Ettler et al. 2008). Concentrations of Ni (>1,000 ppm) and Cu (>2,000 ppm) in two lakes near Sudbury, Ontario were measured by Carignan and Nriagu (1985) and Nriagu et al. (1982). At another industrial site approximately 20 km from a smelter in Flin Flon, Manitoba also indicated an increase in Pb (peak: 550 ppm) and Hg (peak: 3,000 ppb) following the start of smelting operations, accompanied by Cd (peak: 25 ppm), Cu (peak: 800 ppm), and Zn (peak: 3,500 ppm) (Percival and Outridge 2013). In an extreme example, As concentrations of over 30,000 ppm were observed at a lake near Yellowknife, Northwest Territories, although the effect of As deposition was limited to approximately 15 km of processing operations (Thienpont et al. 2016). While Pb and Hg concentrations were also measured by Thienpont et al. (2016), concentrations were not higher than those observed by Ettler et al. (2008) or Percival and Outridge (2013).

While there is compelling evidence that oil upgrading operations near Fort McMurray, Alberta have transported contaminants to nearby lakes and ponds (Kurek et al. 2013), there is a less clear trend with respect to atmospheric transport of trace metals in the region as recorded by bog sediments (Shotyk et al. 2014; Shotyk et al. 2016; Shotyk et al. 2017). Still, Pb, V, Ni, Mo, and Ba were observed at higher concentrations within 20 km of bitumen upgraders, which is a reflection of increased dust input to these systems from upgraders or the open pit mines themselves (Shotyk et al. 2014). Indeed, little to no atmospheric or river-transported trace metal effect of mining operations near Fort McMurray were observed ~200 km north in the Peace-Athabasca Delta, Alberta (Wiklund et al. 2012; Wiklund et al. 2014).

In all cases, the initiation of industrial operations were identifiable in concentrations and accumulation rates of trace metals, although increases due to long-range transport were also identifiable in some cases (Crecelius and Piper 1973; Percival and Outridge 2013; Thienpont et al. 2016), and post-depositional mobility of As and Cu may mean that the timing of Ni, As, Cu concentration changes may not accurately reflect temporal changes in As and Cu supply (Percival and Outridge 2013; Carignan and Nriagu 1985). This is particularly the case with assessing the timing of cessation of industrial inputs, as physical and chemical remobilization processes can result in high concentrations in sediments deposited long after industrial inputs have ceased (Sprague and Vermaire 2018). It is likely that metals in cases of severe contamination are bound to the particulate phase with little physical redistribution (Norton et al. 2004), although chemical remobilization of some metals such as As is common, leading to high concentrations being observed in lake sediments long after the cessation of point source input (Sprague and Vermaire 2018).

2.4 Deposition of Trace Metals in Remote Regions

The case for long-range transport of Pb and Hg is readily made through analysis of remote peat and ice core records (Fitzgerald et al. 1998; Marx et al. 2016). Pb in particular has received much attention in this regard; a number of records are well-summarized by Marx et al. (2016), who reported widespread anthropogenic Pb deposition starting at 1850-1890 AD despite widespread regional differences in Pb deposition (Osterberg et al. 2008; Marx et al. 2016). The timing of long-range anthropogenic Pb deposition is related to the date at which leaded gasoline was used and phased out in various parts of the world: Asian use of leaded gasoline continued until the late 1990s, which resulted in peak Pb concentrations in a Yukon, Canada ice core at 1998 (Osterberg et al. 2008), and peak Pb concentrations in an ice core from the Tibetan plateau at 1997 (Lee et al. 2011). This is in contrast with other northern hemisphere ice core records that record peak Pb concentrations ca. 1950-1980 (McConnell et al. 2002; More et al. 2017; Shotyk et al. 2003). Ice core records from Antarctica also indicate an increase in deposition at the end of the 19th century, with variable dates of peak deposition (Planchon et al. 2003; Vallelonga et al. 2002). Other remote southern hemisphere Pb records share this trend (Marx et al. 2010; Stromsoe et al. 2013).

Atmospheric deposition of Hg in remote locations has received less attention, although there

has long been a compelling case for long-range transport based on ocean, lake, and peat records (Fitzgerald et al. 1998). Recently, 8 lake sediment records from the high Canadian arctic have demonstrated that Hg concentrations from long-range transport increase starting ca. 1850, generating concentrations of up to 150 ppb, although peak concentrations for most lakes were less than 50 ppb (Korosi et al. 2018).

In northern Quebec, Canada, peak Hg concentrations were also between 50 and 150 ppb, with lakes further south having higher peak concentrations (Lucotte et al. 1995). Records reported in Korosi et al. (2018) and Lucotte et al. (1995) did not show a consistent decline in concentration following any specific date; in most records peak concentrations were observed at the top of the core. Lucotte et al. (1995) also measured Pb at 8 lakes in Quebec, the most remote of which had peak Pb concentrations around 50 ppm (n=4).

2.5 Pre-Industrial Trace Metal Mobilization

Prior to industrial deposition of Pb and Hg starting in the 1800s, a number of natural archives have been able to record early mining and smelting activities. In Europe, presumed Roman mining activity has been recorded by increased Pb concentrations in lake sediments in the French Alps at 100 BC-400 AD (Mariet et al. 2018), in the French Alps at 115-330 AD (Guyard et al. 2007), in the Pyrenees at 680 AD (Camarero et al. 1998), in the Pyrenees at 500 BC-500 AD (Hansson et al. 2017), at 16 lakes in southern Sweden at the BC/AD boundary (Renberg et al. 1994), an ice core in the high Canadian arctic (Zheng et al. 2007), and from 500 BC to 300 AD in an ice core from Greenland (Hong et al. 1994). Pre-industrial Pb concentrations in lake sediments ranged from ~50 ppm in the French Alps (Mariet et al. 2018), to 100-400 ppm in Sweden (Renberg et al. 1994), where a factor of 5 increase was reported at the BC/AD boundary.

A period of increased Pb production or transport during the Middle Ages (~1500 AD) was also reported in the French Alps, the high Canadian arctic, and Greenland (Zheng et al. 2007; Mariet et al. 2018; Hong et al. 1994), and minimum Pb deposition in Europe was likely during the black death (1349-1343 AD) as resolved by a high-resolution ice core from the Swiss Alps (More et al. 2017). European smelting operations as early as 1100 BC were likely resolved using Pb isotopes in a high Canadian arctic ice core, although concentrations did not increase to the extent that later smelting operations caused in the core (Zheng et al. 2007).

Pre-industrial records of other trace metals in Europe are less common; however, Mariet et al. (2018) reported concentrations for Zn, Cd, Cu, and As for a 2,000 year lake sediment record from the French Alps, and Hansson et al. (2017) report Sb and Cu concentrations for a 3,000 year lake sediment record from the Pyrenees. While Hansson et al. (2017) note that pre-industrial inputs for Sb and Cu were possibly greater than industrial inputs, this is likely due to mining activities within the catchment, not atmospherically transported pre-industrial inputs.

Outside of Europe, elevated pre-industrial trace metal concentrations were resolved in lake sediments of three Peruvian lakes with watershed mining histories as early as 400 AD (Cooke et al. 2008). There is some indication that Pb, Sb, Cu, and Sn were transported in the pre-industrial atmosphere as recorded by a peat bog in southern Chile (De Vleeschouwer et al. 2014), however pre-industrial increases in metal concentrations were small. In the Tibetan Plateau region, China, atmospheric deposition of Cu to lake sediments from Cu-based metallurgy was inferred as early as 1,500 BC, and Ag metallurgy resulted in peak concentrations of Pb (119 ppm), Ag (3.8 ppm), Cd (0.4 ppm), and Zn (65 ppm) ca. 1,300 AD (Hillman et al. 2015). Hillman et al. (2015) infer atmospheric transport of these trace metals, however given that peak values are ~4 times higher than during industrial-era pollution, there may be a watershed component to delivery of these trace metals to the sediment. Other lakes in the Tibetan plateau region recorded increases in Pb and Hg starting at 500 AD (Hillman et al. 2014), in contrast with lake sediments from central China that document increases in Pb as early as 467 BC, with increases in Cu, Ni, and Zn starting at the BC/AD boundary (Lee et al. 2008).

There are only a few pre-industrial lake sediment records of trace metals in North America. Pompeani et al. (2013) noted near synchronous increases in Pb concentrations at three lakes in northern Michigan ca. 4,000-5,000 BC, although concentrations prior to recent industrial deposition were never greater than 4 ppm. At the New Brunswick-Nova Scotia border region, Dunnington et al. (2017) reported synchronous peaks of Pb (6 ppm), Hg (750 ppb), Cr (100 ppm), and Y (60 ppm) at 3,100 BC, inferred to be a result of a fire event. White (2012) measured Pb at two other lakes in the same region, and found no indication of pre-industrial Pb between 1,000 BC and present.

2.6 Short- and Medium-Range Transport of Trace Metals

Dominating the recent (~1850 AD to present) accumulation history of many trace metals in lake sediments is that of short- and medium-range (<1,000 km). While there are some specific cases where concentrations of trace metals in lake sediments prior to the industrial revolution are higher than those observed from 1850 AD to present, generally this time period represents the highest deposition of trace metals to freshwater systems. The date of 1850 AD applies most broadly to Europe and North America. Increased trace metal deposition is observed more recently in developing countries (Yao et al. 2013; Panizzo et al. 2013). This review focuses on Europe and North America, as the number if studies from locations in these areas is sufficient to make generalizations about the behaviour of trace metals as recorded by lake sediments.

2.6.1 Europe

The earliest studies of trace metal deposition in lake sediments are from the Scandinavian peninsula, where the assessment of acid deposition prompted a number of paleolimnological studies. In Sweden, Norton and Hess (1980) and Davis et al. (1983) measured Zn and Pb concentrations in dated cores from two lakes, noting a synchronous increase in both lakes ca. 1920, a finding which was echoed by a later study of Pb and Zn for two lakes in the same area of Sweden (Bragée et al. 2013). In both studies, peak Pb concentrations were ~200 ppm, and peak Zn concentrations were between 150 and 300 ppm. In Finland, Verta et al. (1989) measured Pb, Zn, Hg, Cd at 18 lakes along a north-south gradient, finding higher Pb, Zn, Hg, and Cd accumulation rates in the southern lakes; the most prominent increase for these accumulation rates occurred after 1900, although concentrations were above background rates by 1800. Verta et al. (1989) reported that concentrations for Cu, Ni, and V were more variable, and tended to increase later in the records (~1950).

In the Pyrenees, recent Pb, Sb, and Cu increases have been observed starting starting ca. ~1950 (Hansson et al. 2017), although there was likely some contribution from remobilized peat impacted by early metallurgical activities in addition to atmospheric deposition. For other records in the Pyrenees, increases in concentrations occurred as early as the mid-1800s, where peak Pb concentrations of 350 ppm were reported (Camarero et al. 1998), and Pb and Hg from atmospheric deposition were observed in peat (Martínez-Cortizas et al. 2012).

In the UK, trace metals have been assessed in lake, pond, and reservoir sediments starting as early as the mid-1960s, when Mackereth (1966) reported post-glacial-present concentrations of Ni, Cu, Co, and Zn at three lakes in the English Lakes district. Mackereth (1966) did not look for or find post-industrial increases in these elements, but later, Hamilton-Taylor (1979) measured Pb concentrations at one of these lakes (Windemere) with a focus on recent sediments. Hamilton-Taylor (1979) noted peak Pb concentrations of 500 ppm that occurred as early as 1900, with first increases occurring in the early 1800s for Pb, Cu (peak: 100 ppm), and Zn (peak: 1,250 ppm). In a study of a lake more proximal to nearby industrial sources, Lang et al. (2018) observed Pb concentrations as high as 600 ppm, with peak concentrations in the mid-1800s. Zn was observed to increase later, with peak concentrations (2,000 ppm) ca. 1950 (Lang et al. 2018). Finally, a study of trace metal accumulation from 5 reservoirs in the north of England did not note major increases or decreases in concentration of most trace metals over time except for Pb and Zn, which increased during the entire period following reservoir creation (Shotbolt et al. 2006). Shotbolt et al. (2006) reported surficial concentrations of Ni (~50 ppm), Cu (30-50 ppm), Zn (100-300 ppm), and Pb (100-300 ppm). Temporal trends in Pb concentrations are similar to those reported by peat core studies, which report peak high Pb deposition from the late 1800s until at least 1950 (Weiss et al. 2002; Kylander et al. 2009; Cloy et al. 2008). Finally, Yang and Rose (2003) measured As at 6 UK lakes and reservoirs, concluding that post-depositional mobility obscured temporal trends, but that anthropogenic input resulted in surficial concentrations between 25 and 800 ppm; most of the As inventory for all lakes was contained in the top 10 cm of sediment.

2.6.2 West, South, and Central North America

It is impossible to discuss short- and medium-range transport of trace metals in North America without the noting the contributions of Stephen Norton, who reviewed this topic in 1990 (Norton et al. 1990), and published a synthesis of trace metals in 30 cores from the four Paleoecological Investigation of Recent Lake Acidification (PIRLA) regions (New England, Adirondacks, northern Great Lakes states, and Florida) (Norton et al. 1992). Some of these data were further synthesized by Blais et al. (1995), who used Pb concentrations from a number of studies to evaluate ^{210}Pb dating techniques. More recently, trace metal concentrations from a number of reservoirs have been collected and synthesized by Mahler et al. (2006), the data and methods for which have been published separately (Van Metre et al. 2006; Van Metre et al. 2004). We

include these studies as they apply regionally to other studies that have since been published.

On the west coast of North America, Crecelius and Piper (1973) measured Pb concentrations in Seattle, Washington, measuring concentrations up to 400 ppm as a result of a Pb smelter (ca. 1890) and automotive emissions (ca. 1920). A subsequent lake sediment core reported similar peak concentrations of Pb and declining concentrations of Cd (peak: 2 ppm), Cr (peak: 90 ppm), Cu (peak: 90 ppm), Hg (peak: 600 ppb), Ni (peak: 80 ppm), Pb (peak: 300 ppm), and Zn (peak: 300 ppm) since 1970 (Mahler et al. 2006). At a more urban lake near Seattle, Mahler et al. (2006) observed steady or increasing concentrations of these elements, except Ni and Pb, both of which had peak concentrations shortly after 1970; concentrations in the urban setting were generally higher by a factor of 2, except for Cd. Just to the north in the Fraser River watershed, Gallagher et al. (2004) noted far lower concentrations of Pb (30 ppm) at a lake 150 km east of Vancouver, Canada, where notable increases in Cr (peak: 120 ppm), Ni (peak: 60 ppm), and Pb occurred ca. 1960. Other lakes in the Fraser River watershed show little trace metal variability except one lake with catchment mining influence (Gallagher et al. 2004). North of Vancouver in Whistler, British Columbia, Dunnington et al. (2016) noted increases in Cu and Zn synchronous ca. 1960, although Pb was below the detection limit in all but two samples.

In the southern United States, there are several reservoir records of trace metal accumulation are available. Rosen and Van Metre (2010) describe Hg, Pb, As, Ni, Cu, Cr, and Zn concentrations near Las Vegas, Nevada, with enrichment of Pb, As, Ni, Cu, and Cr observed in one core as a result of industrial activity, with low concentrations (As: 30 ppm; Pb: 30 ppm) and little trend observed in other cores except for Hg, the concentration of which peaked in 1965. In southern California, concentrations for As, Cd, Cr, Cu, Pb, Hg, Ni and Zn are available in Van Metre et al. (2006), where few trends were observed between 1935 and 2000, except for decreasing Cu observed in all three records after 1960.

Van Metre et al. (2006) also report these data for six reservoirs in Texas, including four reservoirs with reported ages between 1950 and 2000, and two reservoirs with reported ages from 1910 to 2000. In five records, peak Pb concentrations were observed between 1970 and 1980, at which time peaks of Cd, Pb, and Hg were also observed in one reservoir near Dallas. At three other reservoirs near Dallas, trends in Cr, Cd, and Zn were also observed, with concentrations decreasing since 1960 or earlier. Pb (10-400 ppm), Hg (20-500 ppb), and Zn (50-500 ppm)

concentrations were highly dynamic within and between records, whereas As (10-30 ppm), Ni (20-40 ppm), Cd (<2 ppm), Cr (50-70 ppm), and Cu (10-50 ppm) varied less. Several outlying values of Pb (1200 ppm), Cd (182 ppm), As (220 ppm), and Cr (240 ppm) were also observed (Van Metre et al. 2006), likely due to local (watershed transport) effects.

In Georgia, no natural lake trace metal records were available, but four reservoir trace metal records in the Atlanta region have been published by Van Metre et al. (2006) and Callender and Van Metre (1997). At one reservoir, decreasing concentrations of Zn (from 500 ppm) and Cr (from 110 ppm) were observed from 1988-present, and a peak of Cr (~100 ppm) was observed at another reservoir ca. 1971 (Van Metre et al. 2006). Peak Pb concentrations for all four reservoirs occurred between 1970 and 1980, with one reservoir reporting peak Pb concentrations as late as 1988 (Van Metre et al. 2006; Callender and Van Metre 1997). Concentration ranges for other trace metals were similar to ranges reported in Texas reservoirs. In Florida, at least six natural lake records are available as a result of the PIRLA project (Sweets et al. 1990; Blais et al. 1995), which include Pb accumulation rates for 5 lakes, and Zn accumulation rates for 2 lakes. Visually, Pb increases at 5 lakes occur at 1920-1940 (Sweets et al. 1990), although a more thorough analysis revealed that Pb concentrations were above background levels on average around 1920 (Blais et al. 1995). Peak concentrations of 100-300 ppm were reported (Sweets et al. 1990). In addition, Van Metre et al. (2006) measured trace metals at one lake in central Florida, reporting decreasing Pb (peak: 550 ppm), Cu (peak: 450 ppm) and Cr (peak: 120 ppm) since 1970.

The same group of studies also evaluated trace metal concentrations in the Midwest, including lakes and reservoirs in Iowa, Illinois, Minnesota, Michigan, and Wisconsin. At a reservoir in Iowa, Callender and Van Metre (1997) reported low peak Pb accumulation rates compared to other reservoirs in the northeast, with peak accumulation rates occurring between 1980 and 1990. Mahler et al. (2006) found decreasing concentrations of Cd (peak: ~0.8 ppm), Cr (peak: ~90 ppm), Ni (peak: ~50 ppm), and Pb (peak: ~70 ppm) at two lakes in the Chicago area since 1970, in contrast with two lakes in St. Paul, Minnesota, where peak Pb concentrations of 200-400 ppm were observed between 1975 and 1980 (concentrations were similar for other metals) (Van Metre et al. 2006). At the PIRLA lakes in northern Wisconsin and Michigan, anthropogenic Pb deposition was above background as early as 1850, with lakes in Minnesota

reporting increases slightly later (Kingston et al. 1990); on average, the region's Pb concentrations were 1.5 times above background ca. 1884 (Blais et al. 1995). Zn, Cu, and V concentrations in the northern great lake states PIRLA lakes did not show the same degree of enrichment as Pb, except for Zn at two lakes in northern Wisconsin, and general Cu enrichment at the sediment-water interface (Kingston et al. 1990).

2.6.3 Northeast United States

By far, the greatest number of trace metal studies using lake sediment is in the northeast of North America, including Pennsylvania, New York, Ontario, Quebec, and the New England states. This is likely the result of general concern over atmospheric deposition following increased awareness of acid rain, and the fact that lakes are plentiful in this region. Several reviews for specific metals in lake sediments have been written for subsets of this region, including a review of Hg in New York and New England by Perry et al. (2005), a summary of stable Pb rise dates included in Blais et al. (1995), two regional PIRLA syntheses (Davis et al. 1994; Charles et al. 1990; Norton et al. 1992), and several United States Geological Survey (USGS) reservoir studies (Mahler et al. 2006; Van Metre et al. 2006). We include original data and general conclusions from these reviews as they apply to each region discussed.

At the southern boundary of the region, Yuan (2017) measured metals in southwest Lake Erie, finding correlated concentrations of As (peak: 8 ppm), Zn (peak: 200 ppm), Cu (peak: 60 ppm), Ni (peak: 60 ppm), Cr (peak: 60 ppm), Cd (peak: 2 ppm), and Pb (peak: 60 ppm), the concentrations of which peak or reach their modern values ca. 1970. Callender and Van Metre (1997) report Pb concentrations and accumulation rates since 1960 from a reservoir west of Washington, District of Columbia, where concentrations reached 160 ppm ca. 1980. Zn concentrations were generally correlated with Pb concentrations, whereas there was little trend in As, Cr, Cu, Hg, and Ni (Van Metre et al. 2006). One record in Pennsylvania exists, but is dominated by local industrial sources (Rossi et al. 2017).

Some of the earliest studies of trace metals in lakes were conducted in the Adirondacks, New York (Galloway and Likens 1979; Heit et al. 1981), although the first reliably dated trace metal records from this region appear in the literature as part of the regional synthesis of the PIRLA studies (Charles et al. 1990). While the precise date is unclear, Galloway and Likens (1979) noted several peaks (Ag: 0.5 ppm, Cd: 6 ppm, Cr: 30 ppm, Cu: 36 ppm, Pb: 200 ppm, V: 5

ppm, and Zn: 400 ppm) at 5 cm depth from a core collected in 1974, with other metals (Au: 4 ppb, and Sb: 3 ppm) increasing until the sediment-water interface. Heit et al. (1981) measured trace metals at two lakes with differing humic water content, also finding peak concentrations of Cd (~2.5 ppm), Cu (~10 ppm), Hg (~600 ppb), Pb (50-140 ppm), V (~120 ppm), and Zn (150-350 ppm) between 0 and 5 cm, with the largest differences between lakes occurring in Zn, Pb, and Cd. Charles et al. (1990) and Lorey and Driscoll (1999) also noted near-subsurface peaks of Pb, V, and Hg at 8 lakes, which were assigned dates between 1960 and 1980 according to ^{210}Pb chronology. Blais et al. (1995) calculated the average date of the stable Pb rise was approximately 1875 with some variability, but was generally the earliest of the PIRLA regions (Norton et al. 1992). This was consistent with the rises observed in Hg concentrations in the same cores (Lorey and Driscoll 1999).

In southern New England, there is both common ground and intense local variability in sedimentary trace metal occurrence (Norton et al. 1990). At an urban lake in Massachusetts, Chalmers et al. (2007) synthesized data from Van Metre et al. (2006), reporting decreasing Cd (from 13 ppm), Cu (from 600 ppm), Pb (from 1,400 ppm), and Zn (from 3,000 ppm) since 1965. In a nearby reservoir in a light urban setting, Mahler et al. (2006) reported decreasing Pb, Cu, and Hg since 1970, but contrary to Chalmers et al. (2007), found no trend in Zn and increasing Cd; concentrations were much lower than at the urban lake (Pb from 100 ppm, Cu from 200 ppm, Zn at ~200 ppm, and Cd to 1 ppm). An independent multi-element investigation of four lakes in Connecticut reported similar peak concentrations to the light urban lake in Massachusetts (Mahler et al. 2006), but with variable patterns of increase and decrease at each lake (Rogalski 2015). A cross-section of Pb at seven lakes in Connecticut by Siver and Wizniak (2001) revealed that Pb concentrations generally stopped increasing at ca. 1970, but did not necessarily decrease in the decades following.

Vermont and New Hampshire have numerous lakes, that have been cored and assessed for trace metal content since at least 1982, when Hanson et al. (1982) published five short cores of Pb, Zn, and major element concentrations. Three of these records that were dated using ^{210}Pb suggested that Pb and Zn increase ca. 1870 at two of the three lakes, with Zn concentrations of the third apparently controlled by organic content of the core (Hanson et al. 1982). At five different lakes in Vermont and New Hampshire, Kamman and Engstrom (2002) noted a similar initial increase for Hg, but also noted decreases in concentration and accumulation in “recent years”, with concentrations ranging from 150 to 300 ppb. PIRLA cores in Vermont and New

Hampshire suggested that the initial Pb increase was as early as 1800 in this area (Davis et al. 1994). In these cores, Zn concentrations correlated well with Pb in some ponds but not in others, and Cu concentrations generally increased following 1900 but not to the extent that was observed for Zn and Pb (Davis et al. 1994).

To the east, the initial Pb and Hg increases occurred later than in the Adirondacks or New England, exemplified by a paired lake sediment/peat record from coastal Maine, which also showed synchronous Pb, Cd, and Hg accumulation rate peaks at 1970 (Norton et al. 1997; Norton et al. 2007). Norton et al. (2007) found similar Cd accumulation rates at another lake in Maine, but at a third, concentrations were increasing over the entire core. Another record in Maine suggested that Pb concentrations were increasing until at least 1980, whereas Zn concentrations slightly earlier, at 1960. Finally, Perry et al. (2005) collected records of Hg deposition in New York and New England, including a few that were not previously published, finding that total atmospheric contribution of Hg ranged widely among lakes in New England, even within small geographic areas, and most commonly increased through the entirity of each record.

2.6.4 Eastern Canada

The history of measuring trace metals in lake sediment in eastern Canada stretches as far back as in the northeast United States, starting with the work of Evans and Dillon (1982), who found Pb accumulation rates increasing at ~1850 in a southern Ontario lake. At a cluster of six lakes to the west near Sault Ste. Marie, Johnson et al. (1986) found the initial metal accumulation rate increase was at 1875-1900 for Zn (peaks: 200-300 ppm), Pb (peaks: 100-200 ppm), Hg (peaks: 500-1000 ppb), and Cd (peaks: 2-4 ppm); concentrations of Cu (40-80 ppm), Ni (20-40 ppm), and Cr (25-75 ppm) were constant or decreasing for most records in the study. A more extensive study of 15 lakes located across the province showed extensive evidence of post-1900 enrichment of Pb, Zn, and Cd, except in the northwest of the province where increases in Zn, Cd, and As were not observed (Johnson 1987); concentrations were similar to those observed by Johnson et al. (1986) except for several outlying Hg values and peak As values that were between 8 and 16 ppm. Southern Ontario measurements of trace metals suggest that Pb (peak: 80-200 ppm), Zn (peak: 150-250 ppm), Cu (peak: 30-50 ppm), and Cd (peak: 3-4 ppm) concentrations were increasing until at least 1984 at nine lakes in Algonquin Park,

with patterns of Zn, Cd, and Cu accumulation variable between lakes (Wong et al. 1984). A recent study of a central Ontario lake suggested decreasing deposition of Pb, Cu, and Cd since 1978, with initial increases in concentration occurring ca. 1900 for Cd, Co, Ni, Pb, As, and Cu (Watmough 2017). A number of undated records of Pb, Zn, Cd, and Hg are also available (Evans 1986; Evans et al. 1983; Dillon and Evans 1982; Blais and Kalff 1993).

Several trace metal records are available for lakes in Quebec, the most northerly of which show little variability in Pb concentrations, although Hg concentrations are increasing in most cores even as far north as 55 degrees (Lucotte et al. 1995; Ouellet and Jones 1983). In southern Quebec, Pb and Hg concentrations of up to 500 ppm and 500 ppb (respectively) were observed by Lucotte et al. (1995), although east of Montreal peak concentrations of only 125 ppm (Pb) and 200 ppb (Hg) were observed by Gélinas et al. (2000), who also measured V, Cr, Li, Ni, Co, Ga, Cu, Zn, Ag, Sn, Cd, Sb, Th, and U, although age constraint of these sediments was not precise. Near Quebec City, Ouellet and Jones (1983) report Co, Cu, Hg, Ni, Pb, and Zn concentrations at two lakes, with increases in Pb (to 100 ppm) and Zn (to 160 ppm) observed ca. 1940 in both lakes, but in Cu (to 25 ppm) and Hg (to 160 ppb) at only one lake. As concentrations of up to 12 ppm (Couture et al. 2008) and Pb concentrations of 160 ppm (Gallon et al. 2004) were observed at headwater lakes north of the city. Pb concentrations were found to increase at or before 1920, with some contribution from U.S. smelting operations in the mid-1800s (Gobeil et al. 2013; Pratte et al. 2013).

In Atlantic Canada, there is a paucity of dated lake sediment records of trace metal accumulation. Dunnington et al. (2017) and White (2012) report trace metal concentrations at low resolution at three lakes near the New Brunswick/Nova Scotia border region from 8000 BC to 1800 AD, and Sunderland et al. (2008) report Hg concentrations for a lake near the New Brunswick-Maine border, finding peak concentrations of 400 ppb and increases in the late 1800s. All other records of trace metal accumulation in Atlantic Canada are either in peat bogs (Weiss et al. 2002; Kylander et al. 2009), in salt marsh environments (Sunderland et al. 2008), or undated (Dunnington 2011; Nau 2018; McGuire 2018; Holmes 2018; Davidson 2018; Terry 2011; Tymstra 2013; Christopher 1999).

2.7 Conclusion

From this review of trace metal records, it is clear that trace metal accumulation in lake sediments occurs at both regional and local scales. There is considerable evidence that metals such as Pb and Hg can be transported long distances (Fitzgerald et al. 1998; Marx et al. 2016), and possibly to a lesser extent Cd and Zn (Norton et al. 2007; Charles et al. 1990; Norton et al. 1992). While atmospheric deposition at a short- and medium-range is likely a source of As, Cu, and Ni at many sites (Mahler et al. 2006), they often increase at different times than Pb, Hg, and Zn, suggesting a different source or post-depositional mobility (Percival and Outridge 2013; Yang and Rose 2003). Measurements for other metals are more rare, and it is difficult to make generalizations about their origin and transport at a global scale.

Even though the evidence for long-range transport of Pb and Hg is incontrovertible, the accumulation pattern in remote archives is highly variable (Fitzgerald et al. 1998; Marx et al. 2016). For example, most records of Pb, Hg, Cd, and Zn that span the period of 1800-present show a pattern of increasing accumulation rate or concentration starting in the mid-1800s, however the timing of this increase can be as late as the 1940s in some locations (Blais et al. 1995; Perry et al. 2005). Decreases in metal accumulation rates or concentrations following a presumed decrease in atmospheric deposition (e.g., phase-out of Pb in gasoline) can be found in the literature, but are not ubiquitous (Mahler et al. 2006; Perry et al. 2005; Siver and Wizniak 2001). Even whole-lake or focus-corrected burdens of metals can vary considerably in a small area (Blais and Kalff 1993; Dillon and Evans 1982; Perry et al. 2005; Norton et al. 1992). The primary reason for these discrepancies as cited in the literature is watershed-scale effects, including changes in the catchment export rate of a metal due to land use change (Kamman and Engstrom 2002; Lorey and Driscoll 1999), post-depositional sediment redistribution (Dillon and Evans 1982; Blais and Kalff 1993), input of organic matter to the sediment record (Heit et al. 1981; Hanson et al. 1982), or the introduction of a point source near or within the watershed (Norton et al. 2004; Gallagher et al. 2004).

While dated records of trace metals in the industrial era have been measured in many locations around the globe, there are several notable gaps in the literature. First, there are few dated records in Atlantic Canada. As the "tailpipe of North America" (Nova Scotia Environment 2017), there is an opportunity to test models of deposition for the northeast United States proposed by authors such as Perry et al. (2005), Mahler et al. (2006), and Norton et al. (1990).

Second, the majority of records in northeast North America were collected in the 1980s and 1990s, when it would be difficult to observe decreases as a result of the Clean Air Act and/or the phasing out of leaded gasoline (both in the 1970s). Mahler et al. (2006) and Chalmers et al. (2007) partially examine this using reservoir sediment records; however, this has not been done at a regional scale using natural lake records. Third, studies that have assessed the timing of "the first increase" above "background" of trace metals such as Pb, Hg, Cd, and Zn all use a different method to define "background" and "the first increase". Furthermore, none of these studies consider age error due to ^{210}Pb nor accumulation rate error, which in the mid-1800s can be considerable. Given the density of ^{210}Pb-dated cores in the northeast United States, there is considerable opportunity for a quantitative reconstruction of deposition and west-east transport in the region.

Chapter 3

Evaluating the Utility of Elemental Measurements Obtained from Factory-Calibrated Field-Portable X-Ray Fluorescence Units for Aquatic Sediments

Published in *Environmental Pollution* with co-authors Ian S. Spooner[1], Mark L. Mallory[2], Chris E. White[3], and Graham A. Gagnon[4] (Dunnington et al. 2019).

3.1 Abstract

We assessed factory-calibrated field-portable X-ray fluorescence (pXRF) data quality for use with minimally-prepared aquatic sediments, including the precision of replicate pXRF measurements, accuracy of factory-calibrated pXRF values as compared to total digestion/ICP-OES concentrations, and comparability of calibrated pXRF values to extractable concentrations. Data quality levels for precision, accuracy, and comparability were not equivalent for element/analyzer combinations. All analyses of elements that were assessed for precision and accuracy on a single analyzer were both precise (<10% relative standard deviation) and accurate (r^2>0.85) for K, Ca, Ti, Mn, Fe, and Zn. Calibrated pXRF values for Al, K, Ca, Ti, Mn, Fe, Cu, Zn, and Pb were within ~10% relative difference of total digestion/ICP-OES concentrations. Calibrated pXRF values for Fe, Cu, Zn, As, and Pb were within ~20% relative difference of extractable concentrations. Some elements had a higher level of data quality using specific analyzers, but in general, no pXRF analyzer had the highest level of data quality in all categories. Collectively, our data indicate that a wide range of factory-calibrated pXRF units are capable of providing high-quality total concentrations for the analysis of aquatic sediments.

[1]Department of Earth & Environmental Science, Acadia University, 12 University Ave., Wolfville, Nova Scotia, Canada B4P 2R6

[2]Department of Biology, Acadia University, 33 Westwood Ave., Wolfville, Nova Scotia, Canada B4P 2R6

[3]Nova Scotia Department of Energy and Mines, P.O. Box 698, Halifax, Nova Scotia B3J 2T9

[4]Centre for Water Resources Studies, Department of Civil & Resource Engineering, Dalhousie University, 1360 Barrington St., Halifax, Nova Scotia, Canada B3H 4R2

Portable X-ray Fluorescence is a promising analytical method by which high-throughput paleolimnological studies might be conducted at a reasonable cost.

3.2 Introduction

Chapter 2 established that few Pb concentrations have been reported for Maritime Canadian lakes, and that Maritime Canada (New Brunswick, Nova Scotia, and Prince Edward Island) is an excellent location to evaluate the distribution and transport of Pb, particularly if compared to other records from the northeastern United States. Furthermore, Chapter 2 establishes that a high spatial and temporal resolution is needed to capture the high degree of variability observed in previous studies. Such a study is cost-prohibitive without a high-throughput method for measuring Pb and indicators of watershed-scale disturbance in aquatic sediments.

X-Ray Fluorescence (XRF) spectrometry has long been used to measure elemental geochemistry in sediments (Boyle 2000). Recently, factory-calibrated field-portable XRF (pXRF) units have been used to measure trace metal concentrations in algae (Bull et al. 2017; Turner et al. 2017), archaeological remains (Frahm 2014; Hunt and Speakman 2015), contaminated soils (USEPA 1998; Rouillon and Taylor 2016), compost (Sharp and Brabander 2017; Fitzstevens et al. 2017), wetland sediments (Loder et al. 2016; Loder et al. 2017), and in paleolimnological studies (Dunnington et al. 2016; Dunnington et al. 2017). An increasing number of studies use pXRF technology, but whereas many studies have evaluated pXRF data quality for use with polluted soils with minimal sample preparation (Bernick et al. 1995; USEPA 1998; Kalnicky and Singhvi 2001; Kilbride et al. 2006; Mäkinen 2005; Radu and Diamond 2009; Kenna et al. 2011), few studies examine pXRF data quality with respect to aquatic sediments.

Portable XRF is an analytical tool that offers many advantages to other methods of elemental geochemical analyses of aquatic sediment. Sediment core samples have long been used in environmental pollution studies to reconstruct historical pollution load (Thienpont et al. 2016) and/or provide more targeted sampling for potential pollutants (Hoffman et al. 2017). Several studies have demonstrated the benefits of other types of XRF for use with aquatic sediments, including non-destructive measurement of small samples to facilitate future analyses (Rydberg 2014), and analysis of total concentrations (Boyle 2000). Field-portable units offer the additional benefit of increased availability (units can be rented), rapid analysis time (up to hundreds of samples per day), and low cost (Rouillon and Taylor 2016). Extended sample preparation can

detract from these advantages, in some cases requiring specialized equipment, time investment, or additional cost, rendering the method comparable to more traditional methods. However, these advantages can only be realized if the sample preparation/pXRF method can be relied upon to produce measurements that are precise, accurate and comparable to extractable laboratory measurements upon which many guidelines are based (CCME 1999; Kilbride et al. 2006).

It is well-known that XRF measurements are matrix specific and can differ depending on the sample preparation method (Boyle 2000; Rouillon and Taylor 2016). Given limited previous data on pXRF data quality for aquatic sediments and no previous data on pXRF data quality for sediments with minimal anthropogenic impact, there is clearly need for a systematic assessment of data quality for this matrix type. In this study we investigate the relationship between precision of replicate pXRF measurements, accuracy of calibrated pXRF values as compared to lab-assessed total element concentrations, and comparability of calibrated pXRF values to lab-assessed extractable element concentrations (CCME 1999; Kilbride et al. 2006). We do so using a minimal sample preparation method so as to constrain pXRF data quality for aquatic sediments.

3.3 Materials and Methods

3.3.1 Sediment Sampling & Preparation

Sediment samples were analyzed from 17 cores collected from 13 lakes in Nova Scotia, Canada. Approximately 140 samples from First Chain Lake (Halifax), Pockwock Lake (Halifax), and Lake Major (Halifax) were analyzed on all pXRF instruments included in this study. We chose to use sediments that were not necessarily polluted to make sure an adequate range of concentrations were available with which to evaluate data quality, and to assure there was adequate data quality for sediments with lower concentrations of potential pollutants.

Sediments were sampled using a Glew gravity coring device and extruded at 0.5 or 1.0 cm intervals using a portable extrusion platform (Glew 1989; Glew 1988; Glew et al. 2001). Entire slices were dried at 60°C for 48 h, weighed, ground using a mortar and pestle, and stored in pharmaceutical containers. Containers were covered with 80 gauge (20 micron) plastic wrap, which was secured using the container cap and a rubber band. Using a thin (~6 micron) Mylar

film is typically recommended (Kalnicky and Singhvi 2001; Parsons et al. 2013), however we chose to use inexpensive, readily-available material in this study. This may have affected accuracy for lighter elements with lower emission energy peaks (Kalnicky and Singhvi 2001; Parsons et al. 2013), but because the same film was used for all samples, we suspect it did not impact our ability to correct this using laboratory measurements. Similarly, use of a planetary mill and sieving of samples to remove large grains is recommended to ensure samples are homogeneous, neither of which we did in this study. As such, the data quality reported in this paper should be considered a lower bound to the data quality that is possible using pXRF.

3.3.2 XRF Analysis

Between 165 and 378 samples were analyzed on each pXRF instrument using 3-beam soil mode for the X-5000 and Delta instruments, the 2-beam soil mode for the Vanta instrument, and a 4-beam Omnian profile on the Epsilon 1 instrument (Table 3.1). While not a field-portable analyzer, the Epsilon 1 is a small, bench-top unit that is also factory-calibrated, and was thus included in this study. In each case, the detection and processing parameters were chosen as recommended by the instrument provider, to replicate conditions under which these instruments might be obtained in real-world studies, and to ensure some variety in beam configurations such that pXRF as a method could be tested as a whole. For each sample that was run, the cap was removed, then the sample was turned upside-down and placed over the detector (Figure 3.1). Generally, the thickness of sample over the detector was >5 mm (Kalnicky and Singhvi 2001), however several small samples had less than <5 mm of sediment over the detector. Samples ranged in mass from 500 mg to 5 g, with a few samples having a mass <500 mg.

Analyzers reported concentrations of Mg, Al, Si, P, S, Cl, K, Ca, Ti, V, Cr, Mn, Fe, Co, Ni, Cu, Zn, As, Se, Rb, Sr, Y, Zr, Nb, Mo, Ag, Cd, Sn, Sb, Ba, La, Ce, Pr, Nd, Sm, Ta, W, Au, Hg, Pb, Bi, Th, U, and Light Elements (LE). Of these elements, we excluded Mg, Se, Mo, Ag, Cd, Sn, Sb, Ba, Ce, Sm, Au, Th, U, and LE because there was an insufficient range of values in our sediments to test data quality. We excluded Co, La, Pr, Nd, Ta, W, Hg, and Bi from our analysis because there were insufficient values reported above the factory-defined detection limit to test whether or not there was a sufficient range of values with which to test data quality, which we defined as the inter-quartile range (IQR) being greater than two times the 95% confidence interval, calculated using the median standard deviation (SD) of replicate

Table 3.1: Details of pXRF instruments used in this chapter.

XRF ID	Manufacturer	Provider	Number of Samples	Beam Details
X-5000	Olympus	Nova Scotia DEM	378	Ta anode / 30 s (50 kV, 250 µm Cu filter), 30 s (35 kV, 3 mm Al filter), 30 s (15 kV, 200 µm Al filter)
Delta	Olympus	REFLEX Instruments	165	Rh anode / 30 s (40 kV, 150 µm Cu filter), 30 s (40 kV, 2 mm Al filter), 30 s (15 kV, 100 µm Al filter)
Vanta	Olympus	REFLEX Instruments	348	Rh anode / 30 s (40 kV, 2 mm Al filter), 60 s (10 kV, no filter)
Epsilon 1	Panalytical	Panalytical	375	Ag anode / 12 s (50 kV, 100 µm Ag filter), 30 s (50 kV, 500 µm Cu filter), 18 s (12 kV, 50 µm Al filter), 60 s (10 kV, no filter)

elemental measurements (n=3).

The final suite of elements (n=22) tested in this study was Al, Si, P, S, Cl, K, Ca, Ti, V, Cr, Mn, Fe, Ni, Cu, Zn, As, Rb, Sr, Y, Zr, Nb, and Pb. Not all these elements are considered pollutants (e.g., Ca and Mg), however many non-pollutant elements are still important in environmental pollution studies because of multi-element interactions (Hunt and Speakman 2015; Boyle 2000). Therefore, we assessed data quality for all elements for which a reasonable spread of values existed in our sediment samples.

3.3.3 Data Quality

Data quality was assessed using relative standard deviation (RSD), relative difference (RD), and coefficient of determination (r^2) based on criteria established for pXRF data by the USEPA (1998) and used by several evaluations of pXRF data quality (Kilbride et al. 2006; Parsons et al. 2013; Shuttleworth et al. 2014; Rouillon and Taylor 2016) (Table 3.2). The data quality of elemental measurements was classified as definitive, quantitative, or qualitative based on these criteria. When a number of values were available (e.g., RSD and RD values, which have one value per sample), we used the 75% quantile (upper quartile) to evaluate an element/analyzer combination as definitive, quantitative, or qualitative.

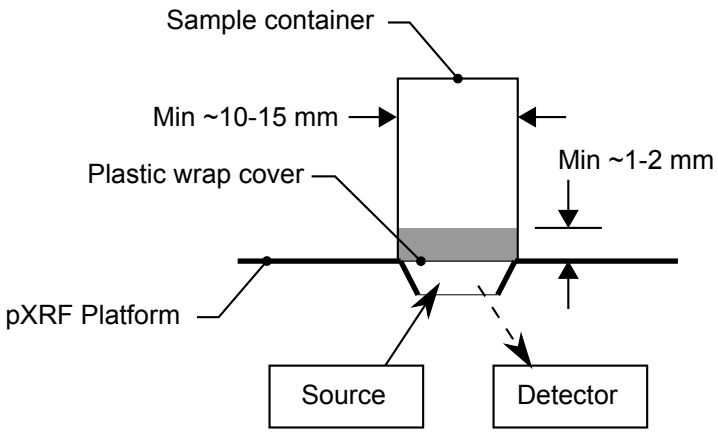

Figure 3.1: Schematic of sample analysis using the pXRF.

Table 3.2: Data and criteria used in this study to establish data quality, after USEPA (1998) and Rouillon and Taylor (2016). For RSD and RD measurements, the 75% quantile was used to classify an element/analyzer combination as qualitative, quantitative, or definitive.

Parameter	Precision	Accuracy	Comparability
Data	%RSD of replicate pXRF measurements	r^2, %RD using pXRF measurements, total digestion/ICP-OES measurements	r^2, %RD using pXRF measurements, partial digestion/ICP-OES measurements
Data Quality Level			
Definitive	RSD ≤ 10%	$0.85 \leq r^2 \leq 1.0$, $\lvert RD \rvert \leq 10\%$	$0.85 \leq r^2 \leq 1.0$, $\lvert RD \rvert \leq 10\%$
Quantitative Screening	10% < RSD ≤ 20%	$0.7 \leq r^2 < 0.85$, $10\% < \lvert RD \rvert \leq 20\%$	$0.7 \leq r^2 < 0.85$, $10\% < \lvert RD \rvert \leq 20\%$
Qualitative Screening	RSD > 20%	$r^2 < 0.7$, $\lvert RD \rvert > 20\%$	$0.85 \leq r^2 \leq 1.0$, $\lvert RD \rvert > 20\%$

3.3.4 Precision of Replicate Measurements

Precision of elemental concentrations was assessed by running every fifth sample in triplicate. For precision analysis, we used standard deviations that were calculated using exactly 3 values above the detection limit as reported by the instrument. A total of 261 replicate samples were evaluated for the X-5000 instrument, 100 replicate samples were evaluated for the Delta instrument, 171 replicate samples were evaluated for the Vanta instrument, and 204 replicate samples were evaluated for the Epsilon 1 instrument. The actual number of RSD values that were available for each element varied because not all samples reported values above the detection limit. We did not evaluate data quality when less than 10 RSD values for an element were available for comparison.

3.3.5 Accuracy of Calibrated Total Concentrations

To test the accuracy of concentrations reported by pXRF analyzers, we sent 24 samples that had been analyzed by all pXRF analyzers in this study to AGAT Laboratories (Mississauga, Ontario, Canada) for total metals analysis. Samples were digested using a 4-acid digestion ($HClO_4$, HF, HNO_3, and HCl) and analyzed for Al, P, S, K, Ca, Ti, V, Cr, Mn, Fe, Ni, Cu, Zn, As, Rb, Sr, Y, Zr, and Pb using ICP-OES. Data quality for each regression was evaluated using an r^2 value between pXRF values and concentrations reported by the laboratory. When the regression resulted in a quantitative or definitive level of data quality for an analyzer/element combination, we applied a correction to instrument-reported values using a linear regression (i.e., transforming pXRF values such that the slope of the regression with laboratory values was 1, and the intercept was 0). We used percent relative difference (%RD) as our metric for accuracy of transformed concentrations (USEPA 1998). Relative differences between total digestion and certified values for 4 lake sediment CRMs (LKSD-1, LKSD-2, LKSD-3, and LKSD-4; Geological Survey of Canada) were used as a comparison to RD values. We did not evaluate data quality when there were less than 5 pairs of values to use for the regression.

On some pXRF units, it is possible to set a calibration for a specific matrix type in advance using a set of total concentrations obtained from a lab. We chose instead to transform factory-calibrated values, as this approach can be taken for any pXRF unit for measurements that were taken at any time in the past. A similar approach has been used by other studies to transform

factory-calibrated pXRF values (Kenna et al. 2011; Frahm 2013; Parsons et al. 2013; Rydberg 2014; Rouillon and Taylor 2016).

3.3.6 Comparability of Calibrated Extractable Concentrations

To test the comparability of concentrations reported by pXRF analyzers to extractable concentrations, we sent 142 samples that had previously been analyzed by at least one pXRF analyzer to AGAT Laboratories (Mississauga, Ontario, Canada) for extractable metals analysis. Samples were digested using a perchloric acid ($HClO_4$) digestion and were analyzed for S, K, Ti, V, Mn, Fe, Cu, Zn, Rb, Zr, and Pb using ICP-OES. Samples were analyzed for As using ICP-MS. This type of digestion does not dissolve silicate minerals and therefore we expect greater deviance from pXRF values (which respond to total concentration), but is important to include in this study because environmental benchmarks are generally based on studies that use this type of digestion (CCME 1999; Kilbride et al. 2006). Each regression was evaluated using an r^2 value between pXRF concentrations and concentrations reported by the laboratory. We did not evaluate data quality for regressions that used less than 5 pairs of values.

As with total digestion values, when data quality for comparability resulted in a quantitative or definitive level of data quality for an analyzer/element combination, we applied a correction to instrument-reported values using a linear regression. CRMs were not available at the time of extractable metals analysis, and so CRMs were not used to compare extractable RD values.

3.4 Results

3.4.1 Precision of Replicate Measurements

RSD values for replicate measurements (n=3) varied by element and by XRF model (Figure 3.2, Table B.1). Overall weighted-average RSDs were classified as definitive for Si, K, Fe, Ti, Mn, Ca, Zn, Al, Sr, Cl, Zr, Rb, P, S, and Y. Some upper quartile RSD values for individual analyzers were classified as definitive, even though the overall level of data quality was quantitative, such as for V on the X-5000 and Delta analyzers, Cr on the Delta analyzer, Pb the Delta and Vanta analyzers, and As on the X-5000 analyzer

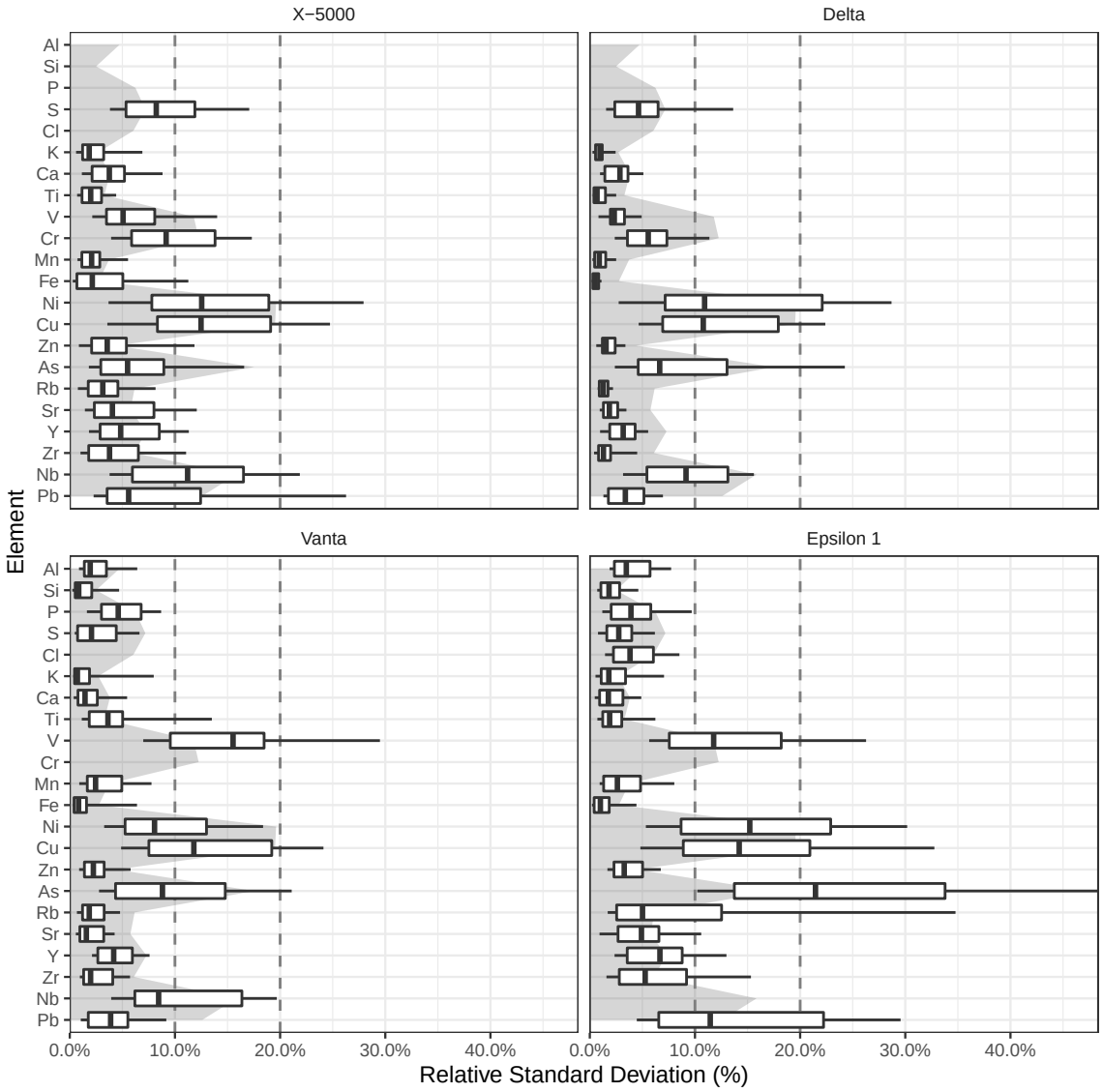

Figure 3.2: Relative standard deviations of replicate values from study pXRF analyzers for elements with a definitive overall level of data quality. Weighted-average upper quartile RSD values for each element are shown as the shaded area on all plots. Whiskers indicate the 10th and 90th percentile; boxes indicate the 25th and 75th percentile.

3.4.2 Accuracy of Calibrated Total Concentrations

Correlations between total concentrations and pXRF values were classified as definitive for K, Mn, Pb, Ti, Fe, Zn, S, Sr, Ca, Cu, As, Zr (Figure B.1, Table B.2). All elements except P, Cr, and Y had at least one analyzer with a definitive correlation between total concentrations and pXRF values; total digestion values were not measured for Si, Cl, and Nb. In particular, correlations for the Epsilon 1 analyzer were classified as definitive for V and Ni, and correlations for the Vanta analyzer were classified as definitive for Al where this was not true for other analyzers. Most relationships were linear but did not have a slope near 1 (Figure B.1), confirming that values reported by the pXRF must be calibrated before being presented as total concentrations.

After the correction was applied, corrected pXRF values were compared with total concentrations to establish the level of accuracy for element/analyzer combinations with a definitive or qualitative correlation (Figure 3.3, Figure B.2). The RD varied by element and analyzer, but in general, element/analyzer combinations that had a high r^2 value were more likely to have a low RD value. Overall RD values were classified as definitive for K, Fe, Mn, Pb Ti, Al, Zn, Ca, and Cu, and individual analyzer RD values were no higher than 12% for these elements. Relative difference values for As were classified as definitive for 3 of 4 analyzers; RD values for Sr were classified as definitive for 2 of 4 analyzers.

3.4.3 Comparability of Calibrated Extractable Concentrations

Correlations between extractable element concentrations and pXRF values for aquatic sediment samples were classified as definitive for As, Mn, Pb, S, Cu, and Fe (Figure B.3, Table B.3). Correlations were classified as quantitative for Zn, and qualitative for Ti, V, K, and Rb. Most relationships had lower correlation coefficients than with total concentrations, which is to be expected as the sample matrix has a large effect on the ability of the digestion to liberate the metal from the sample (Table B.3). In particular, extractable concentrations of Ti, K, and Rb, were not linearly related to pXRF values. Extractable element measurements were made for Zr, but no samples had extractable concentrations above the detection limit of 5 ppm. This was expected given that these elements occur primarily in silicate minerals in lake sediments (Boyle 2000; Rydberg 2014).

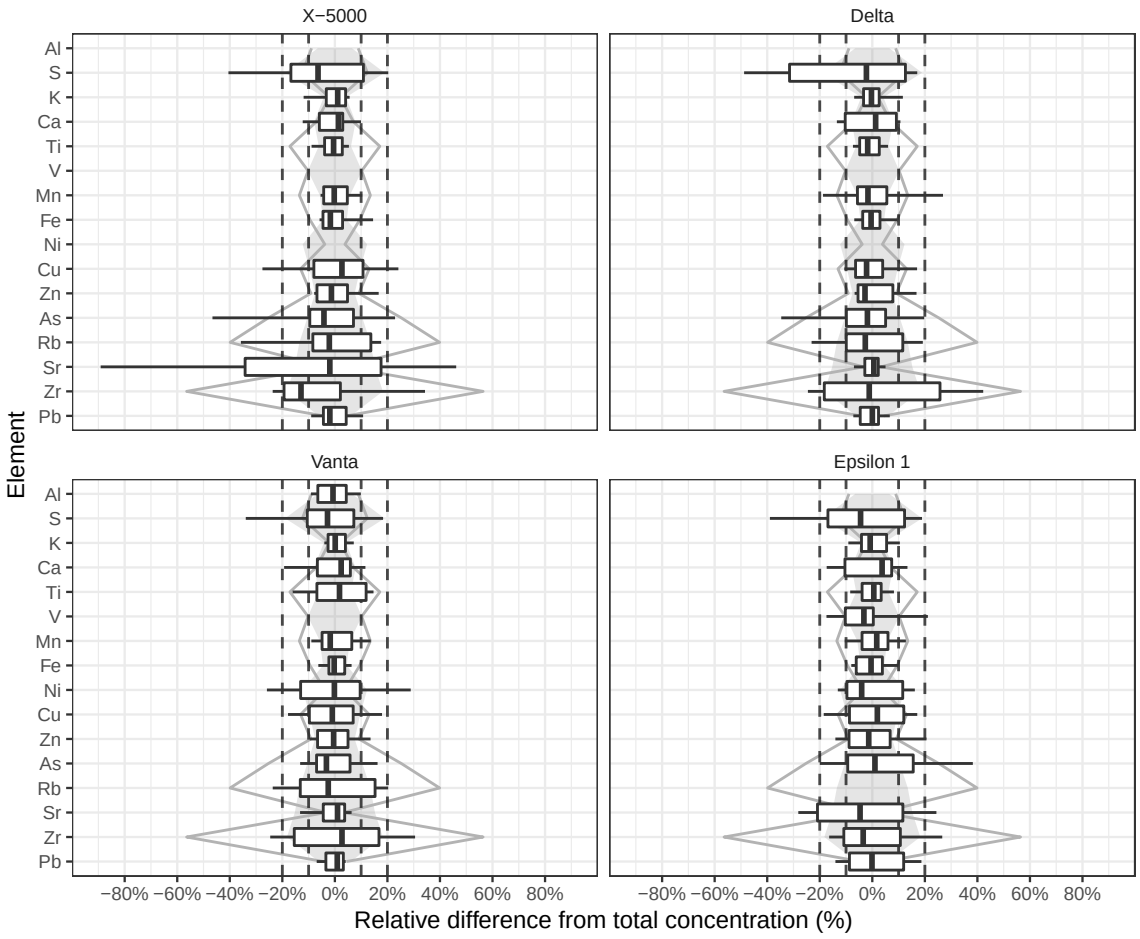

Figure 3.3: Relative difference between calibrated pXRF values and total concentrations for analyzer/element combinations with a quantitative or definitive level of data quality (n=24). Whiskers indicate the 10th and 90th percentile; boxes indicate the 25th and 75th percentile. Shaded area represents the weighted-average upper quartile RD for all analyzers. Gray line represents the upper quartile RD between lab measurements and certified values for CRMs (n=4).

After the correction was applied, calibrated pXRF values were compared with extractable concentrations to establish the ability of pXRF values to predict extractable concentrations. The RD of predicted concentrations varied by element and analyzer, but in general, calibrated pXRF values for heavier elements (Fe, Cu, Zn, As, and Pb) compared more closely with extractable concentrations (Figure 3.4, Figure B.4). RD values for lighter elements, particularly S and Mn, did not always have distributions centered around 0, suggesting that a linear transformation may result in systematically over- or under-predicting extractable equivalent values for that element. In general, absolute RD values were less than 50%, and for Fe, Cu, Zn, As, and Pb were generally within 20%. Only RD values for Fe (2/4 analyzers) and Pb (1/4 analyzers) were classified as definitive.

Aquatic sediment samples are often small (Rydberg 2014), and the analysis of small soil samples using pXRF is the subject of some debate in the literature (Kalnicky and Singhvi 2001; Parsons et al. 2013; Rydberg 2014). We used calibrated pXRF values to evaluate whether small samples (<1.25 g, 8 / 142 samples) were systematically under- or over-predicted. These values often had high RSD values, but did not appear to be systematically under- or over-predicted (Figure B.3, Figure B.4).

3.5 Discussion

3.5.1 Data Quality Relationships

The data quality of elemental pXRF measurements was not identical when assessed for precision of replicate measurements, accuracy with respect to total concentrations, and comparability with respect to extractable concentrations (Table 3.3). In particular, a high level of precision did not guarantee that pXRF measurements were either accurate or comparable, particularly for P and Y, both of which had at least one analyzer which reported a definitive level of precision but little to no correlation between total concentrations and pXRF values. Measurements for V poorly matched extractable concentrations as well despite highly repeatable measurements on some analyzers, likely a result of interference with Ti, which was highly variable in our samples (Hunt and Speakman 2015). Conversely, pXRF measurements of Cu and As, whose pXRF values had highly linear relationships with total concentrations, had high RSD values (low precision) on some units.

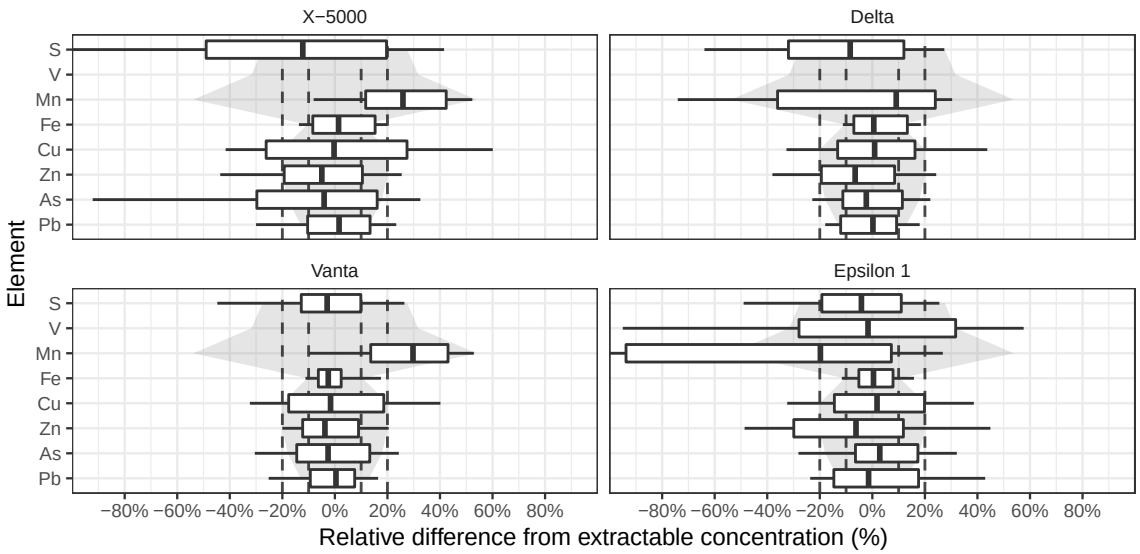

Figure 3.4: Relative difference between calibrated pXRF values and extractable concentrations for analyzer/element combinations with a quantitative or definitive level of data quality (n=142). Whiskers indicate the 10th and 90th percentile; boxes indicate the 25th and 75th percentile. Minimum whisker value for S (X-5000 analyzer) is -120%; minimum whisker value for Mn (Epsilon 1 analyzer) is -270%. Shaded area represents the weighted-average upper quartile RD for all analyzers.

Our data also suggest that agreement with total concentrations and agreement among replicates for a set of samples do not guarantee that measurements will be comparable to extractable values, particularly for elements that are known to occur in silicate minerals (K, Ti, Rb, and Zr), and is likely a result of incomplete digestion rather than poor quality of pXRF measurements (Rouillon and Taylor 2016). Elements whose pXRF values matched extractable concentrations well tended to also match total concentrations well and have a definitive level of precision, except for Cu and As, which had a quantitative level of precision.

3.5.2 Analyzer Data Quality

One of our analyzers (Epsilon 1) used fundamental parameters (FP) quantification algorithm, whereas the other analyzers used a calibration-based quantification algorithm (Kalnicky and Singhvi 2001; Mäkinen et al. 2006). The X-5000 analyzer was the oldest of our analyzers, and the Delta and Vanta units were field-portable models mounted in test stands. Despite these differences, there was no analyzer or groups of analyzers that produced the best data quality for all categories, although certain analyzers quantified specific elements better than others in

our samples. In particular, the Epsilon 1 analyzer produced definitive accuracy and quantitative comparability for V, despite the Delta and Vanta analyzers reporting a qualitative level of accuracy and comparability for the same element. This is likely a result of the FP quantification algorithm performing better than the calibration-based quantification algorithm for that element, although other studies have suggested that empirical calibrations may perform better than FP calibrations for soil samples (Mäkinen et al. 2006).

In general, if an element was measurable on a unit and present in concentrations above the sample-specific detection limit, the instrument configuration did not result in a different level of data quality from other analyzers. However, the anode material, filter materials, and beam configuration did affect which elements were measurable on a unit: Al and Si were not measurable on the X-5000, and Al was not measurable on the Delta instrument.

3.5.3 Elemental Data Quality

In general, when there were sufficient values above the detection limit and a reasonable spread of values with which to assess data quality for an element, pXRF units reported precise (RSD<10%) measurements (Table 3.3). Concentrations reported by pXRF units had a definitive linear relationship (r^2>0.85) with total concentrations for 12 of 19 elements (Table 3.3). At least one analyzer produced precise (RSD<10%) and linearly related measurements for Al, S, K, Ca, Ti, Mn, Fe, Zn, Rb, Sr, Zr, and Pb. Of these, K, Ca, Ti, Mn, Fe, and Zn were both precise and linearly related for all analyzers on which they were measured. Linear relationships with extractable concentrations were generally less definitive than for total concentrations, but could still be classified as such for S, Mn, Fe, Cu, As, and Pb.

Producing calibrated pXRF values that were comparable to total concentrations using a linear correction produced overall RD values <10% for Al, K, Ca, Ti, Mn, Fe, Cu, Zn, and Pb. RD values were centered around 0 for most elements, suggesting that the linear correction did not lead to pXRF values systematically over- or under-predicting total concentrations, and that the calibration was valid for aquatic sediments generally, not just one water body. Producing calibrated pXRF values that were comparable to extractable concentrations was only useful for elements that that are not prevalent in silicate minerals; applying the linear correction for extractable concentrations to pXRF values resulted in calibrated values that had a relative

difference of <~20% for Fe, Cu, Zn, As, and Pb. It is likely that calibrating pXRF values to extractable concentrations is only valid for highly related sediments, such as from a single water body.

Rouillon and Taylor (2016) determined that pXRF measurements for Ti, Cr, Mn, Fe, Cu, Zn, Sr, Cd, and Pb were as good or better than total digestion/ICP-OES analysis for contaminated soils, based on a linear correction similar to that used in this study. Our results were not based on contaminated samples, which is likely the reason why not all pXRF units used in our study reported calibrated Cr and Sr values that were comparable to total digestion/ICP-OES concentrations. Our study did not assess data quality for Cd, and Rouillon and Taylor (2016) did not assess data quality for Al, K, and S, and found, contrary to our results, that pXRF measurements of As were not as good as laboratory-reported concentrations. While limited data exists on pXRF data quality for aquatic sediments, Shuttleworth et al. (2014) found a strong quantitative relationship between extractable Pb and pXRF-reported Pb in peat sediments, which is consistent with the results of this study.

3.5.4 Suitability for Environmental Pollution Studies

In this study we investigated the relationship between precision of replicate pXRF measurements, accuracy of calibrated pXRF values as compared to lab-assessed total element concentrations, and comparability of calibrated pXRF values to extractable element concentrations. Our data were able to assess pXRF as a viable analysis method for (1) time-stratigraphic studies of pollution that require internally-consistent elemental concentrations, and (2) targeted sampling of potential pollutants for comparison with environmental benchmarks. For the assessment of suitability for studies requiring internally-consistent data, we interpreted this to mean values reported by the pXRF should be repeatable and linearly related to the true value. For the assessment of suitability for studies requiring comparison to environmental benchmarks, we interpreted this as the ability of instrument-reported values to be transformed to match extractable concentrations.

Internally consistent studies require precise and accurate elemental measurements, however our findings suggest that evaluating precision is not sufficient to guarantee accuracy, and therefore precision should be evaluated alongside a regression with another analysis method (e.g., 4-acid digestion/ICP-OES) to ensure that reported concentrations are representative of that element,

Table 3.3: Number of analyzers with a definitive level of data quality, per element, per category. Numbers in parentheses indicate the number of analzyers with a quantitative level of data quality.

Element	Precision	Correlation (Total)	Calibrated Values (Total)	Correlation (Extractable)	Calibrated Values (Extractable)
Fe	**4 (0)**	**4 (0)**	**4 (0)**	**3 (1)**	*2 (2)*
Mn	**4 (0)**	**4 (0)**	**4 (0)**	**4 (0)**	0 (0)
Zn	**4 (0)**	**4 (0)**	**4 (0)**	*1 (3)*	0 (3)
K	**4 (0)**	**4 (0)**	**4 (0)**	0 (0)	
Ti	**4 (0)**	**4 (0)**	**3 (1)**	0 (0)	
Ca	**4 (0)**	**4 (0)**	**2 (2)**		
S	**3 (1)**	**4 (0)**	*0 (3)*	**4 (0)**	0 (2)
Sr	**4 (0)**	**3 (1)**	*2 (0)*		
Zr	**4 (0)**	**3 (1)**	*0 (3)*		
Pb	*2 (1)*	**4 (0)**	**3 (1)**	**4 (0)**	*1 (3)*
Cu	*0 (3)*	**4 (0)**	**2 (2)**	**2 (2)**	0 (3)
As	*1 (2)*	**3 (1)**	*3 (1)*	**4 (0)**	*0 (3)*
Al	**2 (0)**	*1 (0)*	**1 (0)**		
Rb	**3 (1)**	*3 (0)*	*0 (3)*	0 (0)	
P	**2 (0)**	0 (0)			
Y	**4 (0)**	0 (0)			
V	*2 (2)*	1 (0)	*0 (1)*	0 (1)	0 (0)
Ni	*0 (2)*	1 (1)	*0 (2)*		
Cr	*1 (1)*	0 (0)			
Si	**2 (0)**				
Cl	**1 (0)**				
Nb	*0 (3)*				

and are not the result of matrix effects or spectral overlaps (Boyle 2000; Kalnicky and Singhvi 2001; Hunt and Speakman 2015). Using this regression to calibrate pXRF values is highly recommended such that reported values can be interpreted as total concentrations. Elements for which low precision exists are still suitable for inclusion in these studies, provided that sample-specific uncertainty is reported (e.g., using error bars generated from replicate measurements). Our method of running every 5th sample in triplicate was able to provide a reasonable characterization of sample-specific uncertainty.

Comparing pXRF-reported concentrations to environmental benchmarks requires that a reasonable linear relationship exists between pXRF concentrations and extractable concentrations for samples with the same sample matrix as the target samples (Kalnicky and Singhvi 2001; Kenna et al. 2011). For our samples and analyzers, correcting pXRF concentrations using this linear relationship resulted in a relative difference of <~20% for Fe, Cu, Zn, As, and Pb, but was greater than 20% on some analyzers. Lab error can be high (Kalnicky and Singhvi 2001; Kane 1993), and our method did not allow for the assessment of laboratory error for extractable concentrations. The USEPA (1998) considered a -20-20% RD an acceptable range for pXRF soil measurements, however element-specific uncertainty should be reported if corrected concentrations are to be compared with environmental benchmarks.

3.5.5 Improving Quantification

We used factory-calibrated pXRF units and minimal sample preparation to assess the lower bound of possible data quality for pXRF units, and to simulate a common circumstance in which analyzers may be used. While we found excellent data quality was achievable for many elements using these methods, the literature suggests several methods by which pXRF data quality could be improved for soil measurements. For example, in this study, we used widely available 80 gauge (20 micron) palate wrap, which may affect the accuracy of lighter elements such as Al and S due to attenuation by the wrap material (Kalnicky and Singhvi 2001; Parsons et al. 2013). Using thin (6 micron) Mylar is generally recommended, and may increase data quality for lighter elements (Kalnicky and Singhvi 2001; Parsons et al. 2013).

Another method for increasing data quality in pXRF measurement is increasing count times. Assuming that counts are Poisson distributed, theoretical RSD should be given by $\sqrt{n}/n$, where n is the number of counts under the peak. Therefore, increasing count time should

increase precision for elements with small peaks. However, many factors contribute to the precision we observed, which was designed to incorporate sample homogeneity for our sample preparation method in addition to probabilistic counting uncertainty (USEPA 1998).

In this study, we used provider-recommended count times, which in general were 90 seconds split between several beam energies. Some studies suggest that increasing count time increases precision (Kalnicky and Singhvi 2001; Shuttleworth et al. 2014), but the longest count time analyzer (Epsilon 1) did not produce more precise results in our study. Thus, for aquatic sediments, we suspect that other factors such as sample homogeneity and quantification algorithms play an equally important role in determining precision (Parsons et al. 2013). Sample homogeneity can be increased by using a planetary mill for homogenization rather than a mortar and pestle, and/or by sieving samples prior to analysis (USEPA 1998).

There is some debate around the minimum amount of sample thickness that can be reliably analyzed by pXRF, with some studies indicating that as little as 5 mm is sufficient (Kalnicky and Singhvi 2001), and others suggesting as much as 12-17 mm is required for heavy elements such as Pb (Parsons et al. 2013). When compared to extractable values, our 8 smallest samples (<1.25 g) were not systematically over- or under-predicted (even for Pb), suggesting that heavy elements in small samples can be reliably measured by pXRF. This observation is consistent with that of Rydberg (2014), who found that 200-mg samples did not produce significantly different values than 500-mg samples when measured by WD-XRF.

3.6 Conclusion

Collectively, our data suggest that pXRF analyzers have a sufficient level of data quality for aquatic sediments to be used in environmental research. Studies using pXRF should provide an application-specific assessment of data quality is reported alongside results, as data quality was variable when assessed by data quality type, by element, and by analyzer. Use of pXRF analyzers is specifically well-suited to studies whose conclusions are based on internally-consistent total concentrations, although with proper reporting of uncertainty, pXRF concentrations can be calibrated and compared to total concentrations or environmental benchmarks. Portable X-ray Fluorescence is a promising analytical method by which high-throughput paleolimnological studies might be conducted at a reasonable cost.

Chapter 4

Visualizing Paleoenvironmental Archives

Submitted to the *Journal of Statistical Software* with co-authors Nell Libera[1], Joshua Kurek[2], Ian S. Spooner[3], and Graham A. Gagnon[4].

4.1 Abstract

This paper presents the *tidypaleo* package for R, which enables high-quality reproducible visualizations of time-stratigraphic multivariate data collected from many locations. Rather than introduce new plotting functions, the *tidypaleo* package defines several orthogonal components of the *ggplot2* package that, when combined, enable most types of stratigraphic diagrams to be created. We do so by conceptualizing multi-parameter data as a series of measurements (rows) with attributes (columns), enabling the use of the *ggplot2* facet mechanism to display multi-parameter data. The orthogonal components include (1) scales that represent relative abundance and concentration values, (2) geometries that are commonly used in paleoenvironmental diagrams created elsewhere, (3) facets that correctly assign scales and sizes to panels representing multiple parameters, and (4) theme elements that enable *tidypaleo* to create elegant graphics. Collectively, this software enables correct analysis of multivariate data from many archives of environmental change that was previously not possible for many investigators.

[1]Paleoecological Environmental Assessment and Research Laboratory (PEARL), Department of Biology, Queen's University, Kingston, Ontario K7L 3N6

[2]Department of Geography and Environment, Mount Allison University, Sackville, New Brunswick E4L 1A7

[3]Department of Earth & Environmental Science, Acadia University, 12 University Ave., Wolfville, Nova Scotia, Canada B4P 2R6

[4]Centre for Water Resources Studies, Department of Civil & Resource Engineering, Dalhousie University, 1360 Barrington St., Halifax, Nova Scotia, Canada B3H 4R2

4.2 Introduction

Chapter 2 identified that variability in Pb deposition can occur at small spatial scales and may require evidence from a many records to confirm spatial trends. Chapter 3 established portable X-Ray Fluorescence (pXRF) as a high-throughput quantitative method to obtain geochemical measurements for lake sediment samples; however, the volume of data that pXRF can provide can only be applied to the study of trace metal deposition at a regional scale if these data can be visualized and analyzed effectively by the average investigator. *tidypaleo* is a package for R statistical software (R Core Team 2019) to create effective visualizations for and conduct analyses of paleoenvironmental data, including records of trace metal pollution and land-use change indicators. These data have several characteristics that distinguish them from traditional time series data (Dunnington and Spooner 2018):

- They are generally multi-proxy and multi-archive, in that evidence from multiple parameters (e.g., the relative abundance of dozens of taxa and/or geochemical measures) and multiple archives (e.g., lake sediment cores from different locations) must be interpreted collectively.
- The connection between position in the archive (e.g., depth in the archive) and calendar age (e.g., AD 1900±15) is subjective and both must be communicated alongside parameter measurements.
- These archives tend to be oriented vertically (e.g., an ice core), and tend to be plotted vertically with parameter measurements on the x-axis and depth or time on the y-axis.

Because of the unique nature of paleoenvironmental data, constructing diagrams that are elegant, technically correct, and reproducible is challenging and often time-consuming. Whereas previous software packages for creating stratigraphic diagrams (e.g., *C2*, *Tilia*Graph*, *rioja*, and *analogue*) use a graphical user interface or base R plotting approach (Grimm 2002; Juggins 2011; Juggins 2019; Simpson and Oksanen 2020), in the *tidypaleo* package, we use the elegant defaults and flexible interface of the *ggplot2* package (Wickham et al. 2020a) as a base on which effective paleoenvironmental diagrams can be built.

4.3 Example Data

In this paper, we use the `kellys_lake_geochem` and `kellys_lake_cladocera` data set, which contain geochemical measurements and microfossil zooplankton (Cladocera) counts from Kellys Lake, Nova Scotia, Canada, to demonstrate the features of the *tidypaleo* package (Figure 4.1; Figure 4.2).

```
data("kellys_lake_geochem", package = "tidypaleo")
data("kellys_lake_cladocera", package = "tidypaleo")

# Figure 4.1
kellys_geochem_plot <- ggplot(
  kellys_lake_geochem,
  aes(x = value, y = depth)
) +
  geom_lineh() +
  geom_point() +
  scale_y_reverse()  +
  facet_geochem_gridh(vars(param)) +
  labs(y = "Depth (cm)", x = NULL)

kellys_geochem_plot
```

```
# Figure 4.2
kellys_abund_plot <- ggplot(
  kellys_lake_cladocera,
  aes(x = rel_abund, y = depth)
) +
  geom_col_segsh() +
  scale_y_reverse()  +
  facet_abundanceh(vars(taxon)) +
  labs(y  = "Depth (cm)")
```

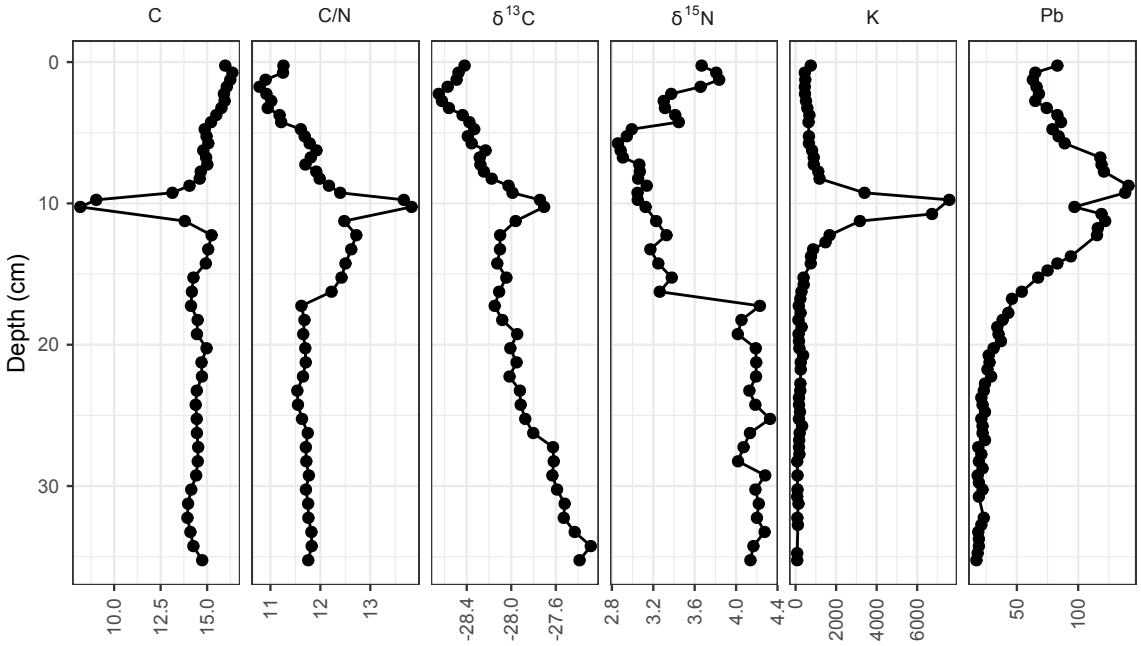

Figure 4.1: Geochemical measurements from Kellys Lake, Nova Scotia, Canada.

```
kellys_abund_plot
```

4.4 Design and Implementation

Like *ggplot2*, the *tidypaleo* package provides a number of reusable components that can be combined in flexible and powerful ways to communicate a wide variety of data types. Here, we use the structure laid out by Wilkinson (2005) when describing the Grammar of Graphics.

4.4.1 Data

Essential to *tidypaleo* is a tabular data structure composed of one row per measurement. Columns contain information about each measurement, including common dimensions (e.g., depth, age, core identifier, and which parameter was measured), and values specific to each measurement (e.g., measured values, units, and errors). This form of data provides an opportunity for measurement-level details to be retained that is not possible with a more traditional "tidy" format (Wickham 2014; Dunnington and Spooner 2018), where columns are

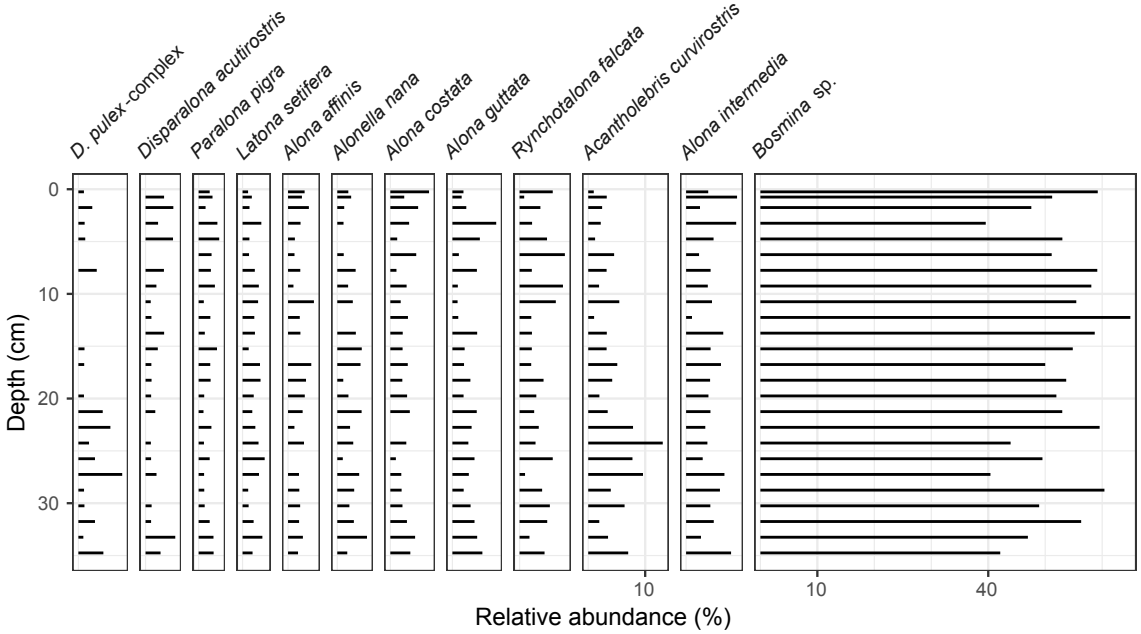

Figure 4.2: Microfossil zooplankton (Cladocera) relative abundances from Kellys Lake, Nova Socita, Canada.

mix of common dimensions and which parameter was measured, rows represent individual sediment samples, and cells can only represent a single value. Data with measurements as rows and attributes as columns (e.g., core identifier and parameter name) allows a natural use of the *ggplot2* grouping and facet mechanisms to plot multiple parameters and locations. Importantly, this also supports communication of error, since value error is just another column in the data structure. The `kellys_lake_geochem` data set used in Figure 1 is shown below.

```
kellys_lake_geochem
```

```
## # A tibble: 305 x 9
##    location param depth age_ad value error
##    <chr>    <chr> <dbl>  <dbl> <dbl> <dbl>
##  1 KLY17-2  C      0.25  2017.  16.0    NA
##  2 KLY17-2  C      0.75  2016.  16.4    NA
##  3 KLY17-2  C      1.25  2015.  16.2    NA
##  4 KLY17-2  C      1.75  2014.  16.1    NA
```

```
##  5 KLY17-2  C      2.25  2013.  15.9    NA
##  6 KLY17-2  C      2.75  2011.  15.9    NA
##  7 KLY17-2  C      3.25  2009.  15.8    NA
##  8 KLY17-2  C      3.75  2007.  15.5    NA
##  9 KLY17-2  C      4.25  2005.  15.2    NA
## 10 KLY17-2  C      4.75  2003.  14.9    NA
## # ... with 295 more rows, and 3 more variables:
## #   error_type <chr>, n_detect <int>, n <int>
```

4.4.2 Scales

Paleoenvironmental data in a one row per measurement structure has several common data types that should be scaled differently when passed to *ggplot2*. Discrete variables such as location, parameter, and sample groupings, such as zones, are well-represented by the existing discrete scales in *ggplot2*. Continuous variables require special consideration, including archive position (typically depth), age, relative abundance, and concentration values.

Position in archive and age are values that are related by a monotonic transformation. Whereas position in the archive is known to a high degree of precision, age values are typically estimated, and communicating uncertainty around this value is essential. In the *tidypaleo* package, the relationship between archive position, age, and age uncertainty is represented by an `age_depth_model()`. An `age_depth_model()` is constructed using previously estimated age and depth values, and provides various options for interpolating and extrapolating. Default interpolation and extrapolation provides a reasonable approximation for visualization, although ideally these values should be provided at a high enough resolution so that interpolation and extrapolation is minimal. Age-depth models can be passed to `scale_(x|y)_depth_age()` and `scale_(x|y)_age_depth()`, which use *ggplot2*'s `sec_axis()` framework to communicate both age and depth (Figure 4.3). These scales also enforce the convention that time should be visualized from bottom to top when on the y-axis, and from left to right when on the x axis.

```
# Figure 4.3
data("kellys_lake_ages", package = "tidypaleo")
```

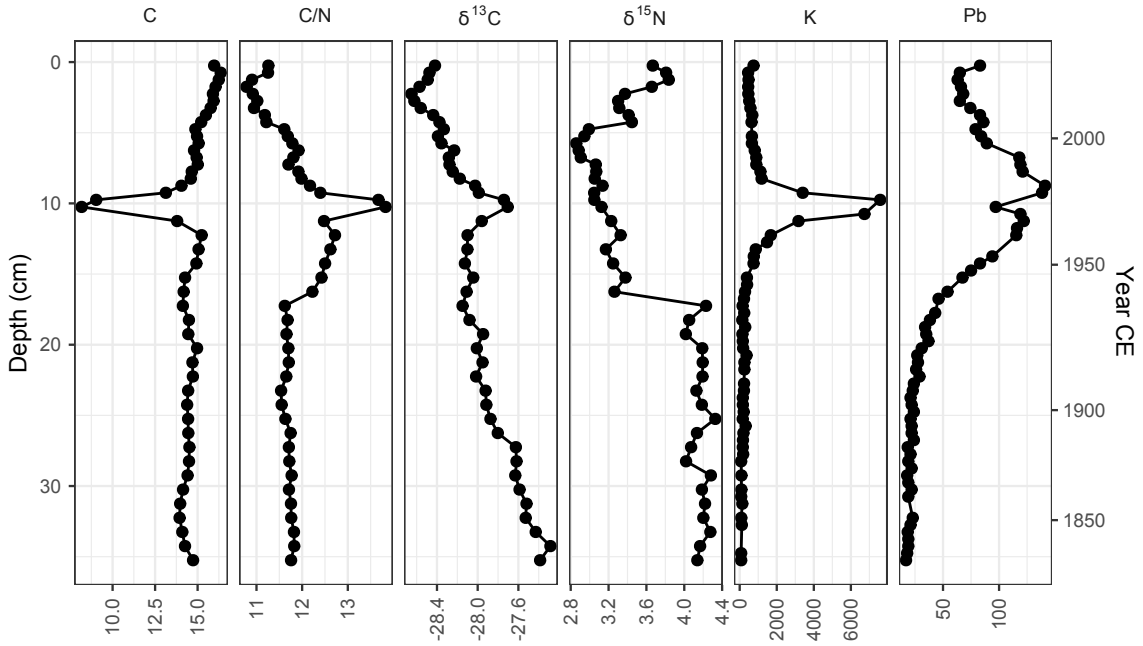

Figure 4.3: Age-depth transformation and scales applied to a stratigraphic plot of geochemical measurements.

```
kellys_adm <- age_depth_model(
  depth = kellys_lake_ages$depth,
  age = kellys_lake_ages$age_ad
)

kellys_geochem_plot +
  scale_y_depth_age(kellys_adm, age_name = "Year CE")
```

Relative abundance of microfossils is a common type of value in paleoenvironmental diagrams. Relative abundance values are always zero or positive, and breaks should always occur at the same intervals on all panels. Because negative values are impossible, zero should always be the minimum limit. Expansion below zero can be misleading and tends to produce unnecessary space. Expansion above the maximum value should be a fixed amount (rather than the default 5%) to keep spacing between panels uniform. These defaults are encapsulated in the `scale_(x|y)_abundance()` scales, which wrap `ggplot2::scale_(x|y)_continuous()` to produce the optimal labels, limits, and

expansion for relative abundance values.

Concentration values are also common in paleoenvironmental diagrams. Concentration values are theoretically always positive, although in practice values below detection or quantification limits are frequently (if incorrectly) encoded as zeroes. Concentration values are usually well-represented by the default continuous scale, which scales to the minimum and maximum of the data. Occasionally it is useful to convey the relative change in concentration between parameters, in which setting the bottom limit to zero (`limits = c(0, NA)`) is appropriate. Similarly, log-scales are appropriate for some parameters (e.g., ^{210}Pb activities). Because the scale modifications required for concentration values are minimal, the *tidypaleo* package does not provide specific scales for concentration values.

4.4.3 Geometries

Two common visual representations of relative abundance values are difficult to recreate using existing *ggplot2* geometries. First, vertical or horizontal segments drawn from the x- or y-axis to the relative abundance value are common and recommended for some types of data (Juggins and Telford 2012). The *tidypaleo* package provides `geom_col_segs()` to create this type of visual representation. This geometry is implemented as a subclass of `ggplot2::GeomSegment`, and is parameterized identically to `geom_col()`, `geom_area()`, `geom_point()`, and `geom_line()`.

Second, "exaggerations" are common to communicate low-magnitude variability when one or more large relative abundance values obscure this trend. From a Grammar of Graphics perspective, these "exaggerations" are statistics, as they modify the original data in such a way that existing graphical representations can be used to draw them (Wilkinson 2005). Pragmatically, these are implemented as subclassses of the existing `ggplot2::Geoms`, because implementing them as subclassess of `ggplot2::Stat` results in the scales expanding to include all exaggerated values. The *tidypaleo* package provides `geom_point_exaggerate()`, `geom_line_exaggerate()`, and `geom_area_exaggerate()` to create this type of graphical representation (Figure 4.4).

```
kellys_demo_base <- kellys_lake_cladocera %>%
  filter(taxon == "Acantholebris curvirostris") %>%
```

```
  ggplot(aes(x = rel_abund, y = depth)) +
  scale_y_reverse()  +
  facet_abundanceh(vars(taxon)) +
  scale_x_abundance(
    breaks = waiver(),
    expand = expansion(add = c(0, 1))
  ) +
  labs(x = "Rel. Abundance (%)", y = "Depth (cm)")

# Figure 4.4
patchwork::wrap_plots(
  kellys_demo_base +
    geom_lineh() +
    geom_lineh_exaggerate(exaggerate_x = 2, col = "grey80"),
  kellys_demo_base +
    geom_areah_exaggerate(exaggerate_x = 2, fill = "grey80") +
    geom_areah(),
  nrow = 1
)
```

In recent *ggplot2* versions (>= 3.3.0), horizontal geometries such as `geom_errorbar()`, `geom_col()`, `geom_line()`, `geom_smooth()`, `geom_ribbon()`, and `geom_area()` can be oriented vertically using `orientation = "y"` (in previous versions of *ggplot2*, vertically-oriented diagrams were more challenging to create). The *tidypaleo* package provides `geom_errorbarh()` `geom_colh()`, `geom_col_segsh()`, `geom_lineh()`, `geom_smoothh()`, `geom_ribbonh()`, and `geom_areah()` to specifically handle vertically-oriented plots, some of which are re-exported from the *ggplot2* and *ggstance* packages (Wickham et al. 2020a; Henry et al. 2020). While these wrappers are minimal, they reflect that vertically-oriented plots are the most common type of paleoenvironmental diagram and make it easier to switch the orientation of a diagram if required (Figure 4.5).

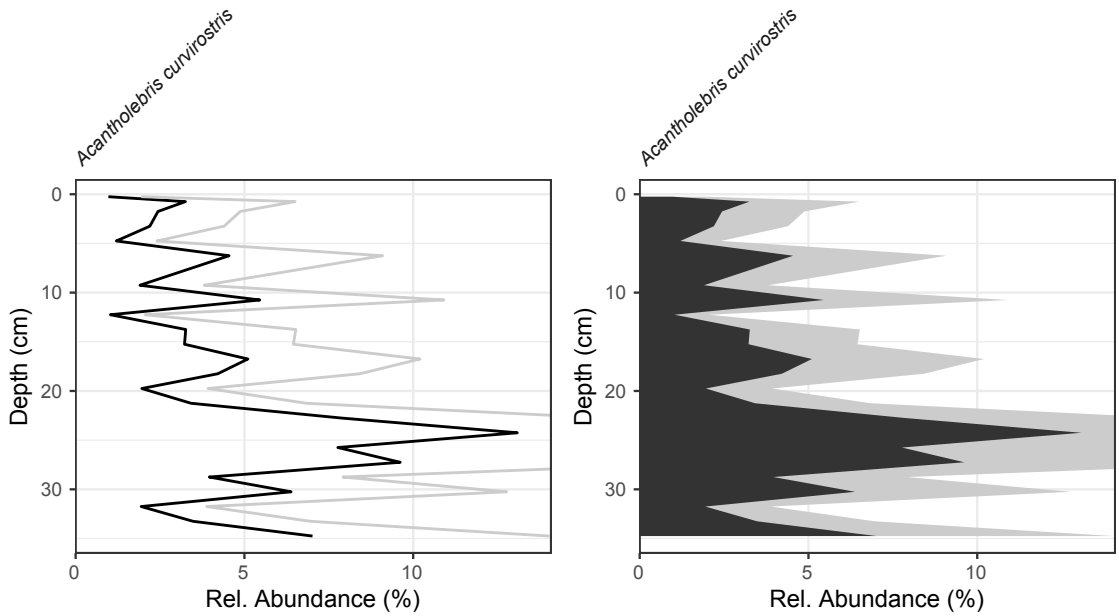

Figure 4.4: Exaggerated line and area geometries for highlighting relative change of parameters with a large change in magnitude.

```
# Figure 4.5
patchwork::wrap_plots(
  kellys_demo_base + geom_col_segsh(),
  kellys_demo_base + geom_lineh(),
  kellys_demo_base + geom_col_segsh() + geom_lineh(),
  kellys_demo_base + geom_areah(),
  nrow = 1
)
```

4.4.4 Facets

In the Grammar of Graphics, facets are defined as displaying subsets of a data set in panels of the same graphic (Wilkinson 2005). Using a data structure with one row per measurement, plotting multiple parameters on same plot using facets is a natural way to represent these data. In *ggplot2*, facets also coordinate the scales and labels for each panel. As noted in Section 4.4.2, different parameter types can have different scaling requirements. Furthermore, proper

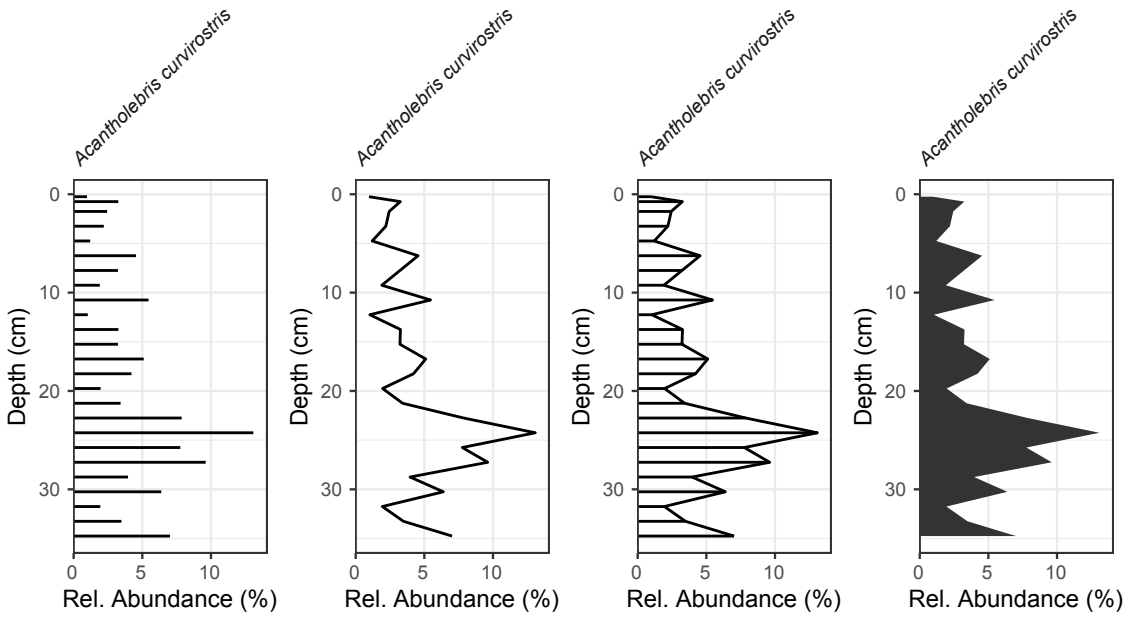

Figure 4.5: Column segment, line, area, and combinations commonly used to represent relative abundance values on stratigraphic diagrams.

labeling of geochemical parameters and species names can be challenging. Facets are a useful way to solve these challenges for diagrams with a common data type. The *tidypaleo* package provides facet types for two common cases: relative abundance data and geochemical data.

Facets for relative abundance data (`facet_abundance()` and `facet_abundanceh()`) wrap `ggplot2::facet_grid()`, applying best-practice rules for the relationship between abundance scales. When plotted, relative abundance values on each panel should have the same weight (i.e., 5% on one panel should take up the same amount of space as 5% on another panel; `space = "free_x"` or `space = "free_y"`). Facet labels must have species names italicized for publication in most journals, but modifiers (e.g., strain III) must not be italicized. This constraint can be accommodated by setting the default labeller to a function that understands the form of most species input (`label_species()`). Finally, facet labels are typically too long to fit horizontally above each panel and must be rotated to be legible. While rotating a facet label is possible using *ggplot2* theme modifications, eliminating the horizontal clip is not. Control over the clip parameter of the strip text is likely in a future *ggplot2* version, however packaging both as part of the facet is a way make this implementation detail transparent to the user.

Panels representing different geochemical parameters do not require `space = "free_x"` or `space = "free_y"`, and thus can wrap either `facet_wrap()` or `facet_grid()`. The *tidypaleo* package provides `facet_geochem_wrap()`, `facet_geochem_grid()`, `facet_geochem_wraph()`, and `facet_geochem_gridh()` for geochemical measurements (Figure 4.1). Scales should be independent between panels representing different parameters, as fixed scales could hide meaningful trends in parameters with a smaller absolute magnitude (for this reason, it is also generally not appropriate to display two geochemical parameters on the same panel). Units of measurement may be different between panels, and thus need to be included in the facet label (Figure 4.6). Furthermore, many common parameter names contain non-ASCII characters that require R plotmath to display on all graphics devices. Both of these labeling constraints are practically difficult to achieve, so we include `label_geochem()` as the default labeller to convert common ASCII representations of parameter names to parseable plotmath and provide an interface to specify measurement units. Finally, including many parameters on a vertically-oriented plot inevitably results in overlapping x-axis labels. Because of this, we also rotate x-axis labels by 90 degrees by default in `facet_geochem_wraph()` and `facet_geochem_gridh()`.

```
# Figure 4.6
kellys_geochem_plot +
  facet_geochem_gridh(
    vars(param),
    units = c(
      "C" = "%", "C/N" = NA, "d13C" = "‰",
      "d15N" = "‰", "Pb" = "ppm", "K" = "ppm"
    )
  )
```

While these facets could be implemented as subclasses of `ggplot2::FacetGrid` and `ggplot2::FacetWrap`, both relative abundance and concentration facets are instead implemented as wrappers around the `ggplot2::facet_grid()` and `ggplot2::facet_wrap()` functions that also add the appropriate scale and theme elements. These labellers, scales, and theme elements are also available as separate components should the user wish to use a different base facet type (e.g., from an extension package).

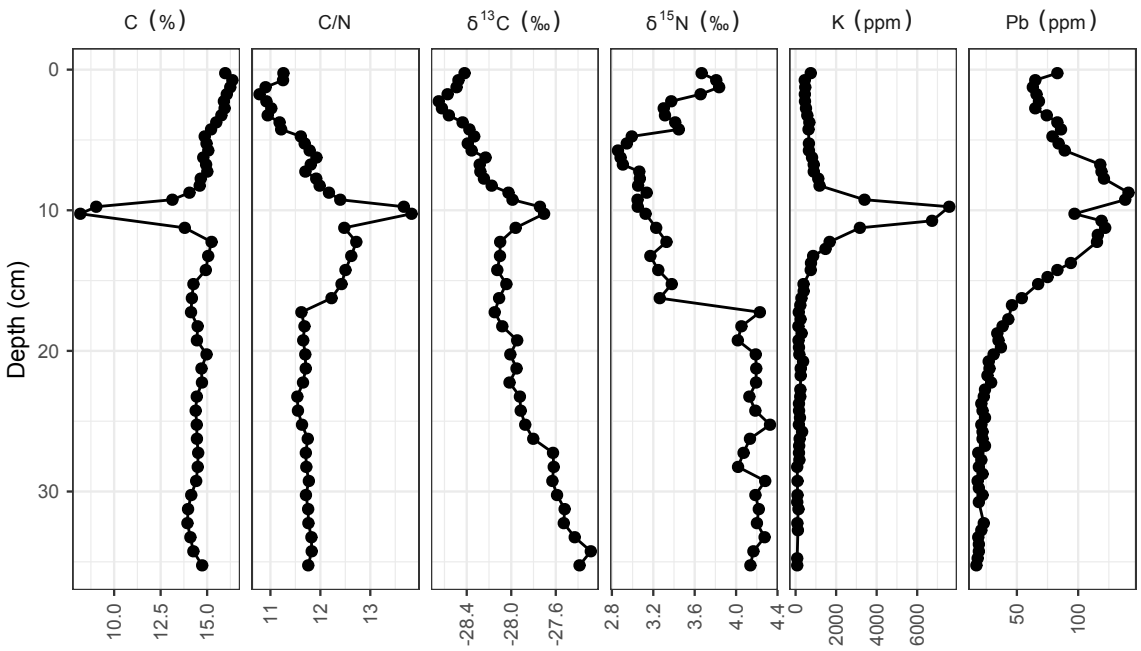

Figure 4.6: Adding units to multi-parameter plots using the geochemistry labeller.

The facets included in the *tidypaleo* package do not solve the problem of paleoenvironmental diagrams that display more than one data type; however, the *patchwork* package provides syntax to align multiple *ggplot2* plots and assign common elements among them (Pedersen 2017). Creating diagrams in this way imposes the constraint that plots with the same data type must be grouped. This constraint makes it easier to describe any differences in plot scales (e.g., for panels where a log scale is appropriate), and we do not think a more complex implementation of a facet would result in better diagrams or syntax.

4.4.5 Theme Elements

This package includes `theme_paleo()`, which is a minimally-modified version of `ggplot2::theme_bw()` that removes the grey background of panel labels. This reflects the look and feel of these diagrams created by other software. Elements of the abundance and geochemical facets are also available as theme modifiers, including `rotated_axis_labels()` and `rotated_facet_labels()`.

4.4.6 Statistical Helpers

The definition of data used by *tidypaleo* is different than the type of data that is needed to compute common multivariate summaries such as ordinations and/or stratigraphically-constrained cluster analysis. To facilitate visualizing the results of these analyses, *tidypaleo* provides a framework for transforming one-row-per-measurement data into a data frame suitable for input to most multivariate summaries (generally one row per sample). The `nested_data()` function exposes the most common transformation options, returning a data frame with list-columns containing the components needed for most analyses.

The options provided by `nested_data()` include (1) the transformation to apply to each column, (2) the filter to apply to the data, and (3) the selection criteria to apply to the data. Option (1) can be used to apply scaling appropriate for a specific statistical analysis (e.g., `scale()` for PCA); options (2) and (3) can be used to handle non-finite values resulting from parameter measurements on different samples.

```
kellys_geochem_nested <- kellys_lake_geochem %>%
  nested_data(
    qualifiers = c(depth, age_ad),
    key = param,
    value = value,
    trans = scale,
    filter_all = all_vars(is.finite(.))
  )

kellys_geochem_nested
```

```
## # A tibble: 1 x 4
##   discarded_colum~ discarded_rows qualifiers data
## * <list>           <list>         <list>     <lis>
## 1 <tibble [70 x 0~ <tibble [36 x~ <tibble [~ <tib~
```

Usable output can be obtained by unnesting one or more columns:

```
kellys_geochem_nested %>%
  unnested_data(qualifiers, data)
```

```
## # A tibble: 34 x 9
##    depth age_ad row_number C[,1] `C/N`[,1]
##    <dbl>  <dbl>      <int> <dbl>     <dbl>
##  1  0.25  2017.          1 1.47    -0.847
##  2  0.75  2016.          2 1.98    -0.863
##  3  1.25  2015.          3 1.83    -1.59
##  4  1.75  2014.          4 1.58    -1.84
##  5  2.25  2013.          5 1.37    -1.55
##  6  2.75  2011.          6 1.42    -1.35
##  7  3.25  2009.          7 1.19    -1.50
##  8  3.75  2007.          8 0.823   -1.01
##  9  4.25  2005.          9 0.451   -0.940
## 10  5.25  2001.         10 0.126    0.0334
## # ... with 24 more rows, and 4 more variables:
## #   d13C[,1] <dbl>, d15N[,1] <dbl>, K[,1] <dbl>,
## #   Pb[,1] <dbl>
```

Analysis helpers `nested_prcomp()` and `nested_chclust()` operate on `nested_data()`, enabling identical analysis to be conducted on potentially many archives:

```
kellys_geochem_clust <- kellys_geochem_nested %>%
  nested_chclust_coniss()

kellys_geochem_clust
```

```
## # A tibble: 1 x 14
##   discarded_colum~ discarded_rows qualifiers data
## * <list>           <list>         <list>     <lis>
```

```
## 1 <tibble [70 x 0~ <tibble [36 x~ <tibble [~ <tib~
## # ... with 10 more variables: distance <list>,
## #   model <list>, n_groups <list>, CCC <list>,
## #   dendro_order <list>, hclust_zone <list>,
## #   zone_info <list>, nodes <list>,
## #   segments <list>, broken_stick <list>
```

The output of these analyses is calculated such that unnesting one or more columns will result in plot-friendly results and diagnostics, such as a broken-stick simulation of a CONISS cluster analysis (Juggins 2019; Grimm 1987; Bennett 1996) or plottable segments:

```
kellys_geochem_clust %>%
  unnested_data(broken_stick)
```

```
## # A tibble: 32 x 3
##    n_groups dispersion broken_stick_dispersion
##       <int>      <dbl>                   <dbl>
##  1        2     17.3                     6.35
##  2        3     10.2                     4.79
##  3        4      3.67                    4.02
##  4        5      4.20                    3.50
##  5        6      2.41                    3.11
##  6        7      1.52                    2.80
##  7        8      1.37                    2.54
##  8        9      1.12                    2.32
##  9       10      1.01                    2.13
## 10       11      0.782                   1.96
## # ... with 22 more rows
```

Whereas a simpler pivot operation, such as that provided by `tidyr::pivot_wider()`, coupled with a more traditional call to an analysis function is effective for a single multivariate

analysis (Wickham and Henry 2020), our approach allows the same rules to be applied to many analyses. This is difficult to recreate with existing tools for pivoting and analysis, which is why we provide these functions in the *tidypaleo* package.

4.5 Example

A motivating example for the development of this package was the ability to create stratigraphic diagrams of multiple archives with statistical summaries. For relative abundance data, it is common to plot the results of an ordination and a cluster analysis alongside the raw data. For this example, we will use diatom count data from lakes in Kejimkujik National Park, Nova Scotia, Canada sourced from the Neotoma paleoecological database (Goring et al. 2015; Ginn et al. 2007).

The stratigraphic diagram for these lakes is an example where exaggerated geometries are useful: while common scales for the same taxa between lakes correctly communicates the difference in magnitude, relative trends are difficult to assess for some taxa without the exaggerated geometry (`geom_areah_exaggerate()`). Relative abundance scales with comparable size across panels are added via `facet_abundanceh()`, which also correctly labels taxa with a rotated facet label.

```
keji_plot <- ggplot(
  keji_lakes_plottable,
  aes(x = rel_abund, y = depth)
) +
  geom_areah_exaggerate(exaggerate_x = 5, alpha = 0.2) +
  geom_areah() +
  scale_y_reverse() +
  facet_abundanceh(
    vars(taxon),
    grouping = vars(location),
    scales = "free"
  ) +
  labs(x = "Relative abundance (%)", y = "Depth (cm)")
```

Using `nested_data()` and `nested_chclust_coniss()`, it is possible to calculate a cluster analysis for both lakes. Here we use a square-root transformation such that the euclidean distance measure used by default in `nested_chclust_coniss()` is useful (Legendre and Birks 2012).

One measure of the quality of a stratigraphically-constrained cluster analysis is a broken-stick analysis to obtain the number of statistically plausible groups (Bennett 1996). These results can be obtained by unnesting the `broken_stick` column in the result of `nested_coniss_chclust()`. For both cores, the cluster analysis identified 3 groups whose dispersion was more than would be expected from a cluster analysis of a random shuffle of the samples.

```
keji_coniss %>%
  unnested_data(broken_stick) %>%
  group_by(location) %>%
  slice(1:4)
```

```
## # A tibble: 8 x 4
## # Groups:   location [2]
##   location   n_groups dispersion broken_stick_dis~
##   <chr>         <int>      <dbl>              <dbl>
## 1 Beaverski~        2       9.27               5.29
## 2 Beaverski~        3       3.24               3.72
## 3 Beaverski~        4       1.53               2.94
## 4 Beaverski~        5       2.17               2.42
## 5 Peskawa L~        2      14.4                6.26
## 6 Peskawa L~        3       4.59               4.50
## 7 Peskawa L~        4       3.27               3.61
## 8 Peskawa L~        5       2.38               3.03
```

The dendrogram associated with these cluster analyses can be added to a plot using `layer_dendrogram()`. Because the scale of the dendrogram is not in relative abundance, a separate plot is needed

```
dendro_plot <- ggplot() +
  layer_dendrogram(keji_coniss, aes(y = depth), label = "CONISS") +
  scale_y_reverse() +
  facet_grid(vars(location), vars(label), scales = "free_y") +
  labs(y = NULL, x = "Dispersion")
```

These plots can be combined using `patchwork::wrap_plots()`, resulting in the finished stratigraphic plot (Figure 4.7).

```
# Figure 4.7
wrap_plots(
  keji_plot +
    theme(
      strip.background = element_blank(),
      strip.text.y = element_blank()
    ),
  dendro_plot +
    theme(
      axis.text.y.left = element_blank(),
      axis.ticks.y.left = element_blank()
    ) +
    labs(y = NULL),
  nrow = 1,
  widths = c(6, 1)
)
```

4.6 Discussion

Several programs are available that are capable of producing paleoenvironmental diagrams of the type produced by this package. In R, the *analogue* and *rioja* packages have functions that specifically produce stratigraphic diagrams (Simpson and Oksanen 2020; Juggins 2019). Functions in both these packages require data with parameters as columns and use dozens

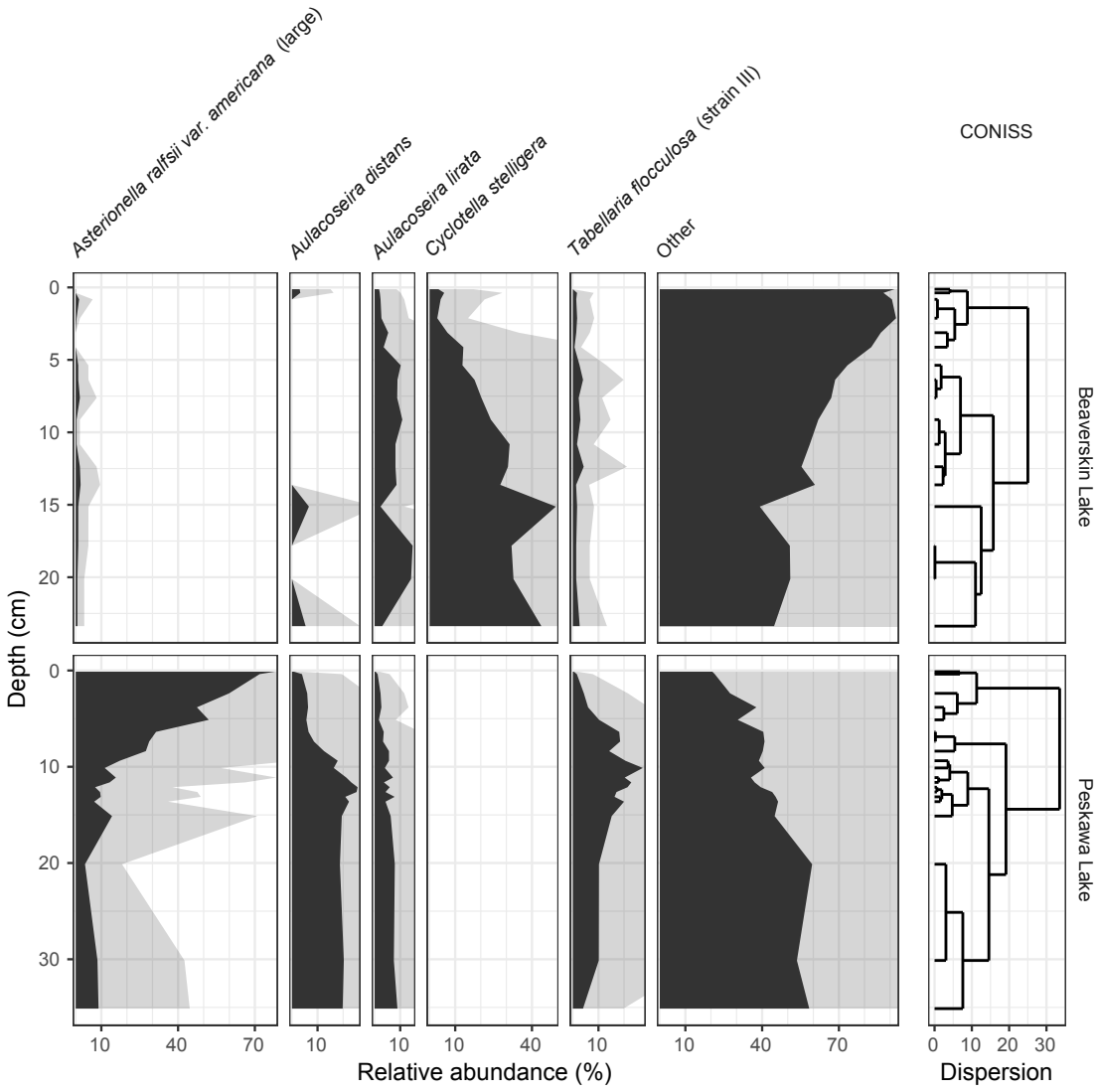

Figure 4.7: Relative abundances and cluster analysis of microfossil diatom relative abundance from two lakes in Kejimkujik National Park, Nova Scotia, Canada.

of arguments to a single function to control the various options for display. This makes the functions highly useful for very specific types of data, but limit their ability to align multiple plots or communicate error (Figure 4.8; Figure 4.9).

Several desktop applications are also commonly used to create paleoenvironmental diagrams, including *Tilla*Graph* (Grimm 2002) and *C2* (Juggins 2011). *Tilla*Graph* creates graphics that are highly customizable, and the program includes the ability to visualize core lithology in addition to plots of multiple parameters (Figure 4.10). *C2* also creates graphics that are highly customizable, and the program includes the ability to use two y-axes next to each other to clearly communicate possible changes to the sedimentation rate (Figure 4.11). Both programs share the disadvantages of many desktop applications, notably, these applications are only available for Windows, and the need for point-and-click edits introduces non-reproducibility if the figure data must be updated.

```
kellys_lake_geochem_wide <- kellys_lake_geochem %>%
  select(location, param, depth, age_ad, value) %>%
  pivot_wider(names_from = param, values_from = value) %>%
  arrange(depth)

# Figure 4.8
withr::with_package("analogue", {
  Stratiplot(
    kellys_lake_geochem_wide %>%
      select(-location, -depth, -age_ad),
    kellys_lake_geochem_wide$depth,
    ylab = "Depth (cm)",
    rev = TRUE,
    varTypes = "absolute"
  )
})
```

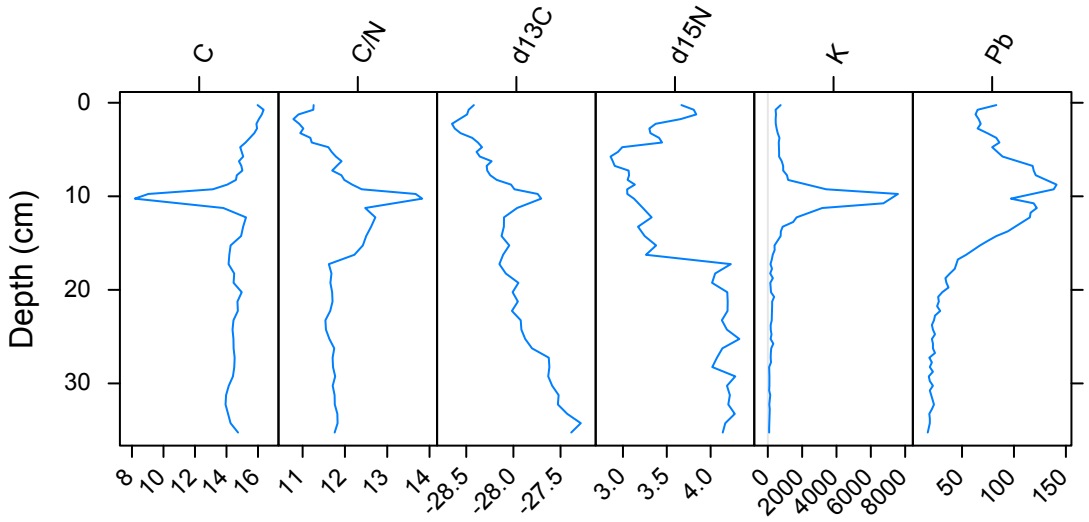

Figure 4.8: A stratigraphic diagram created using the *analogue* package.

```
# Figure 4.9
withr::with_package("rioja", {
  strat.plot(
    kellys_lake_geochem_wide %>%
      select(-location, -depth, -age_ad) %>%
      as.matrix(),
    kellys_lake_geochem_wide$depth,
    xSpace = 0.03,
    ylabel = "Depth (cm)",
    y.rev = TRUE
  )
})
```

The *tidypaleo* package has attempted to build on the best from each of these software packages: functions from *analogue* and *rioja* produce excellent reproducible representations of relative abundance data and include the ability to visualize hierarchical clusters as zones or

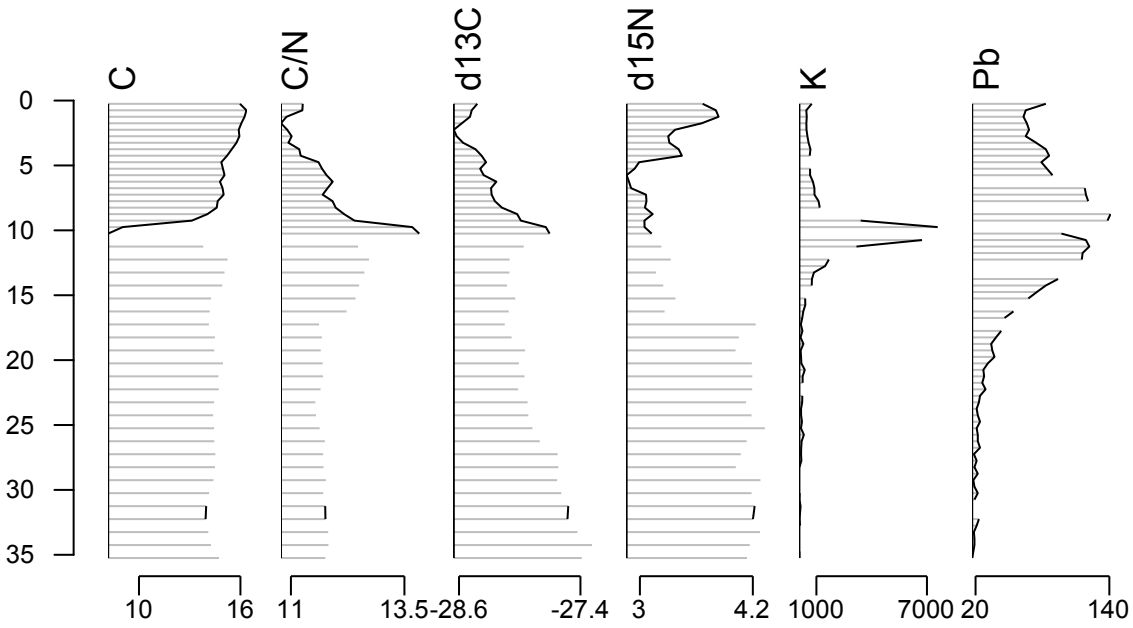

Figure 4.9: A stratigraphic diagram created using the *rioja* package.

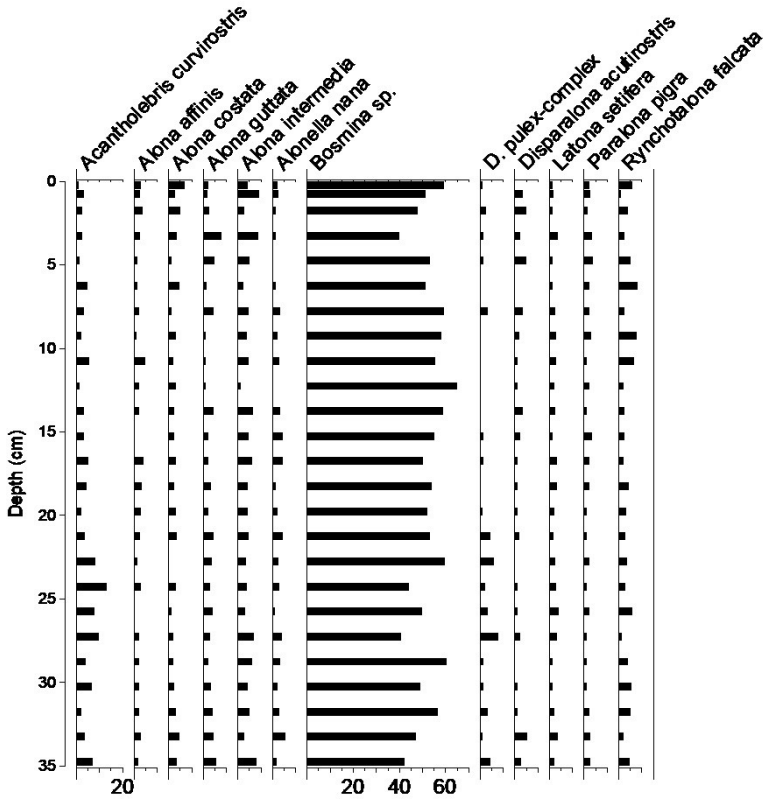

Figure 4.10: A stratigraphic diagram created using *TiliaGraph* software.

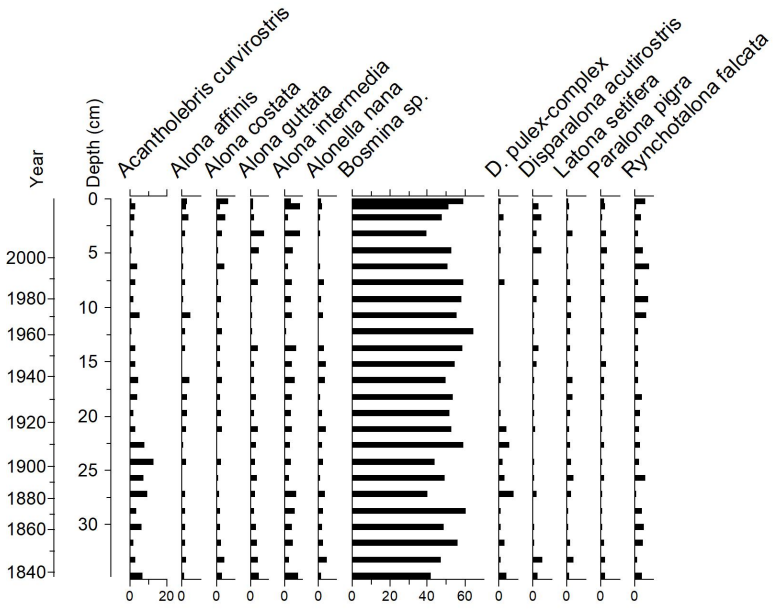

Figure 4.11: A stratigraphic diagram created using *C2* software.

dendrograms as part of the visualization. *Tilla*Graph* and *C2* produce visually appealing diagrams and have interfaces that are well-suited to a non-technical audience. While *tidypaleo* does require coding to make a publishable diagram, there are a large number of resources from which users can draw to learn *ggplot2* (Wickham and Grolemund 2017; Wickham 2009; Healy 2018). We think this also benefits users, who can re-use *ggplot2* concepts from *tidypaleo* to create high-quality diagrams in other disciplines.

4.7 Conclusion

The *tidypaleo* package is an extension of *ggplot2* for R statistical software that provides a number of reusable components for visualizing paleoenvironmental data (Wickham et al. 2020a; R Core Team 2019), such as Pb concentrations and land-use change indicators from many lake sediment records. These components are based on a data structure in the form of one row per measurement, which allows existing concepts in *ggplot2* and the Grammar of Graphics (Wilkinson 2005) to be used to create high-quality paleoenvironmental diagrams. These techniques allow for syntax that might be accessible for the average paleolimnological investigator, such that high-resolution data from many archives can be analyzed and visualized by a wide variety of scientists, engineers, and consultants.

Chapter 5

Anthropogenic Activity in the Halifax Region, Nova Scotia, Canada, as Recorded by Bulk Geochemistry of Lake Sediments

Published in *Lake and Reservoir Management* with co-authors Ian S. Spooner[1], Wendy H. Krkošek[2], Graham A. Gagnon[3], R. Jack Cornett[4], Joshua Kurek[5], Chris E. White[6], Ben Misiuk[7], and Drake Tymstra[8] (Dunnington et al. 2018).

5.1 Abstract

Advances in Portable X-Ray Fluorescence (pXRF) technology have led to the availability of high-resolution, high-quality bulk geochemical data for aquatic sediments, which in combination with Carbon, Nitrogen, $\delta^{13}C$, and $\delta^{15}N$ have the potential to identify watershed-scale disturbance in lake sediment cores. We integrated documented anthropogenic disturbances and changes in bulk geochemical parameters at 8 lakes within the Halifax Regional Municipality (HRM), Nova Scotia, Canada. These data reflect more than two centuries of anthropogenic disturbance in the HRM that included deforestation, urbanization and related development, and water-level change. Deforestation activity was documented at Lake Major and Pockwock Lake by large increases in Ti, Zr, K, and Rb (50–300%), and moderate increases in C/N (>10%). Urbanization was resolved at Lake Fletcher, Lake Lemont, and First Lake by increases in Ti, Zr, K, and Rb (10–300%), decreases in C/N (>10%), and increases in $\delta^{15}N$ (>2.0‰). These

[1]Department of Earth & Environmental Science, Acadia University, 12 University Ave., Wolfville, Nova Scotia, Canada B4P 2R6

[2]Halifax Water, 450 Cowie Hill Road, Halifax, Nova Scotia B3P 2V3

[3]Centre for Water Resources Studies, Department of Civil & Resource Engineering, Dalhousie University, 1360 Barrington St., Halifax, Nova Scotia, Canada B3H 4R2

[4]Andreé E. Lalonde Accelerator Mass Spectrometry Lab, Department of Earth Science, University of Ottawa, Ottawa, Ontario K1N 6N5

[5]Department of Geography and Environment, Mount Allison University, Sackville, New Brunswick E4L 1A7

[6]Nova Scotia Department of Energy and Mines, P.O. Box 698, Halifax, Nova Scotia B3J 2T9

[7]Department of Geography, Memorial University of Newfoundland, St. John's, Newfoundland A1C 5S7

[8]Department of Earth & Environmental Science, Acadia University, 12 University Ave., Wolfville, Nova Scotia, Canada B4P 2R6

data broadly agree with previous paleolimnological bioproxy data, in some cases identifying disturbances that were not previously identified. Collectively these data suggest that bulk geochemical parameters are a useful method with which to identify watershed-scale disturbance in lake sediment archives.

5.2 Introduction

Chapter 2 established the potential importance of watershed-scale disturbance and analysis of multiple lake sediment records to explaining variability of Pb accumulation at the local to regional scale, and Chapter 3 established that several elements traditionally used to infer watershed-scale disturbance are well-characterized by portable X-Ray Fluorescence (pXRF). Chapter 4 established a software package that can be used to visualize and analyze many lake sediment records. Collectively, these methods allow the measurement and analysis of element concentrations that may be useful for reconstructing land-use change at a watershed scale from many lake sediment records; however, these methods are only useful if concentrations of these elements are reliable indicators of disturbance.

Minerogenic elements such as titanium (Ti), potassium (K), rubidium (Rb), zirconium (Zr), and calcium (Ca) are commonly used to reconstruct land-use change or anthropogenic disturbance (Walker et al. 1993; Dixit et al. 2000; Brunschön et al. 2010; Simonneau et al. 2013), although few studies explicitly test the sensitivity of these elements as indicators of watershed disturbance using comparison to historical records. Carbon (C), Nitrogen (N), and stable isotopes of C and N ($\delta^{13}C$ and $\delta^{15}N$, respectively) can be used to infer changes in origin of sedimentary organic matter, changes in nutrient source, and changes in autochthonous productivity (Meyers and Teranes 2001; Mayr et al. 2009) and have the potential to enhance the sensitivity of bulk geochemical indicators when combined with minerogenic elemental geochemistry (Dunnington et al. 2016). C, N, $\delta^{13}C$, and $\delta^{15}N$ are also often compared with historical land-use change, primarily in connection with cultural eutrophication (Brenner et al. 1999; Köster et al. 2005; Routh et al. 2009), however few studies use these parameters in combination with minerogenic elemental geochemistry to enhance the sensitivity of minerogenic parameters to land-use change or anthropogenic disturbance.

The Halifax Regional Municipality (HRM), located on the southeast coast of Nova Scotia, Canada, has a long history of anthropogenic disturbance, including deforestation, land clearing,

agriculture, urbanization, and water-level change. The HRM contains hundreds of lakes, many of which have been previously studied from a land use (Mandell 1994), water quality (Ogden 1971; Anderson et al. 2017; Poltarowicz 2017), or paleolimnological perspective (Tropea et al. 2007; Ginn et al. 2010; Tymstra 2013; Misiuk 2014; Ginn et al. 2015). Lakes serve as the primary drinking water supply for residents of the HRM, and as a result, lake managers have identified long-term data as critical to managing these resources (Anderson et al. 2017). Historical information about the HRM is readily accessible, and much has been documented with respect to historical land-use change in the region. In this study we use dated sediment cores from 8 lakes in the HRM to test the sensitivity of these indicators to historically-documented watershed-scale disturbance, and document how these disturbances are recorded in the bulk geochemical record.

5.3 Study Site

Eight lakes were selected from the HRM that encompassed a variety of land-use histories and watershed characteristics (Table C.1; Figure 5.1). Watershed area for study lakes ranged from <600 ha (Bennery Lake, First Lake, Second Lake, Lake Lemont, First Chain Lake; Table C.1) to >5,000 ha (Lake Major, Pockwock Lake; Table C.1). Lake Fletcher had a watershed area of approximately 16,000 ha, which also contained the watersheds of First and Second Lake. Some watersheds are now primarily forested (>90%: Bennery Lake, Lake Major, Pockwock Lake, Lake Lemont), whereas others now contain widespread residential and/or commercial development (First Lake, Second Lake, Lake Fletcher, First Chain Lake). Six lakes (Bennery Lake, Lake Lemont, First Chain Lake, Lake Major, Pockwock Lake, and Lake Fletcher) currently serve as primary or backup water supplies for Halifax Water, the utility responsible for water and wastewater services in the HRM. The lakes are all oligotrophic on the basis of total phosphorus measurements (Table C.1), however some are mesotrophic on the basis of Secchi depth, possibly due to dissolved organic carbon in some of the lakes (CCME 2004; Carlson and Simpson 1996).

The study lakes were also selected such that previous work was available with which to compare our results. Ginn et al. (2015) performed a diatom-based paleoecological study of anthropogenic stressors on 51 lakes in the HRM and found that Pockwock Lake, First Chain Lake,

and Lake Major were affected primarily by acidification; Lake Fletcher was affected primarily by nutrients; and First Lake, Second Lake, and Lake Lemont were affected primarily by climate. Lake Fletcher, Lake Lemont, and First Lake were additionally found to be affected by an increase in salinity due to road salt application (Ginn et al. 2015). Pockwock Lake has been studied in detail by Tropea et al. (2007), who found two distinct decreases (~1940 and ~1992) in diatom-inferred pH between the early 1800s and 2002, and Ginn et al. (2010), who found little change in chrysophyte assemblages over time. Tymstra (2013) and Misiuk (2014) evaluated the limnology and bulk geochemical paleolimnology of First Lake and Second Lake, respectively, the results of which are used in this study.

Mandell (1994) evaluated water quality and land-use change in 34 lakes in the HRM after Ogden (1971) and found that the primary stressor was road salt input at Second Lake, and regional acidic deposition was the primary stressor at Pockwock Lake. In general, HRM watershed hydrological regimes were often impacted by deforestation within a watershed, new stormwater input from increased watershed impervious surfaces often induced nutrient input leading to eutrophication, and residential lawn development likely increased P concentration in HRM lakes (Mandell 1994). Poltarowicz (2017) quantified phosphorus (P) dynamics at Lake Fletcher, finding that septic systems were likely a major contributor of P to the lake. Fraser (1986) evaluated groundwater contributions to the Chain lakes system, and Anderson et al. (2017) documented recent (since 1999) decreases in sulfate deposition resulting in increased pH and treatment challenges at Lake Major. Finally, Stantec Consulting Ltd. (2012) evaluated the results of the HRM Lakes Water Quality Monitoring program, which measured water quality parameters over 5 years at many HRM lakes, including Lake Fletcher, First Chain Lake, First Lake, and Second Lake.

5.4 Materials and Methods

5.4.1 Historical Methods

Watershed history is critical when evaluating the results of paleolimnological studies, as land-use data provide context for observed trends in geochemical parameters (Smol 1992; Swetnam et al. 1999; Garrison and Wakeman 2000). To obtain historical land-use information, aerial photographs between 1964 and 2013 were georeferenced and evaluated for potential

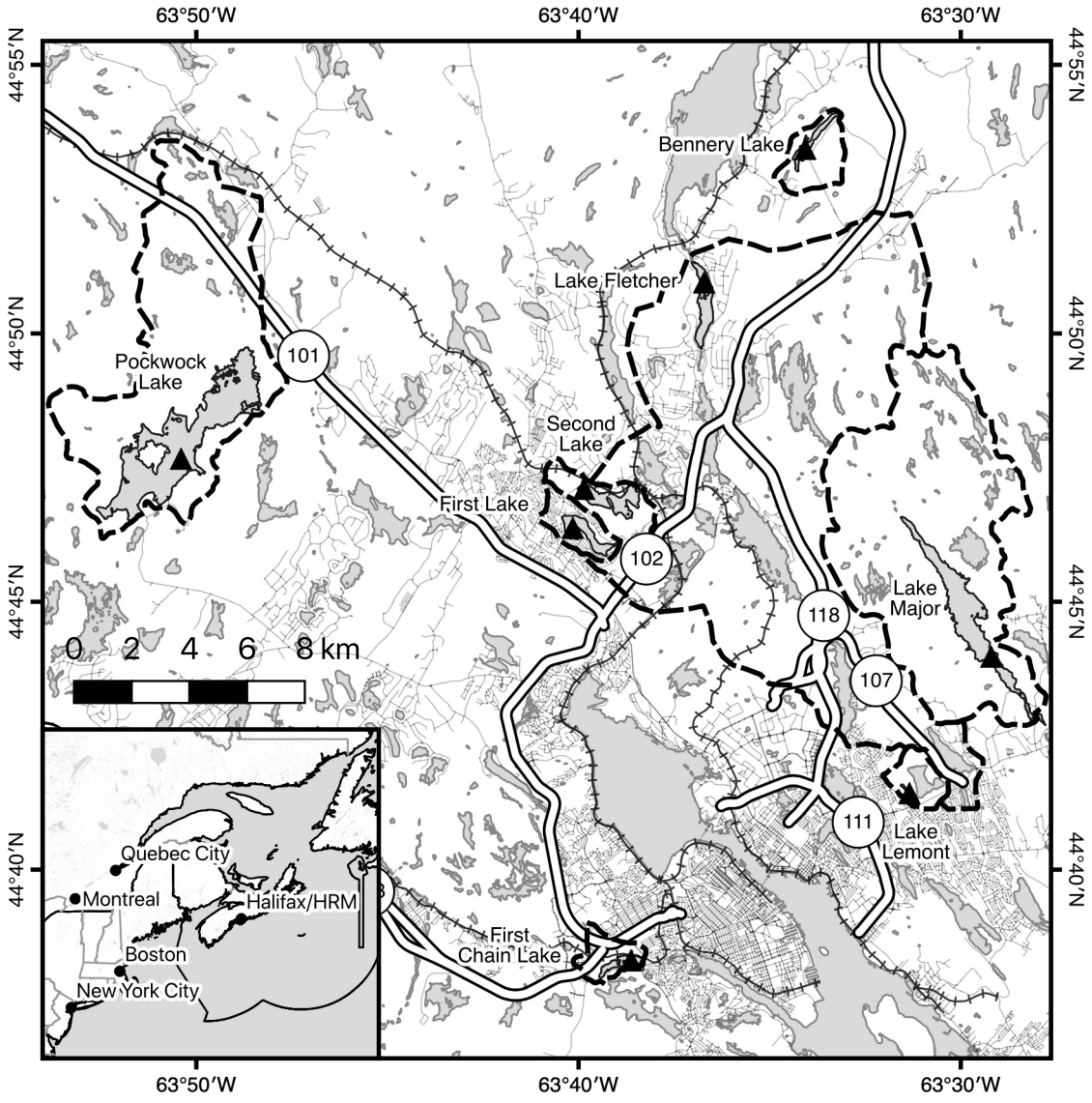

Figure 5.1: Overview of chapter study lakes in the context of the Halifax Regional Municipality (HRM).

watershed disturbances. Aerial photographs were available approximately once per decade for study lakes and were obtained from the Nova Scotia GeoNOVA Aerial Photography Collection (Nova Scotia Department of Natural Resources 2017). Early watershed history was researched by reviewing resources on early deforestation and canal-building in Nova Soctia such as those contributed by Bouchette (1831), Johnson (1986), and Burrows (2003). Additionally, the Nova Scotia Institute of Science archive and the Local History collection at the Halifax Regional Library were reviewed for early material on Halifax area lakes.

Historical periods of disturbance are described in detail in the text, but summarized using the abbreviations Deforestation, Water Works, Agriculture, and Urbanization. Deforestation is used when it is suspected that the land was cleared or logging was active in the watershed. Water Works is used to denote the construction of treatment facilities, which in some cases also involved water level change (e.g., Lake Major, Pockwock Lake). Agriculture is used where there are specific references to a farm in the literature. Finally, Urbanization is used when widespread residential, commercial, and/or industrial development occurred in the watershed.

5.4.2 Coring and Sampling

Sediment gravity cores were collected using a Glew gravity coring device (Glew 1989; Glew et al. 2001) from Lake Major, Pockwock Lake, Bennery Lake, First Chain Lake, Lake Fletcher, and Lake Lemont during 2015 and 2016 (Table C.1); Figure 5.1). Cores from these lakes were extruded using a Glew portable extruder (Glew 1988; Glew et al. 2001) at 0.5 cm intervals for the top 10.0 cm and at 1.0 cm intervals thereafter except the core from Bennery Lake, where samples were extruded at 0.5 cm for the top 5.0 cm and 1.0 cm intervals thereafter. The core from Second Lake was collected in 2013 (Misiuk 2014); the core from First Lake was collected in 2012 (Tymstra 2013). These cores were split and volumetrically subsampled at 1.0 cm intervals. Cores were collected from the deepest basin of each lake except for the core from Lake Major, where the core was collected from the southernmost basin at a depth of 26 m due to field constraints (Table C.1). All sediment samples were dried at 60 C for 48 h and ground using a mortar and pestle prior to geochemical measures.

5.4.3 Bulk Sediment Geochemistry

For this study, we used sedimentary concentrations of Ti, Zr, K, Rb, and Ca, which are elements whose concentrations are both well-characterized by XRF, and have been used in the past to characterize land-use change, particularly erosion (Mackereth 1966; Engstrom and Wright 1984; Garrison and Wakeman 2000; Simonneau et al. 2013; Rouillon and Taylor 2016). Elemental geochemistry was measured in the laboratory using portable X-Ray Fluorescence spectrometer (pXRF). X-Ray Fluorescence has long been used to measure elemental geochemistry in lake sediments (Boyle 2000) and more recently, investigators have reported replicable results from field-portable XRF models for use in aquatic sediments measuring elemental geochemistry of algae (Bull et al. 2017), contaminated soils (Rouillon and Taylor 2016), bedrock (White et al. 2014; Tarr and White 2016), wetland sediments (Loder et al. 2017), and in paleolimnological studies (Dunnington et al. 2016; Dunnington et al. 2017). Elemental concentrations recorded by the pXRF instrument were in parts per million (ppm) according to a factory calibration. Replicates indicated that our data were precise, but because the factory calibration was not matrix-specific to lake sediments, it is challenging to compare absolute concentration values from this study to non-pXRF studies (Hunt and Speakman 2015).

Sediment samples for C, N, and stable isotopes of C and N ($\delta^{13}C$ and $\delta^{15}N$, respectively) were sent to the Stable Isotopes in Nature Laboratory (SINLAB) at the University of New Brunswick. These parameters represent both the organic and inorganic components of the sample. Isotopic composition of carbon ($\delta^{13}C$) was measured relative to the Vienna Pee Dee Belemnite (VPDB), and isotopic composition of nitrogen ($\delta^{15}N$) was measured relative to the atmospheric value. C/N ratios were calculated as mass ratios.

For pXRF analyses, every 5^{th} sample throughout each core was analyzed in triplicate to quantify uncertainty. In addition to standard SINLAB QA/QC protocols for organic analyses, 20 samples were run in duplicate to quantify uncertainty for organic matter parameters. Median relative standard error (RSE) values were less than 4% for all study parameters. Because some individual error values were high (>10%), error bars were included in relevant visualizations. Error bars, when large enough to be visible, represent ± one standard error.

The magnitude of changes in geochemical parameters is reported in this study as (*new value* - *old value*) / *old value*, expressed as a percent. Changes in $\delta^{13}C$ and $\delta^{15}N$ are reported as (*new value* - *old value*) expressed in permille (‰), because these values are not zero-based.

5.4.4 Age-Depth Models

^{210}Pb activity was estimated using a ^{210}Po assay measured by alpha spectroscopy at the André E. Lalonde AMS laboratory at the University of Ottawa. Dating uncertainties were propagated in quadrature based on measurement uncertainties in weighing, radiochemical extraction, and radionuclide counting. Ages and sedimentation rates were calculated according to the constant rate of supply (CRS) model (Appleby and Oldfield 1983). Supported ^{210}Pb activity was estimated using the background ^{210}Pb, propagating the standard deviation of the background ^{210}Pb activity through further calculations in quadrature. Ages for depths prior to the ^{210}Pb background were extrapolated based on the average sedimentation rate of ^{210}Pb-dated depths and were interpreted with caution. Mass accumulation rates (MAR) were calculated using the CRS model and bulk density, which was calculated by weighing the total dry mass of each extruded slice divided by its volume, except for cores FLK12-1 and SLK13-1, for which bulk density was calculated by dividing the dry mass of the volumetric subsample by its volume.

No ^{210}Pb data were available for core FLK12-1 (First Lake), whose chronology was constrained by the point where total elemental Pb concentrations rise above background matched to the core from Second Lake (~1895), the peak of the total elemental Pb concentration matched to the core from Second Lake (~1958), and the time at which the core was collected (2012; Figure C.1). First Lake is adjacent to Second Lake (Figure 5.1), and it is unlikely that the base and peak of the total Pb concentration profile occurred at different times in the sediment profile. Using anthropogenic Pb deposition as an isochronous marker is not precise (Norton et al. 1992; Blais et al. 1995), but was adequate to constrain the chronology for core FLK12-1. Total elemental Pb concentrations for First Lake and Second Lake are provided in the Supplement.

5.4.5 Numerical Analyses

Variation in bulk geochemical parameters was summarized using principal components analysis (PCA). PCA is commonly used in paleolimnological studies to summarize a large number of variables (Legendre and Birks 2012). Variables were scaled to a variance of 1 (grouped by core) prior to the PCA. Both pXRF and organic analyses were performed on most samples. Samples where all values were not available were removed prior to the PCA. For comparability purposes, the sign of the first principal component was adjusted such that Ti was positively

loaded onto the first component. Calculations were performed using R statistical software (R Core Team 2019).

5.5 Results

5.5.1 Historical Observations

The earliest disturbance on HRM lakes was likely deforestation and land-clearing by European settlers. The HRM was settled by the British in the mid-1700s, which likely marked the start of systematic land clearing in the area (Davis and Browne 1996). This early clearing likely would not have affected lakes other than Lake Lemont and First Chain Lake, which are located closest to the population centers of Dartmouth and Halifax, respectively. First Chain Lake was adopted as the city water source for Halifax in 1848, when a canal was constructed between Long Lake (to the southwest) and the Chain lakes for the purposes of increasing the potential drinking water supply of the lakes (Johnston 1908). Several mills used flow from the Chain lakes for power, several farms existed along St. Margret's Bay road to the south of the lake, and granite quarries were located close to the canal (*Province of Nova Scotia, Halifax County, City of Halifax Sheet, No. 68* 1908). As early as 1905, "pollution" in the watershed was identified as a potential problem (Halifax Water Commission 1995). Lake Lemont was adopted as the water supply for Dartmouth in 1891, was the site of a mill as early as the late 1700s, and was the site of a farm and gristmill at the time it was purchased by the Dartmouth Town Council in 1878 (Martin 1957).

In the early 1800s, deforestation was rapidly occurring in the Halifax area, such that in 1838 it was declared that forestry would soon be finished in the province (Creighton 1988). Lakes and streams were efficient methods for transporting lumber prior to widespread railway and road construction (Davis and Browne 1996). The forest composition near Lake Major is mentioned specifically on an 1831 map by Bouchette (1831), at least one mill was located at the outlet of Pockwock Lake in 1823 (Bezanson 1993), and Lake Fletcher was a part of the Shubanacadie Canal route, initially constructed in the mid-1800s (Bouchette 1831). It is likely that these shorelines were logged at some point during the mid-1800s due to ease of transportation to market. Several other mills existed on Pockwock Lake prior to 1970, with the height of productivity between 1880 and 1940 (Bezanson 1993).

Construction of railways in the late-1800s likely expanded the areas that were logged, and according to Dr. B.E. Fernow's forest survey in 1909 and 1910, half of the province was estimated to be cleared (Burrows 2003). The construction of the railways adjacent to First Chain Lake (Canadian National) and Second Lake (Windsor & Annapolis Railway) likely resulted in more rapid clearing in these areas (Smiley 1971), and to some extent the watersheds of First Lake and Bennery Lake, which did not contain a railway but were situated close to well-established rail lines. With construction of roads and the advent of the pulp and paper industry, further clearing of study lake watersheds was likely during the first half of the 20th century (Burrows 2003).

Based on aerial photography available starting in 1964, widespread construction of roads, residential development, and construction of water treatment works were the primary disturbances in study lake watersheds (Nova Scotia Department of Natural Resources 2017). The Lake Lemont area was already well-developed by 1964, although little development was undertaken within the watershed itself except for the road at the south end of the lake, from which stormwater was routed out of the watershed following upgrades in the 1980s and 1990s. The complete Lake Fletcher watershed includes a very large area (16,000 ha) that was also well developed by 1964, although residential development in the immediate watershed also occurred during the 1980s and 1990s. In 1985, a wastewater treatment plant commenced operation, discharging treated wastewater to the inlet of Lake Fletcher. In 2011, a smaller plant started discharging treated wastewater near the outlet of the lake.

In the First Lake watershed, Mandell (1994) reported a 42% increase in urban land use between 1967 and 1986, compared to a 26% increase in urban land use at the adjacent Second Lake, although development at Second Lake only occurred at the outer reaches of its watershed. Construction of the 103 highway and St. Margret's Bay Road occurred prior to 1969 in the Chain lakes watershed, followed by the construction of the Ragged Lake Business Park in the late 1990s. Significant acid rock drainage (ARD) occurred in the Chain lakes watershed because of road and rail construction, commercial development, and infrastructure upgrades (Tarr and White 2016). Aerial photography indicated the Bennery Lake watershed appears to have undergone the least disturbance, with airphotos indicating the construction of a power line across the lake to service the Halifax Airport in the 1960s, and minor logging and peripheral residential development in the late 1990s and early 2000s.

Treatment works at Pockwock Lake were constructed starting in 1977, treatment works on Lake Major were constructed starting in 1999, and treatment works at Bennery Lake were constructed in the 1980s with some infrastructure upgrades in the early 2000s. Treatment works on Pockwock Lake and Lake Major were accompanied by dam construction and water-level increase, although a dam existed at Pockwock Lake at least as early as 1966 (Canadian-British Engineering Consultants 1966). The 101 highway was constructed and some residential development occurred within the Pockwock Lake watershed in the 1970s and 1980s, and by 1992 twinning of the 101 highway was complete. Localized deforestation has been present in the watershed from the 1970s to present (Steenberg et al. 2013). Hurricane Juan (2003) also caused a large amount of destruction in some areas of the Lake Major watershed, and presently small amounts of timber are harvested from the watershed (Steenberg et al. 2013).

5.5.2 Age-Depth Models

Halifax area lake sediments contained enough ^{210}Pb activity to assign dates with low uncertainty from ~1900 to present for most lakes (s.d. <15 years at 1900: Bennery Lake, Second Lake, and First Chain Lake), and from ~1925 for all lakes (Figure 5.2). All lakes exhibit an exponential decline in ^{210}Pb activity with increasing core depth. Stable backgrounds of ^{210}Pb activity are generally recognized between ~15 and 20 cm at each lake. Approximate basal ages for cores ranged from ~1650 (First Chain Lake) to ~1780 (Lake Fletcher). Mean mass accumulation rates (MAR) ranged from 102 g/m^2/yr (First Chain Lake) to 156 g/m^2/yr (Lake Major and Lake Fletcher), except at Second Lake, where the mean sediment accumulation rate was 551 g/m^2/yr. The deepest basin at Second Lake was closer to an inlet stream than the deep basins of other lakes, which is likely responsible for the higher MAR at this site.

5.5.3 Numerical Analyses

PCA summarized 79–95% of the variability of bulk geochemical parameters in the first two principal components (PC1 and PC2; Figure 5.3; Figure C.2). PC1 captured between 53 and 77% of the total variation. Ti was loaded positively on the PC1 axis by definition. K, Rb, and Zr were all positively loaded on the PC1 axis for all lakes, whereas C was negatively loaded on the PC1 axis for all lakes. At Lake Major, Pockwock Lake, and Bennery Lake, δ^{15}N was aligned with C on PC1; at Second Lake, Lake Fletcher, Lake Lemont, First Lake, and Second

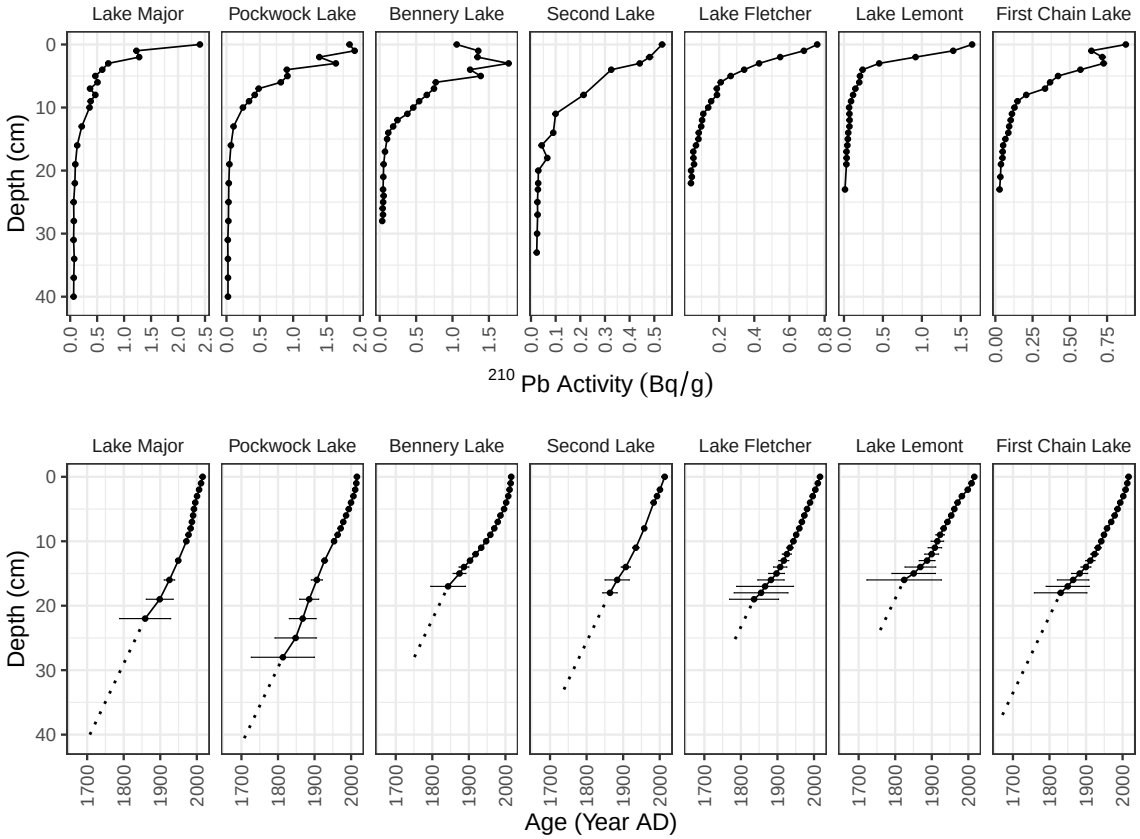

Figure 5.2: ^{210}Pb activity and age for ^{210}Pb-dated cores in this chapter. Dashed line indicates extrapolated ages estimated for depths at and prior to background ^{210}Pb values.

Lake, $\delta^{15}N$ was aligned with Ti on PC1. C/N ratios were generally aligned with C on PC1 except at Lake Major and Pockwock Lake. The loadings of $\delta^{13}C$ and Ca were generally small and were inconsistent between lakes. PC1 scores were interpreted as the combined response of the suite of proxies used in this study.

5.5.4 Bulk Sediment Geochemistry

Deforestation and related activity were the primary disturbances in the catchments of Lake Major, Pockwock Lake, Bennery Lake, and Second Lake; however, these disturbances only appeared to be clearly resolved in Lake Major and Pockwock Lake (Figure 5.3). Early deforestation on Pockwock Lake may have been recorded as an increase in Ti and Ca ~1850; however, the age uncertainty at this depth and stability of other parameters make it difficult to confirm that early deforestation at Pockwock Lake was clearly resolved in the bulk geochemical record. Later (~1880–1940), more intense mill and deforestation activity on Pockwock Lake occurred, resulting in more frequent use of the lake for transporting timber, in addition to deforestation surrounding the lake (Bezanson 1993, D. Haverstock, pers. comm.). During this period C concentrations decreased by 18%, C/N ratios increased by 11%, and minerogenic element concentrations increased (Ti: 110%, Zr: 221%, K: 166%, Rb: 69%, respectively). $\delta^{13}C$ values decreased slightly from −27.4‰ to −27.8‰, and $\delta^{15}N$ increased slightly from 1.9‰ to 2.2‰. During the period of initial deforestation in the Lake Major catchment (1830–1860), responses were similar to those at Pockwock Lake but smaller in magnitude for minerogenic elements (Ti: +86%, Zr: +115%, K: +110%, Rb: +44%). Increases in C/N values for Lake Major during this period were larger than for Pockwock Lake (+26%), but other organic parameters ($\delta^{13}C$, $\delta^{15}N$, C) had opposite trends than those observed at Pockwock Lake. Bulk geochemical changes at the time of estimated deforestation were more subtle for other lakes, where parameter values at this time generally show no consistent pattern. PC1 scores deviated from background values following initial clearing at all study lakes, which likely reflects a combination of anthropogenic disturbances that followed initial clearing of the watershed.

Urbanization was the primary disturbance in the catchments of Lake Fletcher, Lake Lemont, First Lake, and First Chain Lake (Figure 5.4), in addition to several post-1950s disturbances on Bennery Lake and Second Lake (Figure 5.3). At Bennery Lake, airport construction that resulted in a powerline constructed across the north tip of the lake in the 1960s resulted in a

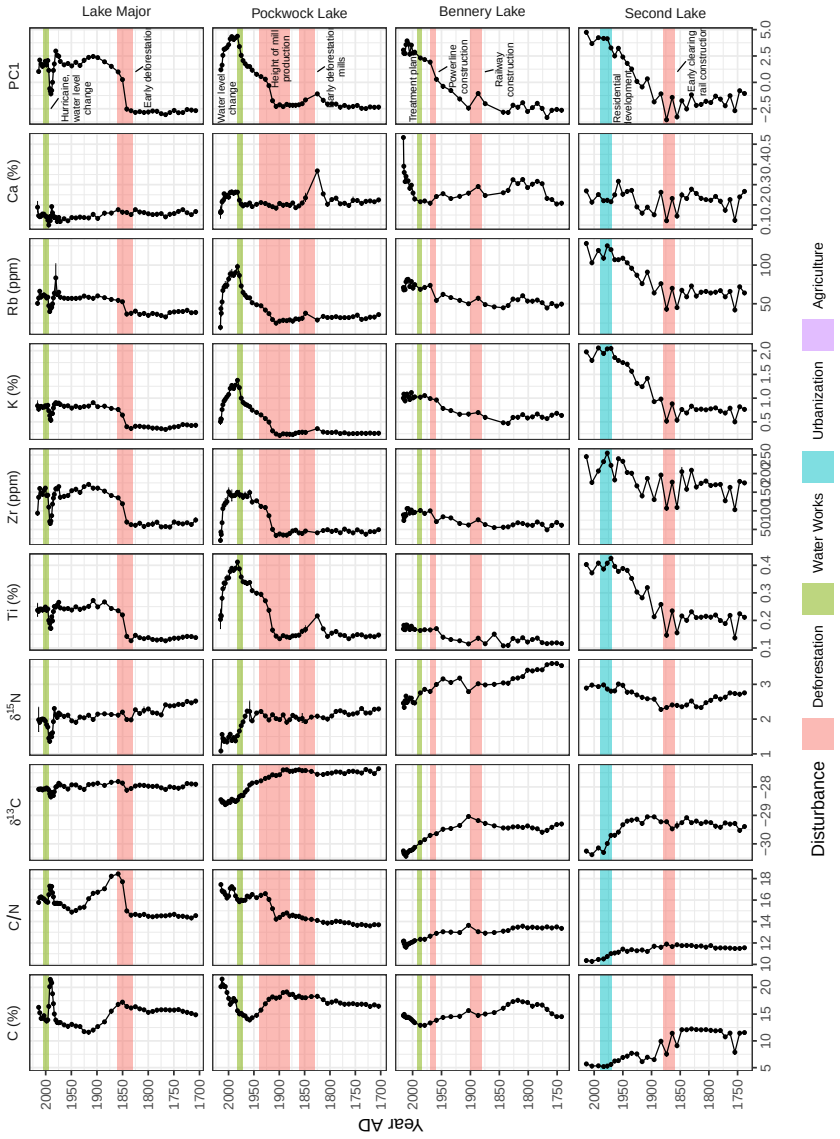

Figure 5.3: Bulk geochemistry, PC1 scores, and periods of probable land disturbance for Lake Major (MAJ15-1), Pockwock Lake (POC15-2), Bennery Lake (BEN15-2), and Second Lake (SLK13-1). Ages prior to 1900 are subject to considerable error, and ages prior to Ĩ850 are estimated using average sedimentation rates over the entire core.

disturbance that was identified by an increase in Rb at this age. Most parameters at Bennery Lake appeared to have a common trend between 1900 and present (C/N: −11%, $\delta^{13}C$: −1.21‰, $\delta^{15}N$: −0.33‰, Ti: +47%, Zr: +44%, K: +51%, Rb: +42%). At Second Lake, the primary disturbance following initial clearing occurred at ~1930, after which C concentrations, C/N ratios, and $\delta^{13}C$ values decreased (C: −25%, C/N: −9%, $\delta^{13}C$: −1.01‰); and $\delta^{15}N$, Ti, Zr, K, and Rb values increased ($\delta^{15}N$: +0.11‰, Ti: +14%, Zr: +22%, K: +25%, Rb: +33%). Mandell (1994) noted that a culvert carrying road runoff entered Second Lake, and it is possible that even though residential development occurred after its installation, initial road construction was better recorded in the bulk geochemical record. Construction of the Windsor & Annapolis Railway in the late 1800s appears to mark the beginning of changes in Ti, Zr, and Rb at Second Lake.

At Lake Fletcher, two periods of urbanization were inferred from the historical record: large-scale urbanization in the upper watershed of the lake (1929–1970), and residential development in the immediate watershed of the lake (1980–2000; Figure 5.4). The onset of urbanization and the end of residential development are resolved reasonably well at Lake Fletcher, the cumulative effect of which appeared to be a decrease in C concentrations and C/N ratios (C: −49%, C/N: −11%), and an increase in $\delta^{13}C$, $\delta^{15}N$, Ti, Zr, K, and Rb ($\delta^{13}C$: +0.49‰, $\delta^{15}N$: +2.48‰, Ti: +78%, Zr: +66%, K: +115%, Rb: +78%). Effects on Lake Fletcher in the mid-1800s due to the construction of the Shubenacadie Canal or deforestation appeared to be minimal. The Lake Lemont watershed adjoins the upper watershed of Lake Fletcher and was also subject to disturbance in the 1800s (e.g., clearing, agriculture, and water works construction). Most urbanization took place outside the Lake Lemont watershed, although a major road was constructed directly adjacent to the lake during this time. Cumulative early disturbance at Lake Lemont resulted in a decrease in C (−49%), and an increase in $\delta^{13}C$, $\delta^{15}N$, Ti, Zr, K, and Rb ($\delta^{13}C$: +0.73‰, $\delta^{15}N$: +1.68‰, Ti: +138%, Zr: +191%, K: +215%, Rb: +112%). Urbanization in the area resulted in further decrease in C concentrations (−17%), and a further increase in $\delta^{15}N$, Ti, Zr, K, and Rb ($\delta^{15}N$: +2.22‰, Ti: +10%, Zr: +4%, K: +17%, Rb: +11%). Peak $\delta^{13}C$ values at Lake Lemont did not occur until ~1990 (peak: −28.00‰).

Urbanization in the watershed of First Lake was intense (Mandell 1994; Tymstra 2013; Misiuk 2014), the onset of which was likely well resolved based on age-depth estimates from stable anthropogenic Pb deposition. From ~1950 to ~2000, C concentrations, C/N ratios, $\delta^{13}C$ values, Zr concentrations, and Rb concentrations decreased (C: −10%, C/N: −6%, $\delta^{13}C$: −0.21‰, Zr:

−12%, Rb: −57%); whereas $\delta^{15}N$ values, Ti concentrations, and K concentrations increased ($\delta^{15}N$: +0.66‰, Ti: +18%, K: 24%). At First Chain Lake geochemical parameters identified two disturbances, likely corresponding to highway construction in the watershed and the construction of the Bayer's Lake industrial park. Between 1920 and 1970, minerogenic element concentrations increased (Ti: +193%, Zr: +327%, K: +302%, Rb: +230%), after which these elements decreased in concentration (Ti: −51%, Zr: −61%, Rb: −51%). C/N ratios and Ca concentrations increased (C/N: +21%, Ca: +77%) and decreased (C/N: −27%, Ca: −56%), but peaked ~1990 instead of ~1970. $\delta^{13}C$ values were increasing from 1970 to the top of the core. Urbanization at First Chain Lake led to widespread bedrock disturbance, which in turn led to acid rock drainage due to the chemical composition of the bedrock (Tarr and White 2016; White et al. 2014; Fraser 1986), which likely dominated how urbanization was recorded in the geochemical record.

At Lake Major, a period of anomalous values was identified ~1984–1995. Historical results suggested two recent disturbances: water-level rise coincident with water works construction ~1999, and Hurricane Juan, which damaged a large amount of forest in the Lake Major watershed. It seems more likely that the anomalous values in this zone are related to one of these two events rather than neither event being recorded in the core as suggested by ^{210}Pb dates, and thus it is likely that the age was estimated incorrectly due to the influx of material caused by the event. The sediment is primarily organic, high C/N material, likely of soil or woody composition. We would expect this type of material to enter the lake either by Hurricane Juan or water level rise. Anomalous values return to pre-disturbance levels following the event. At Pockwock Lake, a disturbance is apparent ~1976, after which time C increased to concentrations slightly greater than prior to 1880 (20%), and Ti, Zr, K, and Rb decreased to concentrations similar to those prior to 1880 (Ti: 0.20%, Zr: 21 ppm, K: 0.51%, Rb: 19 ppm). $\delta^{13}C$ and $\delta^{15}N$ values were both decreasing prior to water level change, and continued to decrease to present.

5.6 Discussion

5.6.1 Watershed Disturbances

The impact of land clearing and deforestation was evident on some but not all lakes despite some evidence of disturbances occurring in all watersheds. Changes were best resolved at

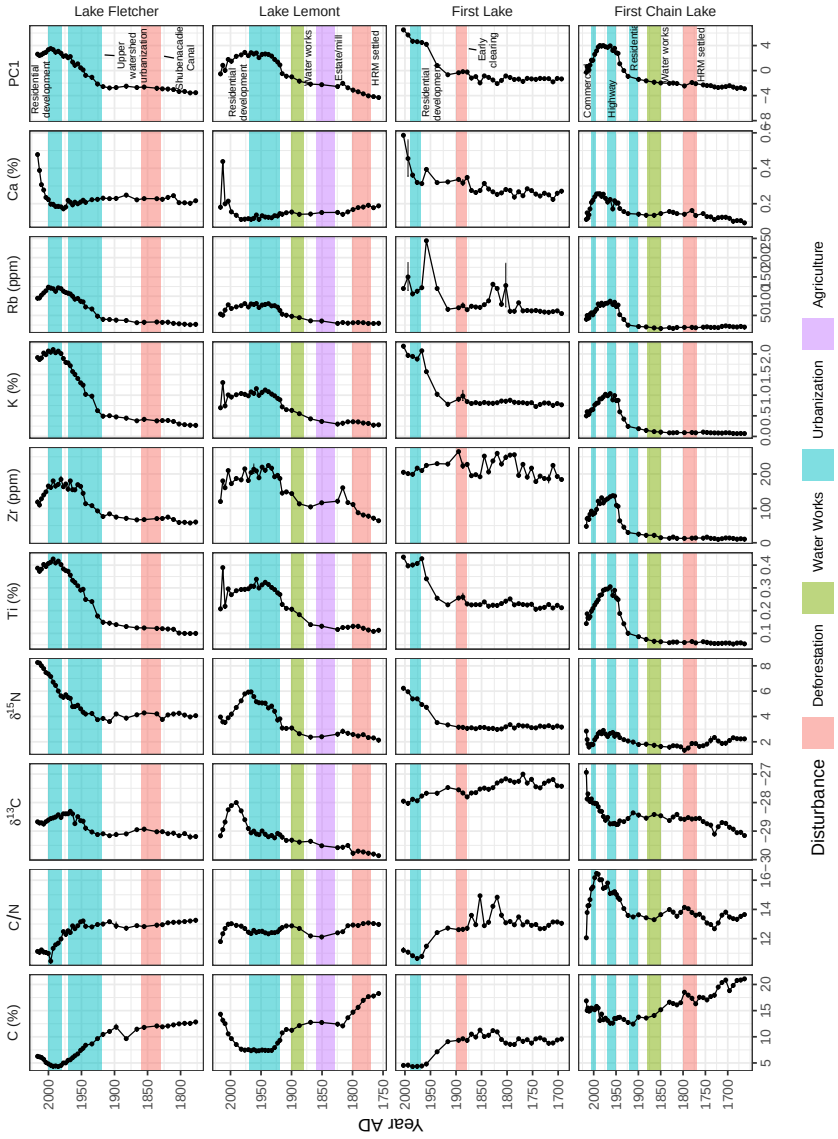

Figure 5.4: Bulk geochemistry, PC1 scores, and periods of probable land disturbance for Lake Fletcher (FLE16-1), Lake Lemont (LEM16-1), First Lake (FLK12-1), and First Chain Lake (FCL16-1). Ages prior to 1900 are subject to considerable error, and ages prior to ĩ850 are estimated using average sedimentation rates over the entire core.

Lake Major and Pockwock Lake, and were recorded in the bulk geochemical sediment record as increases in C/N ratios, Ti, Zr, K, and Rb concentrations, and decreases in C concentrations. Stable isotopes $\delta^{13}C$ and $\delta^{15}N$ did not show a strong trend following deforestation activity at either Lake Major or Pockwock Lake but decreased throughout the period of presumed anthropogenic influence. However, the earliest deforestation activity at Pockwock Lake was not well reflected in the bulk geochemical record, as were other early deforestation activities at other lakes. At Pockwock Lake, an increase in Ti, Zr, K, and Rb (50–300%) suggests increased erosion in the watershed associated with clearing (Engstrom and Wright 1984; Garrison and Wakeman 2000), a decrease in C concentration suggests that clastic input is dominating sedimentation more than any productivity increase associated with soil erosion (Engstrom and Wright 1984), and an increase in C/N ratio indicates organic matter deposition included more terrestrial carbon as compared to autochthonous carbon (Meyers and Teranes 2001). Loadings of C/N and C were aligned on PC1 at these lakes, suggesting that in general, periods of higher C were also periods with a more terrestrial sedimentary organic matter signature (Meyers and Teranes 2001). Previous studies using bioproxies and bulk geochemistry have found that long-term effects from deforestation are small or are not easily resolved in lake sediments, which is consistent with the results of this study (Tremblay et al. 2010; Paterson et al. 1998; Laird et al. 2001).

The period of urbanization as resolved in lakes was also associated with increases in clastic indicators (Ti, Zr, K, and Rb; 10–300%) and a decrease in C concentration; however, unlike the response to deforestation, the C/N ratios decreased during the period of urbanization in all lakes except First Chain Lake. This effect has also been observed in other studies of urbanized watersheds (Rosenmeier et al. 2004; Dunnington et al. 2016). Loadings of C/N and C were not aligned on PC1 at most of these lakes, suggesting that periods of higher C were also periods with a more autochthonous sedimentary organic matter signature. Residents on First Lake and Lake Fletcher have observed deteriorating water quality in the form of algal blooms and decreased clarity (Tymstra 2013; Poltarowicz 2017). These lakes show a high magnitude of decrease in C/N ratios (>10%) and a high magnitude of increase in $\delta^{15}N$ (>2.0‰). At Lake Lemont, $\delta^{15}N$ values also increased by >2.0‰ during the period of urbanization but decreases in C/N ratios were <10%. These data suggest that lower C/N ratios were associated with increased productivity during the period of urbanization, likely in response to increased nutrient input

as suggested by increases in $\delta^{15}N$. Increasing $\delta^{15}N$ has been observed in response to urbanization or increasing population density in a number of studies (Rosenmeier et al. 2004; Köster et al. 2005; O'Reilly et al. 2005; Dunnington et al. 2016), and has been linked to wastewater treatment processes (Leavitt et al. 2006) and increased external nitrate input (Teranes and Bernasconi 2000).

Urbanization at First Chain Lake was not associated with increased $\delta^{15}N$ values or a decrease in C/N ratios to the same extent as First Lake and Lake Fletcher, although $\delta^{15}N$ did increase slightly during this period. The Chain lakes watershed contains bedrock from the Cunard Formation of the Halifax Group (White 2010b), which has a high Sulphur content (White 2010a; White and Barr 2010) and hence a high acid-generating potential (White et al. 2014; Tarr and White 2016). Thus, the effect of development had a markedly different impact on conditions at First Chain Lake than other lakes with urbanized watersheds. During the period of watershed disturbance there was an increase in C/N ratios, and an increase in Ti, Zr, K, and Rb concentrations. First Chain Lake has traditionally had low water-column productivity, likely a result of acidic water column conditions.

Recovery from urbanization or a stabilization of conditions based on bulk geochemical parameter values was observed at lakes with urbanized watersheds following the end of construction (i.e., the end of physical disturbance to the watershed). This effect has also been noted in the literature (Garrison and Wakeman 2000). In particular, $\delta^{15}N$ values at Lake Lemont and First Chain Lake returned to pre-urbanization values following watershed disturbance. $\delta^{15}N$ values in First Lake and Fletcher Lake did not return to pre-urbanization values and continue to increase despite recent stabilization of C/N and clastic indicator elements. This suggests that even though watershed stability increased following the end of new construction, nutrient input may still be occurring in these systems.

Previous paleolimnological studies using minerogenic elemental geochemistry as indicators of urbanization broadly agree with the trend and magnitude of parameters reported in this study. Christopher (1999) observed increases in elemental K concentrations following land clearing, agricultural activity, and urbanization at an urban lake in St. John's, Newfoundland, for which the magnitude of increase was on the order of +100% during combined land clearing and agricultural activity, and +50% during urbanization. Pienitz et al. (2006) observed the opposite

trend at an urban lake in Québec City, Québec: during industrialization and urbanization, elemental C concentrations increased while Al concentrations decreased. It is likely this trend can be attributed to increases in productivity at a magnitude that was not observed in Halifax-area lakes. Rosenmeier et al. (2004) observed a decrease in C/N ratios of about 15% following urbanization at an urban lake in Guatemala, and a $\delta^{15}N$ increase of about 1.5‰ during the same period. Leavitt et al. (2006) reported a 2–5‰ increase in $\delta^{15}N$ values because of treated sewage input to several Canadian prairie lakes.

Construction of water treatment facilities occurred on Lake Major, Pockwock Lake, Bennery Lake, Lake Fletcher, Lake Lemont, and First Chain Lake. In all cases this involved construction of an intake structure, and in other cases involved pipelines/canals to increase the hydrologic throughput of the system (First Chain Lake) or dam construction leading to water level increase (Lake Major, Pockwock Lake). The construction of treatment works was only apparent at Lake Major and Pockwock Lake; other construction was not readily identified. At Lake Major, bulk geochemical parameter values returned to similar levels observed prior to the disturbance; at Pockwock Lake, parameter values changed rapidly following water level change, although this was coincident with mill operations ceasing on the lake. Changes in bulk geochemical parameter values were not consistent between Lake Major and Pockwock Lake at the point of water level change, suggesting that water level change has a lake-specific bulk geochemical signature in these systems.

5.6.2 Interpretation of Geochemical Parameters

As a whole, the bulk sedimentary geochemical parameters used in this study responded strongly to some watershed disturbances (Figure 5.3), primarily driven by changes in Ti, K, Rb, and Zr (Figure C.2). This suggests that erosion of clastic material is well-resolved using elemental concentrations of these four elements, which has long been observed by paleolimnological investigators (Mackereth 1966; Engstrom and Wright 1984; Boyle 2001). In general, concentrations of Ti, K, Rb, Zr, responded together and opposite to C concentrations, which suggests that either organic matter deposition decreased during periods of watershed disturbance, that clastic input diluted organic matter, or both (Cohen 2003). It seems most likely that during periods of watershed disturbance, erosion of inorganic material increased and diluted organic

matter input. The organic matter C/N ratio often changed coincident with watershed disturbance, but sometimes indicated that disturbance resulted in a more terrestrial C/N ratio (Lake Major, Pockwock Lake, and First Chain Lake), or a more autochthonous C/N ratio (First Lake and Lake Fletcher). The greatest changes in $\delta^{15}N$ values occurred when C/N ratios decreased, although it is unclear whether this is a signature of increased anthropogenic nutrient input, increased contribution of autochthonous organic matter, or both.

Several parameters did not systematically respond to watershed-scale land-use change, including Ca and $\delta^{13}C$. These parameters were inconsistently aligned with both historical data (Figure 5.3) and alignment on PC1 (Figure C.2) between lakes. Lime addition was noted at First Chain Lake to control aquatic growth in the late 1800s and early 1900s, likely due to acid-production from erosion of the bedrock exposed during construction of the railway (Johnston 1908). This practice may have occurred on other lakes, complicating the interpretation of Ca concentrations. Ca (Davis and Norton 1978) and $\delta^{13}C$ (O'Reilly et al. 2005) have both been previously noted as varying independent of watershed-scale change, suggesting that they may be representative of autochthonous or atmospheric processes in addition to watershed-scale changes such as carbon source ($\delta^{13}C$) or minerogenic input (Ca).

5.6.3 Comparison to Bioindicator Studies

Several previous paleolimnogical studies examined Pockwock Lake using diatoms (Tropea et al. 2007), scaled chrysophytes (Ginn et al. 2010), and a pre/post anthropogenic impact diatom approach (Ginn et al. 2015), although these studies had a limited ability to evaluate watershed-scale changes that may have influenced observed trends in species composition. Tropea et al. (2007) noted two distinct decreases (~1940 and ~1992) in diatom-inferred pH, neither of which were specifically identified in this study as times of abrupt change. Similarly, the times of abrupt change identified in this study were not identified by Tropea et al. (2007) or Ginn et al. (2010), although the *T. flocculosa* strain III profile from Tropea et al. (2007) appears to respond coincident with lithogenic elements reported in this study. Ginn et al. (2015) reported a decrease in diatom-inferred pH (DI-pH) and diatom-inferred log-specific conductance (DI-SC) from pre-anthropogenic samples to surficial samples, however, because multiple impacts occurred between pre-anthropogenic samples and the time the core was collected, it is uncertain which watershed-scale impact (if any) is responsible for these trends.

Similarly, Ginn et al. (2015) observed trends between pre-anthropogenic sediments and surficial sediments in other study lakes using DI-pH, DI-SC, and diatom-inferred total phosphorous (DI-TP). A slight decrease in DI-pH and DI-TP at First Chain/Second Chain Lakes corresponds to widespread watershed disturbance, which is unique to First Chain/Second Chain lakes due to the high acid rock drainage potential of watershed geology (Tarr and White 2016). DI-TP increased at Lake Fletcher, likely because of widespread catchment urbanization as identified by this study. At Lake Fletcher, Lake Lemont, and First Lake, increases in DI-SC suggest road salt influence because of stormwater input (Ginn et al. 2015). Urbanization at these lakes was resolved in this study as increases in lithogenic element concentrations and $\delta^{15}N$ values. This, in combination with the results of Ginn et al. (2015), suggest that stormwater input may largely be responsible for these changes. In short, the data from this study were able to suggest causal mechanisms for the changes in water quality inferred by previous bioindicator studies.

5.7 Conclusion

Bulk sediment geochemistry from Lake Major, Pockwock Lake, Bennery Lake, Second Lake, Lake Fletcher, Lake Lemont, First Lake, and First Chain Lake reflect more than two centuries of anthropogenic disturbance in the HRM. These impacts include deforestation, urbanization, water works construction, and agriculture. Sediment records from these lakes were used to elucidate the sensitivity of bulk geochemical indicators to watershed-scale disturbances, and how these disturbances are recorded in the bulk geochemical record. Deforestation was resolved at Lake Major and Pockwock Lake by large increases in Ti, Zr, K, and Rb concentrations (50–300%), and moderate increases in C/N ratios (>10%). Urbanization was resolved at Lake Fletcher, Lake Lemont, and First Lake by increases in Ti, Zr, K, and Rb concentrations (10–300%), decreases in C/N ratios (>10%), and increases in $\delta^{15}N$ values (>2.0‰). Collectively these data suggest that bulk geochemical parameters are a useful method to identify watershed-scale disturbance in lake sediment archives.

Chapter 6

Evaluating the Performance of Calculated Elemental Measures in Sediment Archives

Published in the *Journal of Paleolimnology* with co-authors Braden R.B. Gregory[1], Ian S. Spooner[2], Chris E. White[3], and Graham A. Gagnon[4] (Dunnington et al. 2020a). Reprinted by permission from Springer (Appendix A).

6.1 Abstract

Mass accumulation rates, tracer element ratios, enrichment factors, excess measures, and centred log-ratios are elemental measures used in paleolimnological studies when more than one source (e.g., pollution and/or erosion) contributes an element of interest to the sediment archive, or when the closure constraint results in spurious correlations between element concentrations. To determine which measures performed best, we created a model to simulate sediment archives with known inputs from multiple sources. We then calculated each measure and evaluated performance based on whether or not the measure preserved the timing and/or magnitude of mass input from a single source (e.g., pollution). We found that mass accumulation rates performed well when there was a low concentration of the target element in the erosional source, tracer element ratios performed well when erosion was constant, and excess measures performed well when erosion was variable. Enrichment factors did not preserve the magnitude of mass input between simulations with different erosional compositions, and tracer element ratios performed poorly when erosion was not constant. We confirmed these results using real

[1]Department of Earth Sciences, Carleton University, 1125 Colonel By Drive, Ottawa, Ontario K1S 5B6

[2]Department of Earth & Environmental Science, Acadia University, 12 University Ave., Wolfville, Nova Scotia, Canada B4P 2R6

[3]Nova Scotia Department of Energy and Mines, P.O. Box 698, Halifax, Nova Scotia B3J 2T9

[4]Centre for Water Resources Studies, Department of Civil & Resource Engineering, Dalhousie University, 1360 Barrington St., Halifax, Nova Scotia, Canada B3H 4R2

elemental geochemistry from two lakes near Halifax, Nova Scotia, the data from which suggested that the composition of the erosional source is likely to change over time. Collectively our data suggest that while elemental measures are useful interpretive tools, each method has specific numerical and geochemical assumptions that must be evaluated prior to its use. Assumptions of each measure used in a study should be made clear, and concentration profiles should always be made available to the reader.

6.2 Introduction

Multiple sources of Pb pollution to lake sediments are common and investigations of Pb pollution are most effective when the Pb from natural and anthropogenic sources can be separated (Chapter 2). Whereas Chapters 3 and 5 establish the quantification and sensitivity (respectively) of watershed disturbance indicators in lake sediment archives and Chapter 4 establishes methods to visualize and analyze these measures from many records, this chapter examines the utility of watershed disturbance indicators to potentially deconvolute multiple sources of Pb to the lake sediment record.

Because geochemical datasets use proportion of dry mass as a reporting unit, an increase in one element necessitates a decrease in the other elements or the residual fraction of unmeasured material in sample. This closure effect can cause spurious intercorrelations between elements and violates the underlying assumptions of many statistical tests (Aitchison 1986; Kucera and Malmgren 1998; Pawlowsky-Glahn and Egozcue 2006; Boyle 2001). Furthermore, when an element originated from more than one source, separating the contribution of each source is an important precursor to the correct interpretation of an elemental profile (Boyle 2001).

In this chapter we consider a simplified lake sediment record into which is deposited (1) pollution containing lead (Pb), (2) eroded material resulting from watershed disturbance containing Pb and titanium (Ti), and (3) water-column organic matter (OM). Given such a system, several measures to improve the interpretability of elemental concentrations have been proposed. In practice these measures can be used with any element of interest, and elements other than Ti may be better suited to tracing the input of eroded material (Boës et al. 2011; Boyle et al. 2015); we have used Pb and Ti to ensure the readability of equations presented below.

The first measure we will consider is the element-specific mass accumulation rate (MAR),

commonly used in studies of recent pollution and discussed at length by Engstrom and Wright (1984):

$$\mathrm{MAR_{Pb}} = \mathrm{MAR_{dep}} \cdot \mathrm{Pb_{sample}} \tag{6.1}$$

Some studies of recent pollution report the ratio of the element concentration relative to the concentration prior to assumed anthropogenic input (Walters et al. 1974; Blais et al. 1995). This is commonly referred to as the "enrichment factor", and is calculated as:

$$\mathrm{EF_{Pb}} = \frac{\mathrm{Pb_{sample}}}{\mathrm{Pb_{reference}}} \tag{6.2}$$

Next we consider the tracer element ratio, most commonly used in studies of marine sediments or sediments from large lakes (Löwemark et al. 2011; Van Der Weijden 2002), which is calculated as:

$$\mathrm{Pb/Ti} = \frac{\mathrm{Pb_{sample}}}{\mathrm{Ti_{sample}}} \tag{6.3}$$

Studies of recent pollution commonly report the tracer element ratio relative to the same ratio in some reference material (Kemp et al. 1976; Yao et al. 2013; Panizzo et al. 2013; Boës et al. 2011), the reference material for which can be sediments deposited prior to assumed anthropogenic input or a geochemical standard (Kemp et al. 1976; Hilton et al. 1985; Boës et al. 2011). This value is calculated as:

$$\mathrm{EF_{Pb/Ti}} = \frac{\frac{\mathrm{Pb_{sample}}}{\mathrm{Ti_{sample}}}}{\left[\frac{\mathrm{Pb}}{\mathrm{Ti}}\right]_{\mathrm{reference}}} \tag{6.4}$$

Additionally, investigators have calculated the "anthropogenic" or "excess" concentration of an element by calculating the erosional contribution of the target element as a function of the tracer element concentration (Liu et al. 2012; Panizzo et al. 2013). The method of Norton and Kahl (1987) uses the background tracer element ratio as the reference ratio does not use the $\mathrm{Pb_{background}}$ term; the method of Hilton et al. (1985) estimates the reference ratio and the $\mathrm{Pb_{background}}$ term using iterative regression. These can both can be calculated as:

$$\mathrm{Pb_{ex}} = \mathrm{Pb_{sample}} - \mathrm{Pb_{erosion}} - \mathrm{Pb_{background}} \tag{6.5}$$

$$\mathrm{Pb_{ex}} = \mathrm{Pb_{sample}} - \mathrm{Ti_{sample}} \left[\frac{\mathrm{Pb}}{\mathrm{Ti}}\right]_{\mathrm{reference}} - \mathrm{Pb_{background}} \tag{6.6}$$

Finally, we consider log-ratios, which are rarely mentioned in discussions of elemental geochemistry in the field of paleolimnology. Aitchison (1986) showed that using an additive log-ratio (the logarithm of the ratio of two elements; $\ln(\mathrm{Pb}/\mathrm{Ti})$) or centred log-ratios (the logarithm of the ratio of elements over their geometric mean; $\ln(\mathrm{Pb}/g)$)) reduced intercorrelations between elements that resulted from closure effects (Reimann et al. 2012). Although not strictly an example of elemental ratios, we consider centred log-ratios of elements following the formula (Aitchison 1986):

$$\ln(\mathrm{Pb}/g) = \ln\left(\frac{\mathrm{Pb_{sample}}}{g_{\mathrm{sample}}}\right) \tag{6.7}$$

where g is the geometric mean of the sample components under consideration, subject to the constraint that these concentrations add to a constant for each sample. In practice this is achieved by adding a residual component representing the proportion unaccounted for in the known concentrations, or by rescaling the existing components such that the values add to a constant (i.e., a subcomposition).

The variety of measures from which to choose when reporting elemental concentrations suggests the question: which measure should investigators use? In this study we address this question using real and synthesized data to illustrate the potential utility of these measures, and identify situations in which specific measures should be avoided.

6.3 Materials and Methods

6.3.1 Example Data

In this study we use a subset of data from Chapter 5 to test the various elemental measures. Pockwock Lake is the larger and deeper of the two lakes (903 ha, z_{max}=46 m), and has a history of logging and water-level change. It currently serves as the primary drinking water reservoir for the city of Halifax, Nova Scotia. First Chain Lake is a small lake (82 ha) with a z_{max} of 24 m, and has a history of acidification as a result of watershed disturbance of sulfide-bearing bedrock (Chapter 5). It currently serves as a secondary water supply for the city of Halifax,

Nova Scotia. The details of core collection, elemental measurement, and sediment chronology are described in Chapter 5.

We replaced non-detect values with the minimum value for that element observed elsewhere in the core. Based on ages of 1886 and 1875 as the dates at which stable Pb concentrations were >2 times background concentrations in southern Quebec and the Adirondack region of New York (Blais et al. 1995), samples with a ^{210}Pb age before 1870 were considered "background" for the purposes of enrichment factor measures. The geometric mean for the centred log ratio was computed using elements whose concentrations were measured and were above the detection limit (C, Fe, N, K, S, Ca, Ti, Mn, Zn, V, Pb, Sr, Cu, Zr, Rb, As and the residual balance such that the sum of concentrations for each sample was constant).

6.3.2 Synthesized Data

In this study we consider a simple system over a period of 200 years (AD 1800-2000) in which the only sources of mass to the sediment are erosion, water-column organic matter (OM), and pollution (Figure 6.1). The compositions of the erosion, water-column OM, and pollution sources are assumed to be constant through time, with the same mass input time series for pollution in each scenario. Our model was inspired by Boyle (2001), who used a similar model to illustrate the effect of various factors controlling the delivery of trace metals to lake sediment, and by Juggins (2013), who used synthetic data to investigate the assumptions that underlie quantitative reconstructions.

With these constraints, we consider three scenarios: (1) a scenario with constant mass input from erosion and constant water-column OM; (2) a scenario with an increase in mass input from erosion and a constant mass input from water-column OM; and (3) a scenario with an increase in mass input from water-column OM and a constant mass input from erosion. Finally, we evaluate all three scenarios with a low-Pb erosion source.

In the model, the mass accumulation rate (MAR, in relative mass per time) and composition ($C_{S,E}$, in mass E per total mass) of the input for each element (E) from each source (S) is considered at each time step. The sources are assumed to mix completely at each time step, such that mass of deposited sediment can be calculated as the sum of of the mass of sediment from all sources.

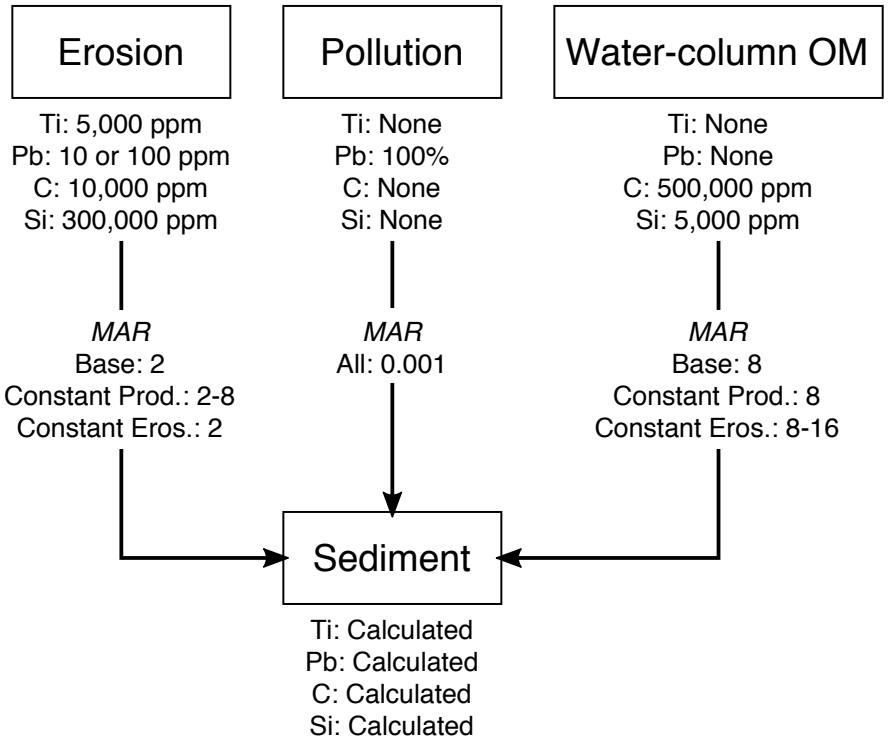

Figure 6.1: A conceptual model of sediment sources to the simplified lake sediment archive.

$$\text{MAR}_{\text{dep}} = \text{MAR}_{\text{erosion}} + \text{MAR}_{\text{water-column OM}} + \text{MAR}_{\text{pollution}} \tag{6.8}$$

The concentration of deposited sediment for a given element at each time step can be calculated as the sum of the masses for each element (the product of the source-specific concentration $C_{S,E}$ and the source-specific flux MAR_S) divided by the total mass (MAR_{dep}). This is essentially a weighted mean of source concentrations weighted by the mass input of each source.

$$C_E = \frac{\text{MAR}_{\text{erosion}} C_{\text{erosion},E} + \text{MAR}_{\text{water-column OM}} C_{\text{water-column OM},E} + \text{MAR}_{\text{pollution}} C_{\text{pollution},E}}{\text{MAR}_{\text{dep}}} \tag{6.9}$$

The parameters controlling the scenarios were the chemical compositions of the three source components and the mass input time series for each source. In this study, the composition of erosion was 300,000 ppm Si, 5,000 ppm Ti, 10 ppm Pb, and 10,000 ppm C; the composition of water-column OM was 5,000 ppm Si and 500,000 ppm C; and the composition of pollution was 100% Pb (Figure 6.1). The composition of the erosion source was derived from the OREAS 46 and OREAS 47 certified reference materials (till). For the high Pb erosion source, a value of 100 ppm of Pb was used. The pollution input mass time series for each scenario was modeled as a Gaussian distribution centred at AD 1980 with a half-width of 50 years; the mass input for the water-column OM and erosion sources were modeled as a Gaussian distribution centered at AD 1960 with a half-width of 50 years, or a constant, depending on the scenario (Table 6.1). The minimum and maximum values for each mass input time series were adjusted such that sediment Pb concentrations were 50-150 ppm and Ti concentrations were 500-4,000 ppm (Table 6.1). These constraining values were matched the observed range of variation observed at Pockwock Lake and First Chain Lake (Figure 6.2). These parameters were not chosen to represent every system, but to represent several plausible systems in which investigators might choose to use various elemental measures.

6.3.3 Software

Computations were performed in R statistical software using the *dplyr* package (R Core Team 2019; Wickham et al. 2020b), and visualizations were created using the *ggplot2* package (Wickham et al. 2020a). Centred log-ratio calculations were verified using the *compositions* package

Table 6.1: Parameters controlling the mass input time series for each source.

Scenario	Source	Base	Peak	Peak Time	Spread
Base	Erosion	2	NA	NA	NA
	Water-column OM	8	NA	NA	NA
	Pollution	0	0.001	1980	50
Constant OM	Erosion	2	8.000	1960	50
	Water-column OM	8	NA	NA	NA
	Pollution	0	0.001	1980	50
Constant Erosion	Erosion	2	NA	NA	NA
	Water-column OM	8	16.000	1960	50
	Pollution	0	0.001	1980	50

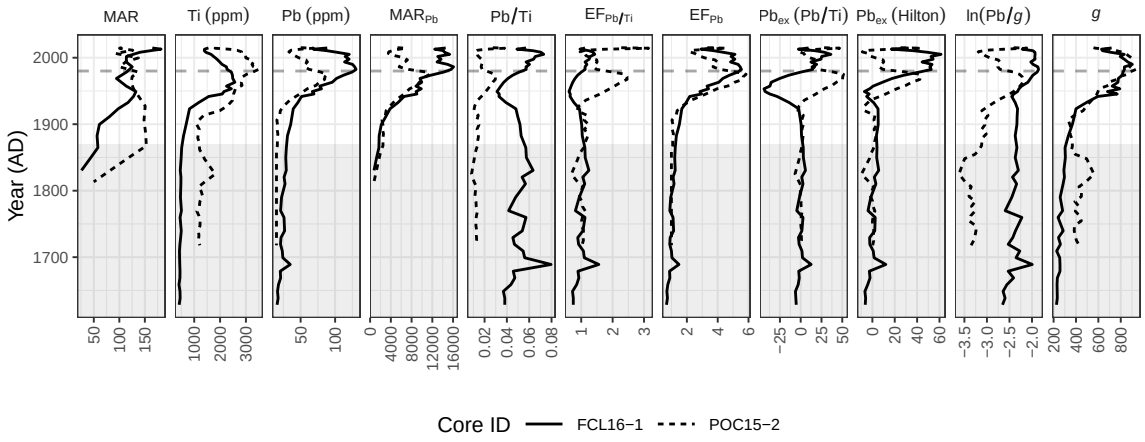

Figure 6.2: Elemental concentrations and ratios at First Chain Lake (FCL16-1) and Pockwock Lake (POC15-2), Halifax, Nova Soctia, Canada. Ti, Pb, Pb_{ex}, and g are in units of parts per million (ppm); MAR is in units of g/m^2/year; all other measures are unitless. Horizontal dashed line indicates the probable peak of Pb mass input from pollution.

(van den Boogaart et al. 2018).

6.4 Results

6.4.1 Example Data

Pb concentrations at First Chain Lake peaked at AD 1980, whereas Ti concentrations peaked at AD 1950, at which time Pb concentrations were only at half their maximum (Figure 6.2). Pb/Ti, $EF_{Pb/Ti}$, and Pb_{ex} values were at their minimum at AD 1950. There was no appreciable decrease in ln(Pb/*g*) coeval with the AD 1950 Ti peak. At Pockwock Lake, Pb concentrations peaked just before AD 1980 but decreased sharply at AD 1980. All measures of Pb at Pockwock Lake capture the pre-1980 Pb peak, then decline sharply at AD 1980. Raw Pb concentrations, EF_{Pb} values, and Pb_{ex}(Hilton) values were the most similar between lakes. The sample geometric mean was also similar in both lakes between 1900 and present, for a reason which we do not know.

6.4.2 Synthesized Data

All scenarios considered in this study had the same time series of Pb mass input from pollution, with a peak at AD 1980. When both water-column OM and erosion were constant (Figure 6.3, rows 1 and 4), all Pb measures including the Pb concentration preserved the timing (i.e., same peak time) of the Pb mass input except Pb_{ex}(Hilton), which could not be calculated when there was no change in Pb concentration from erosion. When both water-column OM and erosion were constant but background concentrations were different, both Pb/Ti (Figure 6.3, panels 1e and 4e) and Pb_{ex}(Pb/Ti) (Figure 6.3, panels 1h and 4h) preserved the magnitude of Pb input from pollution (i.e., the measures were similar despite different background Pb concentrations). Both EF measures (Figure 6.3, panels 1f, 1g, 4f and 4g) and ln(Pb/*g*) (Figure 6.3, panels 1j and 4j) did not have an similar magnitude despite the fact that Pb mass input was identical in both scenarios. Ti concentrations did not vary, thus the Pb-Ti relationship appeared on a biplot as a vertical line (Figure 6.4, panels 1 and 4).

When water-column OM was held constant and erosion was increased with a peak at AD 1960 (Figure 6.3, rows 2 and 5), the Pb concentration contributed by pollution was shifted slightly, such that peak values occurred about 10 years later after the true peak at AD 1980 (Figure 6.3,

panels 2c and 5c). Values of Pb_{ex} and ln(Pb/*g*) demonstrated the same trend, with peak values occurring ca. 1990 (Figure 6.3, panels 2h, 2i, 2j, 5h, 5i, and 5j). Neither Pb/Ti nor $EF_{Pb/Ti}$ preserved the timing of the mass input, and instead shifted the observed peak farther from the true peak, such that the observed peak occurred ca. AD 2000 (Figure 6.3, panels 2e, 2f, 5e, and 5f). Total Pb concentrations were higher when the erosion source contained higher Pb (Figure 6.3, panels 2c and 5c). When the erosion source contained a high concentration of Pb, peak values of MAR_{Pb} occurred about 10 years before the peak of pollution input (Figure 6.3, panels 2d and 5d). Both EF measures and the centred log-ratio did not have an identical magnitude between the High Pb and Low Pb scenarios despite the fact that Pb mass input was identical in both scenarios (Figure 6.3, panels 2f, 2g, 2j, 5f, 5g, and 5j). Ti concentrations increased with increased erosion. The Pb-Ti relationship appeared on a biplot as a generally positive relationship which was reasonably linear prior to increased pollution (Figure 6.4, panels 2 and 5). The iterative regression of the Pb_{ex} (Hilton) method was able to identify this linear relationship, along which Pb_{ex} (Hilton) values were 0 (Figure 6.4, panels 2 and 5).

When erosion was held constant and water-column OM was increased with a peak at AD 1960 Figure 6.3, rows 3 and 6), the effective Pb contributed by pollution was shifted to the same degree as in the scenario where water-column OM was held constant (Figure 6.3, panels 3c and 6c). Values of Pb_{ex} and ln(Pb/*g*) demonstrated the same trend, with peak values occurring ca. 1990 (Figure 6.3, panels 3h, 3j, 6h, and 6j). Values for Pb/Ti and $EF_{Pb/Ti}$ preserved the timing of the Pb mass input (i.e., peak values were at AD 1980), even though peak total Pb concentrations were shifted such that the peak appeared later than AD 1980 (Figure 6.3, panels 3e, 3f, 6e, and 6f). Both EF measures and the ln(Pb/*g*) did not have an identical magnitude between the High Pb and Low Pb scenarios despite the fact that Pb mass input was identical in both scenarios (Figure 6.3, panels 3f, 3g, 3j, 6f, 6g, and 5j). Ti concentrations decreased with increased water-colum OM input as a result of dilution, resulting in little to no relationship between Pb and Ti (Figure 6.4, panels 3 and 6). The iterative regression of the Pb_{ex} (Hilton) method identified a background Pb-Ti relationship with a non-sensical negative slope, suggesting this method should not be used when dilution by water-column OM is suspected.

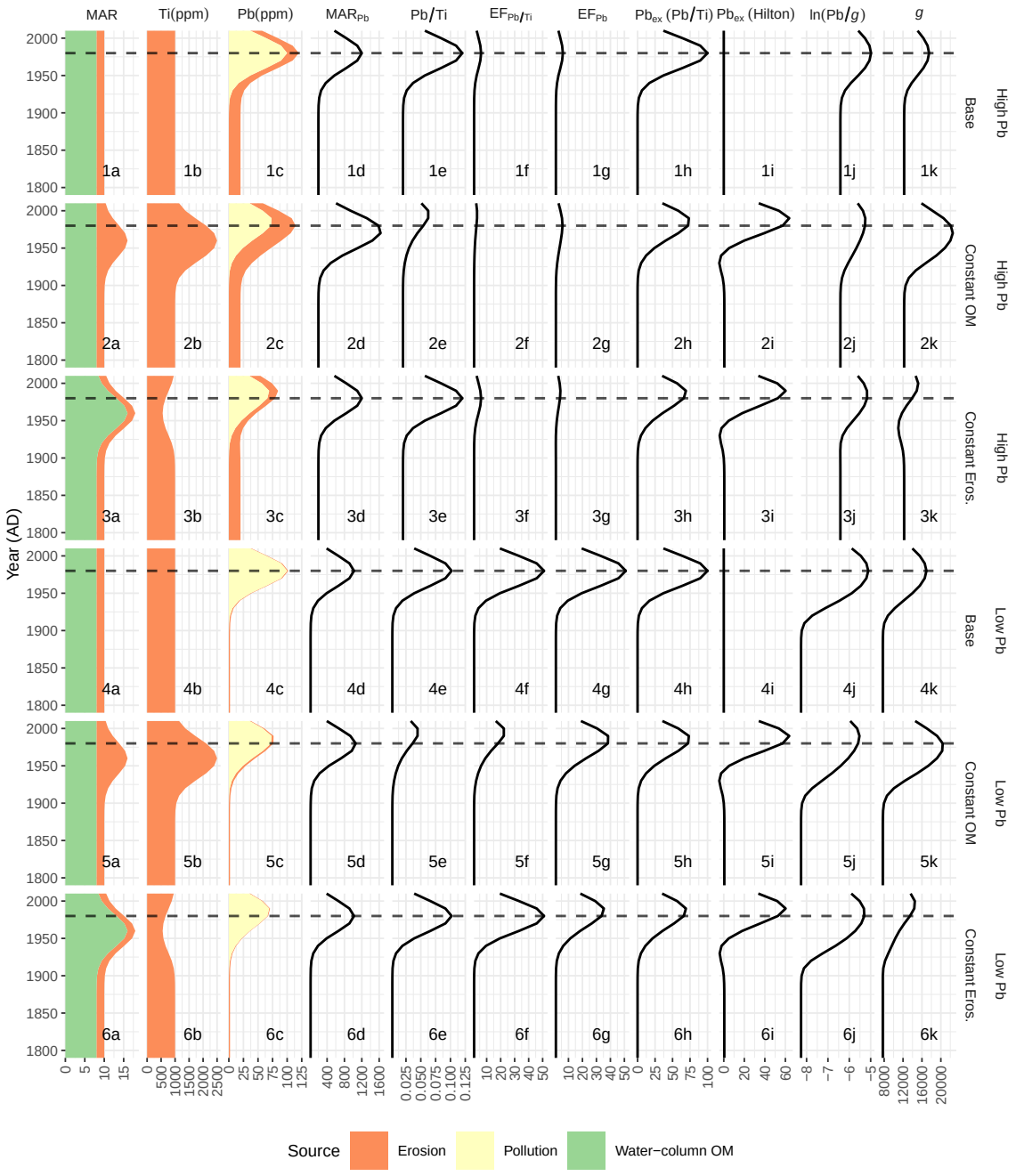

Figure 6.3: Model results and tracer element measures for the modeled scenarios. Ti, Pb, Pb_{ex}, and g are in units of parts per million (ppm); all other measures are unitless. Horizontal dashed line indicates the true peak of Pb mass input from pollution.

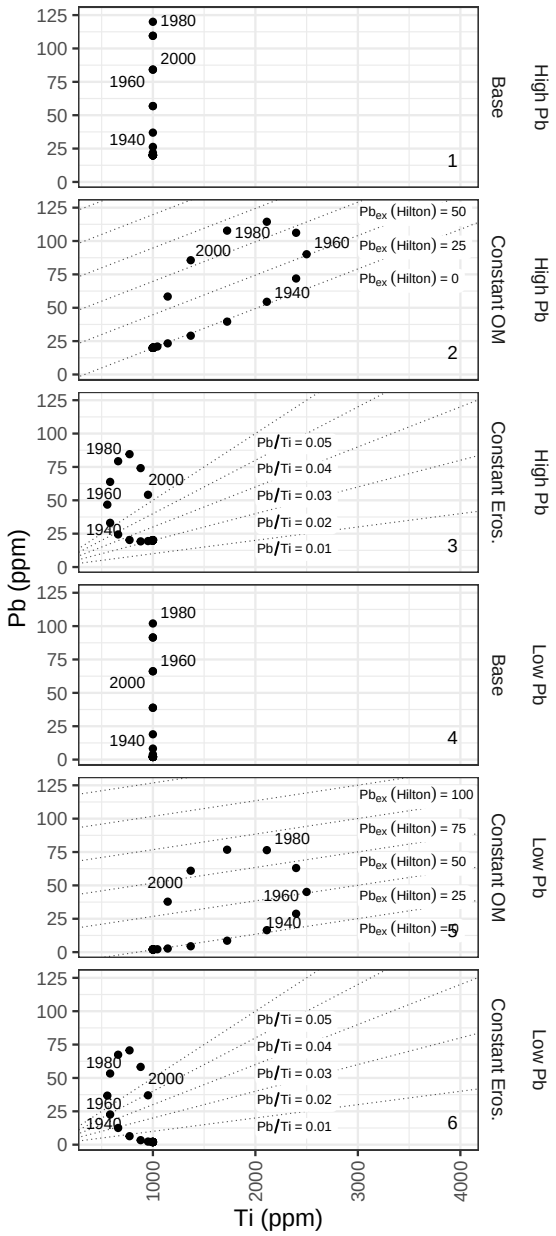

Figure 6.4: Visualization of the Pb-Ti relationship in the model results. A positive relationship was observed when erosion varied (panels 2 and 5), and little to no relationship was observed otherwise. Where Ti concentrations vary as a result of erosion (panels 2 and 5), isolines for Pb_{ex} (Hilton) are shown as dotted lines, as Pb_{ex} (Hilton) is the preferred measure for that scenario. Where Ti concentrations vary as a result of dilution by water column OM (panels 3 and 6), Pb/Ti isolines are shown as dotted lines, as this is the preferred measure for that scenario.

6.5 Discussion

6.5.1 Measure Performance Using Example Data

In two cores from lakes near Halifax, Nova Scotia, Canada, the choice of which measure to report resulted in very different conclusions about the timing and magnitude of Pb deposition within a single core and between cores (Figure 6.2). MAR_{Pb} values suggested that the accumulation of Pb in both systems occurred at a similar rate until AD 1980. Pb/Ti values suggested that an event ca. AD 1700 at First Chain Lake deposited an amount of Pb comparable to that in recent sediments, and that Pb deposition was more significant at First Chain Lake than at Pockwock Lake. $EF_{Pb/Ti}$ values suggested that deposition at Pockwock Lake was far more significant than at First Chain Lake. The centred log-ratio suggested the opposite, with baseline values at First Chain Lake surpassing peak values at Pockwock Lake. It was difficult to interpret the negative Pb_{ex}(Pb/Ti) values at First Chain Lake, whereas the timing of Pb_{ex}(Hilton) values suggested that the timing of anthropogenic Pb varied between the two lakes. Based on our data, the decision of which elemental measure was most representative of actual processes was difficult, and fundamentally altered the interpretation of the geochemical record.

6.5.2 Measure Performance Using Synthetic Data

Raw Pb concentrations were reasonable indicators of Pb input from pollution in all cases, although Pb concentrations were subject to dilution when mass input increased. Interestingly, when mass input increased as a result of erosion and the erosion source contained a high concentration of Pb, the timing of peak Pb concentrations was virtually indistinguishable across scenarios. The differences in Pb concentration were most apparent prior to pollution input (i.e., background concentrations), where Pb concentrations were a function of the Pb concentration in the erosion source and the balance between mass input of erosion and water-column OM.

Mass accumulation rates are commonly used in studies of recent pollution to improve interpretability and remove the closure constraint, however even when the MAR_{dep} can be calculated (usually using ^{210}Pb measurements), the values are less precise than concentration values and introduce unknown biases resulting from interpolation (Engstrom and Wright 1984). The MAR_{Pb} makes no attempt to separate the contribution of Pb from multiple sources: in this study, this was observed as a ~10-year difference between the peak of MAR_{Pb} and Pb input

from erosion when erosion was variable and the erosional source contained high concentrations of Pb.

Tracer element ratios (Pb/Ti) adjusted the magnitude and timing of the original element concentration profiles to reflect the timing and magnitude of the non-erosional source mass input, provided that erosion remained constant. This is the adjustment that was expected based on the "cautionary tale" of Löwemark et al. (2011). When erosion was not constant, the timing and magnitude of the tracer element ratio profile was distorted such that it was not representative of any process that was modeled. This constraint was also noted by Renberg (1986) for a similar measure. In the case of the Pb/Ti ratio, the original concentration profile was more representative of the timing and magnitude of Pb mass input from pollution.

Enrichment factor measures ($EF_{Pb/Ti}$, EF_{Pb}), which have been used to compare elemental profiles between two or more cores (Blais et al. 1995; Walters et al. 1974), were reasonably effective at preserving the timing and magnitude of pollution in the example data. However, in the synthetic data, enrichment factor measures did not preserve the magnitude of Pb mass input from pollution when the composition of the eroded source changed. The magnitude of Pb mass input was not preserved because changing the composition of the eroded source changed the background reference concentration/value, even though the mass input from pollution did not change. Changes in the background mass input of the erosion source would also change the background reference concentration, even if the composition remained the same, and so it is unlikely that enrichment factor measures would preserve the magnitude of Pb mass input from pollution between lakes. This may explain some of the regional variation in metal profiles observed by Blais et al. (1995) and Norton et al. (1992), particularly with Pb, where the majority of deposition is likely atmospheric in origin (Blais and Kalff 1993).

In the example data, Pb_{ex}(Pb/Ti) concentrations were sometimes negative, which is difficult to interpret and unlikely to be representative of anthropogenic Pb contribution at our sites. In a detailed investigation of the Pb_{ex}(Pb/Ti) measure, Boës et al. (2011) found similar results for a lake in northern Sweden, despite the prevalence of using this measure in peat core pollution studies (Martínez Cortizas et al. 2002; Kylander et al. 2006). Kylander et al. (2006) notes that using this method of normalization in peat cores is dependent on airborne dust as a source of Ti, whereas in many lake systems, erosion is also a substantial contributor (Chapter 5. In the synthetic data, Pb_{ex}(Pb/Ti) values were not negative, and in most cases reliably extracted

the expected contribution from pollution, subject to dilution as a result of increased total mass input.

In contrast, Pb_{ex}(Hilton) concentrations reliably extracted the concentration of Pb derived from the pollution source, even when erosion or water-column OM input changed through time. The excess concentrations were still subject to dilution by increased total mass input, which distorted the timing of the observed peak in the opposite direction of the peak of the total mass input in both the example data and the synthetic data. Transforming these excess concentrations into excess accumulation rates is one way to correct this where these data are available. For both synthetic and example data, the Hilton et al. (1985) method likely overestimated the contribution of Pb by erosion, as suggested by small (<5 ppm) negative concentrations of Pb_{ex}(Hilton). Boyle (2001) advised the use of the Hilton et al. (1985) method for identifying concentrations that are a result of pollution, calling it the "best available method" because it does not assume a fixed ratio of Pb to Ti in background samples.

Interpretation of centred log ratios (ln(Pb/*g*)) was difficult in both the example and synthetic data. Low-magnitude variability (i.e., variability in background concentrations) was emphasized when using ln(Pb/*g*) values, but is seldom the focus of environmental pollution studies. Peak values were similar for all scenarios and both example cores, but it is more likely that this is a result of the logarithmic transformation obscuring high-magnitude variability rather than the measure accurately preserving the magnitude of input from pollution. This measure also introduces the geometric mean *g* as a parameter with a subjective interpretation (Figure 6.2; Figure 6.3). Inter-lake comparison of centred log-ratio data may be unreliable as the geometric mean will be substantially different depending on the sub-composition used to calculate the geometric mean of a given sample. As a result, the centred log ratio may be a useful tool for multivariate analysis of compositional data (Aitchison 1986; van den Boogaart et al. 2018; Reimann et al. 2012), but is difficult to interpret in a stratigraphic context.

6.5.3 Geochemical Assumptions

In addition to the numeric assumptions that are considered in this study, geochemical assumptions are critical to consider when interpreting the measures discussed in this paper. In particular, the delivery of the target element to the sediment is often not straightforward: many elements interact with soils, watershed vegetation, water-column OM, and suspended particles,

all of which must be considered prior to assuming a "pollution" source (Boyle 2001; Blais and Kalff 1993; Norton et al. 1992). Post-depositional changes in element concentration will also affect the interpretation of both target and tracer elements (Outridge and Wang 2015). Furthermore, the assumption that the concentration of the tracer element is proportional to the erosional mass input must be evaluated. Changes in the composition of the erosional source over time are likely (Boyle et al. 2015), and the accumulation of atmospherically deposited elements (such as Pb) in watershed soils may increase the concentration of the target element in the erosional source over time (Blais and Kalff 1993). This is likely the reason that Pb mass accumulation rate in the sample cores did not decrease significantly between AD 1980 and present (Figure 6.2).

This study uses a model where erosion is another possible source of the target element, but water-column OM may be a significant source of non-pollution input, particularly for metals that complex with organic matter (Zaferani et al. 2018). For example Renberg (1986) investigated metal/OM ratios as an elemental measure for several lakes in northern Sweden, and Korosi et al. (2018) normalized Hg concentrations to sediment organic carbon for several lakes in northern Canada. Element input as a result of windblown dust was not considered in this study, but is an important source in studies of ombrotrophic peat bogs (Martínez Cortizas et al. 2002; Kylander et al. 2006). As such, the measures discussed in this paper can be (and often are) used in studies of ombrotrophic peat bogs with the erosional source replaced with that of windblown dust.

Whereas Ti is commonly used as the tracer element, other proxies for lithogenic and/or atmospheric input have been used in the literature (Boyle et al. 2015). Boës et al. (2011) obtained different anthropogenic metal fluxes when using Al, Rb, Ti, and Zr as tracers for lithogenic input, suggesting that local mineralogy must be considered before normalizing elemental data. While a detailed examination of catchment mineralogy is not always possible, at the very least investigators should examine the relationship between tracer element concentrations (e.g., Ti) and tracer element concentrations (e.g., Pb; Figure 6.5; Figure 6.4) to verify the relationship between the elements during a period of minimal anthropogenic influence. To use the Hilton et al. (1985) method, this relationship must be positive and reasonably linear. If this relationship is negative or ambiguous, dilution by a non-erosional source such as water-column OM is likely, and Pb/Ti may be a more suitable measure.

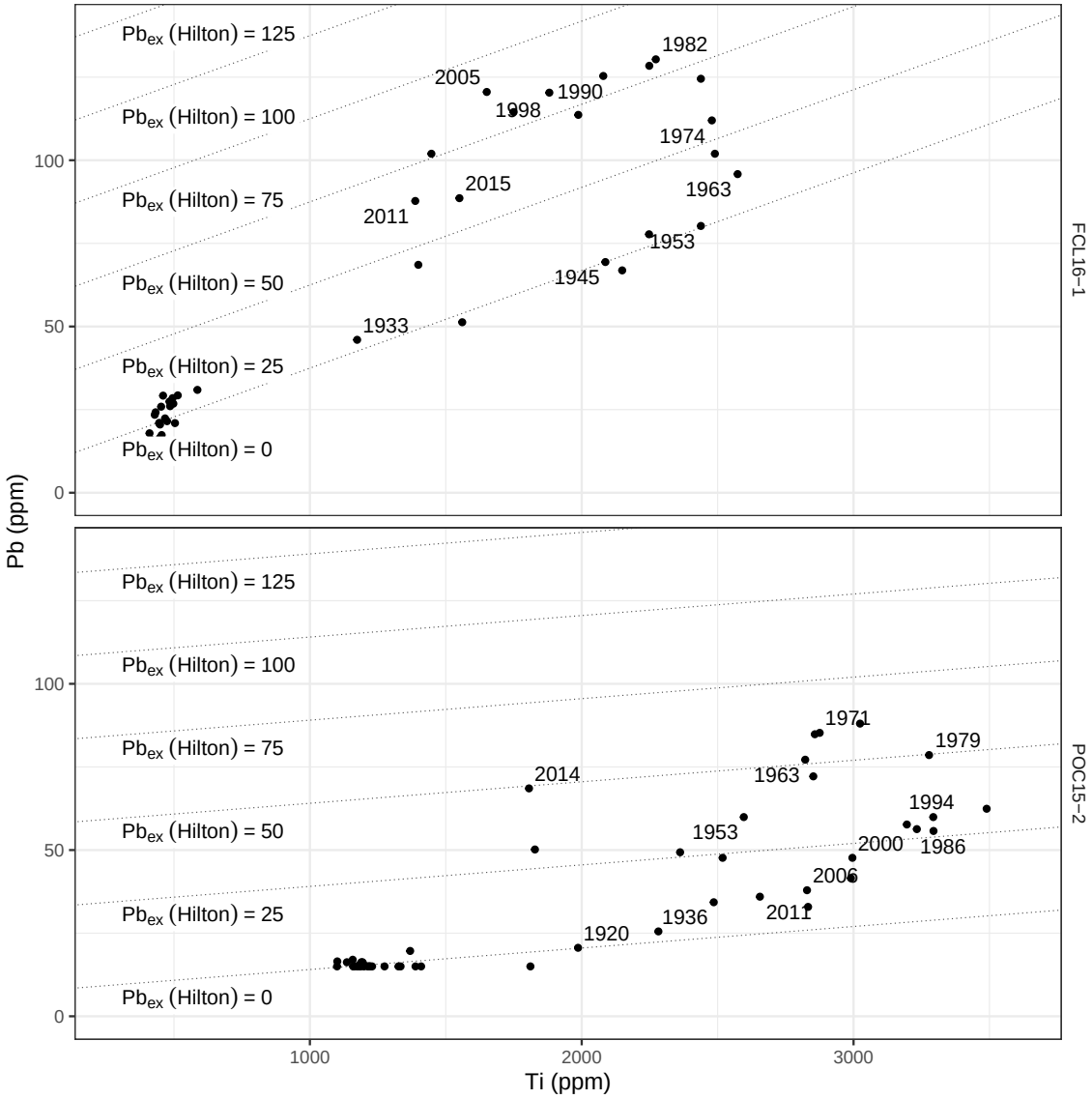

Figure 6.5: Pb concentrations vs. Ti concentrations at First Chain Lake (FCL16-1) and Pockwock Lake (POC15-2), Halifax, Nova Scotia, Canada. Isolines for Pb_{ex} (Hilton) are shown as dotted lines. Pb_{ex} (Hilton) is the preferred measure for these lakes because a positive relationship between Pb and Ti in pre-industrial sediments suggests that erosion (as estimated by Ti concentrations) is responsible for a portion of the total Pb concentration.

6.5.4 Reporting of Elemental Concentrations

Calculated measures can be useful tools to improve the interpretation of elemental geochemistry in paleolimnological studies, however the interpretation of any calculated measure requires implicit assumptions. As such, the original concentration profiles should be made available, and the assumptions of the calculated parameter (both numeric and geochemical) should be explicitly stated in the methods section of paleolimnological publications using such measures. If possible, the numeric concentrations should be made available in supplementary material such that readers can recalculate measures or calculate an alternative measure. In many cases, the concentrations themselves may be a reasonable approximation of both the timing and magnitude of pollution.

Given that many studies that use Pb/Ti and/or $EF_{Pb/Ti}$-like measures report a high degree of correlation between the measure and known or independently measured environmental conditions (Brown 2015; Van Der Weijden 2002; Boës et al. 2011), it is likely that the difficulties associated with using Pb/Ti and/or $EF_{Pb/Ti}$-like measures are avoided in many cases. In particular, the assumption that input from erosion is constant can often be valid in ocean environments or in large lakes where cores are taken far from the shore. Many long-core XRF scanner studies are conducted on cores from these environments, so it is likely that the effects of variable erosion are minor in these studies.

In environments where the assumption of constant input from erosion is not valid (e.g., small lakes or near-shore coring locations), we suggest that it is not valid to use Pb/Ti and/or $EF_{Pb/Ti}$-like measures. Instead, excess measures such as the Hilton et al. (1985) method are most likely to provide a reasonable estimation of elemental input from pollution, particularly if expressed as an accumulation rate or if MAR_{Pb} and MAR_{Ti} are used as inputs rather than concentrations (Norton et al. 1992; Norton et al. 1991). If the concentration of the target element is low in non-pollution sources and high-resolution chronology is available, the element-specific MAR is likely to provide a reasonable estimate of element input from pollution.

The centred log-ratio measure can be difficult to interpret as it only provides an indication of the relative change of a given element. Although this measure is suitable for multivariate analysis and thus an examination of the underlying controls of geochemistry on a system (Aitchison 1986), centred log-ratio data are not suitable for inter-lake comparisons or evaluating the magnitude of change in elemental concentration.

6.6 Conclusion

In this study we evaluated numerical methods to separate multiple sources of Pb input to lake sediments for the purpose of isolating the Pb input due to pollution. We evaluated the effects of variable input as a result of erosion, variable input as a result of increased water-column OM, and variable erosional source composition on elemental concentration profiles and elemental measures. When erosion was constant or nearly constant through time, Pb/Ti and/or $EF_{Pb/Ti}$-like measures were effective proxies for the target element mass input from pollution. When erosion was not constant through time and a sufficient concentration of Pb existed in the erosional input, mass accumulation rates or excess concentration methods such as the Hilton et al. (1985) method were the best suited to preserve the timing and magnitude of the target element mass input from pollution. The Pb–Ti relationship in pre-anthropogenic sediments is likely the best indicator of potential input and/or dilution of Pb as a result of mass input due to erosion.

Chapter 7

The Distribution and Transport of Lead Over Two Centuries as Recorded by Lake Sediments from Northeastern North America

Published in *Science of the Total Environment* with co-authors Sarah Roberts[1], Stephen A. Norton[2], Ian S. Spooner[3], Joshua Kurek[4], Chris E. White[5], and Graham A. Gagnon[6] (Dunnington et al. 2020b).

7.1 Abstract

We evaluated anthropogenic Pb deposition along a west-east transect from the Adirondack Mountains, New York, USA (ADIR) region, the Vermont-New Hampshire-Maine, USA (VT-NH-ME) region, and Nova Scotia, Canada (NS) region using 47 ^{210}Pb-dated lake sediment records. We used focus-corrected Pb inventories to evaluate cumulative deposition and break-point analysis to evaluate possible differences in timings among regions. Peak Pb concentrations decreased from west to east (ADIR region: 52-378 mg kg^{-1}, VT-NH-ME region: 54-253 mg kg^{-1}, NS: 38-140 mg kg^{-1}). Cumulative deposition of anthropogenic Pb also decreased from west to east (ADIR region: 791-1,344 mg m^{-2}, VT-NH-ME region: 209-1,206 mg m^{-2}, NS: 52-421 mg m^{-2}). The initiation of anthropogenic Pb deposition occurred progressively later along the same transect (ADIR region: 1869-1900, VT-NH-ME region: 1874-1905, NS region: 1901-1930). Previous lead isotope studies suggest that eastern Canadian Pb deposition over the past ~150 years has originated from a mix of both Canadian and U.S. sources. The results of this study indicate that anthropogenic Pb from sources west of the ADIR region were

[1]Aquatic Contaminants Research Division, Environment and Climate Change Canada, Burlington, Ontario L7R 46

[2]School of Earth and Climate Sciences, University of Maine, Orono, Maine 04469-5790

[3]Department of Earth & Environmental Science, Acadia University, 12 University Ave., Wolfville, Nova Scotia, Canada B4P 2R6

[4]Department of Geography and Environment, Mount Allison University, Sackville, New Brunswick E4L 1A7

[5]Nova Scotia Department of Energy and Mines, P.O. Box 698, Halifax, Nova Scotia B3J 2T9

[6]Centre for Water Resources Studies, Department of Civil & Resource Engineering, Dalhousie University, 1360 Barrington St., Halifax, Nova Scotia, Canada B3H 4R2

deposited in lesser amounts from west to east and/or Pb sources reflect less population density from west to east. The timing of the initiation of anthropogenic Pb deposition in the NS region suggests that Pb from gasoline may be an important source in this region.

7.2 Introduction

This thesis evaluates the spatial distribution of anthropogenic Pb deposition and informs the nature of west-east Pb transport in northeastern North America. The relevance and environmental consequences of anthropogenic Pb deposition and transport were established in Chapter 1; notably, that the fate of over two centuries of anthropogenic Pb deposition is poorly characterized regionally (Gallon et al. 2005; Graney et al. 1995; Gobeil et al. 2013). The past and present transport of Pb and other compounds in northeastern North America remains relevant as the consequences of related long-term water quality changes become clear (Anderson et al. 2017). Furthermore, the redistribution of atmospherically-deposited Pb from watershed soils is an area of ongoing concern (Boyle 2001; Rose et al. 2012).

Previous chapters provided the conceptual basis for such an evaluation. Chapter 2 provided the basis for using many lake sediment records of Pb from northeastern North America as proxies for atmospheric deposition and transport. The analytical method by which Pb and land-use change indicators can be measured in lake sediments was established in Chapter 3 and software with which to analyze geochemical measurements from many lake sediment records was presented in Chapter 4. Finally, Chapter 5 validates geochemical measurements as indicators of land-use change Chapter 6 presents methods by which indicators of land-use change can be used to assess mass-balance effects on Pb concentrations.

Similarly, previous chapters provided the practical basis for an evaluation of Pb deposition and transport in northeastern North America. This chapter uses newly-collected lake sediment records from Nova Scotia, the paucity of which was noted in the global review presented in Chapter 2, combined with previously-collected sediment records whose existence was also identified in Chapter 2. Bulk geochemistry, including Pb concentrations and concentrations of land-use change indicators were measured on these records using the analytical methods established in Chapter 3. These data were visualized and analyzed using the software developed in Chapter 4 and land-use change indicators identified in Chapter 5 were used to both assess the potential for mass-balance effects on Pb concentrations resulting from pollution and establish

independent age-depth markers to validate the age-depth models constructed in this chapter. A method established in Chapter 6 (visualization of the Pb–Ti relationship in pre-anthropogenic sediments) was used to assess potential mass-balance effects on Pb concentrations resulting from pollution.

7.3 Methods

7.3.1 Record Selection and Parameter Measurement

To characterize Pb deposition in northeastern North America, we assembled existing data for sediment cores for which the Pb concentrations, ^{210}Pb activities, and the ability to estimate dry sediment density existed. For available records that were collected but did not yet have the necessary measurements, we performed additional analyses. Finally, we collected new sediment cores and performed the necessary analyses to ensure the best possible coverage of northeastern North America (Table D.1; Figure D.1). Eleven previously unpublished Pb records and six previously unpublished sediment cores were included in this study (Table D.2). One core per lake was collected, either by piston (all U.S. cores) or gravity coring (all Nova Scotia cores) (Table D.2).

We grouped records into three regions: the Adirondack Mountains, NY (ADIR) region, the Vermont/New Hampshire/ Maine (VT-NH-ME) region, and Nova Scotia (NS). We obtained the appropriate data for 52 lake sediment records, of which we discarded five (Panther Lake, NY; Tumbledown Pond, ME; Laytons Lake, NS; Chance Harbour Lake, NS; and Waterford Lake, NS) because the cores did not achieve background Pb concentrations and/or background ^{210}Pb activities. The earliest cores from the ADIR and VT-NH-ME regions were collected between 1978 and 1985; cores from the NS region were collected between 2006 and 2017 (Table D.2).

For the ADIR and VT-NH-ME regions, we used existing data for lake sediment records which had measurements of total Pb concentrations and ^{210}Pb activities, and the sufficient data to estimate dry density. We digitized over 25,000 measurements for 18 parameters from 34 ADIR and VT-NH-ME lakes. Measurements of total Pb were obtained by Atomic Absorption Spectrometry on a total digestion of ashed sediment that was dried (90°C) then ashed (500°C); ^{210}Pb activities were calculated from ^{210}Po measurements made by alpha spectrometry (Norton et al.

1992; Binford et al. 1993). Many ADIR and VT-NH-ME records were included in the Paleoecological Investigation of Recent Lake Acidification (PIRLA) project (Whitehead et al. 1990), the data from which appear in several related publications (Charles et al. 1990; Norton et al. 1992; Davis et al. 1994; Norton and Kahl 1986; Brewer 1986).

For most cores in the NS region, we measured total Pb using matrix-calibrated X-ray fluorescence spectrometers on dry homogenized sediments (3), and measured total ^{210}Pb activity using alpha spectrometry (200-500 mg dry weight) at MyCore Scientific Inc. (Ottawa). A detailed analysis of the accuracy and precision of these methods is available in Chapters 5 and 3. The analytical precision observed for Pb measurements was generally <10% relative standard deviation (RSD), the relative deviation (RD) from independently measured total concentrations was <10%, and the matrix-specific detection limit was <5 mg kg^{-1}. For the four records from Kejimkujik National Park, Pb was measured by ICP-MS (HNO_3-HCl digestion) with a RSD of <2%, a RD from certified values <15%, and a method detection limit of 0.02 mg kg^{-1} (Roberts et al. 2019). Total ^{210}Pb activities were calculated from alpha- and gamma-ray spectrometry (Roberts et al. 2019). The method used to measure Pb for these lakes was an acid-extractable method rather than a total method, however we did not observe systematically lower inventories from these lakes compared to proximal lakes whose concentrations were measured using a total method.

7.3.2 Age-Depth Models

Previously published age-depth interpretations of ^{210}Pb activities were available for most records used in this study; however, age-depth error was not calculated or reported for most lake sediment records. Because realistic and consistent error estimation was critical to the timing component of our study, we used a Monte Carlo simulation based on the constant rate of supply (CRS) model to produce age-depth models for all records directly from total ^{210}Pb measurements. The CRS model (Appleby and Oldfield 1978) was used because previously-published age-depth models for cores included in this study indicated that this method was appropriate for the corresponding records (36 of 47). Age depth models had not been previously published for 11 of 47 lakes (Mountain (Coburn), Carr, Mud, Salmon, Little Long, Tilden, Nowlans, Torment, Mattatall, Middle, and Kellys). We excluded four of these lakes from the timing component of our study because the log of excess ^{210}Pb activity

showed signs of surface mixing and/or prolonged sedimentation rate changes (Carr, Mud, and Little Long, ME; and Bennery, NS). We excluded three additional lakes (Big Dam, NS; Hilchemakaar, NS; and Cobrielle, NS) from the timing component of our study where independent age-depth markers could not be reconciled. Independent age-depth markers were available and successfully reconciled for 30 of 40 lakes included in the timing component of our study (Table D.3).

The data requirements for the CRS model are (1) the dry density for each sediment interval, (2) total ^{210}Pb activity values and error estimates, and (3) estimated supported ^{210}Pb activity estimates for one or more sediment intervals believed to be below measurable unsupported ^{210}Pb in a record. For all ADIR and VT-NH-ME cores we calculated dry density assuming densities of organic and inorganic material of 1.4 g/cm^3 and 2.4 g/cm^3, respectively, using loss on drying (LOD) and loss on ignition (LOI) (Binford 1990). For most NS cores, we calculated dry density directly from dry mass and known volume. For cores from Roberts et al. (2019), we used the same dry densities that were used to calculate the published cumulative Pb inventories. For sediment depth intervals for which there was insufficient information to estimate dry density, we linearly interpolated using adjacent values.

We used a Monte-Carlo approach to error estimation, which provided us with 1,000 equally plausible age-depth models for each record (Sanchez-Cabeza et al. 2014; Binford 1990). Total ^{210}Pb activity for each depth was modeled as a normal distribution with the sample mean assumed to be the correct activity, and the reported activity error was modeled as the standard error (Aquino-López et al. 2018). Supported ^{210}Pb was calculated using the same samples that were considered supported in the published age-depth model, or using ^{226}Ra measurements if these were available. ^{226}Ra measurements were used to estimate supported ^{210}Pb in four records (Peskowesk, NS; Big Dam, NS; Hilchemakaar, NS; and Cobrielle, NS). Supported ^{210}Pb was modeled in the Monte-Carlo permutations as normal with a standard error estimated as the standard deviation of the background measurements, or the reported error if only one background measurement was available. Measurements of total ^{210}Pb and estimated supported activities are in Figure D.2.

Where activity error was not reported, we assumed a maximum probable error based on the approximately linear upper bound of the known activity error versus the square root of the ^{210}Pb activity for VT-NH-ME records. We estimated errors for 26 records using this method,

including all ADIR records and 12 of 18 VT-NH-ME records. Calculations were performed using the *pb210* package for R statistical software (Dunnington 2020; R Core Team 2019) and validated using previously published age-depth models which were available for most cores. Where available, published ages were within the 5th and 95th percentile of all equally-probable age-depth models (Figure D.3). For unpublished chronologies, we used breaks in erosional element trends and historical records of land-clearing to validate our chronologies (Chapter 5).

7.3.3 Cumulative Anthropogenic Pb Deposition

To compare anthropogenic Pb input in lakes by region, we calculated the cumulative mass of anthropogenic Pb contained in each core based on the dry density and Pb concentration of each interval (7.1).

$$[\text{Pb}_{\text{anthro}}]_i = [\text{Pb}_{\text{total}}]_i - [\text{Pb}_{\text{background}}]_i \tag{7.1}$$

Here, $[\text{Pb}_{\text{background}}]_i$ was calculated as the median $[\text{Pb}_{\text{total}}]_i$ in sediment intervals deposited prior to a CRS-modelled age of 1850. We used a constant background concentration rather than a background concentration that varied for each sediment interval, as there was no evidence that either dilution from water-column organic matter or elevated Pb concentrations occurred during periods of increased erosional input of inorganic matter. We based this methodology on a zero slope of total Pb versus total Ti concentrations in sediments deposited prior to anthropogenic Pb input (Figure D.4; Chapter 6).

The cumulative anthropogenic Pb mass for each slice was calculated from the anthropogenic Pb concentration, the thickness, and the dry density of each interval i for the n sediment intervals in each core with a CRS-modelled age between 1850 and 1978 (7.2).

$$\text{Cumulative Pb}_{\text{anthro}} = \frac{(\sum_{i=1}^{n}[\text{Pb}_{\text{anthro}}]_i \cdot \text{Density}_i \cdot \text{Thickness}_i)}{\text{Focusing Factor}} \tag{7.2}$$

Here, the focusing factor was calculated by dividing the cumulative unsupported ^{210}Pb inventory ($\sum {}^{210}\text{Pb}$) by the estimated regional average unsupported ^{210}Pb inventory of 4,440 Bq m^{-2} (Perry et al. 2005; Cornett et al. 1984) (7.3).

$$\text{Focusing Factor} = \left(\sum {}^{210}\text{Pb}\right) / 4440 \tag{7.3}$$

Excess ^{210}Pb-normalized (focus-corrected) inventories have been used in many studies to compare pollutant inventories from multiple records, as this method can correct for uneven sediment accumulation and wet Pb deposition rates among lakes (Kada and Heit 1992; Perry et al. 2005; Roberts et al. 2019). Because annual precipitation values were relatively consistent across the region (Figure D.7), we expected this approach to primarily correct for sediment focusing. Because 1,000 equally probable ^{210}Pb inventories were calculated, we calculated 1,000 equally probable cumulative anthropogenic Pb masses for each record using randomly selected age-depth models. We evaluated possible explanatory variables using Spearman's correlation coefficient (r_s) between the cumulative anthropogenic Pb mass and available lake/catchment variables (longitude, lake area, catchment area, catchment area:lake area ratio, maximum depth, elevation, and annual precipitation; Figure D.7). We used principal component analysis (PCA) on scaled and centred variables to visualize relationships between explanatory and calculated variables. Both analyses were conducted using R statistical software (R Core Team 2019).

7.3.4 Timing of Pb Deposition

To compare the timing of Pb deposition in lakes by region, we fitted a piecewise linear regression (PLR) for each region (Muggeo 2003). We combined Pb records from each region by rescaling Pb records from each lake such that the "background" concentration was zero and the maximum concentration was one. This approach was used by Kurek et al. (2013) to determine the date at which sedimented polyaromatic hydrocarbon concentrations began increasing at six lakes in northern Alberta, Canada. We only included samples in the PLR with a ^{210}Pb age before 1978 (the earliest collection date of any core in this study) using 1,000 randomly selected age-depth models for each record, for each region. We used the *segmented* package for R statistical software using an initial breakpoint estimate of 1900 (Muggeo 2003). To evaluate if PLR fits were better than the corresponding linear fits, we conducted an ANOVA test between the two models for each set of data. In all cases, the PLR was significantly better than a linear fit (p<0.001).

7.4 Results and Discussion

7.4.1 Pb Concentrations

Sediment Pb concentrations ranged between 2 and 378 mg kg^{-1} (Figure 7.1). While factors other than anthropogenic supply of Pb affect concentration values (e.g., sedimentation rate and/or concentration of organic matter), concentration values are useful indicators and are widely reported in the literature. We observed generally decreasing peak Pb concentrations from west to east: peak concentrations were between 52 and 378 mg kg^{-1} in the ADIR region (median 226 mg kg^{-1}), between 54 and 253 mg kg^{-1} in the VT-NH-ME region (median 150 mg kg^{-1}), and between 38 and 140 mg kg^{-1} in the NS region (median 70 mg kg^{-1}). Background concentrations were generally between 5 and 30 mg kg^{-1} except at Middle Hall Pond (65 mg kg^{-1}) and Windfall Pond (108 mg kg^{-1}) (Figure D.6).

Previous studies have reported similar ranges of concentrations for Pb in northeast North American lakes. In the ADIR region, Galloway and Likens (1979) noted peaks (200 mg kg^{-1}) at 5 cm depth from a core collected in 1974 and Heit et al. (1981) measured Pb at two lakes with differing dissolved organic carbon concentrations, finding peak concentrations of 50 and 140 mg kg^{-1}. Other studies from relatively remote lakes in Ontario and Québec report a similar range of concentrations (Johnson 1987; Ouellet and Jones 1983; Gélinas et al. 2000; Watmough 2017; Blais and Kalff 1993; Dillon and Evans 1982; Sarkar et al. 2015), although several studies report sediment Pb concentrations from southern Québec and Ontario as high as 600 mg kg^{-1} (Evans and Dillon 1982; Lucotte et al. 1995).

In more urban settings, concentrations are commonly much higher. Siver and Wizniak (2001) reported peak sediment Pb concentrations from seven Connecticut lakes between 100 and 400 mg kg^{-1} and surficial concentrations between 100 and 250 mg kg^{-1}. Chalmers et al. (2007) reported surficial sediment Pb concentrations of up to 639 mg kg^{-1} at Upper Mystic Lake, Massachusetts, where peak concentrations were in excess of 1,500 mg kg^{-1}. High concentrations of Pb in urban lakes likely reflect a broader range of Pb sources, including wastewater, stormwater, and short-range atmospheric transport of particulate-bound Pb (Graney et al. 1995). Several lakes in the NS region of this study are near (within 25 km) the city of Halifax, NS (Fletcher, Lemont, First Chain) or Sydney (Middle). However, only one received significant wastewater and/or stormwater (Fletcher) (5), and peak Pb concentrations in these lakes were only slightly

higher than peak concentrations in more rural lakes in the NS region.

The Canadian Council of Ministers of the Environment (CCME) probable effect level (PEL) for the protection of aquatic life is 91.3 mg kg^{-1}, with an interim sediment quality guideline (ISQG) of 35 mg kg^{-1} (CCME 1999). Similar consensus-based estimates of probable Pb toxicity in freshwater sediments were established by MacDonald et al. (2000) (128 mg kg^{-1} probable effect concentration (PEC) and 35.8 mg kg^{-1} threshold effect concentration (TEC), respectively). MacDonald et al. (2000)'s higher consensus-based PEC was exceeded in at least one sample from 13 of 14 ADIR lakes, 12 of 18 VT-NH-ME lakes, and 2 of 15 NS lakes. Cores from the ADIR and VT-NH-ME regions were collected in the late 1970s and early 1980s and thus provide a poor estimate of current conditions. Cores from the NS region, however, were collected between 2006 and 2018. Surficial concentrations of Pb in these cores did not exceed the PEC, but many did exceed the TEC (13 of 15). The potential toxicity of Pb to aquatic life in lake sediments is outside the scope of this study; however, values above MacDonald et al. (2000)'s consensus-based PEL certainly existed at one time in the sediments of all three regions in this study.

7.4.2 Cumulative Anthropogenic Pb Deposition

While sediment Pb concentrations are an indicator of potential impact to aquatic life, cumulative anthropogenic Pb deposition, as used in this study, represents atmospheric deposition at the lake surface normalized for lake- and watershed-specific processes that may affect Pb concentrations (e.g., sedimentation rate and sediment redistribution). Cumulative anthropogenic Pb deposition was highest in ADIR Lakes, lowest in NS lakes, and decreased eastward (r_s=-0.835, $p<0.001$, n=47; Figure 7.2). Values ranged from 791 to 1,344 mg m^{-2} at ADIR lakes, 209 to 1,206 mg m^{-2} at VT-NH-ME lakes, and 52 to 421 mg m^{-2} at NS lakes. Elevation (r_s=0.680, $p<0.001$), lake area (r_s=-0.384, p=0.008), catchment area (r_s=-0.353, p=0.016), and annual precipitation (r_s=-0.290, p=0.049) were all significantly correlated with cumulative anthropogenic deposition (n=47).

We used PCA to examine the relationships among variables calculated for each core, the results of which suggested that annual precipitation, elevation, longitude, and cumulative anthropogenic Pb deposition were all aligned along the same axis in PC1-PC2 space (Figure 7.3).

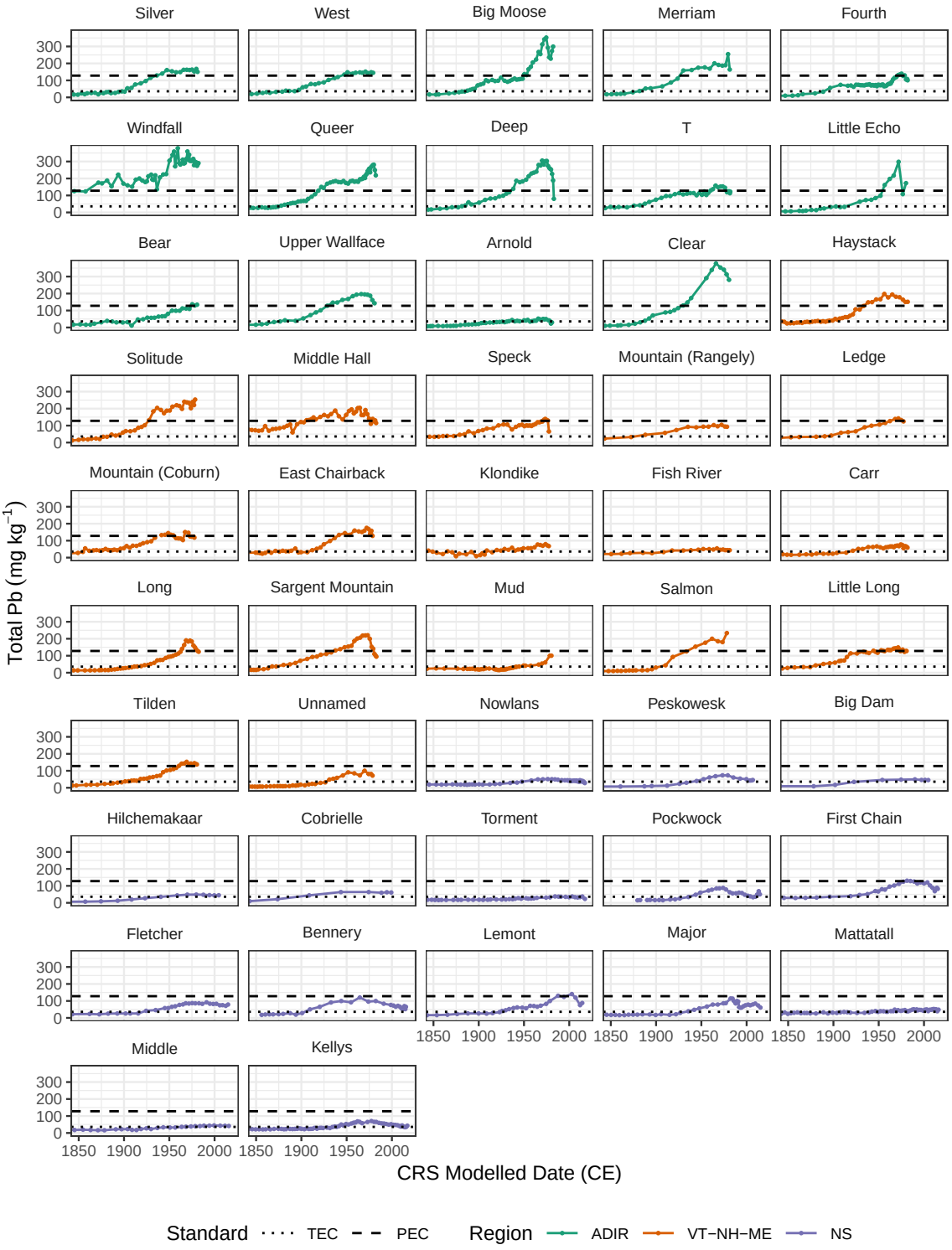

Figure 7.1: Pb concentrations vs. median age of sediment intervals. Records are arranged west to east. Horizontal lines indicate the threshold effect concentration (TEC) and probable effect concentration (PEC) for Pb in freshwater sediments established by MacDonald et al. (2000).

Lake area, catchment area, ^{210}Pb inventory, and maximum depth were aligned along an orthogonal axis. The relationship between these variables is well-established: large lakes tend to be deeper and have larger catchments, with higher excess ^{210}Pb inventories resulting from sediment focusing (Blais and Kalff 1993). This also affects the non-focus-corrected anthropogenic Pb inventory, which was loaded on an axis between longitude and maximum depth. These data suggest that focus correction was able to mitigate the effect of depth on our final calculated Pb inventory. We expected a positive relationship between annual precipitation and Pb inventory, however this relationship was negative (r_s=-0.290) and significant (p=0.049). We think this is a result of slightly increasing precipitation values to the east, and is a secondary result of the strong negative relationship between cumulative anthropogenic Pb deposition and longitude.

The relationship between longitude and cumulative anthropogenic deposition had the highest absolute effect size (r_s=-0.835) with no other reasonable explanation for the trend. The relationship between cumulative anthropogenic deposition and elevation is also worth noting: while positive and significant, this trend was ambiguous within the VT-NH-ME region, where maximum deposition values occurred at approximately 600 m elevation. We argue that while higher elevation lakes may have higher total deposition, these effects are secondary to that of longitude.

While different methods to measure Pb were used in the NS region than the ADIR and VT-NH-ME region, much of the trend is visible within the VT-NH-ME region which used the same dating and chemical methods, suggesting that the trends we observed are not artifacts of the analytical method. Cumulative anthropogenic Pb deposition calculated for clusters of lakes within several kilometers of each other were outside the range of variability that could be explained by ^{210}Pb measurement error. We speculate that this variability did not systematically alter the spatial trend identified in this study; however, it does suggest that there are additional sources of variability that should be examined in future studies.

Previous studies report similar cumulative anthropogenic Pb deposition. Independent of the cores used in this study, Kada and Heit (1992) measured ^{210}Pb and stable Pb at seven lakes in the ADIR region, finding ^{210}Pb-normalized anthropogenic Pb inventories of 800-1100 mg m^{-2}. Elsewhere in northeastern North America, Pratte et al. (2013) noted anthropogenic Pb inventories of 770-1400 mg m^{-2} at three bogs in Québec, in general agreement with the range of 500-1600 mg m^{-2} reported for southern Québec lakes by Blais and Kalff (1993). Smaller

inventories (400-700 mg m^{-2}) occur for eastern Québec and several lakes near Algonquin Park, Ontario (Blais and Kalff 1993; Kada and Heit 1992), with values an order of magnitude lower reported for far northern Québec (Evans and Rigler 1985).

Several studies with widely distributed study sites suggest a spatial component to anthropogenic Pb deposition. Hanson et al. (1983) measured the relative magnitude of Pb deposition along a SW-NE transect from southern Vermont to eastern Québec, finding decreased concentrations of Pb in high elevation sub-alpine forest organic soil (forest floor material). The study was repeated by Evans et al. (2005b) after 17 years. The concentrations, although lower, still showed a decline in concentration to the northeast. Richardson et al. (2014) also noted lower Pb concentrations in mineral soil towards the north and east in their study sites from western Pennsylvania to northern New Hampshire. Ouellet and Jones (1983) used peak-to-background Pb ratios in lake sediments to evaluate the spatial variability of Pb deposition in northern Québec, finding decreasing ratios to the north and west of the St. Lawrence River.

We found decreasing quantities of total Pb deposition along a west-east transect from the ADIR region to NS. In combination with previous studies, this suggests that for Ontario and eastward, the ADIR region represents the region of greatest Pb deposition, with values decreasing to the north and east. While we expect that some variability can be explained by different ranges of years and preservation potential represented by the archives from each study, it is unlikely that this effect is greater than the ubiquitous spatial signature observed within and among previous studies.

Our study was designed to characterize anthropogenic Pb deposition at the regional scale; however, a high degree of variability occurred within small areas. In the ADIR region, five lakes within several km of each other (West, Big Moose, Merriam, Windfall, and Queer) had cumulative anthropogenic Pb deposition ranging between 827 and 1,412 mg m^{-2}; in the VT-NH-ME region, four lakes within 1 km of each other (Mud, Salmon, Little Long, and Tilden) had cumulative anthropogenic Pb deposition ranging between 246 and 484 mg m^{-2}. In NS, the cluster of lakes near Halifax, NS (First Chain, Fletcher, Bennery, Lemont, and Major) had similar variability (222-422 mg m^{-2}). No watershed or morphometric measurement considered in this study systematically explained this variability for these records (Figure 7.2; Figure D.6); however, we did not quantify within-lake basin variability which may be partially responsible (Engstrom and Rose 2013).

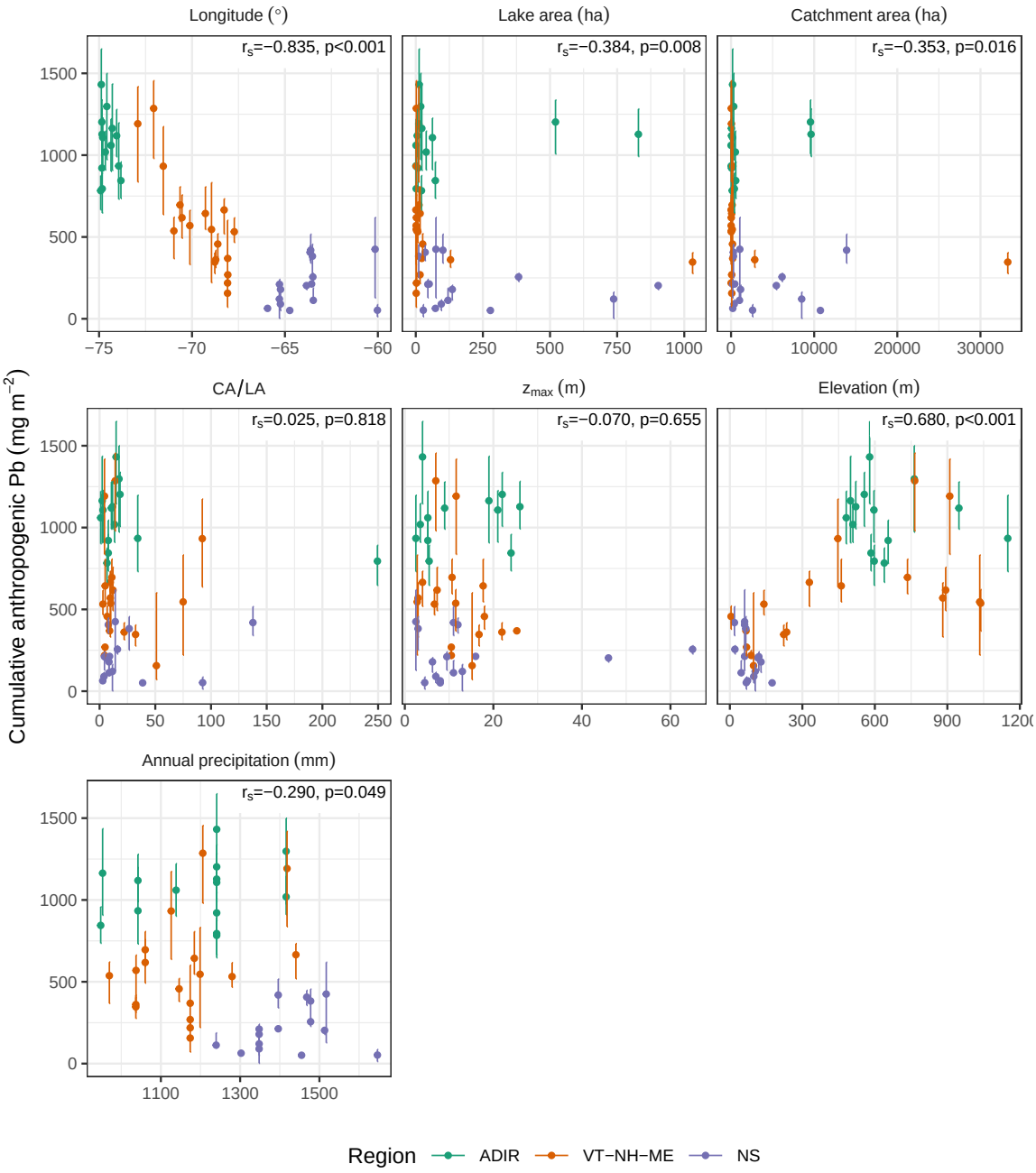

Figure 7.2: Relationship of cumulative focus-corrected anthropogenic Pb deposition to watershed variables. Spearman's correlation coefficients (r s) and p-values of each relationship is shown at the top-right of each panel. The relationship with longitude (upper left) resulted in a significant relationship. Lake specific values are presented in Figures S6 and S7.

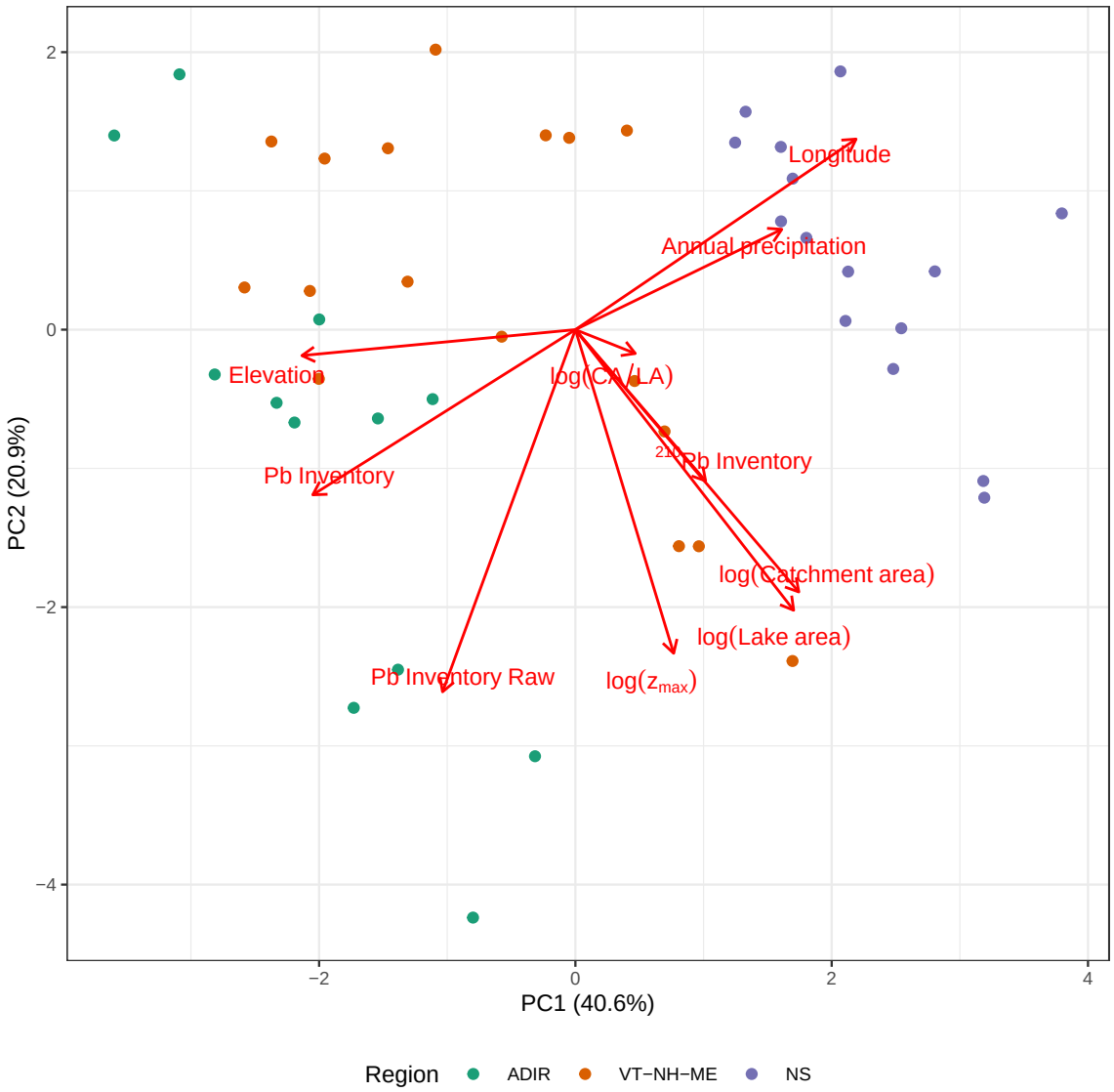

Figure 7.3: Principal components analysis (PCA) biplot of PC1 and PC2 scores with loadings of input variables overlayed. Note that Pb Inventory Raw refers to the non-focus-corrected anthropogenic Pb inventory for each core. Values of variables for each lake are presented in Figures S6 and S7.

7.4.3 Timing of Deposition

The breakpoints identified by piecewise-linear regression identified that anthropogenic Pb concentrations began increasing first in the ADIR region (1869-1900, median 1880), followed by VT-NH-ME region (1874-1905, median 1888), and NS (1901-1933, median 1917) (Figure 7.4). The breakpoints for each region were in the order (ADIR, VT-NH-ME, NS) for 716/1000 simulations; in 965/1000 simulations the breakpoint for the NS region was later than the breakpoints of the other regions. The ordering of regions observed in our Monte Carlo simulations was unlikely to be random ($\chi^2 = 2262$, p<0.001).

Despite a clear trend among regions, there was variation among lakes in the same region. While some of this error may be a result of dating model error, the geographic position of each lake relative to early Pb sources likely affected the timing of Pb increase that was observed. For example, historical gold mining near the four Kejimikujik lakes could have affected the early timing of Pb increase observed at these lakes (Roberts et al. 2019) (Figure 7.1; Figure D.5). Lakes located near the urban center of Halifax, Nova Scotia, did not have earlier timing than surrounding lakes, and in general, we chose lakes for this study that did not have substantial local point sources.

Blais et al. (1995) evaluated the timing of the initial rise in stable Pb using many of the same records that were used in this study, defining the initial rise as the age at which stable Pb was above 1.5 the background value. While their methods were slightly different from this study, they reported a date of 1875±20 for the ADIR region, well within the range observed in this study of 1880 (1869-1900). Other studies that report the timing and magnitude of Pb deposition in northeastern North America use a wider variety of methods and examine data from fewer cores, such as Siver and Wizniak (2001), who reported that increases in Pb concentrations in seven Connecticut lakes did not occur until after 1920. This observation is more similar to our measurements in NS lakes and eastern Québec lakes and bogs than the geographically proximal VT-NH-ME lakes (Gobeil et al. 2013; Pratte et al. 2013). Timing of Pb increases in records from Sargent Mountain Pond and a nearby ombrotrophic bog in eastern Maine generally agreed with the timing of VT-NH-ME lakes (Norton et al. 1997); however, a record from a peat bog in eastern New Brunswick suggests that the main increase in Pb deposition occurred at ca. 1848 (Weiss et al. 2002), earlier than indicated by most of our records in Nova Scotia, and in poor agreement with the timing of smelting operations to the northwest, which did not occur until

1966.

Several studies have noted spatial variability in the timing of Pb deposition at a regional to continental scale. Blais et al. (1995) reported an age of 1886 for 30 cores in southern Québec and Ontario, ages which broadly agree with more contemporary studies of Pb accumulation in lakes (Cheyne et al. 2018). Blais et al. (1995) reported an age of Pb increase at 1884 for 15 lakes in Wisconsin, Minnesota, and Michigan, with later dates for cores in Florida and Northern Québec. In this study we found progressively later dates of Pb increase for VT-NH-ME and NS lakes, similar to observations in lower-deposition areas such as Florida and Northern Québec (Blais et al. 1995; Norton et al. 1990).

Generally, records of Pb accumulation in northeastern North America suggest that Pb increases primarily occurred after 1920 northeast of Maine except in a few lakes where the increase in Pb deposition occurred in the mid-1800s. This may also be true for lakes south of the VT-NH-ME region (Siver and Wizniak 2001). The timing of the increase in Pb concentrations in the ADIR region was earlier than those calculated for records in the VT-NH-ME region, and in general, Pb concentrations began increasing in the ADIR region earlier than in surrounding regions (Blais et al. 1995; Norton et al. 1992).

7.4.4 Implications for Pb Transport

It is possible to make a few generalizations about the nature of regional-scale Pb transport and likely sources of Pb deposition in northeastern North America. While early Pb emissions from coal combustion likely contributed to the earlier timing of Pb increases in ADIR and VT-NH-ME lakes (Norton et al. 1990; Norton et al. 1992; Graney et al. 1995), it seems unlikely that Pb emissions from coal combustion are solely responsible for the increased deposition observed in ADIR lakes compared to NS lakes. The timing of Pb deposition in most NS lakes suggests that Pb emissions from U.S. coal were not transported as far as NS; however, most NS lakes have near-synchronous increases in Pb after 1923, suggesting that Pb from gasoline may be an important source in the NS region. Observations that Pb from U.S. gasoline has been observed in Canadian precipitation and lake sediment suggest that at least some Pb deposited in the NS region may have originated from U.S. sources (Blais 1996; DesJardins et al. 2004). Our results are also consistent with studies that suggest that particulate-bound Pb from coal burning, typically <2 μm in size, does not travel as far as Pb from leaded gasoline (Graney et al. 1995;

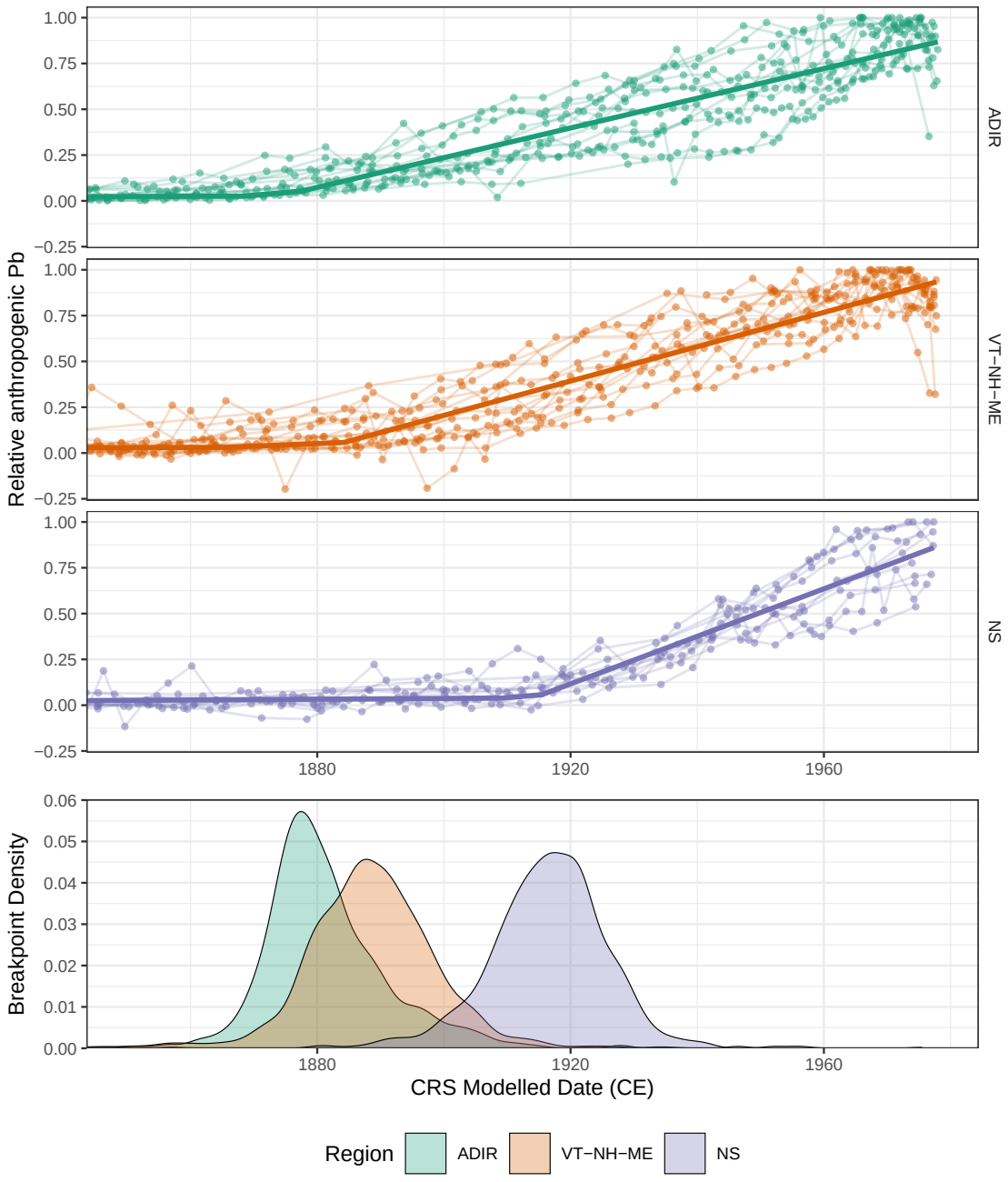

Figure 7.4: Relative anthropogenic Pb concentrations vs. median age (top) and age distributions of breakpoints (bottom). For relative anthropogenic Pb, a value of zero represents the background Pb concentration, and a value of one indicates the maximum concentration observed in a particular record.

Pacyna 1987). Isotopically distinct Pb from U.S. smelting were transported into Québec and Ontario as early as the mid-1800s (Gobeil et al. 2013; Cheyne et al. 2018), but there is limited evidence that this is the case in New Brunswick or eastward (Kylander et al. 2009).

It is possible that the spatial distribution of other atmospherically-transported materials follows a pattern similar to Pb in northeastern North America. The distribution of sulfate (SO_4) during the early 1980s was estimated at >3,000 mg m^{-1} yr^{-1} in the ADIR region, whereas SO_4 deposition for the northern VT-NH-ME and NS regions was 2,000 mg m^{-1} yr^{-1} or lower (Zemba et al. 1988; Fay et al. 1985). Similarly, nitrate (NO_3) deposition was greater in the ADIR region (2,200 mg m^{-1} yr^{-1}) than in the northern VT-NH-ME region (700-900 mg m^{-1} yr^{-1}) (Zemba et al. 1988), in agreement with modern satellite-constrained estimates of NO_3 deposition (Geddes and Martin 2017). Studies in Europe found similar trends for Pb concentrations in cores along a similarly situated transect with respect to atmospheric circulation in the region (Verta et al. 1989; Renberg et al. 1994; Renberg et al. 2000). Verta et al. (1989) noted a correlation between atmospheric deposition of "acidic compounds" and atmospheric deposition of Pb and other trace metals using 18 small lakes in Finland (Verta et al. 1989). Whereas the spatial gradient of Hg deposition is more subtle because Hg travels dominantly as a gas (Perry et al. 2005; Evans et al. 2005b), it is possible that the processes that affect the deposition of SO_4, NO_3, and Pb are similar and result in a more distinct spatial gradient.

The nature of watershed-scale redistribution of atmospherically deposited Pb after 1980 is less clear because many North American studies on Pb in lakes are based on cores that were collected in the late 1970s and early 1980s. Although Pb concentrations in many lakes have decreased since 1980 (Mahler et al. 2006), it is not the case in all NS lakes presented in this study. We see no evidence in our study or elsewhere that Pb concentrations from recently deposited sediments are similar to background concentrations (Figure 7.5) (Siver and Wizniak 2001; Chalmers et al. 2007; Cheyne et al. 2018; Yuan 2017; Sarkar et al. 2015; Aliff et al. 2020), despite little atmospheric deposition of Pb since 1990 (Nriagu 1990).

Sediment mixing and/or sediment resuspension and redeposition is one mechanism by which concentrations in recent sediment would not have returned to background levels (Boyle 2001); however, ^{210}Pb activities did not suggest that mixing was widespread in the cores in this study,

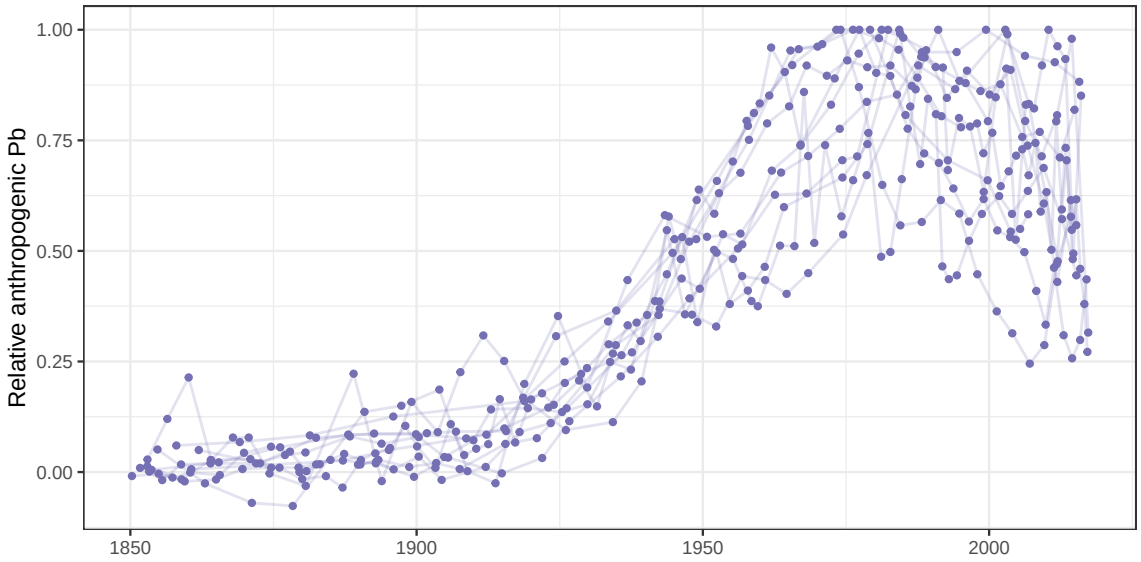

Figure 7.5: Relative anthropogenic Pb for cores collected after 2006. A value of zero represents the background Pb concentration, and a value of 1 indicates the maximum concentration observed in a particular record.

and we find it unlikely that these processes are solely responsible for elevated surficial concentrations in many studies. Robbins et al. (2000) quantified the time-averaging of Pb concentrations, citing a sedimentary reservoir of Pb that delayed the apparent peak of Pb in a coral archive by six years compared to aerial deposition of Pb. This method may be a useful method in future studies with which to quantify the time averaging resulting from watershed delivery, sediment mixing, and sediment resuspension and redeposition.

7.5 Conclusion

While better characterization methods are needed to fingerprint sources of atmospherically-deposited Pb in northeastern North America, the lake sediment cores included in this study suggest decreasing total Pb concentrations, decreasing cumulative deposition of Pb, and Pb deposition starting at a later date from the ADIR region eastward to the VT-NS-ME and NS regions. Previous Pb isotope studies suggest that eastern Canadian Pb deposition over the past ~150 years has originated from a mix of Canadian and U.S. sources. Combined with the results of this study, it is clear that Pb from sources west of the ADIR region were deposited in a progressively decreasing fashion from west to east and/or more easterly sources were later and weaker in their development. The timing of the initiation of anthropogenic Pb deposition

in the NS region suggests that Pb from gasoline became important source after 1923.

Chapter 8

Conclusion

8.1 Conclusion and Implications

This thesis answered two questions. First, was Pb transported to Nova Scotia from U.S. sources? Based on the timing of Pb deposition in 47 dated lake sediment cores (Figure 7.4) and a collection of previous Pb isotope studies from the region reviewed in Chapter 7, Pb from gasoline was an important source to Nova Scotia lake sediment cores and came from a mix of Canadian and U.S. sources. Second, is Nova Scotia the "tailpipe of North America"? Based on the total anthropogenic Pb in Nova Scotia lake sediment cores compared to cores from the northeastern United States (Figure 7.2), there is little evidence that substantial Pb was transported to Nova Scotia suggesting that the title "tailpipe of North America" is a poor characterization of atmospheric Pb transport in Nova Scotia.

Previous studies were unable to draw conclusions about regional transport because they did not evaluate Pb deposition from locations spanning a wide enough area or because they did not analyze deposition over a long enough period of time. A novel contribution of this thesis was to perform such an evaluation: well-dated lake sediments were available from a wide area and provided an archive of Pb deposition over more than two centuries. The analysis in Chapter 7 provided a consistent regional analysis that was able to strengthen the conclusions of previous studies that analyzed a smaller area and/or a shorter period of time.

The implications for west-east transport in northeastern North America extend beyond Pb: Chapter 7 noted similarities between the pattern of Pb deposition observed in this thesis and the distribution of SO_4 and NO_3 around the peak of acid deposition (Zemba et al. 1988; Fay et al. 1985), which may explain the more subtle response to acid precipitation observed in Nova Scotia lakes compared to Adirondack Lakes (Charles et al. 1990; Ginn et al. 2007). Furthermore, this may suggest a common mechanism by which Pb, SO_4, and NO_3 are transported via atmospheric processes; however; a more precise characterization of long-term SO_4 and NO_3

deposition is needed to confirm any connection with Pb deposition.

The impact of decadal- to centennial-scale changes in surface water quality, such as those driven by SO_4 and NO_3 deposition, is increasingly important to water and wastewater treatment (Anderson et al. 2017; Delpla et al. 2009). In areas where SO_4 and NO_3 deposition resulted in reduced dissolved organic carbon (DOC), the reduction of acid deposition has resulted in increased DOC with potentially expensive implications for drinking water treatment (Evans et al. 2005a; Anderson et al. 2017). Furthermore, watershed-scale land-use change is causing widespread changes in global water quality (Mattikalli and Richards 1996). In combination with climate change, these decadal- to centennial-scale changes have the ability to force potentially expensive modifications to treatment infrastructure (Delpla et al. 2009; Qin et al. 2010). Data at a decadal to centennial scale are clearly needed to inform the design of treatment infrastructure whose source water or receiving water quality may change significantly during the design lifetime.

Paleolimnological methods are well-suited to characterizing the decadal- to centennial-scale changes in the source and receiving waters on which modern treatment infrastructure relies. The high-throughput methods developed in this thesis are well-suited to ensuring that applied paleolimnological assessments can be conducted at reasonable cost (e.g., using the analytical method described in Chapter 3) and can be visualized/analyzed effectively (e.g., using the software presented in Chapter 4) by utilities and consultants. The watershed-scale changes for which geochemical proxies were established in Chapter 5 are important for validating age-depth chronologies and determining the potential mass-balance effects on pollutant concentration modeled in Chapter 6.

Paleolimnological methods offer long-term records of environmental change and for many lakes is the only available method by which environmental conditions can be reconstructed at the decadal to centennial scale (Smol 2010; Ginn et al. 2015; Landres et al. 1999; Smol 1992; Smol 1995; Anderson 1995); however, the interpretation of measurements from a single core can be ambiguous. As demonstrated in Chapters 5 and 6, the effects of land-use change on water quality can be difficult to separate from those of climate change and atmospheric deposition. Deconvoluting these interactions requires evidence from many lake sediment archives; however, analyzing, collecting, and interpreting this quantity of data can be time- and/or cost-prohibitive. This thesis demonstrated that portable X-Ray Fluorescence can

mitigate analytical cost (Chapter 3) and provide measurements for elements that can be used to reconstruct watershed-scale disturbance (Chapter 5). Multiple stressors can be simulated and in some cases successfully separated using geochemical measurements of watershed-scale disturbance (Chapter 6). Finally, visualizing lake sediment archives accessibly can be achieved using the software described in Chapter 4. In short, the methods developed in this thesis allow information from a large number of records to be combined to decrease the ambiguity compared to that of a single record, extending the application of paleolimnological methods to domains that require low ambiguity.

8.2 Recomendations for Future Research

Based on the findings of this thesis, several directions for future research are recommended:

- This thesis measured Pb concentrations in lake sediment; however, Pb isotopes in lake sediment are a more precise indicator of source (Blais 1996). A study of similar extent that measured Pb isotopes would be able to quantitatively separate the contribution of multiple sources of Pb to aquatic sediments. The utility of this type of study with a wide regional extent was demonstrated by Renberg et al. (2000) in Sweeden; however, there is no analogue for recent (<200 years) sediments in North America.

- While some literature suggests that catchment loading of Pb to lakes is minimal (Blais and Kalff 1993; Dillon and Evans 1982), over a century of anthropogenic Pb deposition in northeastern North America has resulted in soils as a new source of Pb to lakes that should be studied comprehensively (Rose et al. 2012), in addition to continued sources of atmospheric Pb such as TEL in fuel for small airplanes (Federal Aviation Administration 2019). This is especially true for regions with high potential for impact such as the Adirondack, New York, United States region. Cores from New York, Vermont, New Hampshire, and Maine, United States, were collected in the 1970s and 1980s. As demonstrated in Chapter 7, concentrations of Pb in Nova Scotia, Canada lake sediments do not return to pre-industrial concentrations despite little atmospheric Pb deposition since 1990. A study of more recent cores from New York, Vermont, New Hampshire, and Maine would be able to more precisely identify recent sources of Pb to aquatic sediments that are causing this to occur.

- This study focused on Pb deposition; however, as reviewed in Chapter 2, other potentially toxic trace metals are also transported atmospherically and can be measured by pXRF in aquatic sediments (e.g., Zn, Cu, and As). An assessment of these metals in addition to Pb may be able to more precisely quantify atmospheric transport mechanisms that transport multiple elements. The methods related to watershed-scale transport of trace metals developed in Chapters 5 and 6 are well-suited to quantifying differences between atmospheric and watershed transport that may better constrain the processes that transport these elements.

- The high-throughput methods developed in this thesis were applied to evaluate regional Pb deposition; however, there are potential applications for the assessment of contaminated aquatic sediment and/or water infrastructure planning. Studies that establish the utility of the methods developed in this thesis for each of these applications would be useful and novel contributions.

References

Aitchison, J. (1986). *The Statistical Analysis of Compositional Data*. Monographs on Statistics and Applied Probability. London, England: Chapman & Hall. 416 pp.

Aliff, M. N., E. D. Reavie, S. P. Post, and L. M. Zanko (2020). "Metallic Elements and Oxides and Their Relevance to Laurentian Great Lakes Geochemistry". In: *PeerJ* 8, e9053. DOI: 10.7717/peerj.9053.

Allaire, J., Y. Xie, J. McPherson, J. Luraschi, K. Ushey, A. Atkins, H. Wickham, J. Cheng, W. Chang, and R. Iannone (2019). *rmarkdown: Dynamic Documents for R*. R package version 1.14. URL: https://CRAN.R-project.org/package=rmarkdown.

Anderson, J. N. (1995). "Using the Past to Predict the Future: Lake Sediments and the Modelling of Limnological Disturbance". In: *Ecological Modelling*. Mathematical Modelling in Limnology 78.1–2, pp. 149–172. DOI: 10.1016/0304-3800(94)00124-Z.

Anderson, L. E., W. H. Krkošek, A. K. Stoddart, B. F. Trueman, and G. A. Gagnon (2017). "Lake Recovery Through Reduced Sulfate Deposition: A New Paradigm for Drinking Water Treatment". In: *Environmental Science & Technology* 51.3, pp. 1414–1422. DOI: 10.1021/acs.est.6b04889.

Appleby, P. G. and F. Oldfield (1978). "The Calculation of Lead-210 Dates Assuming a Constant Rate of Supply of Unsupported 210Pb to the Sediment". In: *CATENA* 5.1, pp. 1–8. DOI: 10.1016/S0341-8162(78)80002-2.

— (1983). "The Assessment of ^{210}Pb Data from Sites with Varying Sediment Accumulation Rates". In: *Hydrobiologia* 103.1, pp. 29–35. DOI: 10.1007/BF00028424.

Aquino-López, M. A., M. Blaauw, J. A. Christen, and N. K. Sanderson (2018). "Bayesian Analysis of 210Pb Dating". In: *Journal of Agricultural, Biological and Environmental Statistics* 23.3, pp. 317–333. DOI: 10.1007/s13253-018-0328-7.

Bennett, K. D. (1996). "Determination of the Number of Zones in a Biostratigraphical Sequence". In: *New Phytologist* 132.1, pp. 155–170. DOI: 10.1111/j.1469-8137.1996.tb04521.x.

Bernick, M. B., D. Getty, G. Prince, and M. Sprenger (1995). "Statistical Evaluation of Field-Portable X-Ray Fluorescence Soil Preparation Methods". In: *Journal of Hazardous Materials*. On-Site Analysis of Chemicals at Spill and Hazardous Materials Locations 43.1, pp. 111–116. DOI: 10.1016/0304-3894(95)00031-O.

Bezanson, D. E. (1993). *Hammonds Plains: The First 100 Years*. Halifax, Nova Scotia: Bounty Print Ltd. 152 pp. URL: https://discover.halifaxpubliclibraries.ca/?itemid=%7Clibrary/m/halifax-horizon%7C521860.

Binford, M. W. (1990). "Calculation and Uncertainty Analysis of 210Pb Dates for PIRLA Project Lake Sediment Cores". In: *Journal of Paleolimnology* 3.3, pp. 253–267. DOI: 10.1007/BF00219461.

Binford, M. W., J. S. Kahl, and S. A. Norton (1993). "Interpretation of 210Pb Profiles and Verification of the CRS Dating Model in PIRLA Project Lake Sediment Cores". In: *Journal of Paleolimnology* 9.3, pp. 275–296. DOI: 10.1007/BF00677218.

Blais, J. M. (1996). "Using Isotopic Tracers in Lake Sediments to Assess Atmospheric Transport of Lead in Eastern Canada". In: *Water, Air, and Soil Pollution* 92.3, pp. 329–342. DOI: 10.1007/BF00283566.

Blais, J. M. and J. Kalff (1993). "Atmospheric Loading of Zn, Cu, Ni, Cr, and Pb to Lake Sediments: The Role of Catchment, Lake Morphometry, and Physico-Chemical Properties of the Elements". In: *Biogeochemistry* 23.1, pp. 1–22. DOI: 10.1007/BF00002920.

Blais, J. M., J. Kalff, R. J. Cornett, and R. D. Evans (1995). "Evaluation of ^{210}Pb Dating in Lake Sediments Using Stable Pb, Ambrosia Pollen, and ^{137}Cs". In: *Journal of Paleolimnology* 13.2, pp. 169–178. DOI: 10.1007/BF00678105.

Boës, X., J. Rydberg, A. Martinez-Cortizas, R. Bindler, and I. Renberg (2011). "Evaluation of Conservative Lithogenic Elements (Ti, Zr, Al, and Rb) to Study Anthropogenic Element Enrichments in Lake Sediments". In: *Journal of Paleolimnology* 46.1, pp. 75–87. DOI: 10.1007/s10933-011-9515-z.

Bouchette, J. (1831). *The British Dominions in North America*. London, England: Longman, Rees, Orme, Brown and Green. URL: https://archive.org/details/britishdominions12bouc.

Boyle, J. F. (2000). "Rapid Elemental Analysis of Sediment Samples by Isotope Source XRF". In: *Journal of Paleolimnology* 23.2, pp. 213–221. DOI: 10.1023/A:1008053503694.

— (2001). "Inorganic Geochemical Methods in Paleolimnology". In: *Tracking Environmental Change Using Lake Sediments: Volume 2: Physical and Geochemical Methods*. Ed. by W. M. Last and J. P. Smol. Vol. 2. 4 vols. The Netherlands: Springer Science & Business Media, pp. 83–141. DOI: 10.1007/0-306-47670-3_5.

Boyle, J. F., R. Chiverrell, and D. Schillereff (2015). "Lacustrine Archives of Metals from Mining and Other Industrial Activities—A Geochemical Approach". In: *Environmental Contaminants: Using Natural Archives to Track Sources and Long-Term Trends of Pollution*. Ed. by J. M. Blais, M. R. Rosen, and J. P. Smol. Developments in Paleoenvironmental Research. Dordrecht: Springer Netherlands, pp. 121–159. DOI: 10.1007/978-94-017-9541-8_7.

Bragée, P., P. Choudhary, J. Routh, J. F. Boyle, and D. Hammarlund (2013). "Lake Ecosystem Responses to Catchment Disturbance and Airborne Pollution: An 800-Year Perspective in Southern Sweden". In: *Journal of Paleolimnology* 50.4, pp. 545–560. DOI: 10.1007/s10933-013-9746-2.

Brenner, M., T. J. Whitmore, J. H. Curtis, D. A. Hodell, and C. L. Schelske (1999). “Stable Isotope (δ13C and δ15N) Signatures of Sedimented Organic Matter as Indicators of Historic Lake Trophic State”. In: *Journal of Paleolimnology* 22.2, pp. 205–221. DOI: 10.1023/A:1008078222806.

Brewer, G. F. (1986). “Sulfur, Heavy Metal, and Major Element Chemistry of Sediments from Four Eastern Maine Ponds”. M.Sc. Thesis. Orono, Maine: University of Maine. 139 pp. URL: http://ursus.maine.edu/record=b3616142.

Brown, E. T. (2015). “Estimation of Biogenic Silica Concentrations Using Scanning XRF: Insights from Studies of Lake Malawi Sediments”. In: *Micro-XRF Studies of Sediment Cores*. Developments in Paleoenvironmental Research. Springer, Dordrecht, pp. 267–277. DOI: 10.1007/978-94-017-9849-5_9.

Brunschön, C., T. Haberzettl, and H. Behling (2010). “High-Resolution Studies on Vegetation Succession, Hydrological Variations, Anthropogenic Impact and Genesis of a Subrecent Lake in Southern Ecuador”. In: *Vegetation History and Archaeobotany* 19.3, pp. 191–206. DOI: 10.1007/s00334-010-0236-4.

Bull, A., M. T. Brown, and A. Turner (2017). “Novel Use of Field-Portable-XRF for the Direct Analysis of Trace Elements in Marine Macroalgae”. In: *Environmental Pollution* 220, pp. 228–233. DOI: 10.1016/j.envpol.2016.09.049.

Burrows, K. C. (2003). *Nova Scotia Through The Trees 1761-1930*. Wellington, Nova Scotia: Terra Firma Press. 150 pp.

Callender, E. and P. C. Van Metre (1997). “Environmental Policy Analysis, Peer Reviewed: Reservoir Sediment Cores Show U.S. Lead Declines”. In: *Environmental Science & Technology* 31.9, 424A–428A. DOI: 10.1021/es972473k.

Camarero, L., P. Masqué, W. Devos, I. Ani-Ragolta, J. Catalan, H. C. Moor, S. Pla, and J. A. Sanchez-Cabeza (1998). “Historical Variations in Lead Fluxes in the Pyrenees (Northeast Spain) from a Dated Lake Sediment Core”. In: *Water, Air, and Soil Pollution* 105, pp. 439–449. DOI: 10.1023/A:1005005625972.

Canadian-British Engineering Consultants (1966). *Report on Use of Lake Major for the Greather Halifax Area*. Public Service Comission of Halifax, p. 35.

Carignan, R. and J. Nriagu (1985). “Trace Metal Deposition and Mobility in the Sediments of Two Lakes near Sudbury, Ontario”. In: *Geochimica et Cosmochimica Acta* 49, pp. 1753–1764. DOI: 10.1016/0016-7037(85)90146-2.

Carlson, R. E. and J. Simpson (1996). *A Coordinator’s Guide to Volunteer Monitoring*. Boulder, Colorado: North American Lake Management Society, p. 92.

CCME, ed. (1999). *Canadian Environmental Quality Guidelines*. Publication / Canadian Council of Ministers of the Environment no. 1299. Hull, QC: CCME.

— (2004). *Phosphorus: Canadian Guidance Framework for the Management of Freshwater Systems*. Ottawa, Ontario: Canadian Council of Ministers of the Environment, p. 6.

Chalmers, A. T., P. C. Van Metre, and E. Callender (2007). "The Chemical Response of Particle-Associated Contaminants in Aquatic Sediments to Urbanization in New England, U.S.A." In: *Journal of Contaminant Hydrology*. Issues in Urban Hydrology: The Emerging Field of Urban Contaminant Hydrology 91.1, pp. 4–25. DOI: 10.1016/j.jconhyd.2006.08.007.

Charles, D. F., M. W. Binford, E. T. Furlong, R. A. Hites, M. J. Mitchell, S. A. Norton, F. Oldfield, M. J. Paterson, J. P. Smol, and A. J. Uutala (1990). "Paleoecological Investigation of Recent Lake Acidification in the Adirondack Mountains, NY". In: *Journal of Paleolimnology* 3.3, pp. 195–241. DOI: 10.1007/BF00219459.

Cheyne, C. A. L., A. M. Thibodeau, G. F. Slater, and B. A. Bergquist (2018). "Lead Isotopes as Particulate Contaminant Tracers and Chronostratigraphic Markers in Lake Sediments in Northeastern North America". In: *Chemical Geology* 477, pp. 47–57. DOI: 10.1016/j.chemgeo.2017.11.043.

Christopher, T. K. (1999). "Paleolimnology in an Urban Environment : The History of Environmental Change in St. John's, Newfoundland". Ph.D. Thesis. St. John's, Newfoundland: Memorial University of Newfoundland. 378 pp. URL: http://research.library.mun.ca/9445/ (visited on 10/06/2017).

Cloy, J. M., J. G. Farmer, M. C. Graham, A. B. MacKenzie, and G. T. Cook (2008). "Historical Records of Atmospheric Pb Deposition in Four Scottish Ombrotrophic Peat Bogs: An Isotopic Comparison with Other Records from Western Europe and Greenland". In: *Global Biogeochemical Cycles* 22.2. DOI: 10.1029/2007GB003059.

Cohen, A. S. (2003). *Paleolimnology : The History and Evolution of Lake Systems: The History and Evolution of Lake Systems*. Oxford, UK: Oxford University Press. 540 pp.

Cooke, C. A., M. B. Abbott, and A. P. Wolfe (2008). "Late-Holocene Atmospheric Lead Deposition in the Peruvian and Bolivian Andes". In: *The Holocene* 18.2, pp. 353–359. DOI: 10.1177/0959683607085134.

Cornett, R. J., L. Chant, and D. Link (1984). "Sedimentation of Pb-210 in Laurentian Shield Lakes". In: *Water Quality Research Journal* 19.2, pp. 97–109. DOI: 10.2166/wqrj.1984.018.

Couture, R.-M., C. Gobeil, and A. Tessier (2008). "Chronology of Atmospheric Deposition of Arsenic Inferred from Reconstructed Sedimentary Records". In: *Environmental Science & Technology* 42.17, pp. 6508–6513. DOI: 10.1021/es800818j.

Crecelius, E. A. and D. Z. Piper (1973). "Particulate Lead Contamination Recorded in Sedimentary Cores from Lake Washington, Seattle". In: *Environmental Science & Technology* 7.11, pp. 1053–1055. DOI: 10.1021/es60083a005.

Creighton, W. (1988). *Forestkeeping: A History of the Lands and Forests of Nova Scotia 1926-1969*. Halifax, Nova Scotia: Nova Scotia Department of Government Services.

Croudace, I. W., A. Rindby, and R. G. Rothwell (2006). “ITRAX: Description and Evaluation of a New Multi-Function X-Ray Core Scanner”. In: *Geological Society, London, Special Publications* 267.1, pp. 51–63. DOI: 10.1144/GSL.SP.2006.267.01.04.

Davidson, K. B. (2018). “Spatiotemporal Assessment of Metal Concentrations of Pre-Effluent Estuarine Sediments in a Freshwater Kraft Pulp Mill Tailings Pond Using Paleolimnological Methods, A’se’k, Pictou, Nova Scotia”. Acadia University. 98 pp. URL: https://scholar.acadiau.ca/islandora/object/theses%3A2616/ (visited on 11/01/2018).

Davis, D. S. and S. Browne, eds. (1996). *Natural History of Nova Scotia*. Vol. 1. Halifax, Nova Scotia: Nova Scotia Museum.

Davis, R. B., D. S. Anderson, S. A. Norton, and M. C. Whiting (1994). “Acidity of Twelve Northern New England (U.S.A.) Lakes in Recent Centuries”. In: *Journal of Paleolimnology* 12.2, pp. 103–154. DOI: 10.1007/BF00678090.

Davis, R. B. and S. A. Norton (1978). “Paleolimnologic Studies of Human Impact on Lakes in the United States, with Emphasis on Recent Research in New England”. In: *Polskie Archiwum Hydrobiologii* 25.1/2, pp. 99–115.

Davis, R. B., S. A. Norton, C. T. Hess, and D. F. Brakke (1983). “Paleolimnological Reconstruction of the Effects of Atmospheric Deposition of Acids and Heavy Metals on the Chemistry and Biology of Lakes in New England and Norway”. In: *Hydrobiologia* 103.1, pp. 113–123. DOI: 10.1007/BF00028438.

De Vleeschouwer, F., H. Vanneste, D. Mauquoy, N. Piotrowska, F. Torrejón, T. Roland, A. Stein, and G. L. Roux (2014). “Emissions from Pre-Hispanic Metallurgy in the South American Atmosphere”. In: *PLOS ONE* 9.10, e111315. DOI: 10.1371/journal.pone.0111315.

Delpla, I., A. .-V. Jung, E. Baures, M. Clement, and O. Thomas (2009). “Impacts of Climate Change on Surface Water Quality in Relation to Drinking Water Production”. In: *Environment International* 35.8, pp. 1225–1233. DOI: 10.1016/j.envint.2009.07.001.

DesJardins, M. J., K. Telmer, and S. Beauchamp (2004). “Apportioning Atmospheric Pollution to Canadian and American Sources in Kejimkujik National Park, Nova Scotia, Using Pb Isotopes in Precipitation”. In: *Atmospheric Environment* 38.39, pp. 6875–6881. DOI: 10.1016/j.atmosenv.2004.08.039.

Dillon, P. J. and R. D. Evans (1982). “Whole-Lake Lead Burdens in Sediments of Lakes in Southern Ontario, Canada”. In: *Hydrobiologia* 91-92.1, pp. 121–130. DOI: 10.1007/BF00940101.

Dixit, S. S., A. S. Dixit, J. P. Smol, R. M. Hughes, and S. G. Paulsen (2000). “Water Quality Changes from Human Activities in Three Northeastern USA Lakes”. In: *Lake and Reservoir Management* 16.4, pp. 305–321. DOI: 10.1080/07438140009354238.

Dixon, S. L., J. M. Gaitens, D. E. Jacobs, W. Strauss, J. Nagaraja, T. Pivetz, J. W. Wilson, and P. J. Ashley (2009). "Exposure of U.S. Children to Residential Dust Lead, 1999–2004: II. The Contribution of Lead-Contaminated Dust to Children's Blood Lead Levels". In: *Environmental Health Perspectives* 117.3, pp. 468–474. DOI: 10.1289/ehp.11918. pmid: 19337524.

Dunnington, D., B. R. B. Gregory, I. S. Spooner, C. E. White, and G. A. Gagnon (2020a). "Evaluating the Performance of Calculated Elemental Measures in Sediment Archives". In: *Journal of Paleolimnology*. DOI: 10.1007/s10933-020-00123-3.

Dunnington, D. (2020). *pb210: Lead-210 dating utilities*. https://paleolimbot.github.io/pb210/, https://github.com/paleolimbot/pb210.

Dunnington, D. W. (2011). "Using Paleolimnological Methods to Track Late Holocene Environmental Change at Long Lake, New Brunswick - Nova Scotia Border Region, Canada". B.Sc.H. Thesis. Wolfville, Nova Scotia: Acadia University. 93 pp. URL: http://scholar.acadiau.ca/islandora/object/theses:847.

Dunnington, D. W., S. Roberts, S. A. Norton, I. S. Spooner, J. Kurek, J. L. Kirk, D. C. G. Muir, C. E. White, and G. A. Gagnon (2020b). "The Distribution and Transport of Lead over Two Centuries as Recorded by Lake Sediments from Northeastern North America". In: *Science of The Total Environment*, p. 140212. DOI: 10.1016/j.scitotenv.2020.140212.

Dunnington, D. W., I. S. Spooner, W. H. Krkošek, G. A. Gagnon, R. J. Cornett, C. E. White, B. Misiuk, and D. Tymstra (2018). "Anthropogenic Activity in the Halifax Region, Nova Scotia, Canada, as Recorded by Bulk Geochemistry of Lake Sediments". In: *Lake and Reservoir Management* 34.4, pp. 334–348. DOI: 10.1080/10402381.2018.1461715.

Dunnington, D. W. and I. S. Spooner (2018). "Using a Linked Table-Based Structure to Encode Self-Describing Multiparameter Spatiotemporal Data". In: *FACETS* 3.1, pp. 326–337. DOI: 10.1139/facets-2017-0026.

Dunnington, D. W., I. S. Spooner, M. L. Mallory, C. E. White, and G. A. Gagnon (2019). "Evaluating the Utility of Elemental Measurements Obtained from Factory-Calibrated Field-Portable X-Ray Fluorescence Units for Aquatic Sediments". In: *Environmental Pollution* 249, pp. 45–53. DOI: 10.1016/j.envpol.2019.03.001.

Dunnington, D. W., I. S. Spooner, C. E. White, R. J. Cornett, D. Williamson, and M. Nelson (2016). "A Geochemical Perspective on the Impact of Development at Alta Lake, British Columbia, Canada". In: *Journal of Paleolimnology* 56.4, pp. 315–330. DOI: 10.1007/s10933-016-9919-x.

Dunnington, D. W., H. White, I. S. Spooner, M. L. Mallory, C. White, N. J. O'Driscoll, and N. R. McLellan (2017). "A Paleolimnological Archive of Metal Sequestration and Release in the Cumberland Basin Marshes, Atlantic Canada". In: *FACETS* 2.1, pp. 440–460. DOI: 10.1139/facets-2017-0004.

Engstrom, D. R. and N. L. Rose (2013). “A Whole-Basin, Mass-Balance Approach to Paleolimnology”. In: *Journal of Paleolimnology* 49.3, pp. 333–347. DOI: 10.1007/s10933-012-9675-5.

Engstrom, D. R. and H. E. Wright (1984). “Chemical Stratigraphy of Lake Sediments as a Record of Environmental Change”. In: *Lake Sediments and Environmental History: Studies in Palaeolimnology and Palaeoecology in Honour of Winifred Tutin*. Ed. by E. Y. Haworth, J. W. G. Lund, and W. Tutin. Leicester: Leicester University Press, pp. 11–67.

Ettler, V., T. Navrátil, M. Mihaljevič, J. Rohovec, M. Zuna, O. Šebek, L. Strnad, and M. Hojdová (2008). “Mercury Deposition/Accumulation Rates in the Vicinity of a Lead Smelter as Recorded by a Peat Deposit”. In: *Atmospheric Environment* 42.24, pp. 5968–5977. DOI: 10.1016/j.atmosenv.2008.03.047.

Evans, C. D., D. T. Monteith, and D. M. Cooper (2005a). “Long-Term Increases in Surface Water Dissolved Organic Carbon: Observations, Possible Causes and Environmental Impacts”. In: *Environmental Pollution*. Recovery from Acidificationin the UK: Evidence from 15 Years of Acid Waters Monitoring 137.1, pp. 55–71. DOI: 10.1016/j.envpol.2004.12.031.

Evans, G. C., S. A. Norton, I. J. Fernandez, J. S. Kahl, and D. Hanson (2005b). “Changes in Concentrations of Major Elements and Trace Metals in Northeastern U.S.-Canadian Sub-Alpine Forest Floors”. In: *Water, Air, and Soil Pollution* 163.1-4, pp. 245–267. DOI: 10.1007/s11270-005-0435-2.

Evans, H. E., P. J. Smith, and P. J. Dillon (1983). “Anthropogenic Zinc and Cadmium Burdens in Sediments of Selected Southern Ontario Lakes”. In: *Canadian Journal of Fisheries and Aquatic Sciences* 40.5, pp. 570–579. DOI: 10.1139/f83-076.

Evans, R. D. and P. J. Dillon (1982). “Historical Changes in Anthropogenic Lead Fallout in Southern Ontario, Canada”. In: *Hydrobiologia* 91.1, pp. 131–137. DOI: 10.1007/BF02391928.

Evans, R. D. (1986). “Sources of Mercury Contamination in the Sediments of Small Headwater Lakes in South-Central Ontario, Canada”. In: *Archives of Environmental Contamination and Toxicology* 15.5, pp. 505–512. DOI: 10.1007/BF01056562.

Evans, R. D. and F. H. Rigler (1985). “Long Distance Transport of Anthropogenic Lead as Measured by Lake Sediments”. In: *Water, Air, and Soil Pollution* 24.2, pp. 141–151. DOI: 10.1007/BF00285439.

Fay, J. A., D. Golomb, and S. Kumar (1985). “Source Apportionment of Wet Sulfate Deposition in Eastern North America”. In: *Atmospheric Environment (1967)* 19.11, pp. 1773–1782. DOI: 10.1016/0004-6981(85)90004-6.

Federal Aviation Administration (2019). *Fact Sheet – Leaded Aviation Fuel and the Environment*. URL: https://www.faa.gov/news/fact_sheets/news_story.cfm?newsId=14754 (visited on 02/28/2020).

Fitzgerald, W. F., D. R. Engstrom, R. P. Mason, and E. A. Nater (1998). “The Case for Atmospheric Mercury Contamination in Remote Areas”. In: *Environmental Science & Technology* 32.1, pp. 1–7. DOI: 10.1021/es970284w.

Fitzstevens, M. G., R. M. Sharp, and D. J. Brabander (2017). “Biogeochemical Characterization of Municipal Compost to Support Urban Agriculture and Limit Childhood Lead Exposure from Resuspended Urban Soils”. In: *Elem Sci Anth* 5.0. DOI: 10.1525/elementa.238.

Frahm, E. (2013). “Validity of “off-the-Shelf” Handheld Portable XRF for Sourcing Near Eastern Obsidian Chip Debris”. In: *Journal of Archaeological Science* 40.2, pp. 1080–1092. DOI: 10.1016/j.jas.2012.06.038.

— (2014). “Characterizing Obsidian Sources with Portable XRF: Accuracy, Reproducibility, and Field Relationships in a Case Study from Armenia”. In: *Journal of Archaeological Science* 49, pp. 105–125. DOI: 10.1016/j.jas.2014.05.003.

Fraser, J. H. (1986). “An Evaluation of Bedrock Groundwater Flow in the Long and Chain Lake Watersheds, Halifax County, Nova Scotia”. M.Sc. Thesis. Halifax, Nova Scotia: Nova Scotia Technical University. 69 pp.

Gallagher, L., R. W. Macdonald, and D. W. Paton (2004). “The Historical Record of Metals in Sediments from Six Lakes in the Fraser River Basin, British Columbia”. In: *Water, Air, and Soil Pollution* 152.1-4, pp. 257–278. URL: http://link.springer.com/article/10.1023/B:WATE.0000015349.25371.af (visited on 02/17/2014).

Gallon, C., A. Tessier, C. Gobeil, and M. C. Alfaro-De La Torre (2004). “Modeling Diagenesis of Lead in Sediments of a Canadian Shield Lake 11Associate Editor: K. K. Falkner”. In: *Geochimica et Cosmochimica Acta* 68.17, pp. 3531–3545. DOI: 10.1016/j.gca.2004.02.013.

Gallon, C., A. Tessier, C. Gobeil, and L. Beaudin (2005). “Sources and Chronology of Atmospheric Lead Deposition to a Canadian Shield Lake: Inferences from Pb Isotopes and PAH Profiles”. In: *Geochimica et Cosmochimica Acta* 69.13, pp. 3199–3210. DOI: 10.1016/j.gca.2005.02.028.

Galloway, J. N. and G. E. Likens (1979). “Atmospheric Enhancement of Metal Deposition in Adirondack Lake Sediments”. In: *Limnology and Oceanography* 24.3, pp. 427–433. DOI: 10.4319/lo.1979.24.3.0427.

Garrison, P. J. and R. S. Wakeman (2000). “Use of Paleolimnology to Document the Effect of Lake Shoreland Development on Water Quality”. In: *Journal of Paleolimnology* 24.4, pp. 369–393. URL: http://link.springer.com/article/10.1023/A:1008107706726 (visited on 02/17/2014).

Geddes, J. A. and R. V. Martin (2017). “Global Deposition of Total Reactive Nitrogen Oxides from 1996 to 2014 Constrained with Satellite Observations of NO_2 Columns”. In: *Atmospheric Chemistry and Physics* 17.16, pp. 10071–10091. DOI: 10.5194/acp-17-10071-2017.

Gélinas, Y., M. Lucotte, and J.-P. Schmit (2000). “History of the Atmospheric Deposition of Major and Trace Elements in the Industrialized St. Lawrence Valley, Quebec, Canada”. In: *Atmospheric Environment* 34.11, pp. 1797–1810. DOI: 10.1016/S1352-2310(99)00336-2.

Ginn, B. K., B. F. Cumming, and J. P. Smol (2007). “Assessing pH Changes since Pre-Industrial Times in 51 Low-Alkalinity Lakes in Nova Scotia, Canada”. In: *Canadian Journal of Fisheries and Aquatic Sciences* 64.8, pp. 1043–1054. DOI: 10.1139/f07-078.

Ginn, B. K., T. Rajaratnam, B. F. Cumming, and J. P. Smol (2015). “Establishing Realistic Management Objectives for Urban Lakes Using Paleolimnological Techniques: An Example from Halifax Region (Nova Scotia, Canada)”. In: *Lake and Reservoir Management* 31.2, pp. 92–108. DOI: 10.1080/10402381.2015.1013648.

Ginn, B. K., M. Rate, B. F. Cumming, and J. P. Smol (2010). “Ecological Distribution of Scaled-Chrysophyte Assemblages from the Sediments of 54 Lakes in Nova Scotia and Southern New Brunswick, Canada”. In: *Journal of Paleolimnology* 43.2, pp. 293–308. DOI: 10.1007/s10933-009-9332-9.

Glew, J. R. (1989). “A New Trigger Mechanism for Sediment Samplers”. In: *Journal of Paleolimnology* 2.4, pp. 241–243. DOI: 10.1007/BF00195474.

Glew, J. R. (1988). “A Portable Extruding Device for Close Interval Sectioning of Unconsolidated Core Samples”. In: *Journal of Paleolimnology* 1.3, pp. 235–239. DOI: 10.1007/BF00177769.

Glew, J. R., J. P. Smol, and W. M. Last (2001). “Sediment Core Collection and Extrusion”. In: *Tracking Environmental Change Using Lake Sediments*. Ed. by W. M. Last and J. P. Smol. Developments in Paleoenvironmental Research 1. The Netherlands: Kluwer Academic Publishers, pp. 73–105. URL: http://link.springer.com/chapter/10.1007/0-306-47669-X_5 (visited on 11/24/2014).

Gobeil, C., A. Tessier, and R.-M. Couture (2013). “Upper Mississippi Pb as a Mid-1800s Chronostratigraphic Marker in Sediments from Seasonally Anoxic Lakes in Eastern Canada”. In: *Geochimica et Cosmochimica Acta* 113, pp. 125–135. DOI: 10.1016/j.gca.2013.02.023.

Goring, S., A. Dawson, G. Simpson, K. Ram, R. Graham, E. Grimm, and J. Williams (2015). “Neotoma: A Programmatic Interface to the Neotoma Paleoecological Database”. In: *Open Quaternary* 1.1, Art. 2. DOI: 10.5334/oq.ab.

Graney, J. R., A. N. Halliday, G. J. Keeler, J. O. Nriagu, J. A. Robbins, and S. A. Norton (1995). “Isotopic Record of Lead Pollution in Lake Sediments from the Northeastern United States”. In: *Geochimica et Cosmochimica Acta* 59.9, pp. 1715–1728. DOI: 10.1016/0016-7037(95)00077-D.

Grégoire, D. S. and A. J. Poulain (2018). “Shining Light on Recent Advances in Microbial Mercury Cycling”. In: *FACETS*. DOI: 10.1139/facets-2018-0015.

Grimm, E. (2002). *Tilia*Graph*. URL: http://www.ncdc.noaa.gov/paleo/tiliafaq.html.

Grimm, E. C. (1987). “CONISS: A FORTRAN 77 Program for Stratigraphically Constrained Cluster Analysis by the Method of Incremental Sum of Squares”. In: *Computers & Geosciences* 13.1, pp. 13–35. DOI: 10.1016/0098-3004(87)90022-7.

Guyard, H., E. Chapron, G. St-Onge, F. S. Anselmetti, F. Arnaud, O. Magand, P. Francus, and M.-A. Mélières (2007). “High-Altitude Varve Records of Abrupt Environmental Changes and Mining Activity over the Last 4000 Years in the Western French Alps (Lake Bramant, Grandes Rousses Massif)”. In: *Quaternary Science Reviews* 26.19–21, pp. 2644–2660. DOI: 10.1016/j.quascirev.2007.07.007.

Halifax Water Commission (1995). *Downstream: An (Sic) Historical Reflection of the Halifax Water Supply System*. Halifax, Nova Scotia: Halifax Water Comission. 68 pp.

Hamilton-Taylor, J. (1979). “Enrichments of Zinc, Lead, and Copper in Recent Sediments of Windermere, England”. In: *Environmental Science & Technology* 13.6, pp. 693–697. DOI: 10.1021/es60154a008.

Hanson, D. W., S. A. Norton, and J. S. Williams (1983). “Spatial and Temporal Trends in the Chemistry of Atmospheric Deposition in New England”. In: *International Symposium on Hydrometeorology, June 13-17, 1982, Denver, Colorado*. Ed. by A. I. Johnson and R. A. Clark. Denver, Colorado: American Water Resources Association, pp. 25–33. Google Books: WNgsAQAAMAAJ. URL: https://books.google.ca/books/about/?id=WNgsAQAAMAAJ.

Hanson, D. W., S. A. Norton, and J. S. Williams (1982). “Modern and Paleolimnological Evidence for Accelerated Leaching and Metal Accumulation in Soils in New England, Caused by Atmospheric Deposition”. In: *Water, Air, and Soil Pollution* 18.1, pp. 227–239. DOI: 10.1007/BF02419415.

Hansson, S. V., A. Claustres, A. Probst, F. De Vleeschouwer, S. Baron, D. Galop, F. Mazier, and G. Le Roux (2017). “Atmospheric and Terrigenous Metal Accumulation over 3000 Years in a French Mountain Catchment: Local vs Distal Influences”. In: *Anthropocene* 19, pp. 45–54. DOI: 10.1016/j.ancene.2017.09.002.

Healy, K. (2018). *Data Visualization: A Practical Introduction*. 1 edition. Princeton, NJ: Princeton University Press. 296 pp.

Heit, M., Y. Tan, C. Klusek, and J. C. Burke (1981). “Anthropogenic Trace Elements and Polycyclic Aromatic Hydrocarbon Levels in Sediment Cores from Two Lakes in the Adirondack Acid Lake Region”. In: *Water, Air, and Soil Pollution* 15.4, pp. 441–464. DOI: 10.1007/BF00279426.

Henry, L., H. Wickham, and W. Chang (2020). *ggstance: Horizontal ’ggplot2’ Components*. R package version 0.3.4. URL: https://CRAN.R-project.org/package=ggstance.

Hillman, A. L., M. B. Abbott, J. Yu, D. J. Bain, and T. Chiou-Peng (2015). “Environmental Legacy of Copper Metallurgy and Mongol Silver Smelting Recorded in Yunnan Lake Sediments”. In: *Environmental Science & Technology* 49.6, pp. 3349–3357. DOI: 10.1021/es504934r.

Hillman, A. L., J. Yu, M. B. Abbott, C. A. Cooke, D. J. Bain, and B. A. Steinman (2014). "Rapid Environmental Change during Dynastic Transitions in Yunnan Province, China". In: *Quaternary Science Reviews* 98, pp. 24–32. DOI: 10.1016/j.quascirev.2014.05.019.

Hilton, J., W. Davison, and U. Ochsenbein (1985). "A Mathematical Model for Analysis of Sediment Core Data: Implications for Enrichment Factor Calculations and Trace-Metal Transport Mechanisms". In: *Chemical Geology* 48.1–4, pp. 281–291. DOI: 10.1016/0009-2541(85)90053-1.

Hoffman, E., J. Lyons, J. Boxall, C. Robertson, C. B. Lake, and T. R. Walker (2017). "Spatiotemporal Assessment (Quarter Century) of Pulp Mill Metal(Loid) Contaminated Sediment to Inform Remediation Decisions". In: *Environmental Monitoring and Assessment* 189.6, p. 257. DOI: 10.1007/s10661-017-5952-0.

Holmes, B. E. (2018). "Application of the Paleolimnological Method in the Environmental Assessment of Pulp Mill Effluent-Influenced Freshwater Sediment in Pictou County, Nova Scotia". B.Sc.H. Thesis. Wolfville, Nova Scotia: Acadia University. 108 pp. URL: https://scholar.acadiau.ca/islandora/object/theses:3239 (visited on 11/01/2018).

Hong, S., J.-P. Candelone, C. C. Patterson, and C. F. Boutron (1994). "Greenland Ice Evidence of Hemispheric Lead Pollution Two Millennia Ago by Greek and Roman Civilizations". In: *Science* 265.5180, pp. 1841–1843. DOI: 10.1126/science.265.5180.1841. pmid: 17797222.

Horowitz, A. J., K. A. Elrick, J. A. Robbins, and R. B. Cook (1995). "Effect of Mining and Related Activities on the Sediment Trace Element Geochemistry of Lake Coeur D'Alene, Idaho, USA Part II: Subsurface Sediments". In: *Hydrological Processes* 9.1, pp. 35–54. DOI: 10.1002/hyp.3360090105.

Hubeny, J. B., E. Kristiansen, A. Danikas, J. Zhu, F. M. G. McCarthy, M. G. Cantwell, B. Warren, and D. Allen (2018). "Multi-Century Record of Anthropogenic Impacts on an Urbanized Mesotidal Estuary: Salem Sound, MA". In: *Estuaries and Coasts* 41.2, pp. 404–420. DOI: 10.1007/s12237-017-0298-y.

Hunt, A. M. W. and R. J. Speakman (2015). "Portable XRF Analysis of Archaeological Sediments and Ceramics". In: *Journal of Archaeological Science* 53, pp. 626–638. DOI: 10.1016/j.jas.2014.11.031.

Johnson, M. G., L. R. Culp, and S. E. George (1986). "Temporal and Spatial Trends in Metal Loadings to Sediments of the Turkey Lakes, Ontario". In: *Canadian Journal of Fisheries and Aquatic Sciences* 43.4, pp. 754–762. DOI: 10.1139/f86-093.

Johnson, M. G. (1987). "Trace Element Loadings to Sediments of Fourteen Ontario Lakes and Correlations with Concentrations in Fish". In: *Canadian Journal of Fisheries and Aquatic Sciences* 44.1, pp. 3–13. DOI: 10.1139/f87-002.

Johnson, R. S. (1986). *Forests of Nova Scotia*. Halifax, Nova Scotia: Nova Scotia Department of Lands and Forests. 407 pp.

Johnston, H. W. (1908). “Halifax Water Works”. In: *Proceedings and Transactions of the Nova Scotian Institute of Science* 12.1, pp. 72–118. URL: http://dalspace.library.dal.ca/handle/10222/12631 (visited on 08/09/2017).

Juggins, S. (2011). *C2*. Version 1.7.6. URL: https://www.staff.ncl.ac.uk/stephen.juggins/software/C2Home.htm.

— (2013). “Quantitative Reconstructions in Palaeolimnology: New Paradigm or Sick Science?” In: *Quaternary Science Reviews* 64, pp. 20–32. DOI: 10.1016/j.quascirev.2012.12.014.

— (2019). *rioja: Analysis of Quaternary Science Data*. R package version 0.9-21. URL: https://CRAN.R-project.org/package=rioja.

Juggins, S. and R. J. Telford (2012). “Exploratory Data Analysis and Data Display”. In: *Tracking Environmental Change Using Lake Sediments*. Ed. by H. J. B. Birks, A. F. Lotter, S. Juggins, and J. P. Smol. Vol. 5. Dordrecht: Springer Netherlands, pp. 123–141. DOI: 10.1007/978-94-007-2745-8_5.

Kada, J. and M. Heit (1992). “The Inventories of Anthropogenic Ph, Zn, As, Cd, and the Radionuclides 137Cs and Excess 210Pb in Lake Sediments of the Adirondack Region, USA”. In: *Hydrobiologia* 246.3, pp. 231–241. DOI: 10.1007/BF00005700.

Kalnicky, D. J. and R. Singhvi (2001). “Field Portable XRF Analysis of Environmental Samples”. In: *Journal of Hazardous Materials*. On-Site Analysis 83.1, pp. 93–122. DOI: 10.1016/S0304-3894(00)00330-7.

Kamman, N. C. and D. R. Engstrom (2002). “Historical and Present Fluxes of Mercury to Vermont and New Hampshire Lakes Inferred from 210Pb Dated Sediment Cores”. In: *Atmospheric Environment*. NADP 2000 - Ten Years After the Clean Air Act Amendments 36.10, pp. 1599–1609. DOI: 10.1016/S1352-2310(02)00091-2.

Kane, J. S. (1993). “Reference Materials”. In: *American Laboratory* 25.2, pp. 96–97.

Kay, M. L., J. A. Wiklund, C. R. Remmer, T. J. Owca, W. H. Klemt, L. K. Neary, K. Brown, E. MacDonald, K. Thomson, J. M. Vucic, K. Wesenberg, R. I. Hall, and B. B. Wolfe (2020). “Evaluating Temporal Patterns of Metals Concentrations in Floodplain Lakes of the Athabasca Delta (Canada) Relative to Pre-Industrial Baselines”. In: *Science of The Total Environment* 704, p. 135309. DOI: 10.1016/j.scitotenv.2019.135309.

Kemp, A. L. W., R. L. Thomas, C. I. Dell, and J.-M. Jaquet (1976). “Cultural Impact on the Geochemistry of Sediments in Lake Erie”. In: *Journal of the Fisheries Research Board of Canada* 33.3, pp. 440–462. DOI: 10.1139/f76-065.

Kenna, T. C., F. O. Nitsche, M. M. Herron, B. J. Mailloux, D. Peteet, S. Sritrairat, E. Sands, and J. Baumgarten (2011). “Evaluation and Calibration of a Field Portable X-Ray Fluorescence Spectrometer for Quantitative Analysis of Siliciclastic Soils and Sediments”. In: *Journal of Analytical Atomic Spectrometry* 26.2, pp. 395–405. DOI: 10.1039/C0JA00133C.

Kilbride, C., J. Poole, and T. R. Hutchings (2006). “A Comparison of Cu, Pb, As, Cd, Zn, Fe, Ni and Mn Determined by Acid Extraction/ICP–OES and Ex Situ Field Portable X-Ray Fluorescence Analyses”. In: *Environmental Pollution* 143.1, pp. 16–23. DOI: 10.1016/j.envpol.2005.11.013.

Kingston, J. C., R. B. Cook, R. G. Kreis, K. E. Camburn, S. A. Norton, P. R. Sweets, M. W. Binford, M. J. Mitchell, S. C. Schindler, L. C. K. Shane, and G. A. King (1990). “Paleoecological Investigation of Recent Lake Acidification in the Northern Great Lakes States”. In: *Journal of Paleolimnology* 4.2, pp. 153–201. DOI: 10.1007/BF00226322.

Korosi, J. B., K. Griffiths, J. P. Smol, and J. M. Blais (2018). “Trends in Historical Mercury Deposition Inferred from Lake Sediment Cores across a Climate Gradient in the Canadian High Arctic”. In: *Environmental Pollution* 241, pp. 459–467. DOI: 10.1016/j.envpol.2018.05.049.

Köster, D., R. Pienitz, B. B. Wolfe, S. Barry, D. R. Foster, and S. S. Dixit (2005). “Paleolimnological Assessment of Human-Induced Impacts on Walden Pond (Massachusetts, USA) Using Diatoms and Stable Isotopes”. In: *Aquatic Ecosystem Health & Management* 8.2, pp. 117–131. DOI: 10.1080/14634980590953743.

Kucera, M. and B. A. Malmgren (1998). “Logratio Transformation of Compositional Data: A Resolution of the Constant Sum Constraint”. In: *Marine Micropaleontology* 34.1, pp. 117–120. DOI: 10.1016/S0377-8398(97)00047-9.

Kurek, J., J. L. Kirk, D. C. Muir, X. Wang, M. S. Evans, and J. P. Smol (2013). “Legacy of a Half Century of Athabasca Oil Sands Development Recorded by Lake Ecosystems”. In: *Proceedings of the National Academy of Sciences* 110.5, pp. 1761–1766. DOI: 10.1073/pnas.1217675110.

Kylander, M. E., D. J. Weiss, E. Peiteado Varela, T. Taboada Rodriguez, and A. Martínez Cortizas (2006). “Archiving Natural and Anthropogenic Lead Deposition in Peatlands”. In: *Developments in Earth Surface Processes*. Ed. by I. P. Martini, A. Martínez Cortizas, and W. Chesworth. Vol. 9. Peatlands. Elsevier, pp. 479–497. DOI: 10.1016/S0928-2025(06)09021-3.

Kylander, M. E., D. J. Weiss, and B. Kober (2009). “Two High Resolution Terrestrial Records of Atmospheric Pb Deposition from New Brunswick, Canada, and Loch Laxford, Scotland”. In: *Science of The Total Environment* 407.5, pp. 1644–1657. DOI: 10.1016/j.scitotenv.2008.10.036.

Laird, K., B. Cumming, and R. Nordin (2001). “A Regional Paleolimnological Assessment of the Impact of Clear-Cutting on Lakes from the West Coast of Vancouver Island, British Columbia”. In: *Canadian Journal of Fisheries and Aquatic Sciences* 58.3, pp. 479–491. DOI: 10.1139/f00-265.

Landers, D. H., C. Gubala, M. Verta, M. Lucotte, K. Johansson, T. Vlasova, and W. L. Lockhart (1998). "Using Lake Sediment Mercury Flux Ratios to Evaluate the Regional and Continental Dimensions of Mercury Deposition in Arctic and Boreal Ecosystems". In: *Atmospheric Environment*. Atmospheric Transport, Chemistry and Deposition of Mercury 32.5, pp. 919–928. DOI: 10.1016/S1352-2310(97)00116-7.

Landres, P. B., P. Morgan, and F. J. Swanson (1999). "Overview of the Use of Natural Variability Concepts in Managing Ecological Systems". In: *Ecological Applications* 9.4, pp. 1179–1188. DOI: 10.1890/1051-0761(1999)009[1179:OOTUON]2.0.CO;2.

Lang, B., A. S. Medeiros, A. Worsley, A. Bedford, and S. J. Brooks (2018). "Influence of Industrial Activity and Pollution on the Paleoclimate Reconstruction from a Eutrophic Lake in Lowland England, UK". In: *Journal of Paleolimnology* 59.4, pp. 397–410. DOI: 10.1007/s10933-017-9995-6.

Leavitt, P. R., C. S. Brock, C. Ebel, and A. Patoine (2006). "Landscape-Scale Effects of Urban Nitrogen on a Chain of Freshwater Lakes in Central North America". In: *Limnology and Oceanography* 51.5, pp. 2262–2277.

Lee, C. S. L., S.-h. Qi, G. Zhang, C.-l. Luo, L. Y. L. Zhao, and X.-d. Li (2008). "Seven Thousand Years of Records on the Mining and Utilization of Metals from Lake Sediments in Central China". In: *Environmental Science & Technology* 42.13, pp. 4732–4738. DOI: 10.1021/es702990n.

Lee, K., S. D. Hur, S. Hou, L. J. Burn-Nunes, S. Hong, C. Barbante, C. F. Boutron, and K. J. R. Rosman (2011). "Isotopic Signatures for Natural versus Anthropogenic Pb in High-Altitude Mt. Everest Ice Cores during the Past 800years". In: *Science of The Total Environment* 412-413, pp. 194–202. DOI: 10.1016/j.scitotenv.2011.10.002.

Legendre, P. and H. J. B. Birks (2012). "From Classical to Canonical Ordination". In: *Tracking Environmental Change Using Lake Sediments*. Ed. by H. J. B. Birks, A. F. Lotter, S. Juggins, and J. P. Smol. Vol. 5. Dordrecht: Springer Netherlands, pp. 201–248. DOI: 10.1007/978-94-007-2745-8_8.

Liu, X., S. Jiang, P. Zhang, and L. Xu (2012). "Effect of Recent Climate Change on Arctic Pb Pollution: A Comparative Study of Historical Records in Lake and Peat Sediments". In: *Environmental Pollution* 160 (Supplement C), pp. 161–168. DOI: 10.1016/j.envpol.2011.09.019.

Loder, A. L., M. L. Mallory, I. Spooner, C. McLauchlan, P. O. Englehardt, N. McLellan, and C. White (2016). "Bioaccumulation of Lead and Arsenic in Gastropods Inhabiting Salt Marsh Ponds in Coastal Bay of Fundy, Canada". In: *Water, Air, & Soil Pollution* 227.3, p. 75. DOI: 10.1007/s11270-016-2774-6.

Loder, A. L., M. L. Mallory, I. Spooner, N. R. McLellan, C. White, and J. P. Smol (2017). "Do Rural Impoundments in Coastal Bay of Fundy, Canada Sustain Adequate Habitat for Wildlife?" In: *Wetlands Ecology and Management*, pp. 1–18. DOI: 10.1007/s11273-017-9566-7.

Lorey, P. and C. T. Driscoll (1999). “Historical Trends of Mercury Deposition in Adirondack Lakes”. In: *Environmental Science & Technology* 33.5, pp. 718–722. DOI: 10.1021/es9800277.

Löwemark, L., H. .-F. Chen, T. .-N. Yang, M. Kylander, E. .-F. Yu, Y. .-W. Hsu, T. .-Q. Lee, S. .-R. Song, and S. Jarvis (2011). “Normalizing XRF-Scanner Data: A Cautionary Note on the Interpretation of High-Resolution Records from Organic-Rich Lakes”. In: *Journal of Asian Earth Sciences*. Quaternary Paleoclimate of the Western Pacific and East Asia: State of the Art and New Discovery 40.6, pp. 1250–1256. DOI: 10.1016/j.jseaes.2010.06.002.

Lucotte, M., A. Mucci, C. Hillaire-Marcel, P. Pichet, and A. Grondin (1995). “Anthropogenic Mercury Enrichment in Remote Lakes of Northern Québec (Canada)”. In: *Water, Air, and Soil Pollution* 80.1, pp. 467–476. DOI: 10.1007/BF01189696.

MacDonald, D. D., C. G. Ingersoll, and T. A. Berger (2000). “Development and Evaluation of Consensus-Based Sediment Quality Guidelines for Freshwater Ecosystems”. In: *Archives of Environmental Contamination and Toxicology* 39.1, pp. 20–31. DOI: 10.1007/s002440010075.

Mackereth, F. J. H. (1966). “Some Chemical Observations on Post-Glacial Lake Sediments”. In: *Philosophical Transactions of the Royal Society of London. Series B, Biological Sciences* 250.765, pp. 165–213. JSTOR: 2416701.

Mahler, B. J., P. C. van Metre, and E. Callender (2006). “Trends in Metals in Urban and Reference Lake Sediments across the United States, 1970 to 2001”. In: *Environmental Toxicology and Chemistry* 25.7. data_link: https://pubs.usgs.gov/ds/2006/166/, pp. 1698–1709. DOI: 10.1897/05-459R.1.

Mäkinen, E., M. Korhonen, E.-L. Viskari, S. Haapamäki, M. Järvinen, and L. Lu (2006). “Comparison of Xrf and Faas Methods in Analysing Cca Contaminated Soils”. In: *Water, Air, & Soil Pollution* 171.1-4, pp. 95–110. DOI: 10.1007/s11270-005-9017-6.

Mäkinen, J. (2005). “A Comparison of the Geochemistry of Aquatic Sediments and the Fine (<63 Mm) till Fraction in Finland”. In: *Geochemistry: Exploration, Environment, Analysis* 5.2, pp. 159–167. DOI: 10.1144/1467-7873/03-034.

Mandell, P. R. (1994). “The Effects of Land Use Changes on Water Quality of Urban Lakes in the Halifax/Dartmouth Region”. M.Sc. Thesis. Halifax, Nova Scotia: Dalhousie University. 186 pp.

Mariet, A.-L., F. Monna, F. Gimbert, C. Bégeot, C. Cloquet, S. Belle, L. Millet, D. Rius, and A.-V. Walter-Simonnet (2018). “Tracking Past Mining Activity Using Trace Metals, Lead Isotopes and Compositional Data Analysis of a Sediment Core from Longemer Lake, Vosges Mountains, France”. In: *Journal of Paleolimnology* 60.3, pp. 399–412. DOI: 10.1007/s10933-018-0029-9.

Martin, J. P. (1957). *The Story of Dartmouth*. Halifax, Nova Scotia: Atlantic Nova Print Ltd. 561 pp. URL: https://discover.halifaxpubliclibraries.ca/?itemid=%7Clibrary/m/halifax-horizon%7C1278572.

Martínez-Cortizas, A., E. P. Varela, R. Bindler, H. Biester, and A. Cheburkin (2012). "Reconstructing Historical Pb and Hg Pollution in NW Spain Using Multiple Cores from the Chao de Lamoso Bog (Xistral Mountains)". In: *Geochimica et Cosmochimica Acta*. Environmental Records of Anthropogenic Impacts 82, pp. 68–78. DOI: 10.1016/j.gca.2010.12.025.

Martínez Cortizas, A., E. García-Rodeja Gayoso, and D. Weiss (2002). "Peat Bog Archives of Atmospheric Metal Deposition". In: *Science of The Total Environment*. Peat Bog Archives of Atmospheric Metal Deposition 292.1, pp. 1–5. DOI: 10.1016/S0048-9697(02)00024-4.

Marx, S. K., B. S. Kamber, H. A. McGowan, and A. Zawadzki (2010). "Atmospheric Pollutants in Alpine Peat Bogs Record a Detailed Chronology of Industrial and Agricultural Development on the Australian Continent". In: *Environmental Pollution* 158.5, pp. 1615–1628. DOI: 10.1016/j.envpol.2009.12.009.

Marx, S. K., S. Rashid, and N. Stromsoe (2016). "Global-Scale Patterns in Anthropogenic Pb Contamination Reconstructed from Natural Archives". In: *Environmental Pollution* 213, pp. 283–298. DOI: 10.1016/j.envpol.2016.02.006.

Mattikalli, N. M. and K. S. Richards (1996). "Estimation of Surface Water Quality Changes in Response to Land Use Change: Application of The Export Coefficient Model Using Remote Sensing and Geographical Information System". In: *Journal of Environmental Management* 48.3, pp. 263–282. DOI: 10.1006/jema.1996.0077.

Mayr, C., A. Lücke, N. I. Maidana, M. Wille, T. Haberzettl, H. Corbella, C. Ohlendorf, F. Schäbitz, M. Fey, S. Janssen, and B. Zolitschka (2009). "Isotopic Fingerprints on Lacustrine Organic Matter from Laguna Potrok Aike (Southern Patagonia, Argentina) Reflect Environmental Changes during the Last 16,000 Years". In: *Journal of Paleolimnology* 42.1, pp. 81–102. DOI: 10.1007/s10933-008-9249-8.

McConnell, J. R., G. W. Lamorey, and M. A. Hutterli (2002). "A 250-Year High-Resolution Record of Pb Flux and Crustal Enrichment in Central Greenland". In: *Geophysical Research Letters* 29.23, p. 2130. DOI: 10.1029/2002GL016016.

McGuire, H. E. (2018). "Metal Mobility and Retention Associated with Salt Water Inundation at Laytons Lake, Nova Scotia". B.Sc.H. Thesis. Acadia University. 72 pp. URL: https://scholar.acadiau.ca/islandora/object/theses%3A2705/ (visited on 11/01/2018).

Meyers, P. A. and J. L. Teranes (2001). "Sediment Organic Matter". In: *Tracking Environmental Change Using Lake Sediments: Volume 2: Physical and Geochemical Methods*. Ed. by W. M. Last and J. P. Smol. Vol. 2. 4 vols. The Netherlands: Kluwer Academic Publishers, pp. 239–269. DOI: 10.1007/0-306-47670-3_9.

Mielke, H. W., M. A. S. Laidlaw, and C. R. Gonzales (2011). "Estimation of Leaded (Pb) Gasoline's Continuing Material and Health Impacts on 90 US Urbanized Areas". In: *Environment International* 37.1, pp. 248–257. DOI: 10.1016/j.envint.2010.08.006.

Misiuk, B. (2014). “A Multi-Proxy Comparative Paleolimnological Study of Anthropogenic Impact between First and Second Lake, Lower Sackville, Nova Scotia”. B.Sc.H. Thesis. Wolfville, NS: Acadia University. 67 pp. URL: http://scholar.acadiau.ca/islandora/object/theses:1148.

More, A. F., N. E. Spaulding, P. Bohleber, M. J. Handley, H. Hoffmann, E. V. Korotkikh, A. V. Kurbatov, C. P. Loveluck, S. B. Sneed, M. McCormick, and P. A. Mayewski (2017). “Next-Generation Ice Core Technology Reveals True Minimum Natural Levels of Lead (Pb) in the Atmosphere: Insights from the Black Death”. In: *GeoHealth*, pp. 1–9. DOI: 10.1002/2017GH000064.

Muggeo, V. M. R. (2003). “Estimating Regression Models with Unknown Break-Points”. In: *Statistics in Medicine* 22.19, pp. 3055–3071. DOI: 10.1002/sim.1545.

Nau, G. (2018). “Fishway Passage of Alewife, Alosa Pseudoharengus (Wilson, 1811), and Marine Nutrient Transfer to Freshwater Ecosystems in Three River Systems in Nova Scotia and New Brunswick, Canada”. M.Sc. Thesis. Acadia University. 72 pp. URL: https://scholar.acadiau.ca/islandora/object/theses%3A2701/ (visited on 11/01/2018).

Norton, S. A., G. C. Evans, and J. S. Kahl (1997). “Comparison of Hg and Pb Fluxes to Hummocks and Hollows of Ombrotrophic Big Heath Bog and to Nearby Sargent Mt. Pond, Maine, USA”. In: *Water, Air, and Soil Pollution* 100.3, pp. 271–286. DOI: 10.1023/A:1018380610893.

Norton, S. A. (2007). “Atmospheric Metal Pollutants-Archives, Methods, and History”. In: *Acid Rain - Deposition to Recovery*. Ed. by P. Brimblecombe, H. Hara, D. Houle, and M. Novak. Dordrecht: Springer Netherlands, pp. 93–98. DOI: 10.1007/978-1-4020-5885-1_11.

Norton, S. A., R. W. Bienert, M. W. Binford, and J. S. Kahl (1992). “Stratigraphy of Total Metals in PIRLA Sediment Cores”. In: *Journal of Paleolimnology* 7.3, pp. 191–214. DOI: 10.1007/BF00181714.

Norton, S. A., P. J. Dillon, R. D. Evans, G. Mierle, and J. S. Kahl (1990). “The History of Atmospheric Deposition of Cd, Hg, and Pb in North America: Evidence from Lake and Peat Bog Sediments”. In: *Acidic Precipitation: Sources, Deposition, and Canopy Interactions*. Ed. by S. E. Lindberg, A. L. Page, and S. A. Norton. Advances in Environmental Science. New York, NY: Springer New York, pp. 73–102. DOI: 10.1007/978-1-4612-4454-7_4.

Norton, S. A. and T. C. Hess (1980). “Atmospheric Deposition in Norway during the Last 300 Years as Recorded in SNSF Lake Sediments. I. Sediment Dating and Chemical Stratigraphy”. In: *Ecological Impact of Acid Precipitation : Proceedings of an International Conference, Sandefjord, Norway, March 11-14, 1980*. Ed. by D. Drabløs and A. Tollan. Oslo : SNSF Project. URL: https://trove.nla.gov.au/version/24031620 (visited on 09/16/2018).

Norton, S. A. and J. S. Kahl (1987). “A Comparison of Lake Sediments and Ombrotrophic Peat Deposits as Long-Term Monitors of Atmospheric Pollution”. In: *New Approaches to Monitoring Aquatic Ecosystems*. Ed. by T. Boyle. West Conshohocken, PA: ASTM International, pp. 40–57. DOI: 10.1520/STP28580S.

Norton, S. A. and J. S. Kahl (1986). “Atmospheric Deposition of Lead in Sediments and Peat”. In: *Pathways, Cycling, and Transformation of Lead in the Environment*. Toronto, Ontario: The Royal Society of Canada, pp. 97–132.

Norton, S. A., E. R. Perry, T. A. Haines, and A. C. Dieffenbacher-Krall (2004). “Paleolimnological Assessment of Grove and Plow Shop Ponds, Ayer, Massachusetts, USA – A Superfund Site”. In: *Journal of Environmental Monitoring* 6.5, pp. 457–465. DOI: 10.1039/B315640K.

Norton, S. A., M. Verta, and J. S. Kahl (1991). “Relative Contributions to Lake Sediment Chemistry by Atmospheric Deposition”. In: *Verhandlungen des Internationalen Verein Limnologie* 24.5, pp. 2989–2993. DOI: 10.1080/03680770.1989.11899215.

Norton, S. A., T. Wilson, M. Handley, and E. C. Osterberg (2007). “Atmospheric Deposition of Cadmium in the Northeastern USA”. In: *Applied Geochemistry*. Selected Papers from the 7th International Conference on Acid Deposition, Prague, Czech Republic, 12–17 June, 2005 22.6, pp. 1217–1222. DOI: 10.1016/j.apgeochem.2007.03.014.

Nova Scotia Department of Natural Resources (2017). *Aerial Photography Collection | GeoNOVA*. URL: https://geonova.novascotia.ca/aerial-photography-collection (visited on 02/01/2017).

Nova Scotia Environment (2017). *Air Quality Forum*. URL: https://novascotia.ca/nse/air/airqualityforumpresentations.asp (visited on 01/02/2020).

Nriagu, J. O. (1990). “The Rise and Fall of Leaded Gasoline”. In: *Science of The Total Environment* 92, pp. 13–28. DOI: 10.1016/0048-9697(90)90318-O.

Nriagu, J. O., H. K. T. Wong, and R. D. Coker (1982). “Deposition and Chemistry of Pollutant Metals in Lakes around the Smelters at Sudbury, Ontario”. In: *Environmental Science & Technology* 16.9, pp. 551–560. DOI: 10.1021/es00103a004.

O’Reilly, C. M., D. L. Dettman, and A. S. Cohen (2005). “Paleolimnological Investigations of Anthropogenic Environmental Change in Lake Tanganyika: VI. Geochemical Indicators”. In: *Journal of Paleolimnology* 34.1, pp. 85–91. DOI: 10.1007/s10933-005-2399-z.

Ogden, J. (1971). *Water Quality Survey of Selected Metropolitan Area Lakes*. Halifax, Nova Scotia: Metropolitain Area Planning Comittee.

Osterberg, E., P. Mayewski, K. Kreutz, D. Fisher, M. Handley, S. Sneed, C. Zdanowicz, J. Zheng, M. Demuth, M. Waskiewicz, and J. Bourgeois (2008). “Ice Core Record of Rising Lead Pollution in the North Pacific Atmosphere”. In: *Geophysical Research Letters* 35.5. DOI: 10.1029/2007GL032680.

Oudijk, G. (2010). “The Rise and Fall of Organometallic Additives in Automotive Gasoline”. In: *Environmental Forensics* 11.1-2, pp. 17–49. DOI: 10.1080/15275920903346794.

Ouellet, M. and H. G. Jones (1983). “Paleolimnological Evidence for the Long-Range Atmospheric Transport of Acidic Pollutants and Heavy Metals into the Province of Quebec, Eastern Canada”. In: *Canadian Journal of Earth Sciences* 20.1, pp. 23–36. DOI: 10.1139/e83-003.

Outridge, P. M. and F. Wang (2015). “The Stability of Metal Profiles in Freshwater and Marine Sediments”. In: *Environmental Contaminants*. Ed. by J. M. Blais, M. R. Rosen, and J. P. Smol. Developments in Paleoenvironmental Research 18. Springer Netherlands, pp. 35–60. DOI: 10.1007/978-94-017-9541-8_3.

Pacyna, J. M. (1987). “Atmospheric Emissions of Arsenic, Cadmium, Lead and Mercuryfrom High Temperature Processes in Power Generation and Industry”. In: *Lead, Mercury, Cadmium and Arsenic in the Environment*. Ed. by T. C. Hutchinson and K. M. Memma. New York: John Wiley & Sons, pp. 69–87.

Panizzo, V. N., A. W. Mackay, N. L. Rose, P. Rioual, and M. J. Leng (2013). “Recent Palaeolimnological Change Recorded in Lake Xiaolongwan, Northeast China: Climatic versus Anthropogenic Forcing”. In: *Quaternary International*. The Baikal-Hokkaido Archaeology Project: Environmental Archives, Proxies and Reconstruction Approaches 290-291 (Supplement C), pp. 322–334. DOI: 10.1016/j.quaint.2012.07.033.

Parsons, C., E. Margui Grabulosa, E. Pili, G. H. Floor, G. Roman-Ross, and L. Charlet (2013). “Quantification of Trace Arsenic in Soils by Field-Portable X-Ray Fluorescence Spectrometry: Considerations for Sample Preparation and Measurement Conditions”. In: *Journal of Hazardous Materials* 262, pp. 1213–1222. DOI: 10.1016/j.jhazmat.2012.07.001.

Paterson, A. M., B. F. Cumming, J. P. Smol, J. M. Blais, and R. L. France (1998). “Assessment of the Effects of Logging, Forest Fires and Drought on Lakes in Northwestern Ontario: A 30-Year Paleolimnological Perspective”. In: *Canadian Journal of Forest Research* 28.10, pp. 1546–1556. DOI: 10.1139/x98-138.

Pawlowsky-Glahn, V. and J. J. Egozcue (2006). “Compositional Data and Their Analysis: An Introduction”. In: *Geological Society, London, Special Publications* 264.1, pp. 1–10. DOI: 10.1144/GSL.SP.2006.264.01.01.

Pedersen, T. L. (2017). *patchwork: The Composer of ggplots*. R package version 0.0.1. URL: https://github.com/thomasp85/patchwork.

Percival, J. B. and P. M. Outridge (2013). “A Test of the Stability of Cd, Cu, Hg, Pb and Zn Profiles over Two Decades in Lake Sediments near the Flin Flon Smelter, Manitoba, Canada”. In: *Science of The Total Environment* 454-455, pp. 307–318. DOI: 10.1016/j.scitotenv.2013.03.011.

Perry, E., S. A. Norton, N. C. Kamman, P. M. Lorey, and C. T. Driscoll (2005). “Deconstruction of Historic Mercury Accumulation in Lake Sediments, Northeastern United States”. In: *Ecotoxicology* 14.1, pp. 85–99. DOI: 10.1007/s10646-004-6261-2.

Pienitz, R., K. Roberge, and W. F. Vincent (2006). “Three Hundred Years of Human-Induced Change in an Urban Lake: Paleolimnological Analysis of Lac Saint-Augustin, Québec City, Canada”. In: *Canadian Journal of Botany* 84.2, pp. 303–320. DOI: 10.1139/b05-152.

Planchon, F. A. M., K. van de Velde, K. J. R. Rosman, E. W. Wolff, C. P. Ferrari, and C. F. Boutron (2003). “One Hundred Fifty–Year Record of Lead Isotopes in Antarctic Snow from Coats Land”. In: *Geochimica et Cosmochimica Acta* 67.4, pp. 693–708. DOI: 10.1016/S0016-7037(02)01136-5.

Poltarowicz, J. (2017). “An Analysis of Phosphorus Loading and Trophic State in Fletchers Lake, Nova Scotia”. M.Sc. Thesis. Halifax, Nova Scotia: Dalhousie University. URL: http://DalSpace.library.dal.ca/handle/10222/72830 (visited on 04/12/2017).

Pompeani, D. P., M. B. Abbott, B. A. Steinman, and D. J. Bain (2013). “Lake Sediments Record Prehistoric Lead Pollution Related to Early Copper Production in North America”. In: *Environmental Science & Technology* 47.11, pp. 5545–5552. DOI: 10.1021/es304499c.

Pratte, S., A. Mucci, and M. Garneau (2013). “Historical Records of Atmospheric Metal Deposition along the St. Lawrence Valley (Eastern Canada) Based on Peat Bog Cores”. In: *Atmospheric Environment* 79, pp. 831–840. DOI: 10.1016/j.atmosenv.2013.07.063.

Province of Nova Scotia, Halifax County, City of Halifax Sheet, No. 68 (1908). In collab. with E. Fairibault. Publication No. 1019. Ottawa, Ontario.

QGIS Development Team (2020). *QGIS Geographic Information System*. Open Source Geospatial Foundation Project. Vienna, Austria. URL: http://qgis.osgeo.org.

Qin, B., G. Zhu, G. Gao, Y. Zhang, W. Li, H. W. Paerl, and W. W. Carmichael (2010). “A Drinking Water Crisis in Lake Taihu, China: Linkage to Climatic Variability and Lake Management”. In: *Environmental Management* 45.1, pp. 105–112. DOI: 10.1007/s00267-009-9393-6.

R Core Team (2019). *R: A Language and Environment for Statistical Computing*. R Foundation for Statistical Computing. Vienna, Austria. URL: https://www.R-project.org/.

Radu, T. and D. Diamond (2009). “Comparison of Soil Pollution Concentrations Determined Using AAS and Portable XRF Techniques”. In: *Journal of Hazardous Materials* 171.1, pp. 1168–1171. DOI: 10.1016/j.jhazmat.2009.06.062.

Reimann, C., P. Filzmoser, K. Fabian, K. Hron, M. Birke, A. Demetriades, E. Dinelli, and A. Ladenberger (2012). “The Concept of Compositional Data Analysis in Practice — Total Major Element Concentrations in Agricultural and Grazing Land Soils of Europe”. In: *Science of The Total Environment* 426, pp. 196–210. DOI: 10.1016/j.scitotenv.2012.02.032.

Renberg, I. (1986). “Concentration and Annual Accumulation Values of Heavy Metals in Lake Sediments: Their Significance in Studies of the History of Heavy Metal Pollution”. In: *Hydrobiologia* 143.1, pp. 379–385. DOI: 10.1007/BF00026686.

Renberg, I., M.-L. Brännvall, R. Bindler, and O. Emteryd (2000). "Atmospheric Lead Pollution History during Four Millennia (2000 BC to 2000 AD) in Sweden". In: *AMBIO: A Journal of the Human Environment* 29.3, pp. 150–157. DOI: 10.1579/0044-7447-29.3.150.

Renberg, I., M. W. Persson, and O. Emteryd (1994). "Pre-Industrial Atmospheric Lead Contamination Detected in Swedish Lake Sediments". In: *Nature* 368.6469, pp. 323–326. DOI: 10.1038/368323a0.

Richardson, J. B., A. J. Friedland, J. M. Kaste, and B. P. Jackson (2014). "Forest Floor Lead Changes from 1980 to 2011 and Subsequent Accumulation in the Mineral Soil across the Northeastern United States". In: *Journal of Environmental Quality* 43.3, pp. 926–935. DOI: 10.2134/jeq2013.10.0435.

Robbins, J. A., C. Holmes, R. Halley, M. Bothner, E. Shinn, J. Graney, G. Keeler, M. tenBrink, K. A. Orlandini, and D. Rudnick (2000). "Time-Averaged Fluxes of Lead and Fallout Radionuclides to Sediments in Florida Bay". In: *Journal of Geophysical Research: Oceans* 105.C12, pp. 28805–28821. DOI: 10.1029/1999JC000271.

Roberts, S., J. L. Kirk, J. A. Wiklund, D. C. G. Muir, F. Yang, A. Gleason, and G. Lawson (2019). "Mercury and Metal(Loid) Deposition to Remote Nova Scotia Lakes from Both Local and Distant Sources". In: *Science of The Total Environment* 675, pp. 192–202. DOI: 10.1016/j.scitotenv.2019.04.167.

Rogalski, M. A. (2015). "Tainted Resurrection: Metal Pollution Is Linked with Reduced Hatching and High Juvenile Mortality in Daphnia Egg Banks". In: *Ecology* 96.5, pp. 1166–1173. DOI: 10.1890/14-1663.1.

Rose, N. L., H. Yang, S. D. Turner, and G. L. Simpson (2012). "An Assessment of the Mechanisms for the Transfer of Lead and Mercury from Atmospherically Contaminated Organic Soils to Lake Sediments with Particular Reference to Scotland, UK". In: *Geochimica et Cosmochimica Acta*. Environmental Records of Anthropogenic Impacts 82, pp. 113–135. DOI: 10.1016/j.gca.2010.12.026.

Rosen, M. R. and P. C. Van Metre (2010). "Assessment of Multiple Sources of Anthropogenic and Natural Chemical Inputs to a Morphologically Complex Basin, Lake Mead, USA". In: *Palaeogeography, Palaeoclimatology, Palaeoecology*. Paleolimnology 294.1, pp. 30–43. DOI: 10.1016/j.palaeo.2009.03.017.

Rosenmeier, M. F., M. Brenner, W. F. Kenney, T. J. Whitmore, and C. M. Taylor (2004). "Recent Eutrophication in the Southern Basin of Lake Petén Itzá, Guatemala: Human Impact on a Large Tropical Lake". In: *Hydrobiologia* 511.1-3, pp. 161–172. DOI: 10.1023/B:HYDR.0000014038.64403.4d.

Rossi, R. J., D. J. Bain, A. L. Hillman, D. P. Pompeani, M. S. Finkenbinder, and M. B. Abbott (2017). "Reconstructing Early Industrial Contributions to Legacy Trace Metal Contamination in Southwestern Pennsylvania". In: *Environmental Science & Technology*. DOI: 10.1021/acs.est.6b03372.

Rouillon, M. and M. P. Taylor (2016). "Can Field Portable X-Ray Fluorescence (pXRF) Produce High Quality Data for Application in Environmental Contamination Research?" In: *Environmental Pollution* 214, pp. 255–264. DOI: 10.1016/j.envpol.2016.03.055.

Routh, J., P. Choudhary, P. A. Meyers, and B. Kumar (2009). "A Sediment Record of Recent Nutrient Loading and Trophic State Change in Lake Norrviken, Sweden". In: *Journal of Paleolimnology* 42.3, pp. 325–341. DOI: 10.1007/s10933-008-9279-2.

Rydberg, J. (2014). "Wavelength Dispersive X-Ray Fluorescence Spectroscopy as a Fast, Non-Destructive and Cost-Effective Analytical Method for Determining the Geochemical Composition of Small Loose-Powder Sediment Samples". In: *Journal of Paleolimnology* 52.3, pp. 265–276. DOI: 10.1007/s10933-014-9792-4.

Sanchez-Cabeza, J.-A., A. C. Ruiz-Fernández, J. F. Ontiveros-Cuadras, L. H. Pérez Bernal, and C. Olid (2014). "Monte Carlo Uncertainty Calculation of 210Pb Chronologies and Accumulation Rates of Sediments and Peat Bogs". In: *Quaternary Geochronology* 23, pp. 80–93. DOI: 10.1016/j.quageo.2014.06.002.

Sarkar, S., T. Ahmed, K. Swami, C. D. Judd, A. Bari, V. A. Dutkiewicz, and L. Husain (2015). "History of Atmospheric Deposition of Trace Elements in Lake Sediments, 1880 to 2007". In: *Journal of Geophysical Research: Atmospheres* 120.11, pp. 5658–5669. DOI: 10.1002/2015JD023202.

Sharp, R. M. and D. J. Brabander (2017). "Lead (Pb) Bioaccessibility and Mobility Assessment of Urban Soils and Composts: Fingerprinting Sources and Refining Risks to Support Urban Agriculture". In: *GeoHealth* 1.10, pp. 333–345. DOI: 10.1002/2017GH000093.

Shotbolt, L., S. M. Hutchinson, and A. D. Thomas (2006). "Sediment Stratigraphy and Heavy Metal Fluxes to Reservoirs in the Southern Pennine Uplands, UK". In: *Journal of Paleolimnology* 35.2, pp. 305–322. DOI: 10.1007/s10933-005-1594-2.

Shotyk, W., M. E. Goodsite, F. Roos-Barraclough, R. Frei, J. Heinemeier, G. Asmund, C. Lohse, and T. S. Hansen (2003). "Anthropogenic Contributions to Atmospheric Hg, Pb and As Accumulation Recorded by Peat Cores from Southern Greenland and Denmark Dated Using the 14C "Bomb Pulse Curve"". In: *Geochimica et Cosmochimica Acta* 67.21, pp. 3991–4011. DOI: 10.1016/S0016-7037(03)00409-5.

Shotyk, W., P. G. Appleby, B. Bicalho, L. J. Davies, D. Froese, I. Grant-Weaver, G. Magnan, G. Mullan-Boudreau, T. Noernberg, R. Pelletier, B. Shannon, S. van Bellen, and C. Zaccone (2017). "Peat Bogs Document Decades of Declining Atmospheric Contamination by Trace Metals in the Athabasca Bituminous Sands Region". In: *Environmental Science & Technology*. DOI: 10.1021/acs.est.6b04909.

Shotyk, W., P. G. Appleby, B. Bicalho, L. Davies, D. Froese, I. Grant-Weaver, M. Krachler, G. Magnan, G. Mullan-Boudreau, T. Noernberg, R. Pelletier, B. Shannon, S. van Bellen, and C. Zaccone (2016). "Peat Bogs in Northern Alberta, Canada Reveal Decades of Declining Atmospheric Pb Contamination". In: *Geophysical Research Letters* 43.18, 2016GL070952. DOI: 10.1002/2016GL070952.

Shotyk, W., R. Belland, J. Duke, H. Kempter, M. Krachler, T. Noernberg, R. Pelletier, M. A. Vile, K. Wieder, C. Zaccone, and S. Zhang (2014). "Sphagnum Mosses from 21 Ombrotrophic Bogs in the Athabasca Bituminous Sands Region Show No Significant Atmospheric Contamination of "Heavy Metals"". In: *Environmental Science & Technology* 48.21, pp. 12603–12611. DOI: 10.1021/es503751v.

Shuttleworth, E. L., M. G. Evans, S. M. Hutchinson, and J. J. Rothwell (2014). "Assessment of Lead Contamination in Peatlands Using Field Portable XRF". In: *Water, Air, & Soil Pollution* 225.2, p. 1844. DOI: 10.1007/s11270-013-1844-2.

Simonneau, A., E. Doyen, E. Chapron, L. Millet, B. Vannière, C. Di Giovanni, N. Bossard, K. Tachikawa, E. Bard, P. Albéric, M. Desmet, G. Roux, P. Lajeunesse, J. F. Berger, and F. Arnaud (2013). "Holocene Land-Use Evolution and Associated Soil Erosion in the French Prealps Inferred from Lake Paladru Sediments and Archaeological Evidences". In: *Journal of Archaeological Science* 40.4, pp. 1636–1645. DOI: 10.1016/j.jas.2012.12.002.

Simpson, G. L. and J. Oksanen (2020). *analogue: Analogue and Weighted Averaging Methods for Palaeoecology*. R package version 0.17-4. URL: https://CRAN.R-project.org/package=analogue.

Siver, P. A. and J. A. Wizniak (2001). "Lead Analysis of Sediment Cores from Seven Connecticut Lakes". In: *Journal of Paleolimnology* 26.1, pp. 1–10. DOI: 10.1023/A:1011131201092.

Smiley, M. (1971). *Historical Recordings of Beaver Bank 1798-1968 Halifax County Nova Scotia*. Halifax, Nova Scotia: Maribelle Smiley. URL: https://discover.halifaxpubliclibraries.ca/?itemid=%7Clibrary/m/halifax-horizon%7C1354669.

Smol, J. P. (1992). "Paleolimnology: An Important Tool for Effective Ecosystem Management". In: *Journal of Aquatic Ecosystem Health* 1.1, pp. 49–58. URL: http://link.springer.com/article/10.1007/BF00044408 (visited on 02/17/2014).

— (1995). "Paleolimnological Approaches to the Evaluation and Monitoring of Ecosystem Health: Providing a History for Environmental Damage and Recovery". In: *Evaluating and Monitoring the Health of Large-Scale Ecosystems*. Ed. by D. J. Rapport, C. L. Gaudet, and P. Calow. NATO ASI Series 28. Berlin: Springer-Verlag, pp. 301–318. DOI: 10.1007/978-3-642-79464-3_19. (Visited on 06/03/2015).

— (2010). "The Power of the Past: Using Sediments to Track the Effects of Multiple Stressors on Lake Ecosystems". In: *Freshwater Biology* 55, pp. 43–59. DOI: 10.1111/j.1365-2427.2009.02373.x.

Sprague, D. D. and J. C. Vermaire (2018). "Legacy Arsenic Pollution of Lakes Near Cobalt, Ontario, Canada: Arsenic in Lake Water and Sediment Remains Elevated Nearly a Century After Mining Activity Has Ceased". In: *Water, Air, & Soil Pollution* 229.3, p. 87. DOI: 10.1007/s11270-018-3741-1.

Stantec Consulting Ltd. (2012). *An Analysis of the HRM Lakes Water Quality Monitoring Program (2007-2011)*. Halifax, Nova Scotia: Halifax Regional Municipality, p. 180.

Steenberg, J. W. N., P. N. Duinker, and P. G. Bush (2013). "Modelling the Effects of Climate Change and Timber Harvest on the Forests of Central Nova Scotia, Canada". In: *Annals of Forest Science* 70.1, pp. 61–73. DOI: 10.1007/s13595-012-0235-y.

Stromsoe, N., J. N. Callow, H. A. McGowan, and S. K. Marx (2013). "Attribution of Sources to Metal Accumulation in an Alpine Tarn, the Snowy Mountains, Australia". In: *Environmental Pollution* 181, pp. 133–143. DOI: 10.1016/j.envpol.2013.05.051.

Sunderland, E. M., M. D. Cohen, N. E. Selin, and G. L. Chmura (2008). "Reconciling Models and Measurements to Assess Trends in Atmospheric Mercury Deposition". In: *Environmental Pollution* 156.2, pp. 526–535. DOI: 10.1016/j.envpol.2008.01.021.

Sweets, P. R., R. W. Bienert, T. L. Crisman, and M. W. Binford (1990). "Paleoecological Investigations of Recent Lake Acidification in Northern Florida". In: *Journal of Paleolimnology* 4.2, pp. 103–137. DOI: 10.1007/BF00226320.

Swetnam, T. W., C. D. Allen, and J. L. Betancourt (1999). "Applied Historical Ecology: Using the Past to Manage for the Future". In: *Ecological Applications* 9.4, pp. 1189–1206. DOI: 10.1890/1051-0761(1999)009[1189:AHEUTP]2.0.CO;2.

Tarr, C. and C. E. White (2016). "Acid Rock Drainage in the Chain Lakes Watershe, Halifax Regional Municipality, Nova Scotia". In: *Geoscience and Mines Branch Report ME 2016-001: Report of Activities 2015*. Halifax, Nova Scotia: Nova Scotia Department of Natural Resources, pp. 109–119.

Teranes, J. L. and S. M. Bernasconi (2000). "The Record of Nitrate Utilization and Productivity Limitation Provided by d15N Values in Lake Organic Matter—a Study of Sediment Trap and Core Sediments from Baldeggersee, Switzerland". In: *Limnology and Oceanography* 45.4, pp. 801–813. URL: http://aslo.net/lo/toc/vol_45/issue_4/0801.pdf (visited on 10/02/2014).

Terry, D. B. (2011). "The Effects of Water Level Fluctuations and Sediment Resuspension on Water Quality at Tupper Lake, Nova Scotia". B.Sc.H. Thesis. Wolfville, NS: Acadia University. URL: http://openarchive.acadiau.ca/cdm/singleitem/collection/HTheses/id/700/rec/12.

Thienpont, J. R., J. B. Korosi, K. E. Hargan, T. Williams, D. C. Eickmeyer, L. E. Kimpe, M. J. Palmer, J. P. Smol, and J. M. Blais (2016). "Multi-Trophic Level Response to Extreme Metal Contamination from Gold Mining in a Subarctic Lake". In: *Proc. R. Soc. B* 283.1836, p. 20161125. DOI: 10.1098/rspb.2016.1125. pmid: 27534958.

Tremblay, V., I. Larocque-Tobler, and P. Sirois (2010). "Historical Variability of Subfossil Chironomids (Diptera: Chironomidae) in Three Lakes Impacted by Natural and Anthropogenic Disturbances". In: *Journal of Paleolimnology* 44.2, pp. 483–495. DOI: 10.1007/s10933-010-9429-1.

Tropea, A. E., B. K. Ginn, B. F. Cumming, and J. P. Smol (2007). "Tracking Long-Term Acidification Trends in Pockwock Lake (Halifax, Nova Scotia), the Water Supply for a Major Eastern Canadian City". In: *Lake and Reservoir Management* 23.3, pp. 279–286. DOI: 10.1080/07438140709354016.

Turner, A., H. Poon, A. Taylor, and M. T. Brown (2017). "In Situ Determination of Trace Elements in Fucus Spp. by Field-Portable-XRF". In: *Science of The Total Environment* 593-594, pp. 227–235. DOI: 10.1016/j.scitotenv.2017.03.091.

Tymstra, D. (2013). "A Paleolimnological Record of Anthropogenic Impact on Water Quality in First Lake, Lower Sackville, Nova Scotia". B.Sc.H. Thesis. Wolfville, NS: Acadia University. 72 pp. URL: http://scholar.acadiau.ca/islandora/object/theses:1014.

United States Environmental Protection Agency (2020). *Chemview*. URL: https://chemview.epa.gov/ (visited on 02/28/2020).

USEPA (1998). *Environmental Technology Verification Report: Field Portable X-Ray Fluorescence Analyzer*. EPA/600/R-97/146. United States Environmental Protection Agency. URL: https://nepis.epa.gov/Adobe/PDF/30003LR0.pdf (visited on 06/28/2017).

Vallelonga, P., K. Van de Velde, J. .-P. Candelone, V. I. Morgan, C. F. Boutron, and K. J. R. Rosman (2002). "The Lead Pollution History of Law Dome, Antarctica, from Isotopic Measurements on Ice Cores: 1500 AD to 1989 AD". In: *Earth and Planetary Science Letters* 204.1, pp. 291–306. DOI: 10.1016/S0012-821X(02)00983-4.

van den Boogaart, K. G., R. Tolosana-Delgado, and M. Bren (2018). *compositions: Compositional Data Analysis*. R package version 1.40-2. URL: https://CRAN.R-project.org/package=compositions.

Van Der Weijden, C. H. (2002). "Pitfalls of Normalization of Marine Geochemical Data Using a Common Divisor". In: *Marine Geology* 184.3, pp. 167–187. DOI: 10.1016/S0025-3227(01)00297-3.

Van Metre, P., J. T. Wilson, C. C. Fuller, E. Callender, and B. J. Mahler (2004). *Collection, Analysis, and Age-Dating of Sediment Cores from 56 U.S. Lakes and Reservoirs Sampled by the U.S. Geological Survey, 1992-2001*. USGS Numbered Series 2004-5184. U.S. Geological Survey, p. 187. DOI: 10.3133/sir20045184.

Van Metre, P. C., B. J. Mahler, and J. T. Wilson (2006). *Major and Trace Elements in 35 Lake and Reservoir Sediment Cores From Across the United States, 1994–2001*. Data Series 166. Denver, Colorado: United States Geological Survey, p. 36. DOI: 10.3133/ds166.

Verta, M., K. Tolonen, and H. Simola (1989). "History of Heavy Metal Pollution in Finland as Recorded by Lake Sediments". In: *Science of The Total Environment*. Trace Metals in Lakes 87-88, pp. 1–18. DOI: 10.1016/0048-9697(89)90222-2.

Walker, I. R., E. D. Reavie, S. Palmer, and R. N. Nordin (1993). "A Palaeoenvironmental Assessment of Human Impact on Wood Lake, Okanagan Valley, British Columbia, Canada". In: *Quaternary International* 20, pp. 51–70. DOI: 10.1016/1040-6182(93)90036-F.

Walters, L. J., T. J. Wolery, and R. D. Myser (1974). "Occurrence of As, Cd, Co, Cr, Cu, Fe, Hg, Ni, Sb, and Zn in Lake Erie Sediments". In: *Proceedings: Seventeenth Conference on Great Lakes Research*. Conference on Great Lakes Research. Hamilton, Ontario: International Association for Great Lakes Research, pp. 219–234.

Watmough, S. A. (2017). "Historical and Contemporary Metal Budgets for a Boreal Shield Lake". In: *Science of The Total Environment* 598, pp. 49–57. DOI: 10.1016/j.scitotenv.2017.04.077.

Weiss, D., W. Shotyk, E. A. Boyle, J. D. Kramers, P. G. Appleby, and A. K. Cheburkin (2002). "Comparative Study of the Temporal Evolution of Atmospheric Lead Deposition in Scotland and Eastern Canada Using Blanket Peat Bogs". In: *Science of The Total Environment* 292, pp. 7–18. DOI: 10.1016/S0048-9697(02)00025-6.

White, C. E. (2010a). *Compilation of Geochemical and Petrographic Data from the Western and Southern Parts of the Goldenville and Halifax Groups, Nova Scotia*. Digital Open File Report ME2010-001. Halifax, Nova Scotia: Department of Natural Resources, Mineral Resources Branch, p. 18.

— (2010b). "Stratigraphy of the Lower Paleozoic Goldenville and Halifax Groups in the Western Part of Southern Nova Scotia". In: *Atlantic Geology* 46, pp. 136–154. DOI: 10.4138/atlgeol.2010.008.

White, C. E. and S. M. Barr (2010). "Lithochemistry of the Lower Paleozoic Goldenville and Halifax Groups, Southwestern Nova Scotia, Canada: Implications for Stratigraphy, Provenance, and Tectonic Setting of the Meguma Terrane". In: *Geological Society of America Memoirs*. Ed. by R. Tollo, M. Bartholomew, J. P. Hibbard, and P. Karabinos. Vol. 206. Geological Society of America, pp. 347–366. DOI: 10.1130/2010.1206(15).

White, C. E., L. Trudell, and R. Hamblin (2014). "An Update on the Acid-Generating Potential of Rocks in Southwestern Nova Scotia with Emphasis on the Metropolitan Halifax Regional Municipality". In: *Geoscience and Mines Branch Report ME 2014-001: Report of Activities 2013*. Ed. by D. MacDonald and E. MacDonald. Halifax, Nova Scotia: Nova Scotia Department of Natural Resources, pp. 67–80.

White, H. E. (2012). "Paleolimnological Records of Post-Glacial Lake and Wetland Evolution from the Isthmus of Chignecto Region, Eastern Canada". M.Sc. Thesis. Wolfville, NS: Acadia University. URL: http://scholar.acadiau.ca/islandora/object/theses:247.

Whitehead, D. R., D. F. Charles, and R. A. Goldstein (1990). "The PIRLA Project (Paleoecological Investigation of Recent Lake Acidification): An Introduction to the Synthesis of the Project". In: *Journal of Paleolimnology* 3.3, pp. 187–194. URL: http://link.springer.com/article/10.1007/BF00219458 (visited on 02/17/2014).

Wickham, H. (2009). *Ggplot2: Elegant Graphics for Data Analysis*. Use R! New York: Springer-Verlag. URL: / / www . springer . com / gp / book / 9780387981413 (visited on 12/06/2018).

— (2014). "Tidy Data". In: *Journal of Statistical Software* 59.10. DOI: 10.18637/jss.v059.i10.

Wickham, H. (2019). *tidyverse: Easily Install and Load the 'Tidyverse'*. R package version 1.3.0. URL: https://CRAN.R-project.org/package=tidyverse.

Wickham, H., W. Chang, L. Henry, T. L. Pedersen, K. Takahashi, C. Wilke, K. Woo, H. Yutani, and D. Dunnington (2020a). *ggplot2: Create Elegant Data Visualisations Using the Grammar of Graphics*. R package version 3.3.1. URL: https://CRAN.R-project.org/package=ggplot2.

Wickham, H., R. François, L. Henry, and K. Müller (2020b). *dplyr: A Grammar of Data Manipulation*. R package version 1.0.0. URL: https://CRAN.R-project.org/package=dplyr.

Wickham, H. and G. Grolemund (2017). *R for Data Science: Import, Tidy, Transform, Visualize, and Model Data*. 1 edition. Sebastopol, CA: O'Reilly Media. 522 pp.

Wickham, H. and L. Henry (2020). *tidyr: Tidy Messy Data*. R package version 1.1.0. URL: https://CRAN.R-project.org/package=tidyr.

Wiklund, J. A., R. I. Hall, B. B. Wolfe, T. W. Edwards, A. J. Farwell, and D. G. Dixon (2012). "Has Alberta Oil Sands Development Increased Far-Field Delivery of Airborne Contaminants to the Peace–Athabasca Delta?" In: *Science of The Total Environment* 433, pp. 379–382. DOI: 10.1016/j.scitotenv.2012.06.074.

— (2014). "Use of Pre-Industrial Floodplain Lake Sediments to Establish Baseline River Metal Concentrations Downstream of Alberta Oil Sands: A New Approach for Detecting Pollution of Rivers". In: *Environmental Research Letters* 9.12, p. 124019. DOI: 10.1088/1748-9326/9/12/124019.

Wilkinson, L. (2005). *The Grammar of Graphics*. 2nd ed. Statistics and Computing. New York: Springer-Verlag. URL: //www.springer.com/gp/book/9780387245447 (visited on 11/09/2018).

Wong, H. K. T., J. O. Nriagu, and R. D. Coker (1984). "Atmospheric Input of Heavy Metals Chronicled in Lake Sediments of the Algonquin Provincial Park, Ontario, Canada". In: *Chemical Geology*. Geochronology of Recent Deposits 44.1, pp. 187–201. DOI: 10.1016/0009-2541(84)90072-X.

Xie, Y. (2019). *bookdown: Authoring Books and Technical Documents with R Markdown*. R package version 0.11. URL: https://CRAN.R-project.org/package=bookdown.

— (2020). *knitr: A General-Purpose Package for Dynamic Report Generation in R*. R package version 1.28. URL: https://CRAN.R-project.org/package=knitr.

Yang, H. and N. L. Rose (2003). "Arsenic Distribution in the UK Lake Sediments". In: *Journal de Physique IV (Proceedings)* 107, pp. 1389–1392. DOI: 10.1051/jp4:20030561.

Yao, S., B. Xue, and Y. Tao (2013). "Sedimentary Lead Pollution History: Lead Isotope Ratios and Conservative Elements at East Taihu Lake, Yangtze Delta, China". In: *Quaternary International*. Larger Asian Rivers: Changes in Hydro-Climate and Water Environments 304 (Supplement C), pp. 5–12. DOI: 10.1016/j.quaint.2012.10.058.

Yuan, F. (2017). “A Multi-Element Sediment Record of Hydrological and Environmental Changes from Lake Erie since 1800”. In: *Journal of Paleolimnology* 58.1, pp. 23–42. DOI: 10.1007/s10933-017-9953-3.

Zaferani, S., M. Pérez-Rodríguez, and H. Biester (2018). “Diatom Ooze—A Large Marine Mercury Sink”. In: *Science* 361.6404, pp. 797–800. DOI: 10.1126/science.aat2735. pmid: 30049786.

Zemba, S. G., D. Golomb, and J. A. Fay (1988). “Wet Sulfate and Nitrate Deposition Patterns in Eastern North America”. In: *Atmospheric Environment (1967)* 22.12, pp. 2751–2761. DOI: 10.1016/0004-6981(88)90442-8.

Zheng, J., W. Shotyk, M. Krachler, and D. A. Fisher (2007). “A 15,800-Year Record of Atmospheric Lead Deposition on the Devon Island Ice Cap, Nunavut, Canada: Natural and Anthropogenic Enrichments, Isotopic Composition, and Predominant Sources”. In: *Global Biogeochemical Cycles* 21.2. DOI: 10.1029/2006GB002897.

Zhu, H. (2019). *kableExtra: Construct Complex Table with ’kable’ and Pipe Syntax*. R package version 1.1.0. URL: https://CRAN.R-project.org/package=kableExtra.

Appendix A

Copyright Permissions

The original version of Chapter 3 appeared in *Environmental Pollution* (Dunnington et al. 2019). *Environmental Pollution*, as an Elsevier journal, allows authors to reuse content in a thesis/dissertation: "Please note that, as the author of this Elsevier article, you retain the right to include it in a thesis or dissertation, provided it is not published commercially. Permission is not required, but please ensure that you reference the journal as the original source. For more information on this and on your other retained rights, please visit: https://www.elsevier.com/about/our-business/policies/copyright#Author-rights."

The original version of Chapter 4 may appear in the *Journal of Statistical Software*, if accepted for publication. The *Journal of Statistical Software* publishes articles under the Creative Commons Attribution License (CCAL), under which authors retain ownership of the copyright for their article, but authors allow anyone to download, reuse, reprint, modify, distribute, and/or copy articles in Journal of Statistical Software, so long as the original authors and source are credited. For more information, visit https://creativecommons.org/licenses/by/3.0/.

The original version of Chapter 5 appeared in *Lake and Reservoir Management* (Dunnington et al. 2018). *Lake and Reservoir Management*, as a Taylor & Francis journal, allows authors to reuse content in a thesis/dissertation: "Taylor & Francis is pleased to offer reuses of its content for a thesis or dissertation free of charge contingent on resubmission of permission request if work is published."

The original version of Chapter 7 appeared in *Science of the Total Environment* (Dunnington et al. 2020b). *Science of the Total Environment*, as an Elsevier journal, allows authors to reuse content in a thesis/dissertation: "Please note that, as the author of this Elsevier article, you retain the right to include it in a thesis or dissertation, provided it is not published commercially. Permission is not required, but please ensure that you reference the journal as the original source. For more information on this and on your other retained rights, please visit: https://www.elsevier.com/about/our-business/policies/copyright#Author-rights."

The original version of Chapter 6 appeared in the *Journal of Paleolimnology* (Dunnington et al. 2020a). It appears in this thesis under the following terms and conditions:

SPRINGER NATURE LICENSE TERMS AND CONDITIONS

Jun 12, 2020

This Agreement between Mr. Dewey Dunnington ("You") and Springer Nature ("Springer Nature") consists of your license details and the terms and conditions provided by Springer Nature and Copyright Clearance Center.

- License Number: 4846620314222

- License date: Jun 12, 2020
- Licensed Content Publisher: Springer Nature
- Licensed Content Publication: Journal of Paleolimnology
- Licensed Content Title: Evaluating the performance of calculated elemental measures in sediment archives
- Licensed Content Author: Dewey W. Dunnington et al
- Licensed Content Date: May 19, 2020
- Type of Use: Thesis/Dissertation
- Requestor type: academic/university or research institute
- Format: print and electronic
- Portion: full article/chapter
- Will you be translating?: no
- Circulation/distribution: 1000 - 1999
- Author of this Springer Nature content: yes
- Title: Using High-Throughput Paleolimnological Methods to Evaluate the Distribution and Transport of Lead in Northeastern North America
- Institution name: Dalhousie University
- Expected presentation date: Aug 2020
- Requestor Location: Mr. Dewey Dunnington, 1 Cherry Dr, Dartmouth, NS B3A2Z1, Canada, Attn: Mr. Dewey Dunnington
- Total: 0.00 CAD

Springer Nature Customer Service Centre GmbH: Terms and Conditions

This agreement sets out the terms and conditions of the licence (the Licence) between you and Springer Nature Customer Service Centre GmbH (the Licensor). By clicking 'accept' and completing the transaction for the material (Licensed Material), you also confirm your acceptance of these terms and conditions.

A.0.0.0.1 Grant of License

The Licensor grants you a personal, non-exclusive, non-transferable, world-wide licence to reproduce the Licensed Material for the purpose specified in your order only. Licences are granted for the specific use requested in the order and for no other use, subject to the conditions below.

The Licensor warrants that it has, to the best of its knowledge, the rights to license reuse of the Licensed Material. However, you should ensure that the material you are requesting is original to the Licensor and does not carry the copyright of another entity (as credited in the published version).

If the credit line on any part of the material you have requested indicates that it was reprinted or adapted with permission from another source, then you should also seek permission from that source to reuse the material.

A.0.0.0.2 Scope of Licence

You may only use the Licensed Content in the manner and to the extent permitted by these Ts&Cs and any applicable laws.

A separate licence may be required for any additional use of the Licensed Material, e.g. where a licence has been purchased for print only use, separate permission must be obtained for electronic re-use. Similarly, a licence is only valid in the language selected and does not apply for editions in other languages unless additional translation rights have been granted separately in the licence. Any content owned by third parties are expressly excluded from the licence.

Similarly, rights for additional components such as custom editions and derivatives require additional permission and may be subject to an additional fee. Please apply to Journalpermissions@springernature.com / bookpermissions@springernature.com for these rights.

Where permission has been granted free of charge for material in print, permission may also be granted for any electronic version of that work, provided that the material is incidental to your work as a whole and that the electronic version is essentially equivalent to, or substitutes for, the print version.

An alternative scope of licence may apply to signatories of the STM Permissions Guidelines, as amended from time to time.

A.0.0.0.3 Duration of Licence

A licence for is valid from the date of purchase ('Licence Date') at the end of the relevant period in the below table:

- *Scope of Licence*: Duration of Licence
- *Post on a website*: 12 months
- *Presentations*: 12 months
- *Books and journals*: Lifetime of the edition in the language purchased

A.0.0.0.4 Acknowledgement

The Licensor's permission must be acknowledged next to the Licenced Material in print. In electronic form, this acknowledgement must be visible at the same time as the figures/tables/illustrations or abstract, and must be hyperlinked to the journal/book's homepage. Our required acknowledgement format is in the Appendix below.

A.0.0.0.5 Restrictions on use

Use of the Licensed Material may be permitted for incidental promotional use and minor editing privileges e.g. minor adaptations of single figures, changes of format, colour and/or style where the adaptation is credited as set out in Appendix 1 below. Any other changes including but not

limited to, cropping, adapting, omitting material that affect the meaning, intention or moral rights of the author are strictly prohibited.

You must not use any Licensed Material as part of any design or trademark.

Licensed Material may be used in Open Access Publications (OAP) before publication by Springer Nature, but any Licensed Material must be removed from OAP sites prior to final publication.

A.0.0.0.6 Ownership of Rights

Licensed Material remains the property of either Licensor or the relevant third party and any rights not explicitly granted herein are expressly reserved.

A.0.0.0.7 Warranty

IN NO EVENT SHALL LICENSOR BE LIABLE TO YOU OR ANY OTHER PARTY OR ANY OTHER PERSON OR FOR ANY SPECIAL, CONSEQUENTIAL, INCIDENTAL OR INDIRECT DAMAGES, HOWEVER CAUSED, ARISING OUT OF OR IN CONNECTION WITH THE DOWNLOADING, VIEWING OR USE OF THE MATERIALS REGARDLESS OF THE FORM OF ACTION, WHETHER FOR BREACH OF CONTRACT, BREACH OF WARRANTY, TORT, NEGLIGENCE, INFRINGEMENT OR OTHERWISE (INCLUDING, WITHOUT LIMITATION, DAMAGES BASED ON LOSS OF PROFITS, DATA, FILES, USE, BUSINESS OPPORTUNITY OR CLAIMS OF THIRD PARTIES), AND WHETHER OR NOT THE PARTY HAS BEEN ADVISED OF THE POSSIBILITY OF SUCH DAMAGES. THIS LIMITATION SHALL APPLY NOTWITHSTANDING ANY FAILURE OF ESSENTIAL PURPOSE OF ANY LIMITED REMEDY PROVIDED HEREIN.

A.0.0.0.8 Limitations

BOOKS ONLY:Where ‘reuse in a dissertation/thesis’ has been selected the following terms apply: Print rights of the final author’s accepted manuscript (for clarity, NOT the published version) for up to 100 copies, electronic rights for use only on a personal website or institutional repository as defined by the Sherpa guideline (www.sherpa.ac.uk/romeo/).

A.0.0.0.9 Termination and Cancellation

Licences will expire after the period shown in Clause 3 (above).

Licensee reserves the right to terminate the Licence in the event that payment is not received in full or if there has been a breach of this agreement by you.

A.0.0.0.10 Appendix 1 — Acknowledgements:

For Journal Content: Reprinted by permission from [the Licensor]: [Journal Publisher (e.g. Nature/Springer/Palgrave)] [JOURNAL NAME] [REFERENCE CITATION (Article name, Author(s) Name), [COPYRIGHT] (year of publication)

For Advance Online Publication papers: Reprinted by permission from [the Licensor]: [Journal Publisher (e.g. Nature/Springer/Palgrave)] [JOURNAL NAME] [REFERENCE CITATION (Article name, Author(s) Name), [COPYRIGHT] (year of publication), advance online publication, day month year (doi: 10.1038/sj.[JOURNAL ACRONYM].)

For Adaptations/Translations: Adapted/Translated by permission from [the Licensor]: [Journal Publisher (e.g. Nature/Springer/Palgrave)] [JOURNAL NAME] [REFERENCE CITATION (Article name, Author(s) Name), [COPYRIGHT] (year of publication)

Note: For any republication from the British Journal of Cancer, the following credit line style applies:

Reprinted/adapted/translated by permission from [the Licensor]: on behalf of Cancer Research UK: : [Journal Publisher (e.g. Nature/Springer/Palgrave)] [JOURNAL NAME] [REFERENCE CITATION (Article name, Author(s) Name), [COPYRIGHT] (year of publication)

For Advance Online Publication papers: Reprinted by permission from The [the Licensor]: on behalf of Cancer Research UK: [Journal Publisher (e.g. Nature/Springer/Palgrave)] [JOURNAL NAME] [REFERENCE CITATION (Article name, Author(s) Name), [COPYRIGHT] (year of publication), advance online publication, day month year (doi: 10.1038/sj.[JOURNAL ACRONYM])

For Book content: Reprinted/adapted by permission from [the Licensor]: [Book Publisher (e.g. Palgrave Macmillan, Springer etc) [Book Title] by [Book author(s)] [COPYRIGHT] (year of publication)

A.0.0.0.11 Other Conditions

Version 1.2

Questions? customercare@copyright.com or +1-855-239-3415 (toll free in the US) or +1-978-646-2777.

Appendix B

Supplemental Information: Evaluating the Utility of Elemental Measurements Obtained from Factory-Calibrated Field-Portable X-Ray Fluorescence Units for Aquatic Sediments

This appendix contains supplemental tables and figures for Chapter 3.

Table B.1: Relative standard deviations of replicate values from study pXRF analyzers. NA indicates that the element was not measured on the XRF model, or that too few samples had values above the detection limit for that element. Bold indicates a definitive level of data quality, italics represent a quantitative level of data quality, and normal formatting indicates a qualitative level of data quality.

Element	Overall RSD	X-5000	Delta	Vanta	Epsilon 1
Si	**2.5%**	NA	NA	**2.1%** (n=55)	**2.8%** (n=68)
K	**2.7%**	**3.2%** (n=83)	**1.2%** (n=30)	**1.9%** (n=53)	**3.4%** (n=68)
Fe	**2.8%**	**5.0%** (n=83)	**0.8%** (n=31)	**1.6%** (n=57)	**1.8%** (n=68)
Ti	**3.3%**	**3.0%** (n=83)	**1.5%** (n=32)	**5.0%** (n=56)	**3.0%** (n=68)
Mn	**3.7%**	**2.9%** (n=83)	**1.5%** (n=31)	**4.9%** (n=57)	**4.8%** (n=68)
Ca	**3.8%**	**5.2%** (n=83)	**3.6%** (n=18)	**2.6%** (n=55)	**3.2%** (n=68)
Zn	**4.4%**	**5.4%** (n=83)	**2.4%** (n=31)	**3.3%** (n=57)	**5.0%** (n=68)
Al	**4.7%**	NA	NA	**3.5%** (n=55)	**5.7%** (n=68)
Sr	**5.8%**	**8.0%** (n=83)	**2.7%** (n=31)	**3.2%** (n=57)	**6.6%** (n=68)
Cl	**6.0%**	NA	NA	NA	**6.0%** (n=68)
Zr	**6.1%**	**6.5%** (n=81)	**2.0%** (n=32)	**4.1%** (n=57)	**9.2%** (n=68)
Rb	**6.2%**	**4.6%** (n=82)	**1.7%** (n=31)	**3.3%** (n=57)	*12.5%* (n=68)
P	**6.2%**	NA	NA	**6.8%** (n=55)	**5.8%** (n=68)
S	**7.2%**	*11.9%* (n=83)	**6.5%** (n=31)	**4.4%** (n=55)	**4.0%** (n=68)
Y	**7.3%**	**8.5%** (n=82)	**4.3%** (n=32)	**6.0%** (n=57)	**8.8%** (n=48)
V	*11.8%*	**8.1%** (n=83)	**3.3%** (n=31)	*18.5%* (n=22)	*18.2%* (n=66)
Cr	*12.3%*	*13.8%* (n=79)	**7.3%** (n=25)	NA	NA
Pb	*12.6%*	*12.4%* (n=73)	**5.1%** (n=32)	**5.5%** (n=57)	22.2% (n=68)
Nb	*15.9%*	*16.5%* (n=76)	*13.1%* (n=29)	*16.4%* (n=57)	NA
As	*17.5%*	**8.9%** (n=80)	*13.1%* (n=32)	*14.8%* (n=57)	33.8% (n=61)
Cu	*19.5%*	*19.1%* (n=61)	*17.9%* (n=31)	*19.2%* (n=51)	20.9% (n=65)
Ni	*19.6%*	*18.9%* (n=39)	22.1% (n=22)	*13.0%* (n=38)	22.9% (n=68)

Table B.2: Pearson correlation coefficient and RD values between total concentrations and pXRF measurements. NA indicates that the element was not measured on the XRF model, or that too few total concentration values were available for that element. Bold indicates a definitive level of data quality, italics represent a quantitative level of data quality, and normal formatting indicates a qualitative level of data quality.

Element	Overall RD	Overall r^2	X-5000	Delta	Vanta	Epsilon 1
K	**4.2%**	**0.990**	r^2=**0.992**, RD=**4.1%** (n=23)	r^2=**0.991**, RD=**3.3%** (n=23)	r^2=**0.996**, RD=**4.0%** (n=24)	r^2=**0.979**, RD=**5.4%** (n=24)
Fe	**4.5%**	**0.950**	r^2=**0.933**, RD=**4.5%** (n=23)	r^2=**0.953**, RD=**3.6%** (n=25)	r^2=**0.963**, RD=**3.8%** (n=24)	r^2=**0.948**, RD=**6.1%** (n=24)
Mn	**5.7%**	**0.988**	r^2=**0.987**, RD=**4.7%** (n=23)	r^2=**0.983**, RD=**5.7%** (n=25)	r^2=**0.988**, RD=**6.4%** (n=24)	r^2=**0.994**, RD=**6.0%** (n=24)
Pb	**6.1%**	**0.976**	r^2=**0.980**, RD=**4.4%** (n=23)	r^2=**0.986**, RD=**4.6%** (n=25)	r^2=**0.995**, RD=**3.4%** (n=24)	r^2=**0.944**, RD=*11.9%* (n=24)
Ti	**6.1%**	**0.971**	r^2=**0.990**, RD=**3.9%** (n=23)	r^2=**0.984**, RD=**4.8%** (n=25)	r^2=**0.934**, RD=*11.9%* (n=24)	r^2=**0.975**, RD=**3.9%** (n=24)
Al	**6.5%**	**0.798**	NA	NA	r^2=**0.912**, RD=**6.5%** (n=24)	r^2=0.684, RD=NA% (n=24)
Zn	**7.5%**	**0.944**	r^2=**0.945**, RD=**6.8%** (n=23)	r^2=**0.952**, RD=**7.8%** (n=25)	r^2=**0.978**, RD=**6.6%** (n=24)	r^2=**0.900**, RD=**8.8%** (n=24)
Ca	**7.9%**	**0.919**	r^2=**0.943**, RD=**5.9%** (n=23)	r^2=**0.871**, RD=*10.3%* (n=6)	r^2=**0.892**, RD=**6.7%** (n=24)	r^2=**0.935**, RD=*10.4%* (n=24)
Cu	**9.6%**	**0.916**	r^2=**0.876**, RD=*10.7%* (n=21)	r^2=**0.956**, RD=**6.4%** (n=25)	r^2=**0.912**, RD=**9.7%** (n=24)	r^2=**0.913**, RD=*12.0%* (n=24)
V	*10.3%*	*0.622*	r^2=0.558, RD=NA% (n=23)	r^2=0.512, RD=NA% (n=25)	r^2=0.426, RD=NA% (n=9)	r^2=**0.870**, RD=*10.3%* (n=24)
As	*10.5%*	*0.886*	r^2=*0.825*, RD=**9.5%** (n=23)	r^2=**0.908**, RD=**9.9%** (n=25)	r^2=**0.922**, RD=**7.0%** (n=22)	r^2=**0.891**, RD=*15.6%* (n=22)
Ni	*12.3%*	*0.625*	r^2=0.158, RD=NA% (n=19)	r^2=0.613, RD=NA% (n=21)	r^2=*0.771*, RD=*13.0%* (n=21)	r^2=**0.876**, RD=*11.6%* (n=24)
Rb	*13.5%*	*0.813*	r^2=**0.903**, RD=*13.7%* (n=19)	r^2=**0.895**, RD=*11.6%* (n=20)	r^2=**0.892**, RD=*15.3%* (n=19)	r^2=0.556, RD=NA% (n=19)

Table B.2: Pearson correlation coefficient and RD values between total concentrations and pXRF measurements. NA indicates that the element was not measured on the XRF model, or that too few total concentration values were available for that element. Bold indicates a definitive level of data quality, italics represent a quantitative level of data quality, and normal formatting indicates a qualitative level of data quality. *(continued)*

Element	Overall RD	Overall r^2	X-5000	Delta	Vanta	Epsilon 1
Sr	*15.2%*	*0.928*	r^2=*0.776*, RD=34.2% (n=23)	r^2=**0.991**, RD=**2.8%** (n=25)	r^2=**0.986**, RD=**4.4%** (n=24)	r^2=**0.948**, RD=20.9% (n=24)
Zr	*18.3%*	*0.872*	r^2=*0.738*, RD=*19.3%* (n=23)	r^2=**0.905**, RD=25.8% (n=25)	r^2=**0.909**, RD=*16.8%* (n=24)	r^2=**0.928**, RD=*10.8%* (n=24)
S	*18.9%*	*0.942*	r^2=**0.938**, RD=*16.7%* (n=23)	r^2=**0.934**, RD=31.5% (n=24)	r^2=**0.953**, RD=*10.5%* (n=24)	r^2=**0.945**, RD=*16.9%* (n=24)
Cr	NA%	0.611	r^2=0.673, RD=NA% (n=23)	r^2=0.482, RD=NA% (n=11)	NA	NA
P	NA%	0.412	NA	r^2=0.015, RD=NA% (n=14)	r^2=0.616, RD=NA% (n=24)	r^2=0.440, RD=NA% (n=24)
Y	NA%	0.245	r^2=0.358, RD=NA% (n=23)	r^2=0.182, RD=NA% (n=25)	r^2=0.068, RD=NA% (n=24)	r^2=0.387, RD=NA% (n=23)

Table B.3: Pearson correlation coefficient and RD values between extractable concentrations and pXRF measurements. NA indicates that the element was not measured on the XRF model, or that too few total concentration values were available for that element. Bold indicates a definitive level of data quality, italics represent a quantitative level of data quality, and normal formatting indicates a qualitative level of data quality.

Element	Overall RD	Overall r^2	X-5000	Delta	Vanta	Epsilon 1
Fe	*10.5%*	*0.878*	r^2=*0.826*, RD=*15.3%* (n=123)	r^2=**0.857**, RD=*13.3%* (n=130)	r^2=**0.905**, RD=**6.3%** (n=142)	r^2=**0.917**, RD=**7.9%** (n=130)
Pb	*13.0%*	*0.938*	r^2=**0.936**, RD=*13.4%* (n=122)	r^2=**0.975**, RD=*12.1%* (n=130)	r^2=**0.973**, RD=**9.4%** (n=142)	r^2=**0.866**, RD=*17.6%* (n=130)
As	*18.0%*	*0.974*	r^2=**0.954**, RD=29.7% (n=76)	r^2=**0.972**, RD=*11.4%* (n=81)	r^2=**0.985**, RD=*14.5%* (n=93)	r^2=**0.983**, RD=*17.3%* (n=71)
Zn	20.0%	0.792	r^2=*0.770*, RD=*19.3%* (n=123)	r^2=*0.787*, RD=*19.4%* (n=130)	r^2=**0.888**, RD=*12.3%* (n=142)	r^2=*0.712*, RD=29.9% (n=130)
Cu	20.1%	0.882	r^2=*0.836*, RD=27.5% (n=101)	r^2=**0.941**, RD=*16.2%* (n=130)	r^2=**0.906**, RD=*18.6%* (n=135)	r^2=*0.831*, RD=*19.9%* (n=125)
S	27.5%	0.930	r^2=**0.875**, RD=49.0% (n=122)	r^2=**0.914**, RD=31.9% (n=128)	r^2=**0.970**, RD=*12.8%* (n=142)	r^2=**0.954**, RD=*19.2%* (n=130)
V	31.7%	0.497	r^2=0.461, RD=NA% (n=123)	r^2=0.407, RD=NA% (n=130)	r^2=0.125, RD=NA% (n=56)	r^2=*0.783*, RD=31.7% (n=129)
Mn	53.9%	0.960	r^2=**0.956**, RD=42.4% (n=123)	r^2=**0.990**, RD=36.1% (n=126)	r^2=**0.952**, RD=43.1% (n=142)	r^2=**0.945**, RD=93.7% (n=130)
K	NA%	0.441	r^2=0.457, RD=NA% (n=123)	r^2=0.307, RD=NA% (n=117)	r^2=0.504, RD=NA% (n=142)	r^2=0.479, RD=NA% (n=130)
Rb	NA%	0.129	r^2=0.142, RD=NA% (n=108)	r^2=0.119, RD=NA% (n=114)	r^2=0.126, RD=NA% (n=114)	r^2=0.131, RD=NA% (n=114)
Ti	NA%	0.543	r^2=0.538, RD=NA% (n=123)	r^2=0.560, RD=NA% (n=130)	r^2=0.502, RD=NA% (n=136)	r^2=0.575, RD=NA% (n=130)

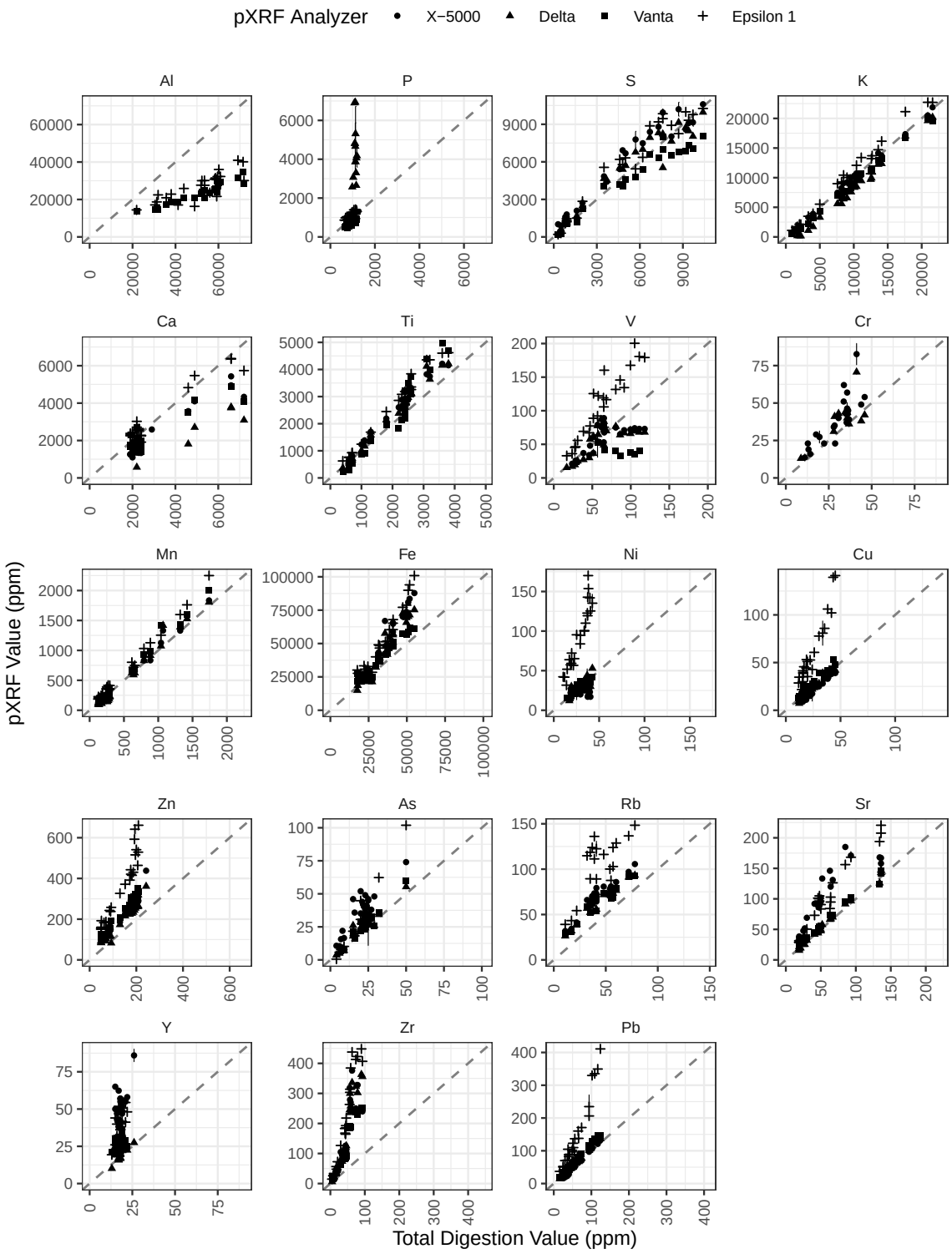

Figure B.1: Total concentrations (4-acid digestion/ICP-OES) compared to pXRF values. Dashed line indicates the y=x line.

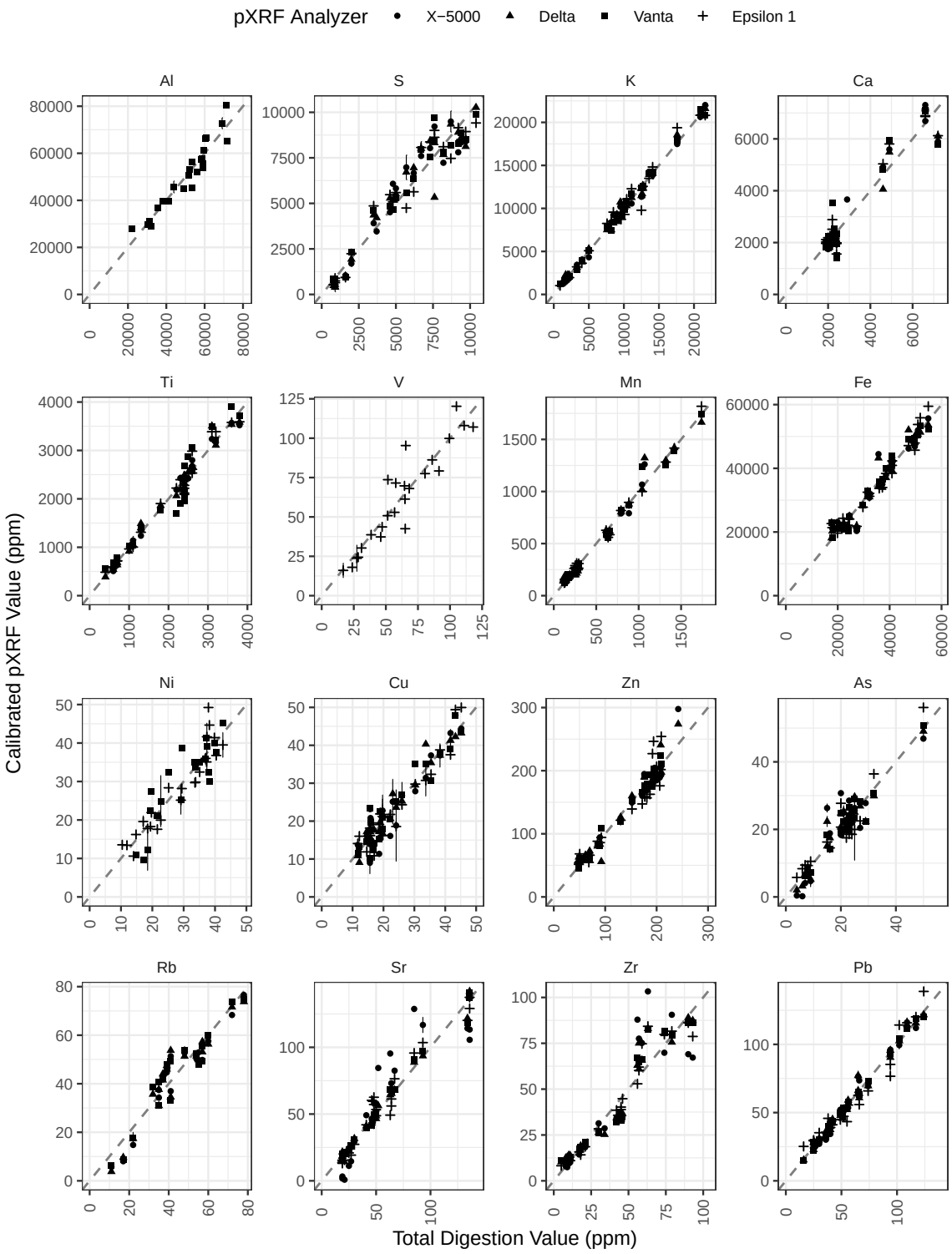

Figure B.2: Total concentrations (4-acid digestion/ICP-OES) compared to calibrated pXRF values. Dashed line indicates the y=x line.

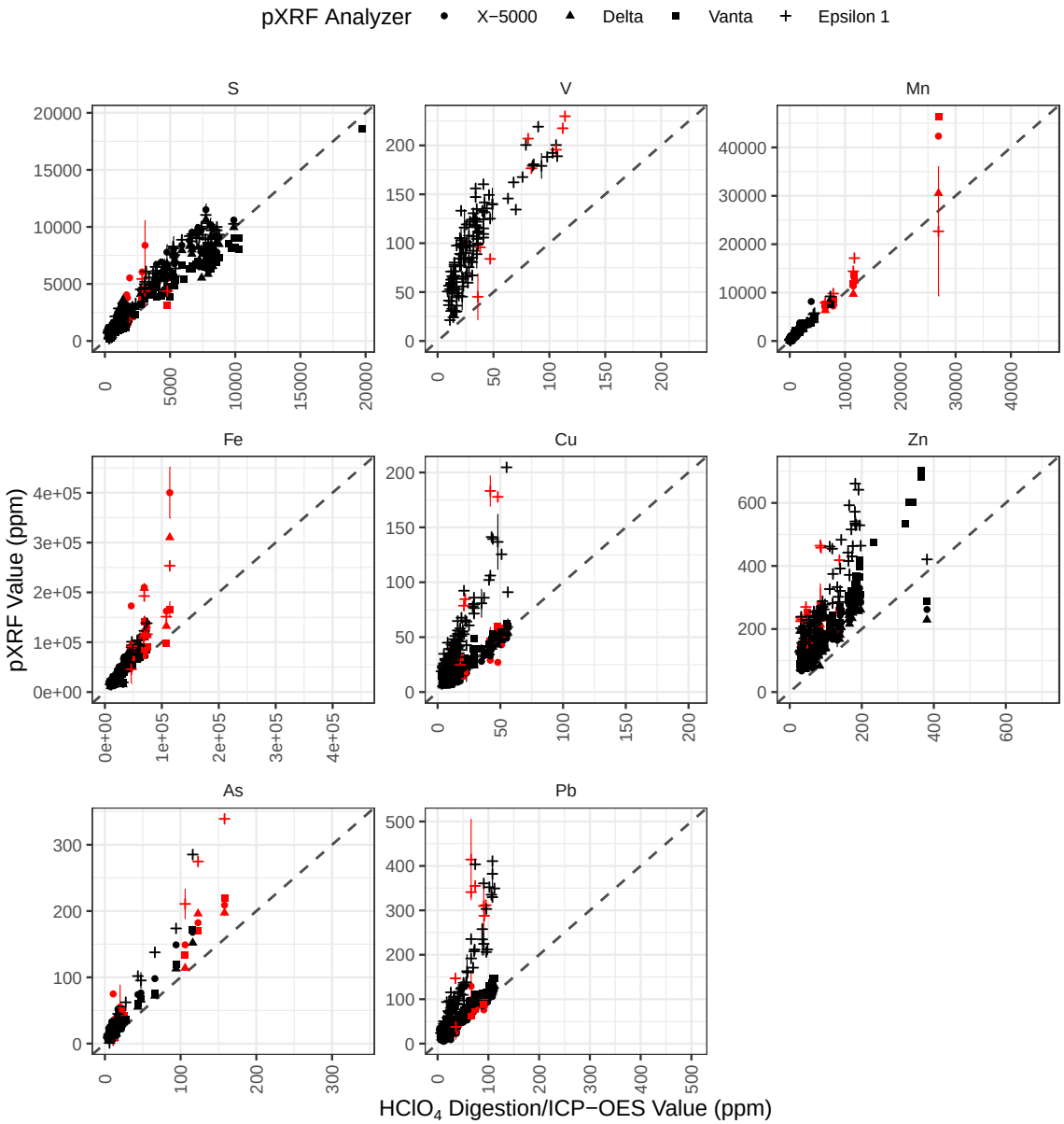

Figure B.3: Extractable concentrations ($HClO_4$ digestion/ICP-OES) compared to pXRF values. Dashed line indicates the y=x line. Samples with a mass <1.25 g are shown in red.

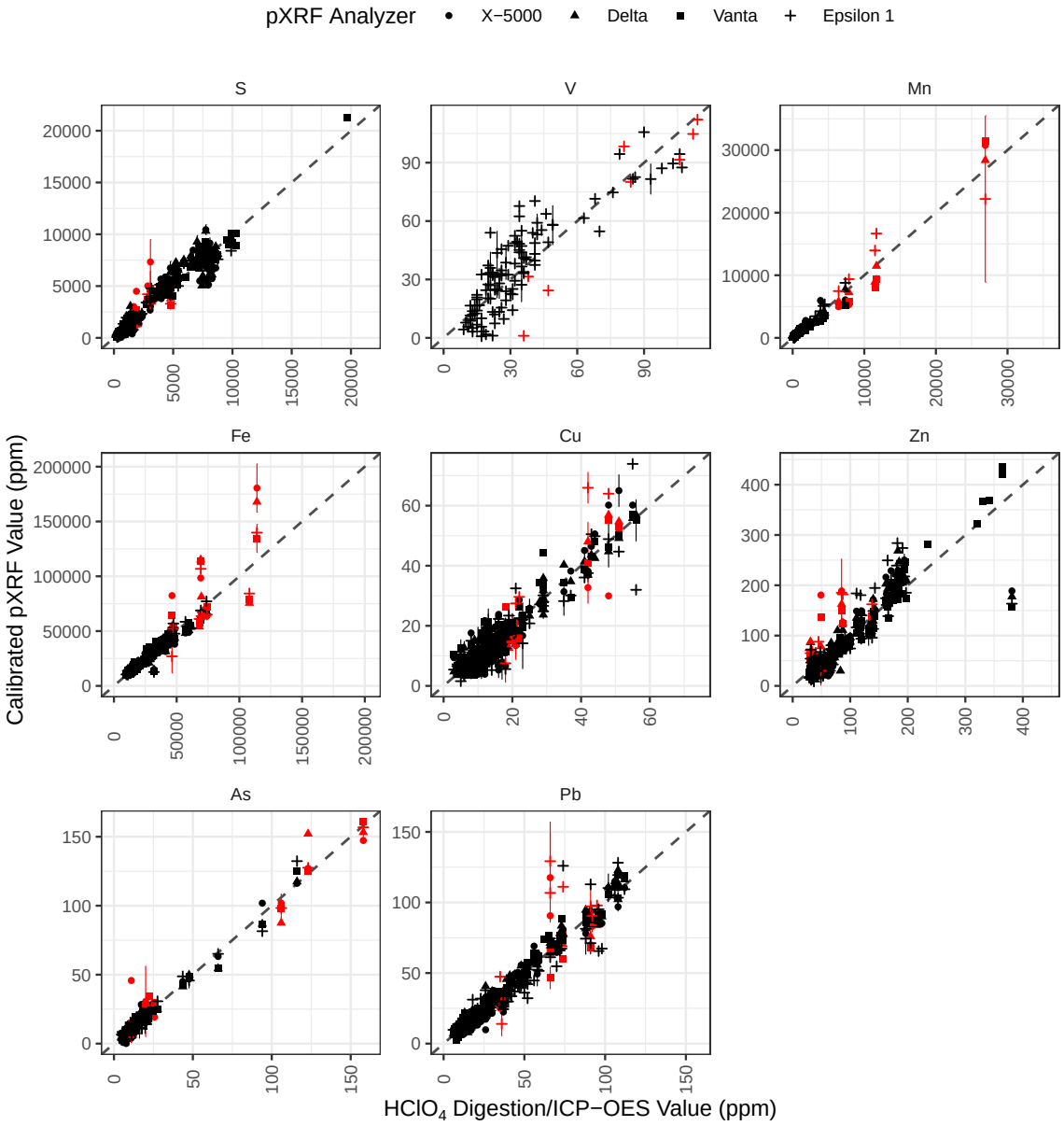

Figure B.4: Extractable concentrations ($HClO_4$ digestion/ICP-OES) compared to calibrated pXRF values. Dashed line indicates the y=x line. Samples with a mass <1.25 g are shown in red.

Appendix C

Supplemental Information: Anthropogenic Activity in the Halifax Region, Nova Scotia, Canada, as Recorded by Bulk Geochemistry of Lake Sediments

This appendix contains supplemental tables and figures for Chapter 5.

Table C.1: Selected watershed parameters for lakes in Chapter 5. Bathymetry data were not available Lake Lemont; First/Second Chain Lake bathymetry data were provided by Fraser (1986). Surface water quality data are presented as mean ± one standard deviation during 2015 and 2016, and are courtesy of the Halifax Water lake sampling program. Water quality for First Lake and Second Lake were obtained from Tymstra (2013) and Misiuk (2014), respectively. ND is used when all samples from 2015 and 2016 were non-detect. The variable "z" denotes water depth; SD denotes Secchi depth. Trophic state was calculated as the minimum and maximum trophic state using the minimum and maximum of all available parameters, using criteria from CCME (2004) and Carlson and Simpson (1986).

Parameter	Lake Major	Pockwock Lake	Bennery Lake	Second Lake	Lake Fletcher	Lake Lemont	First Lake	First Chain Lake
Watershed (ha)	6137	5450	447	509	13903	292	356	274
Area (ha)	383	903	50	113	101	11	82	35
z_{max} (m)	65	46	16	14	11	-	24	12
z_{mean} (m)	22.1	11.7	3.8	3.9	2.3	-	6.4	4.4
Vol (10^6 m^3)	83.6	106.0	1.9	4.4	2.3	-	5.3	12.1
DO (mg/L)	8.7±1.9	8.8±1.1	9.6±2.4	7.8±0.6	9.0±1.0	8.6±1.4	8.8±1.1	9.4±1.1
pH	4.7±0.1	5.3±0.3	5.8±0.6	7.0±0.4	6.4±0.2	6.4±0.2	7.6±0.5	5.1±0.7
SD (m)	-	5.0±1.0	3.7±0.7	3.7±0.8	3.6±0.7	3.6±0.1	4.3±1.5	4.6±0.2
Temp (C)	19.7±1.0	14.7±5.6	16.5±8.3	23.6±0.5	20.3±1.0	19.9±0.6	18.6±5.3	19.3±2.0
TN (mg/L)	0.30±0.08	0.23±0.22	0.33±0.05	-	0.35±0.06	0.30±0.14	-	0.17±0.13
TOC (mg/L)	4.43±0.61	3.05±0.19	4.62±0.52	-	3.13±0.31	2.60±0.10	-	0.76±0.18
TP (µg/L)	ND	6.50±4.95	8.67±5.51	-	6.33±1.53	5.00±0.00	-	ND
Chl-*a* (µg/L)	1.34±0.49	1.11±0.58	1.42±0.71	-	0.89±0.29	0.49±0.29	-	0.14±0.14
Trophic State	Oligotrophic	Oligo-Mesotrophic	Oligo-Mesotrophic	Oligo-Mesotrophic	Oligo-Mesotrophic	Oligo-Mesotrophic	Oligo-Mesotrophic	Oligotrophic
Core ID	MAJ15-1	POC15-2	BEN15-2	SLK13-1	FLE16-1	LEM16-1	FLK12-1	FCL16-1
Date	2015/11	2015/12	2015/11	2013/7	2016/6	2016/6	2012/6	2016/6
Depth (m)	25.9	43.9	12.8	12.2	7.6	3.7	19.8	12.2
Long	-63.48662	-63.83998	-63.56771	-63.66418	-63.61184	-63.52228	-63.66913	-63.64374
Lat	44.73295	44.79445	44.89064	44.78511	44.84920	44.69045	44.77297	44.63839

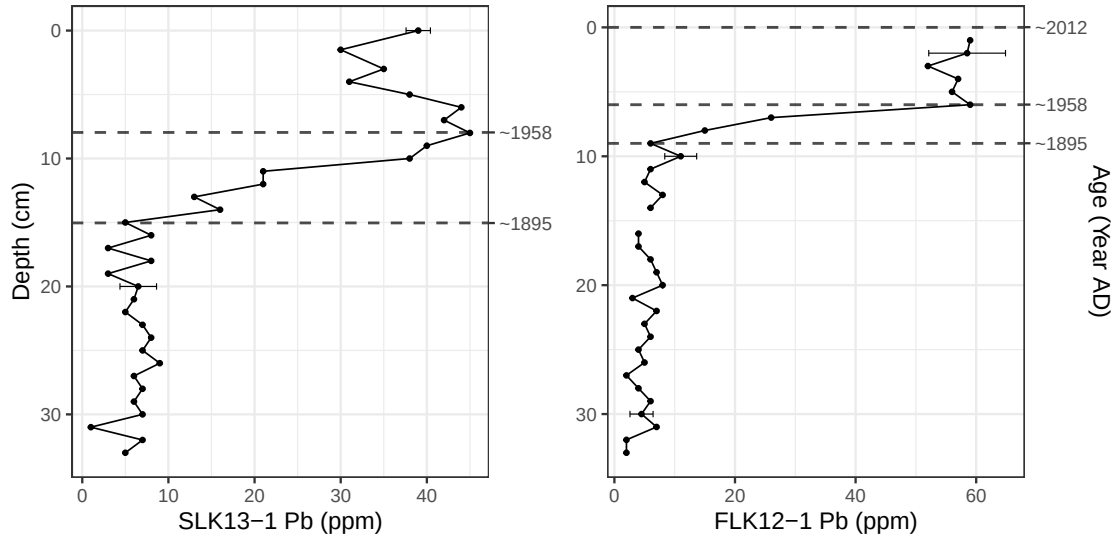

Figure C.1: Total elemental Pb concentrations for First Lake (FLK12-1) and Second Lake (SLK13-1). The age-depth model for Second Lake is based on ^{210}Pb activity; the age-depth model for First Lake is based on the point where total elemental Pb concentrations rise above background matched to the core from Second Lake (ca. 1895), the peak of the total elemental Pb concentration matched to the core from Second Lake (ca. 1958), and the time at which the core was collected (2012).

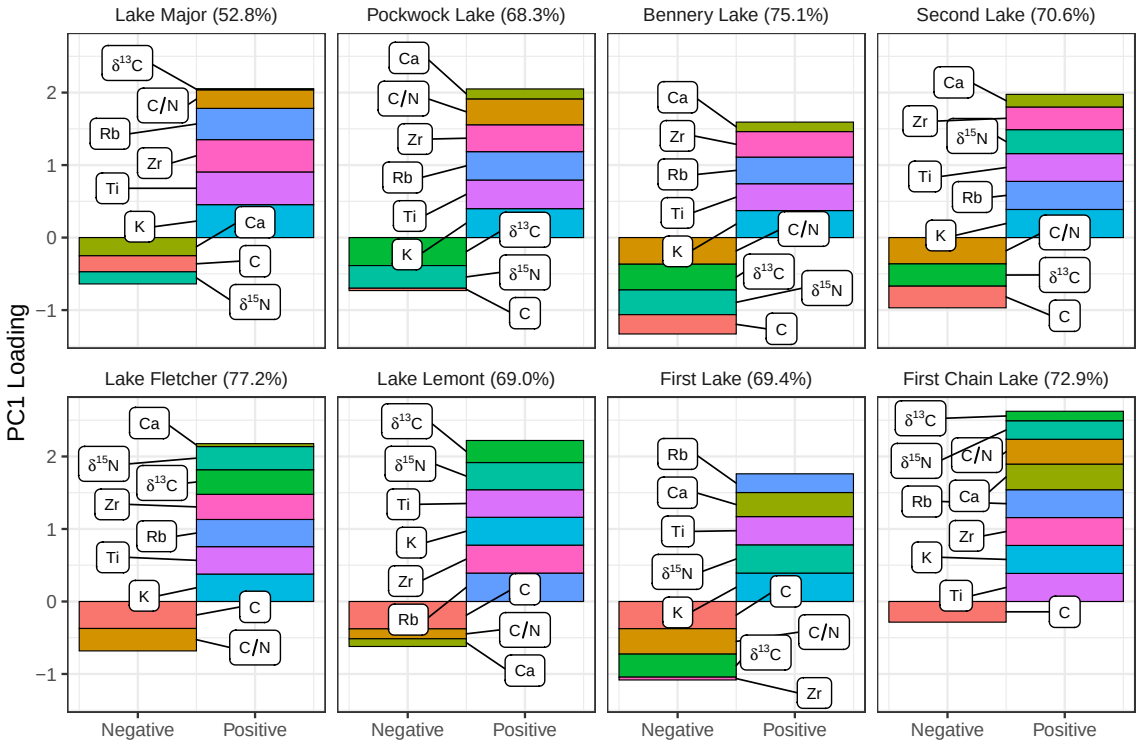

Figure C.2: PCA loadings for the first principal component for lakes in Chapter 5.

Appendix D

Supplemental Information: The Distribution and Transport of Lead Over Two Centuries as Recorded by Lake Sediments from Northeastern North America

This appendix contains supplemental tables and figures for Chapter 7.

Table D.1: List of cores included in this study and associated metrics. CA/LA denotes Catchment Area:Lake Area ratio; z max denotes maximum depth; ADIR denotes the Adirondack Region; VT-NH-ME denotes the Vermont-New Hampshire-Maine region; NS denotes the Nova Scotia region. We used one core from each lake for each lake included in this study.

Region	Lake	Longitude	Latitude	Lake area (ha)	Catchment area (ha)	CA/LA	z_{max} (m)	Elevation (m)
ADIR	Silver	-74.9123	43.8440	21.4	142	6.67	NA	639
	West	-74.8791	43.8113	12.4	184	14.8	4	578
	Big Moose	-74.8483	43.8308	520	9555	18.4	22	556
	Merriam	-74.8460	43.8575	8.2	64	7.8	5.2	655
	Fourth	-74.8396	43.7549	829	9628	11.6	26	521
	Windfall	-74.8288	43.8054	1.6	399	249	5.5	597
	Queer	-74.7993	43.8115	62	187	3.01	21	596
	Deep	-74.6624	43.6187	38.8	521	13.4	3.5	509
	T	-74.5820	43.4553	18.5	322	17.4	NA	763
	Little Echo	-74.3572	44.3058	1	1	1	5.2	482
	Bear	-74.2874	44.3990	22.6	52.9	2.34	19	499
	Upper Wallface	-74.0559	44.1482	5.5	58.3	10.6	9	948
	Arnold	-73.9439	44.1310	0.4	13.7	34.2	2.5	1150
	Clear	-73.8237	43.9990	73	567	7.77	24	584
VT-NH-ME	Haystack	-72.9164	42.9180	11.2	49.7	4.42	11.6	910
	Solitude	-72.0630	43.3075	2	28	14	7	765
	Middle Hall	-71.5455	43.8593	2.28	210	92.2	NA	447
	Speck	-70.9732	44.5637	4	40	10	11.5	1038
	Mountain (Rangely)	-70.6446	44.8950	12.2	134	11	10.7	735
	Ledge	-70.5379	44.9133	2.4	28.8	12	7.3	893
	Mountain (Coburn)	-70.1150	45.4788	1.25	12	9.62	3	881
	East Chairback	-69.2787	45.4639	16.2	81	5	17.7	461
	Klondike	-68.9501	45.9279	2	150	75	2.8	1034
	Fish River	-68.7731	46.8283	1031	33289	32.3	16.8	223
	Carr	-68.7224	46.7655	129	2856	22.1	21.9	235
	Long	-68.6119	44.0389	25.7	175	6.82	18	5

Table D.1: List of cores included in this study and associated metrics. CA/LA denotes Catchment Area:Lake Area ratio; z max denotes maximum depth; ADIR denotes the Adirondack Region; VT-NH-ME denotes the Vermont-New Hampshire-Maine region; NS denotes the Nova Scotia region. We used one core from each lake for each lake included in this study. *(continued)*

Region	Lake	Longitude	Latitude	Lake area (ha)	Catchment area (ha)	CA/LA	z_{max} (m)	Elevation (m)
	Sargent Mountain	-68.2695	44.3345	0.52	5	9.62	4	329
	Mud	-68.0886	44.6339	1.7	86.7	51	15.2	98
	Salmon	-68.0849	44.6329	2.6	11.5	4.42	10.5	88
	Little Long	-68.0776	44.6379	22.3	201	9	25.3	67
	Tilden	-68.0720	44.6351	16	78.4	4.9	10.5	69
	Unnamed	-67.7244	44.9092	7.7	23.1	3	6.7	141
NS	Nowlans	-65.9342	44.3121	73.2	208	2.84	8	73
	Peskowesk	-65.2963	44.3140	737	8500	11.5	13	105
	Big Dam	-65.2911	44.4606	45	200	4.4	9.5	120
	Hilchemakaar	-65.2402	44.2891	95	380	3.98	7	99
	Cobrielle	-65.2361	44.3140	136	1150	8.46	6.25	129
	Torment	-64.7402	44.7310	278	10747	38.7	8	175
	Pockwock	-63.8392	44.8004	903	5450	6.04	46	116
	First Chain	-63.6444	44.6386	35	274	7.83	12	61
	Fletcher	-63.6121	44.8408	101	13903	138	11	19
	Bennery	-63.5651	44.8928	50	447	8.94	16	61
	Lemont	-63.5217	44.6897	11	292	26.5	3	66
	Major	-63.4972	44.7462	383	6137	16	65	21
	Mattatall	-63.4741	45.6907	120	1016	8.47	11	47
	Middle	-60.1483	46.0625	75	1055	14.1	2.5	61
	Kellys	-60.0237	45.9279	28	2590	92.5	4.5	68

Table D.2: Annual precipitation estimates, collection methods, and references for lakes included in Chapter 7. Annual precipitation is based on the 1981-2010 climate normals published by the National Oceanic and Atmospheric Administration (NOAA) for U.S. locations, and Environment and Climate Change Canada for Canadian locations.

Region	Lake	Annual precip (mm)	Climate station (distance)	Collection Date	Collection method	Core reference	Pb record reference
ADIR	Silver	1241	BIG MOOSE 3 SE (6.1 km)	1982	Piston core	Norton and Kahl (1986)	Norton and Kahl (1986)
	West	1241	BIG MOOSE 3 SE (1.6 km)	1981	Piston core	Charles et al. (1990)	Charles et al. (1990)
	Big Moose	1241	BIG MOOSE 3 SE (3.7 km)	May 1982	Piston core	Charles et al. (1990)	Charles et al. (1990)
	Merriam	1241	BIG MOOSE 3 SE (6.6 km)	Mar 1982	Piston core	Charles et al. (1990)	Charles et al. (1990)
	Fourth	1241	BIG MOOSE 3 SE (5.5 km)	1982	Piston core	Norton and Kahl (1986)	Norton and Kahl (1986)
	Windfall	1241	BIG MOOSE 3 SE (3.1 km)	Aug 1982	Piston core	Charles et al. (1990)	Charles et al. (1990)
	Queer	1241	BIG MOOSE 3 SE (5.6 km)	Aug 1982	Piston core	Charles et al. (1990)	Charles et al. (1990)
	Deep	1416	PISECO (20.8 km)	Apr 1983	Piston core	Charles et al. (1990)	Charles et al. (1990)
	T	1416	PISECO (4.8 km)	1982	Piston core	Norton and Kahl (1986)	Norton and Kahl (1986)
	Little Echo	1138	TUPPER LAKE SUNMOUNT (10.6 km)	1981	Piston core	Charles et al. (1990)	Charles et al. (1990)
	Bear	953	SARANAC RGNL AP (6.6 km)	Oct 1981	Piston core	Charles et al. (1990)	Charles et al. (1990)
	Upper Wallface	1042	LAKE PLACID 2 S (12.1 km)	Nov 1981	Piston core	Charles et al. (1990)	Charles et al. (1990)

Table D.2: Annual precipitation estimates, collection methods, and references for lakes included in Chapter 7. Annual precipitation is based on the 1981-2010 climate normals published by the National Oceanic and Atmospheric Administration (NOAA) for U.S. locations, and Environment and Climate Change Canada for Canadian locations. *(continued)*

Region	Lake	Annual precip (mm)	Climate station (distance)	Collection Date	Collection method	Core reference	Pb record reference
	Arnold	1042	LAKE PLACID 2 S (13.0 km)	Jul 1981	Piston core	Charles et al. (1990)	Charles et al. (1990)
	Clear	948	ELIZABETHTOWN (29.9 km)	Oct 1981	Piston core	Charles et al. (1990)	Charles et al. (1990)
VT-NH-ME	Haystack	1418	WEST WARDSBORO (13.9 km)	1983	Piston core	Davis et al. (1994)	Davis et al. (1994)
	Solitude	1206	MT SUNAPEE (3.3 km)	1979	Piston core	Davis et al. (1994)	Davis et al. (1994)
	Middle Hall	1126	PLYMOUTH (11.9 km)	1983	Piston core	Norton et al. (1990)	Norton et al. (1990)
	Speck	970	BERLIN MUNI AP (16.4 km)	1978	Piston core	Davis et al. (1994)	Davis et al. (1994)
	Mountain (Rangely)	1060	RANGELEY (10.7 km)	1979	Piston core	Hanson et al. (1983)	Hanson et al. (1983)
	Ledge	1060	RANGELEY (13.5 km)	1978	Piston core	Davis et al. (1994)	Davis et al. (1994)
	Mountain (Coburn)	1037	JACKMAN (19.4 km)	1978	Piston core	Norton et al. (1981)	Norton et al. (1981)
	East Chairback	1184	BARNARD (22.1 km)	1979	Piston core	Davis et al. (1994)	Davis et al. (1994)
	Klondike	1199	RIPOGENUS DAM (18.8 km)	1978	Piston core	Davis et al. (1994)	Davis et al. (1994)
	Fish River	1037	PORTAGE (22.9 km)	1982	Piston core	Hanson et al. (1983)	Hanson et al. (1983)
	Carr	1037	PORTAGE (19.0 km)	1982	Piston core	This thesis	This thesis

Table D.2: Annual precipitation estimates, collection methods, and references for lakes included in Chapter 7. Annual precipitation is based on the 1981-2010 climate normals published by the National Oceanic and Atmospheric Administration (NOAA) for U.S. locations, and Environment and Climate Change Canada for Canadian locations. *(continued)*

Region	Lake	Annual precip (mm)	Climate station (distance)	Collection Date	Collection method	Core reference	Pb record reference
	Long	1146	LINCOLN SAN DIST WTP (38.2 km)	1983	Piston core	Norton and Kahl (1986)	Norton and Kahl (1986)
	Sargent Mountain	1441	ACADIA NP (4.5 km)	1983	Piston core	Norton and Kahl (1986)	Norton and Kahl (1986)
	Mud	1174	ELLSWORTH (29.6 km)	Feb 1981	Piston core	Brewer (1986)	Brewer (1986)
	Salmon	1174	ELLSWORTH (29.8 km)	Feb 1981	Piston core	Brewer (1986)	Brewer (1986)
	Little Long	1174	ELLSWORTH (30.5 km)	Feb 1981	Piston core	Brewer (1986)	Brewer (1986)
	Tilden	1174	ELLSWORTH (30.8 km)	Feb 1981	Piston core	Brewer (1986)	Brewer (1986)
	Unnamed	1280	WESLEY (6.5 km)	1979	Piston core	Davis et al. (1994)	Davis et al. (1994)
NS	Nowlans	1302	WEYMOUTH FALLS (9.9 km)	May 2017	Gravity core	This thesis	This thesis
	Peskowesk	1348	KEJIMKUJIK PARK (15.3 km)	Jul 2009	Gravity core	Roberts et al. (2019)	Roberts et al. (2019)
	Big Dam	1348	KEJIMKUJIK PARK (7.9 km)	Oct 2008	Gravity core	Roberts et al. (2019)	Roberts et al. (2019)
	Hilchemakaar	1348	KEJIMKUJIK PARK (16.3 km)	Feb 2008	Gravity core	Roberts et al. (2019)	Roberts et al. (2019)
	Cobrielle	1348	KEJIMKUJIK PARK (13.5 km)	Jan 2006	Gravity core	Roberts et al. (2019)	Roberts et al. (2019)
	Torment	1455	SPRINGFIELD (11.2 km)	Jun 2017	Gravity core	This thesis	This thesis

Table D.2: Annual precipitation estimates, collection methods, and references for lakes included in Chapter 7. Annual precipitation is based on the 1981-2010 climate normals published by the National Oceanic and Atmospheric Administration (NOAA) for U.S. locations, and Environment and Climate Change Canada for Canadian locations. *(continued)*

Region	Lake	Annual precip (mm)	Climate station (distance)	Collection Date	Collection method	Core reference	Pb record reference
	Pockwock	1513	POCKWOCK LAKE (3.7 km)	Dec 2015	Gravity core	This thesis	This thesis
	First Chain	1468	HALIFAX CITADEL (5.0 km)	Jun 2016	Gravity core	This thesis	This thesis
	Fletcher	1396	HALIFAX STANFIELD INT'L A (9.9 km)	Jun 2016	Gravity core	This thesis	This thesis
	Bennery	1396	HALIFAX STANFIELD INT'L A (5.3 km)	Nov 2015	Gravity core	This thesis	This thesis
	Lemont	1478	WESTPHAL (0.8 km)	Jun 2016	Gravity core	This thesis	This thesis
	Major	1478	WESTPHAL (7.2 km)	Nov 2015	Gravity core	This thesis	This thesis
	Mattatall	1239	MIDDLEBORO (11.1 km)	Aug 2016	Gravity core	This thesis	This thesis
	Middle	1517	SYDNEY A (14.0 km)	Jun 2017	Gravity core	This thesis	This thesis
	Kellys	1646	LOUISBOURG (3.6 km)	May 2017	Gravity core	This thesis	This thesis

Table D.3: List of independent age-depth markers used to assess reconstructed age-depth models. Watershed disturbance denotes historically-documented logging or other watershed disturbance, the depth for which was assessed using erosional indicators such as K, Ti, and/or Rb (Chapter 6). Cores that did not pass validation were not included in the timing component of this study.

Region	Lake	Marker	Marker depth (cm)	Marker age (Year CE)	CRS Modelled age (Year CE)	Pass	Marker Source
ADIR	West	Watershed Disturbance	10.00	1890	1880-1917	Yes	Charles et al. (1990)
	Big Moose	Train Soot	17.00	1894	1878-1920	Yes	Binford et al. (1993)
	Big Moose	Charcoal	16.00	1900	1888-1922	Yes	Binford et al. (1993)
	Merriam	Watershed Disturbance	8.00	1900	1860-1916	Yes	Charles et al. (1990)
	Windfall	PAH Rise	36.00	1848	1766-1916	Yes	Binford et al. (1993)
	Windfall	Ambrosia Rise	32.50	1869	1848-1923	Yes	Binford et al. (1993)
	Windfall	Fly Ash	32.50	1869	1848-1923	Yes	Binford et al. (1993)
	Queer	Ambrosia Rise	19.00	1893	1878-1919	Yes	Binford et al. (1993)
	Queer	Fly Ash	17.50	1902	1891-1924	Yes	Binford et al. (1993)
	Deep	Fly Ash	14.00	1894	1893-1918	Yes	Binford et al. (1993)
	Deep	Fly Ash	17.00	1858	1855-1898	Yes	Binford et al. (1993)
	Little Echo	Lime/Chrysophytes	2.00	1964	1964-1969	Yes	Binford et al. (1993)
	Clear	Watershed Disturbance	12.00	1870-1900	1834-1880	Yes	Charles et al. (1990)

Table D.3: List of independent age-depth markers used to assess reconstructed age-depth models. Watershed disturbance denotes historically-documented logging or other watershed disturbance, the depth for which was assessed using erosional indicators such as K, Ti, and/or Rb (Chapter 6). Cores that did not pass validation were not included in the timing component of this study. *(continued)*

Region	Lake	Marker	Marker depth (cm)	Marker age (Year CE)	CRS Modelled age (Year CE)	Pass	Marker Source
VT-NH-ME	Solitude	^{137}Cs	4.50	1960-1970	1957-1964	Yes	This thesis
	Speck	^{137}Cs	3.50	1960-1970	1967-1971	Yes	This thesis
	Ledge	Watershed Disturbance	10.00	1850-1870	1676-1918	Yes	Davis et al. (1994)
	East Chairback	^{137}Cs	4.00	1960-1970	1968-1972	Yes	This thesis
	Fish River	Watershed Disturbance	9.00	1955	1944-1960	Yes	Hanson et al. (1983)
	Long	Charcoal	16.00	1880	1870-1928	Yes	Binford et al. (1993)
	Sargent Mountain	Watershed Disturbance	12.00	1913	1884-1917	Yes	This thesis
	Mud	Watershed Disturbance	20.00	1870-1900	1717-1939	Yes	Brewer (1986)
	Salmon	Watershed Disturbance	10.00	1870-1900	1889-1910	Yes	Brewer (1986)
	Little Long	Watershed Disturbance	30.00	1870-1900	1809-1849	No	Brewer (1986)
	Tilden	Watershed Disturbance	30.00	1870-1900	1871-1903	Yes	Brewer (1986)
	Unnamed	^{137}Cs	2.25	1960-1970	1962-1967	Yes	This thesis
NS	Nowlans	Watershed Disturbance	24.00	1900	1857-1942	Yes	This thesis
	Peskowesk	^{137}Cs	7.50	1960-1970	1945-1999	Yes	Roberts et al. (2019)
	Big Dam	^{137}Cs	3.00	1960-1970	1986-1993	No	Roberts et al. (2019)

Table D.3: List of independent age-depth markers used to assess reconstructed age-depth models. Watershed disturbance denotes historically-documented logging or other watershed disturbance, the depth for which was assessed using erosional indicators such as K, Ti, and/or Rb (Chapter 6). Cores that did not pass validation were not included in the timing component of this study. *(continued)*

Region	Lake	Marker	Marker depth (cm)	Marker age (Year CE)	CRS Modelled age (Year CE)	Pass	Marker Source
	Hilchemakaar	^{137}Cs	4.00	1960-1970	1984-1994	No	Roberts et al. (2019)
	Cobrielle	^{137}Cs	2.00	1960-1970	1985-1992	No	Roberts et al. (2019)
	Torment	Watershed Disturbance	14.00	1900	1890-1926	Yes	This thesis
	Pockwock	Watershed Disturbance	8.00	1970	1968-1973	Yes	This thesis
	First Chain	Watershed Disturbance	12.00	1920	1910-1930	Yes	This thesis
	Fletcher	Watershed Disturbance	13.00	1920	1870-1938	Yes	This thesis
	Lemont	Watershed Disturbance	14.00	1920	1825-1938	Yes	This thesis
	Major	Watershed Disturbance	25.00	1850	1794-1903	Yes	This thesis
	Mattatall	Watershed Disturbance	28.00	1870-1900	1800-1894	Yes	This thesis
	Middle	Watershed Disturbance	8.00	1870-1900	1865-1984	Yes	This thesis
	Kellys	Watershed Disturbance	10.00	1975	1893-1988	Yes	This thesis

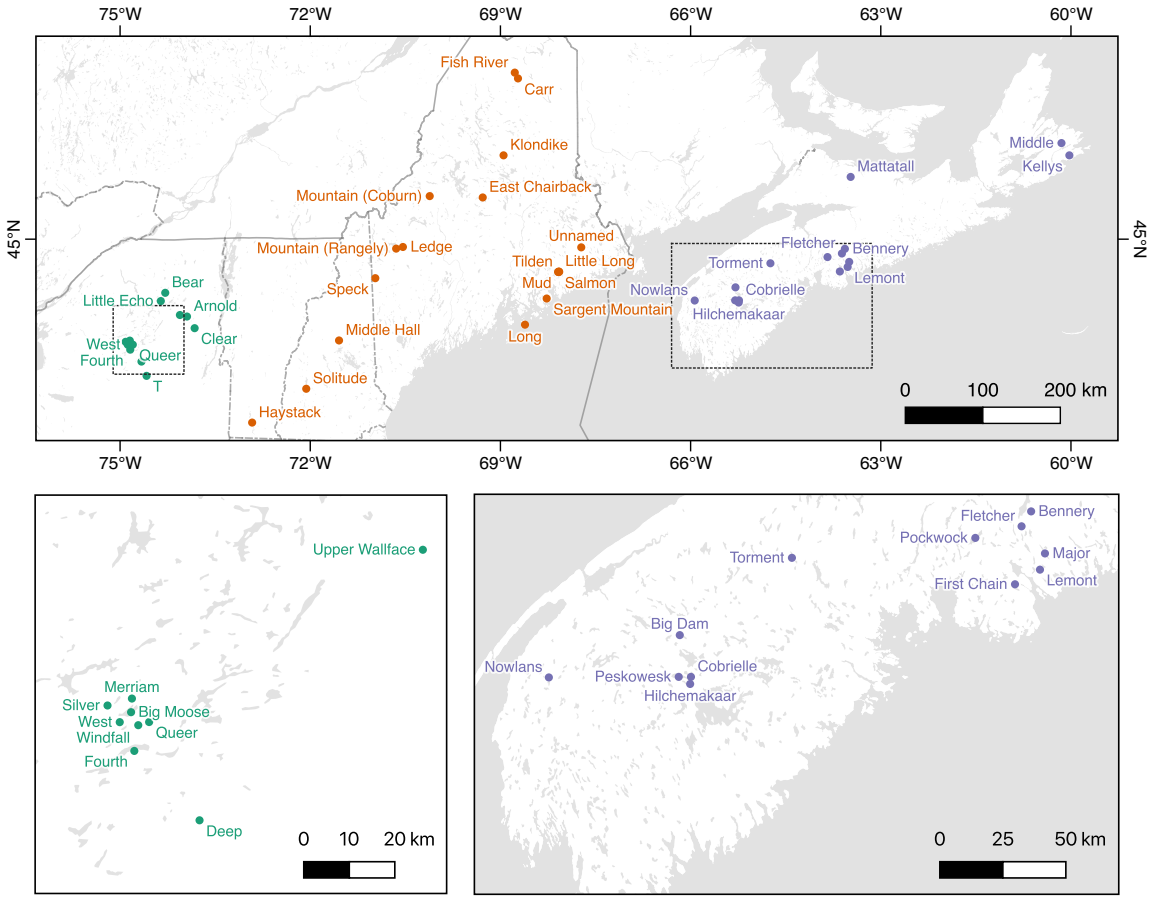

Figure D.1: Location of cores included in Chapter 7. Tilden, Little Long, Mud, and Salmon ponds are within 3 km^2 of each other in eastern Maine.

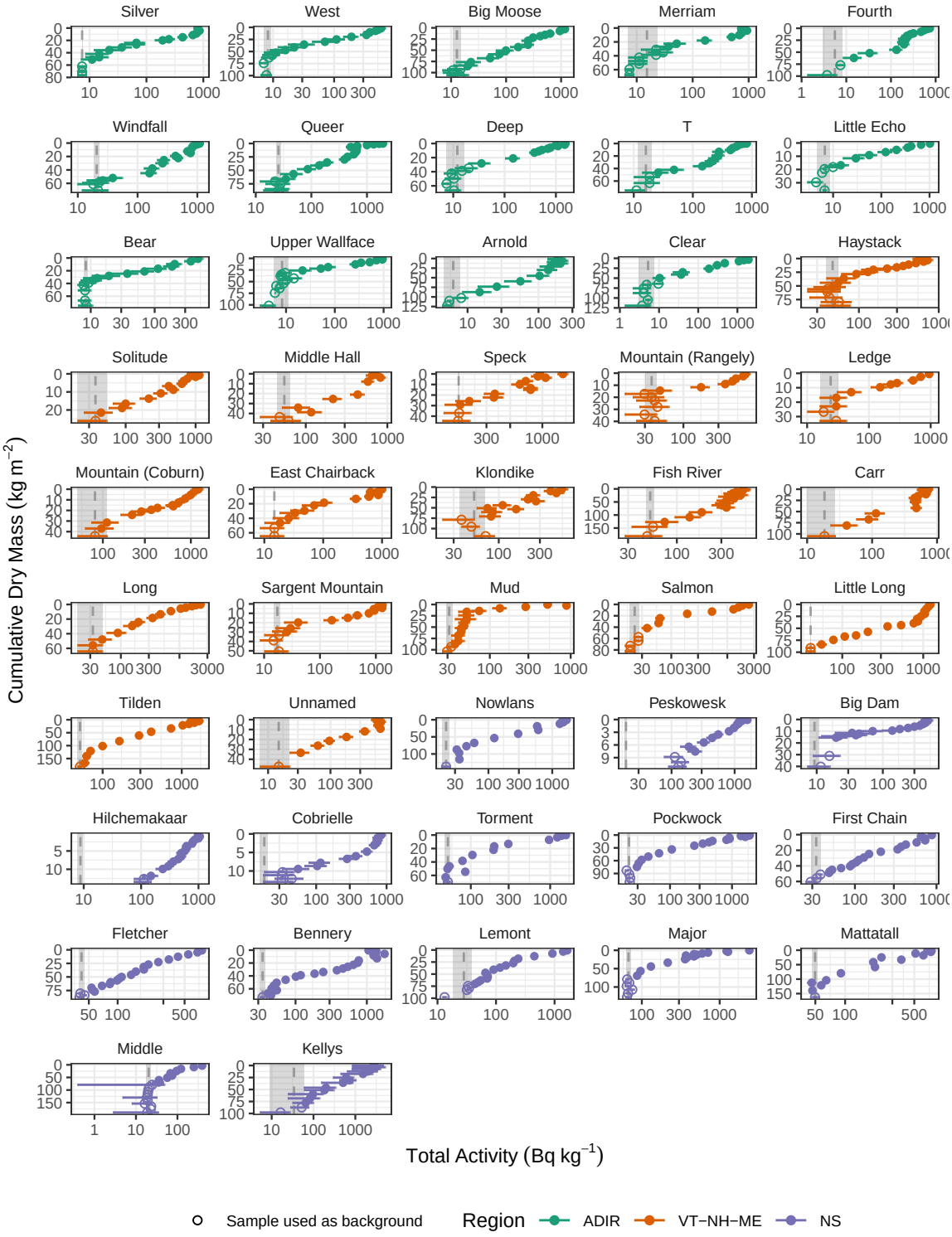

Figure D.2: Total ^{210}Pb activities and calculated background values (shaded area). ADIR denotes the Adirondack Region; VT-NH-ME denotes the Vermont-New Hampshire-Maine region; NS denotes the Nova Scotia region.

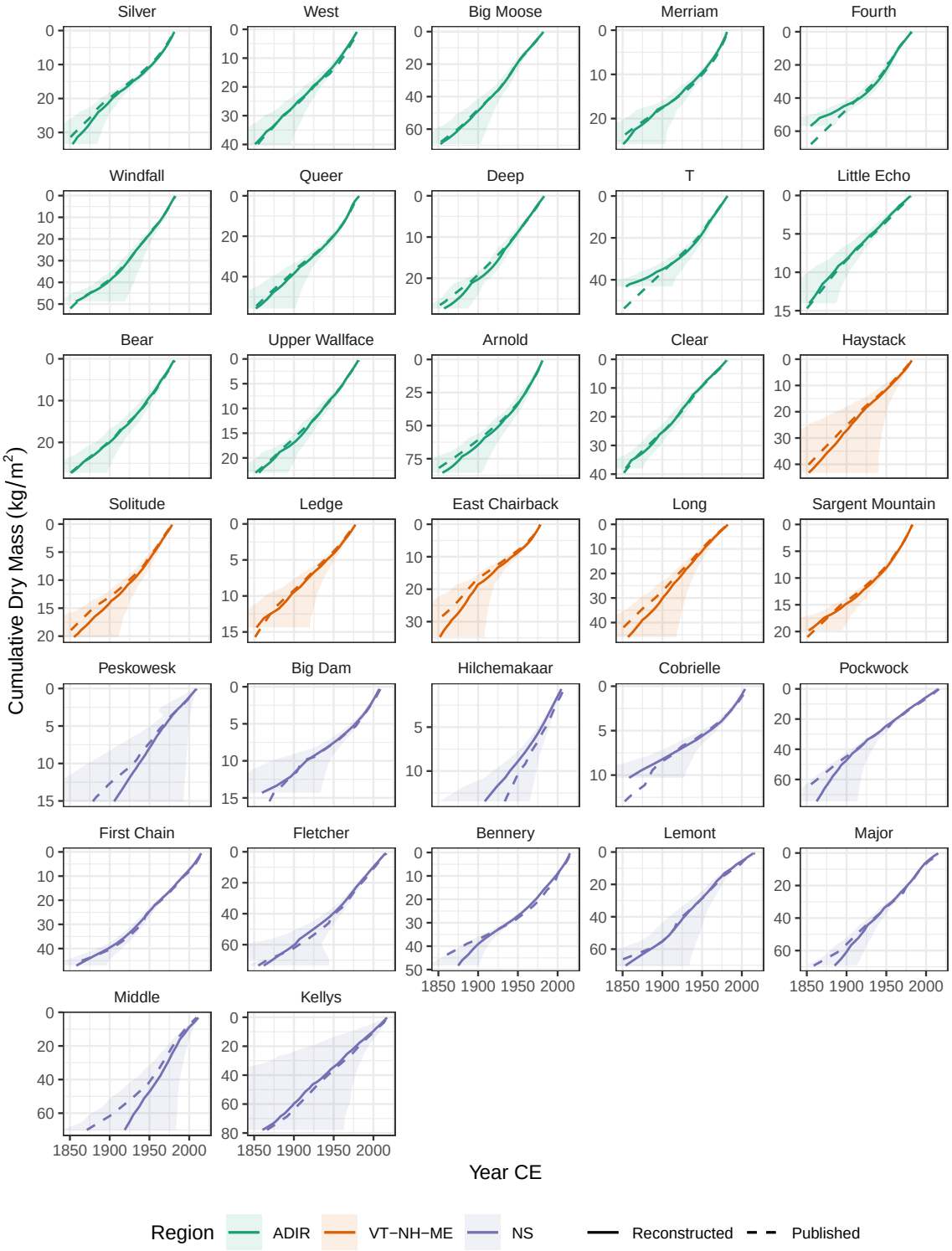

Figure D.3: Comparison of recalculated age-depth models with original published models, if available. The shaded area indicates the 5th and 95th percentile ages of all 1,000 equally probable age-depth models used in this study.

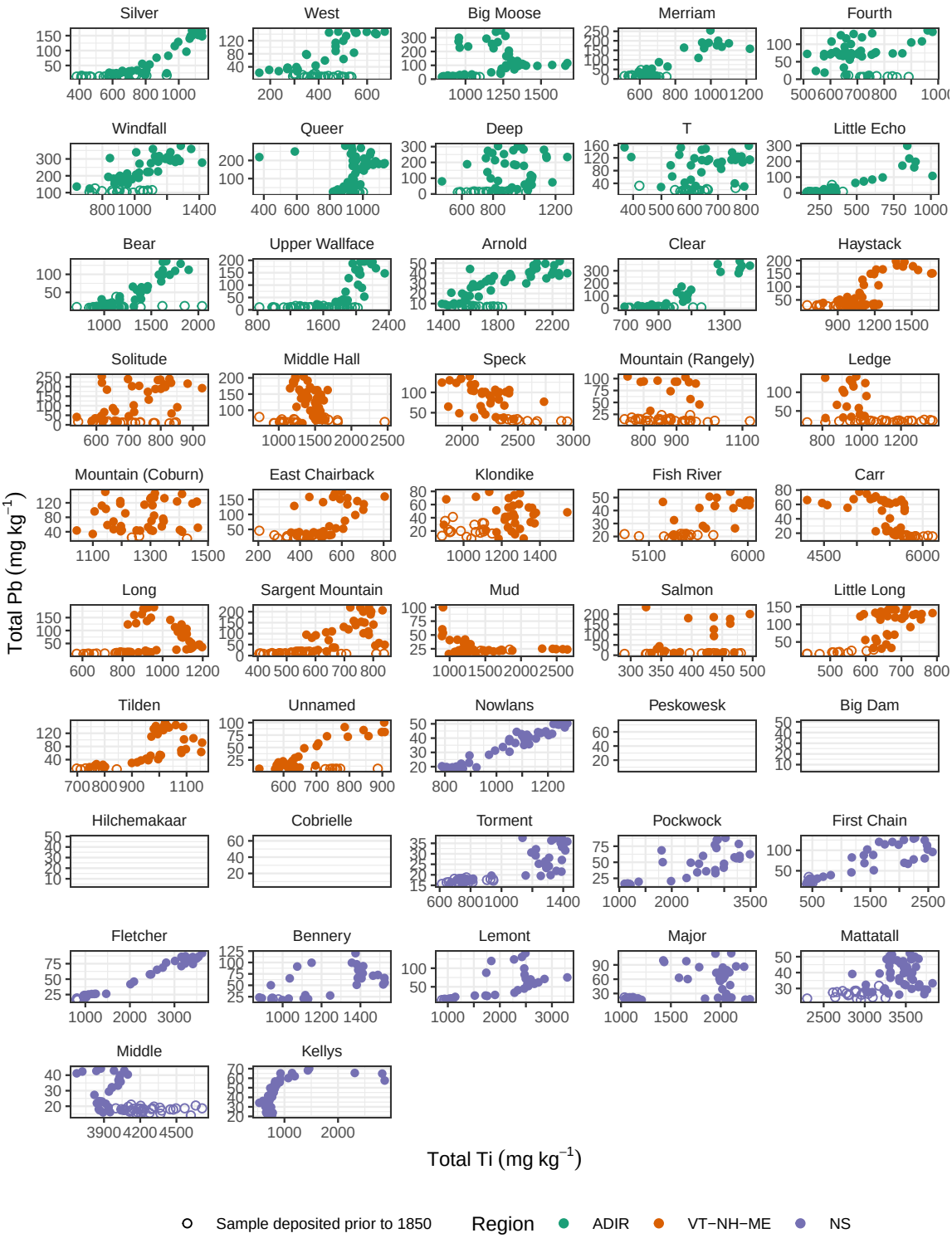

Figure D.4: Total Pb and Total Ti concentrations for study lakes, where available.

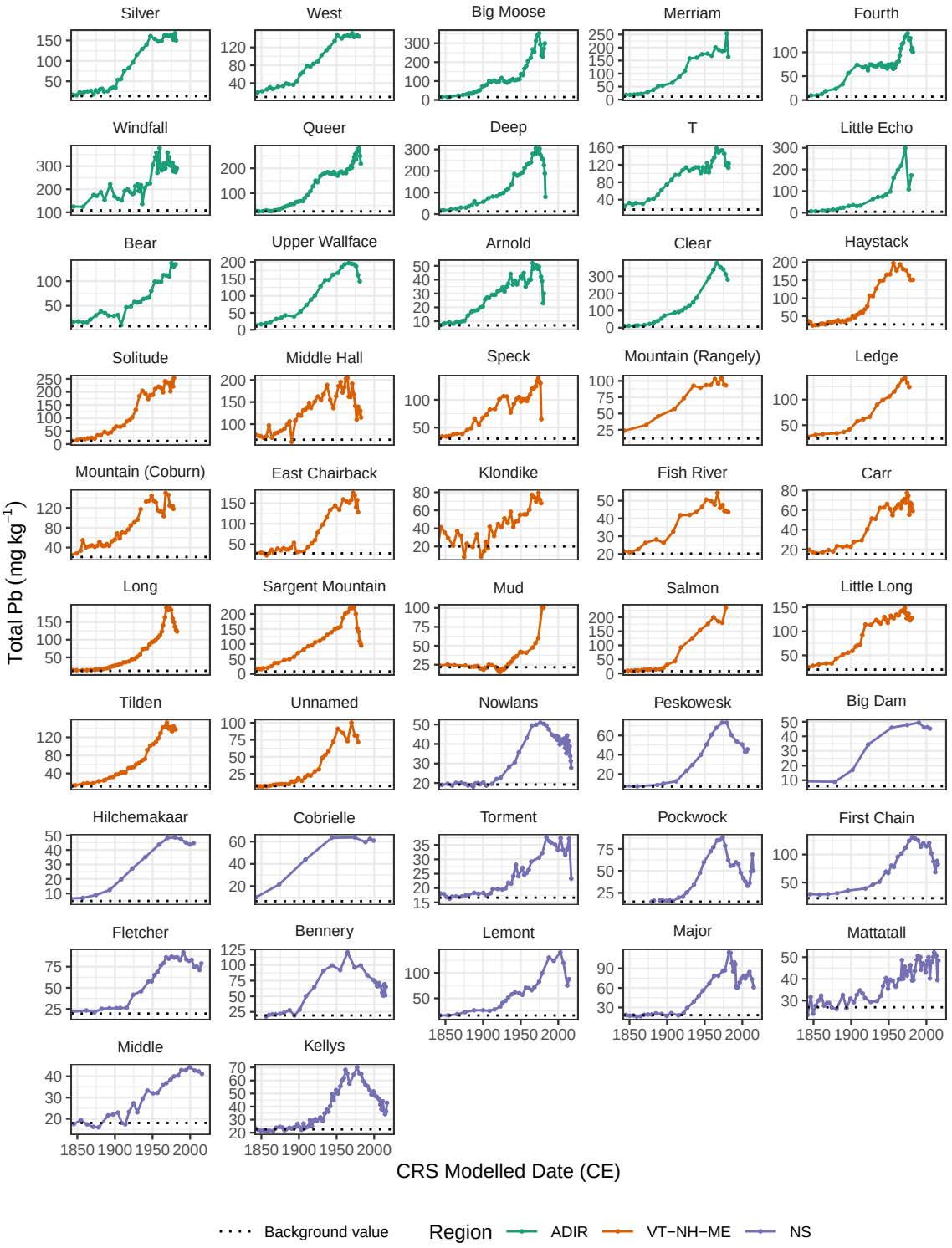

Figure D.5: Pb concentrations vs. median age of sediment intervals. Records are arranged west to east; horizontal dashed line indicates the calculated background concentration for Pb.

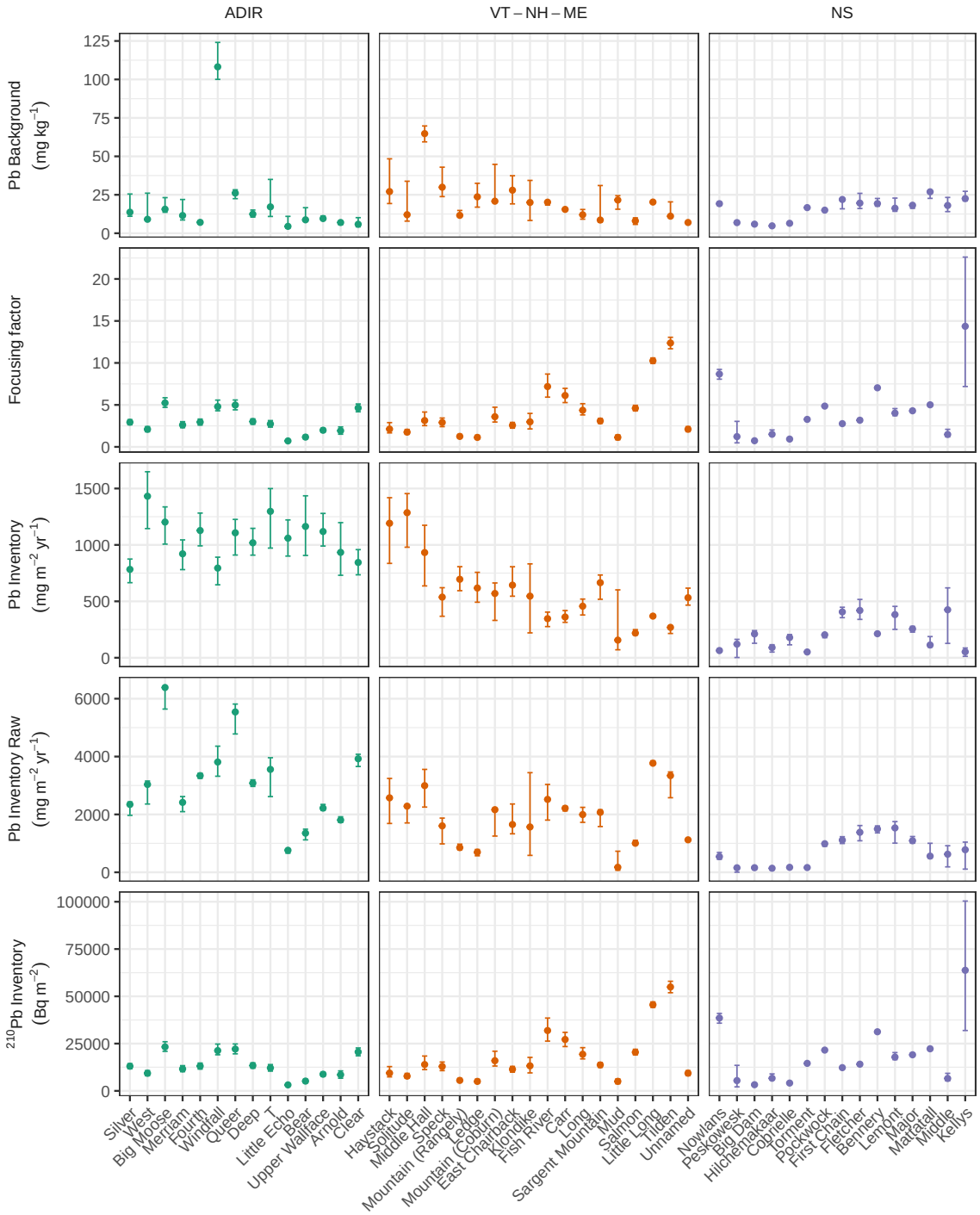

Figure D.6: Calculated backgrounds and inventories for each location. Pb inventories are focus-corrected cumulative anthropogenic deposition calculated using samples deposted between 1850 and 1978; Raw Pb inventories are cumulative anthropogenic deposition prior to focus correction. Inventories for ^{210}Pb are the basis for focus correction and are the estimated inventory of excess ^{210}Pb for the entire core.

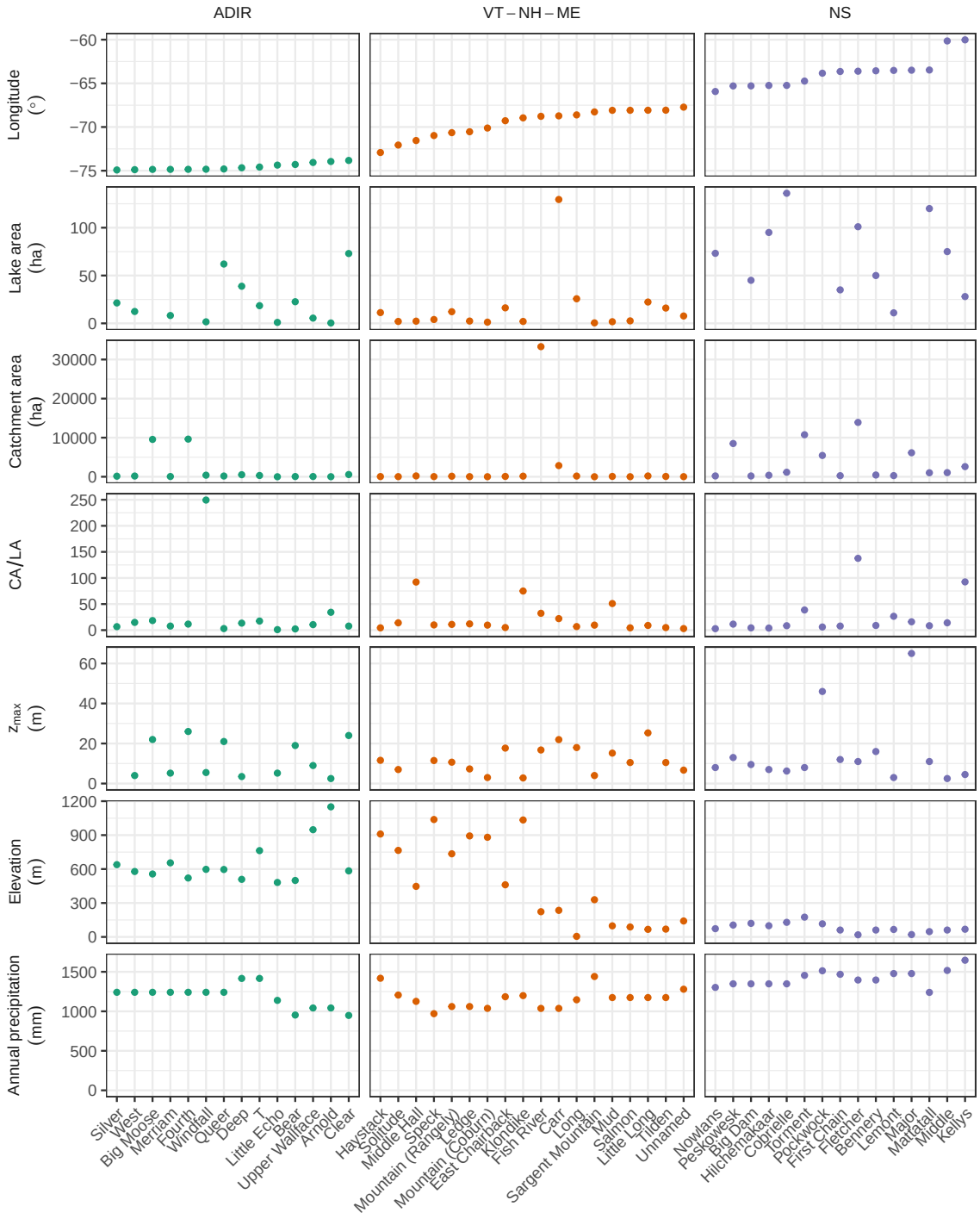

Figure D.7: Explanatory variable values for each lake. CA/LA denotes the ratio between the catchment area and lake area and z_{max} denotes the maximum depth. Lake areas greater than 200 ha (Big Moose, Fourth, Fish River, Peskowesk, Torment, Pockwock, and Major) are not shown to highlight variability between smaller values.